Fonctionnalité et dynamique des microvillosités intestinales : rôles clés des protéines de liaison à l'actine

Florent Ubelmann

THESE DE DOCTORAT DE

L'UNIVERSITE PIERRE ET MARIE CURIE

Spécialité : Complexité du Vivant

Présentée par

M. Florent Ubelmann

Pour obtenir le grade de

DOCTEUR de l'UNIVERSITÉ PIERRE ET MARIE CURIE

Fonctionnalité et dynamique des microvillosités intestinales : Rôles clés des protéines de liaison à l'actine

Pivotal role of actin binding proteins for proper microvilli function and plasticity

Thèse effectuée à l'Institut Curie, Paris

Equipe de Morphogenèse et Signalisation cellulaires

UMR 144 CNRS/Institut Curie

soutenue le 18 septembre 2012

devant le jury composé de :

Pr Germain Trugnan	Président du jury
Pr Inke Näthke	Rapporteur
Dr Florence Niedergang	Rapporteur
Dr Nadine Cerf-Bensussan	Examinateur
Dr Edith Brot Laroche	Examinateur
Dr Delphine Delacour	Examinateur
Pr Daniel Louvard	Examinateur
Dr Sylvie Robine	Directeur de thèse

Mots clés : actine, microvillosités, lésions, plasticité, physiologie de l'intestin.

Keywords : actin, microvilli, wound healing, plasticity, intestinal physiology

Résumé

Les microvillosités du pôle apical des cellules intestinales, sont de fines expansions membranaires structurées par un réseau de filaments d'actine organisé par plusieurs protéines de liaison à l'actine. L'objectif de ce travail de thèse consiste à mieux comprendre comment ces protéines de liaison à l'actine régulent deux fonctions critiques de ces organelles : leur fonctionnalité et leur plasticité.

Nous nous sommes tout d'abord intéressés aux trois protéines de liaison à l'actine qui organisent le réseau de microfilaments soutenant les microvillosités : villine, espine et plastine 1. Nous avons montré que ces protéines ne sont pas essentielles à la formation des microvillosités. En revanche, elles assurent l'agencement d'une fine architecture d'actine qui est requise pour la rétention à la membrane des microvillosités des protéines nécessaires pour la physiologie intestinale.

En plus de sa fonction structurale, la villine fragmente les filaments d'actine, suggérant un rôle central dans la dynamique du cytosquelette de la microvillosité. Celles-ci sont en effet sujettes à des réorganisations morphologiques majeures lors de stress intestinaux. Nous avons apporté les preuves définitives montrant que la villine joue un rôle critique au cours de la réparation tissulaire en participant au processus de migration cellulaire par l'initiation du désassemblage du pôle apical. Le pool d'actine microvillositaire est alors remobilisé pour assurer la formation de structures migratoires efficaces.

Ces travaux de thèse documentent ainsi deux aspects importants de la biologie de la cellule épithéliale intestinale: l'établissement de la fonctionnalité du pôle apical et son remodelage dynamique permettant une réponse rapide à un stress.

Abstract

Covering the apex of intestinal cells, microvilli are microscopic membrane protrusions structured by a network of actin filaments organized by actin binding proteins. The objective of my thesis consists on investigating how the microvillar actin binding proteins regulate two key features of these organelles: their functionality and plasticity.

From a structural point of view, the actin filaments supporting microvilli are tightly packed together by three actin bundling proteins: villin, espin and plastin-1. Using a combined knockout approach, we demonstrate that these three proteins are dispensable to enable and maintain microvilli protrusions. They however confer the appropriate actin organization required for the apical retention of proteins essential for normal intestinal physiology.

Besides its structural role, villin also nucleates, caps, and severs actin filaments in a calcium dependent manner, suggesting a central role in microvilli cytoskeleton dynamics. The brush border is indeed subject to major morphological remodeling upon various intestinal stresses (nutrition, pathogen infection, mechanical stress, injury....), which highlights the importance of such cell shape changes. We provide evidences that villin plays a critical role during tissue healing through the initiation of apex disassembly. Such cellular remodeling releases a pool of actin that is remobilized to build efficient migratory structures.

Overall, this thesis work documents two important aspects of the epithelial cell biology of the intestine: how the functionality of the apical cellular domain is established and how it can be dynamically remodelled allowing the enterocytes to rapidly respond to a stress.

Acknowledgments

I would like to start by deeply acknowledging Inke and Florence for their time and their valuable comments that helped to significantly improve this thesis manuscript. I also thank Germain Trugnan, Nadine, Delphine and Edith for having kindly accepted to be part of the jury.

This work would not have been possible without the support, help and advices of many persons. Above all, I would like to express my immense gratitude to Sylvie, for your trust, your enthusiasm, the constant support and the exceptional atmosphere that you were able to build in your group. Thank you very much as well for your expertise and for the sufficient degree of liberty that allowed me to learn how to independently think. I owe to you a lot. I am also profoundly grateful to Pr. Daniel Louvard for the opportunity to work in his lab, an environment of high scientific and technical knowledge. Thank you very much for your priceless advices and support.

I would like to particularly thank Céline, who I followed in the lab. Thank you very much for teaching me the basics of cell biology. Thank you for the continuous help and support throughout these years. I also express special thanks to Delphine Delacour for teaching me everything about immunohistochemistry and proteomics and for the numerous fruitful and friendly discussions. Thank you also Edith, for your time and expertise on mouse intestinal physiology. I am especially grateful to Mathias Chamaillard for the fruitful collaboration on colonoscopy and for giving me the opportunity to stay for a few days in Lille. I would like to additionally thank Gyorgy Hutvagner and Leggy Arnold for making me discover research, for teaching me how to work independently and for the very enriching stays in Dundee and in Memphis.

I warmly acknowledge all the past and current members of Sylvie's group that I had the chance to meet: Fati, Silvia, Cédric, Mathilde, Maia, Jeanne, Giuseppe and Silvina. Thanks a lot for your advices and your friendship. I also thank Monique, Evelyne, Dominique and Renata for their very kind help, advices and comments. Thank you Danijela for "adopting" me in your labmeetings and for your precious help. I am very grateful to Toto, for your help, your enthusiasm and your friendship. I am also profoundly indebted to Ilse for her exceptional skills and for the beautiful EM imaging. I thank the mass spectrometry team, for

their very important help and advices, the animal facility team and especially Stéphanie and Virginie and the FACS team. And to Marie Ange and Julie, I really appreciated your advices and support. l also thank all the members of the 2nd floor for the very friendly and pleasant working atmosphere and especially Nadia, Alex, Sara, Shannon, Daniel, Dora, Véro, Carole, Maria, Claudia, Olga, Priscilla and Davide for our discussions and your friendship. Thank you also to the "bombardier" team, Guimo, Patou, Loredana, Florent and to the members of the ADIC.

I also thank my dear friends from university Manue, Pau, Mica, Mag, Hadley, and Lolo for all the adventures we had together and for their support. Thank you Ana for the time we spent together, for our long-lasting deep friendship and for making me discover Colombia. Teresa, I am very grateful for your time, our numerous discussions, your invaluable support during the writing and before and also for widening my mind - *tudo vale a pena se a alma não é pequena* -. I wish you the best for your future. And I finally would like to thank my family, my mom and dad, who I admire a lot, my grandparents and Anaïs, Gabrielle and Thomas. Thank you all for your support and for your understanding. I wish I was more present during these four years.

Foreword

This thesis manuscript describes the scientific works achieved during my four years of PhD that I conducted in the Institut Curie under the supervision of Sylvie Robine, in the Morphogenesis and Cell Signaling team led by Pr. Daniel Louvard. Since many years, our laboratory is interested in the biology of the intestine and more specifically has become specialized in a cellular domain found on the apex of intestinal cells: the brush border. The intestinal brush border is constituted by numerous microvilli, which are microscopic membrane protrusions supported by a network of actin filaments organized by several actin binding proteins. This structure maximizes the absorptive and digestive functions of the intestinal epithelium. The important contribution of Daniel Louvard and Sylvie Robine regarding the cell biology of the microvillus has set the basis for this study. Indeed, they were the first to report that each of the proteins organizing the microvillar actin filaments is not individually required to maintain microvilli. In addition, they could reveal an unexpected role for one of these proteins, villin, in cell reorganization elicited by various signals.

During my PhD, I explored how these actin binding proteins ensure two important characteristics of the epithelial cells: the establishment of the apical domain functionality and its dynamic remodeling, which allows the cells to rapidly respond to a stress. In particular, the analysis of the synergic contribution of these proteins revealed that their function is not to enable the microvillar protrusions, as often assumed, but to confer the appropriate actin organization for the apical retention of proteins essential to microvilli physiological functions. This study was already initated when I join the lab. In a second aspect, I pursued the investigations on the villin role in cell plasticity and could demonstrate unambiguously its central role during wound healing process in the intestine. More specifically, results obtained using a combination of cell culture and animal models show that villin actively participates in cell migration, a critical process during wound healing, through microvilli disassembly. Such cell reorganization releases an important pool of actin monomers that is remobilized to build efficient migratory structures.

In the introductory part, I will briefly depict the cytoskeletal elements which shape the cells. I will then focus on the establishment and maintenance of polarity in polarized epithelial cells such as the enterocytes. Polarity implies the generation of asymmetrical membrane domains of distinct morphological and functional characteristics. These aspects will hence be discussed before

giving a description of the model used in this study: the intestinal epithelium. I will particularly focus on the brush border that covers each intestinal cell.

The core of the manuscript is subdivided in two parts, each of them treating the different aspects that I developed during my PhD.

Finally in the appendix, I enclosed the reprints of the different scientific reports which resulted from this study. The main part of the work is represented by two articles, one of them already in press and the other one in the process of being published. I also had the opportunity to write a chapter focused on the structure and functionality of microvilli for the book “Cellular domains”. In addition, I could participate as a collaborator to a study demonstrating the importance of actin dynamics to ensure vesicle fission on highly tensed membrane such as found in the intestinal brush border.

Index

Figures index

Introduction

In multicellular organisms, numerous vital functions are rationally compartmentalized in specialized units made up of specialized cells. Cell specialization enhances the efficiency of these biological functions and reduces global energy consumption. Cells achieve specialization by acquiring a differentiated state, which is defined by the establishment of adapted structures associated to the synthesis of suited proteins. In complex organisms such as mammals, specialized cells executing a common function are usually grouped together to form a tissue. Tissues can furthermore be assembled into an organ to perform more complex functions. Due to the broad variety of functions achieved by organs, specialized cells present an immense diversity of expression profiles and structural properties. Such differentiated state is beautifully exemplified in the cells that constitute the model we used in this study: the intestine, the organ dedicated to digestion and absorption. Before describing our working model, I will give a description of the cytoskeleton and define its role in the establishment of epithelial polarity. Epithelium and polarity are indeed two notions that characterize the intestinal tissue.

A. The cytoskeleton: the building block of cell specializations

A fundamental aspect of differentiation resides in the design of specialized cellular domains within the cell. This compartmentalization into organelles segregates biochemical reactions and increases locally the concentration of molecules, thereby promoting cellular processes. Their efficiency can be further enhanced by a structural specialization of some organelles, such as those found on the apex of intestinal cells. Structural specializations are typically shaped by the cytoskeleton, which brings mechanical support to cellular components. The cytoskeleton consists on an organized and intricate network of cytoplasmic fibrilar proteins present in the cytoplasm. This key element of cell architecture is additionally critical to elaborate the proper intracellular organization. In eukaryotic cells, three main types of fibers compose the cytoskeleton: the actin filaments (or micro-filaments), the intermediate filaments and the microtubules.

Microtubules are long tube-like polymers made up of ubiquitous and conserved globular proteins: α and β tubulin. These tubulin heterodimers assemble to form the protofilaments, the building block of the microtubules. Microtubules are polarized fibers; they present two distinct extremities, termed + and -, on which different subunits of the dimer are exposed. Elongation of microtubules essentially occurs at the + end **(Figure 1)**. Even if exceptions do exist, microtubules typically arise from the microtubule-organizing center where they are nucleated. Among the diverse functions carried out by microtubules in the cell, they play major role in intracellular trafficking. Two families of specialized molecular motors moving vesicular cargoes along microtubules have been characterized: dyneins and kinesins which differ in their polarity of displacement. Indeed, dyneins move preferentially towards the + ends of microtubule whereas kinesins are - end directed motors. In addition to molecular motors, various proteins regulate microtubule assembly or disassembly, thereby conferring a dynamic property to this cytoskeletal element.

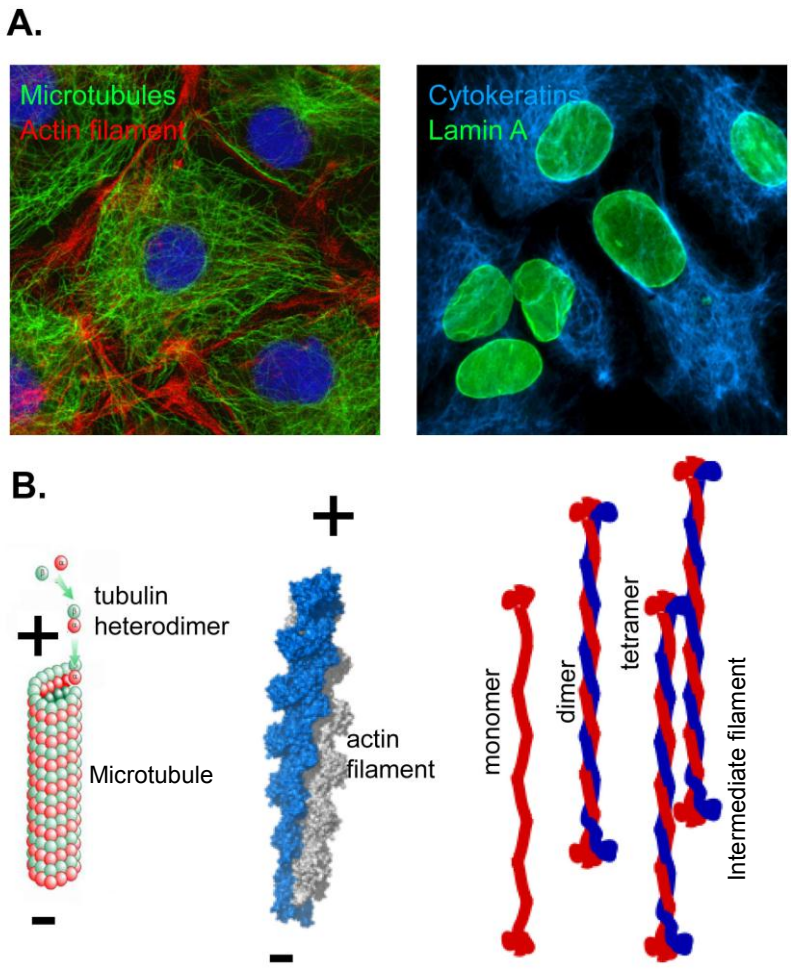

Figure 1: The three cytoskeletal filamentous elements of the cell
A. Immunostainings against the different fibers that constitute the cytoskeleton. Left micrograph: actin filaments (red) and microtubules (green); nuclei are shown in blue. Right image: Cytokeratins (blue) and thee nucleus specific intermediate filament protein Lamin A (green). Micrographs obtained from: http://www.bscb.org/softcell/images/mp_tripple.gif and http://www.piercenet.com/media/000022-ICC-cytokeratin-DyLight-405-lamin-488.jpg. **B.** The highly conserved proteins tubulins and actin form two types of polarized filaments: microtubules and actin filaments. Intermediate filaments arise from multimerisation of intermediate filament monomers. Images obtained from Wikipedia.

In contrast to microtubules, intermediate filaments do not present any polarity and are composed by molecules encoded by a very diverse array of genes. This heterogeneity is mainly based on the high divergence of the N- and C- terminal domains. The central domain, more conserved among the intermediate filaments molecules, allows their dimerization **(Figure 1)**. Assembly of these dimers creates stable and deformable fibers. The high number of different intermediate filaments molecules reflects their diverse intracellular functions and the different cell types from where they originate. For instance, lamins form a meshwork in the inner layer of nuclei. Keratins are found in epithelial cells whereas vimentin is characteristic of mesenchymal cells **(Figure 1)**. The intermediate filaments do not seem to have any function in intracellular trafficking. Their primary role seems rather to confer mechanical resistance to the cell owing to their elastic properties.

The last element that constitutes the cytoskeleton, the actin filaments, or microfilaments, shares two important characteristics with microtubules. Both of them are polarized fibers and made of polymers of globular proteins ubiquitous among different cell types **(Figure 1)**. Actin filaments also play a major role in intracellular trafficking in concert with molecular motors: the myosins.

Actin: a highly conserved protein.

Actin filaments are constituted by monomers of actin – or G-actin -, a globular protein of around 42 kDa found in virtually all eukaryotic cells. Its considerable importance is illustrated by a highly conserved sequence among different species. Structurally, G-actin is composed of four domains that appear as two lobes organized around a central cleft. The cleft binds ATP or ADP and a divalent cation, calcium or magnesium, which results in ADP- and ATP-bound monomers of different conformations **(Figure 2A)**. These actin monomers can assemble into filament composed of two intertwined helices. The actin filament – F-actin – exhibits a polar organization owing to the intrinsic horizontal asymmetry of globular actin. Their polarity can be revealed experimentally by the ability of the head domain – S1 - of myosin II to bind specifically microfilaments. When bound to an actin filament the S1 fragments, which appear as arrowheads at the ultra-structural level, uniformly point towards one extremity: the pointed end. The additional extremity is usually named the barbed end. Besides this discernible polar structure revealed by myosin S1 decoration, polarity is functional, as the two extremities present different biochemical properties **(Figure 2)** (Pollard and Borisy, 2003).

Generation of actin filaments.

Actin monomers spontaneously assemble, or nucleate, into filaments *in vitro* upon addition of salts in the solution. The inherent instability of actin dimers and trimers makes however this process unfavorable, resulting in a latency period observed when measuring polymerization rate *in vitro*. Once this step is overcome, actin polymerizes rapidly until reaching a plateau corresponding to a rate limiting availability of G-actin. Concentration of actin monomers is thus a critical parameter influencing actin polymerization.

Assembly of monomers into microfilaments obeys to a critical concentration, above which all G-actin will polymerize. For Mg-ATP-actin, the critical concentration is lower at the barbed end than at the pointed end, whereas they are identical for ADP bound actin **(Figure 2B)**. Indeed, albeit dispensable for polymerization, Mg-ATP bound to the cleft stabilizes the molecule and favors its addition to an existing filament. Consequently, at steady state, addition of ATP linked monomers is favored at the barbed ends, or growing ends. Upon ATP-actin insertion into a filament, actin starts undergoing ATP hydrolysis. As mentioned earlier, ADP-actin monomers are less stabilized within the filament and thus progressively dissociate from the filament. Thereby, ATP hydrolysis appears to act as an internal clock that determines ageing of actin molecules within a filament by inducing dissociation of "aged" molecules. This intrinsic property of actin biochemistry gives rise to the treadmilling process, in which ATP-bound monomers addition at the barbed end is compensated by dissociation of ADP-bound monomers at the pointed ends. Nevertheless, F-actin treadmilling is a relatively slow process that cannot account for the explosive bursts of actin polymerization found in highly dynamic structures such

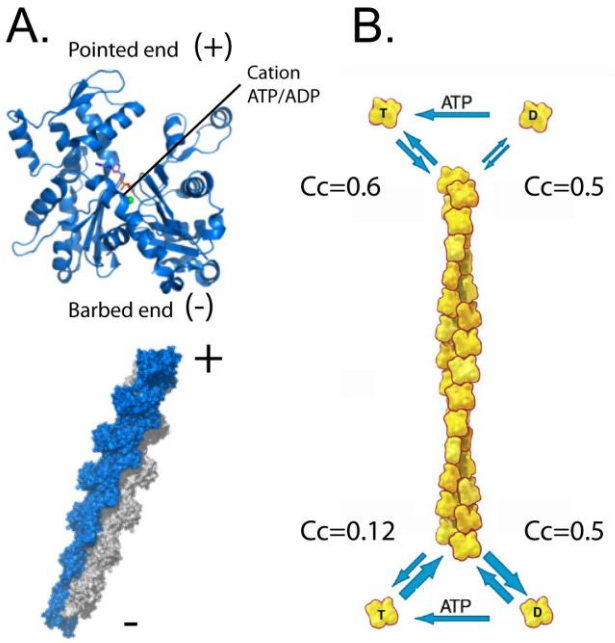

Figure 2: Actin filament assembly
A. Structural model of an actin monomer and an actin filament. The actin monomer is constituted by two lobes separated by the central cleft where a cation and ATP or ADP bind. Actin monomers assemble into polarized filaments. Note the intrinsic rotation due to the helical arrangement of the filament. Images are taken from Wikipedia. **B.** Characteristics of the dynamics of polymerization/depolymerization of an actin filament. The critical concentrations (Cc) from filament extremities for ATP bound actin differ at the barbed and pointed ends, giving rise to a slow treadmilling. ATP or ADP bound monomers are indicated with T or D, respectively. Modified from Pollard and Borisy, 2003.

as lamellipodia or filopodia of migrating cells. Likewise, the design of specialized cellular domains requires generation of elaborate actin networks. Therefore, cells express a cohort of actin binding proteins which exploit diverse aspects of actin biochemistry to control actin assembly and disassembly (Pollard and Borisy, 2003).

Cells regulate the availabilities of actin monomers and filament growing ends to control the polymerization rate.

The actin binding protein profilin catalyzes the ADP nucleotide exchange for ATP thus increasing the pool of monomers ready to polymerize. Following nucleotide exchange, profilin stays bound to actin monomer and does not impede its association to existing filaments. In contrast, thymosin B4 which also binds monomers, blocks their nucleation and association. Thus competition between these small actin sequestering proteins regulates the quantity of monomers available for polymerization **(Figure 3)** (Pollard and Borisy, 2003).

Another level of regulation is provided by capping proteins which bind to barbed ends and terminate their growth **(Figure 3)**. Capping prevents rapid depletion of available monomers that would occur in case of uncontrolled growth of barbed ends. Therefore, capping of growing filaments counterintuitively allows bursts of high actin polymerization. Indeed, the free actin monomers are directed to the few barbed ends that remain uncapped, in a "funneling" effect (Cooper and Schafer, 2000; Le Clainche and Carlier, 2008).

Finally, proteins that accelerate actin disassembly from filaments to exceed the natural dissociation by ATP hydrolysis replenish the actin monomers pool. The most studied member is certainly cofilin, from the actin depolymerizing factor – ADF – family. ADF/cofilin is thought to promote monomer disassembly by two mechanisms. ADF/cofilin binds preferentially to ADP bound monomers and *in vitro* studies have shown that cofilin enhances monomers off rate – or dissociation – from pointed ends. ADF/cofilin also cuts – or severs – actin filaments, leading to their depolymerization in coordination with capping proteins which stop actin assembly. In fact, recent experimental data suggest that ADF/cofilin replenishes the monomer pool through severing rather than by facilitating dissociation **(Figure 3)** (Kiuchi et al., 2007). In contrast to ADF/cofilin, proteins from the gelsolin family harbor a capping activity in addition to their F-actin severing property. These proteins are therefore sufficient to increase the quantity of monomeric actin available for polymerization without the support of additional capping proteins.

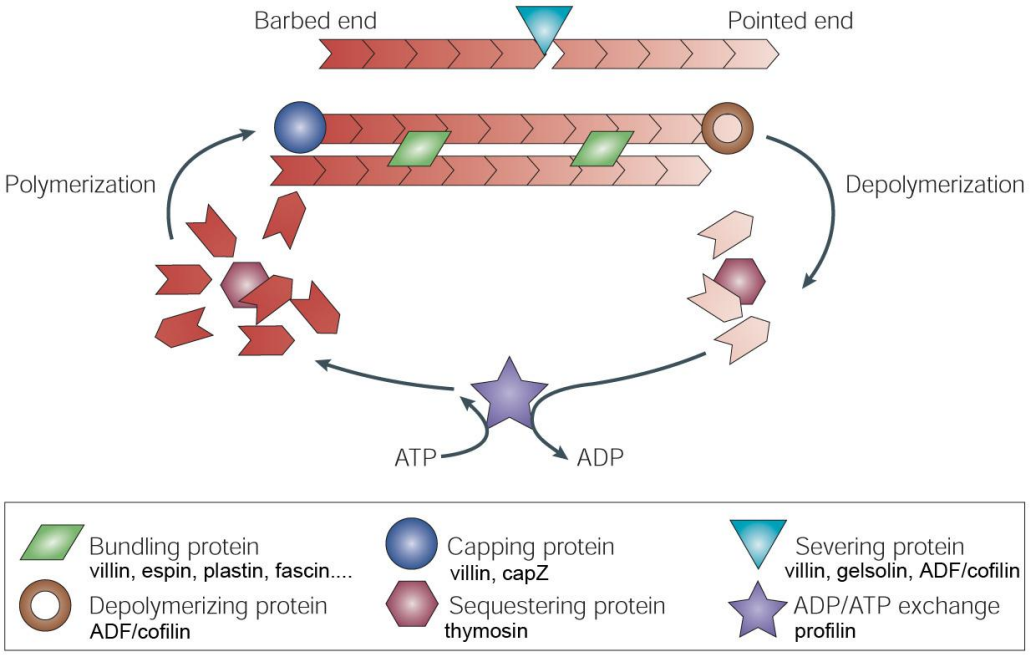

Figure 3: A cohort of actin binding proteins regulates actin dynamics and organization
Actin depolymerization at the pointed end is favored by proteins of the ADF/cofilin family which sever filaments and/or favor disassembly. Actin assembly at the barbed end is regulated by profilin, thymosin B4 and capping proteins. Actin dynamics is additionally regulated by actin severing proteins which create barbed and pointed ends. The actin network can be subsequently structured and stabilized by actin cross-linking and bundling proteins. Adapted from Revenu et al., 2004.

Facilitated initiation of new actin filaments.

The initiation of new actin filaments is an unfavorable event. Nevertheless, a prompt generation of a large number of new filaments, required in many cellular processes, is achieved by several actin binding proteins that trigger nucleation of new filaments. So far two sub-classes of actin nucleators have been described. They are characterized by the architecture of the actin network which results from nuclation: branched or unbranched.

Responsible for branched nucleation, the Arp2/3 complex binds to a pre-existing filament and initiates the formation of a newborn filament at a 70° angle from the mother filament. Arp2/3 mediated nucleation thus results in a dendritic array of actin filaments. Nucleation occurs as Arp2 and Arp3 subunits structurally resemble monomeric actin and mimic the first monomers of the filament. Originally in an inactive state, Arp2/3 is activated by upstream nucleating promoting factors. Depending on the biological process it is involved in, different factors activate Arp2/3. As an example, the Wiskott-Aldrich symptom protein – WASp – triggers Arp2/3 activation during cellular motility whereas the related protein WASH is rather involved during vesicular fission (Yarar et al., 1999; Derivery et al., 2009). This discrepancy illustrates the versatility and importance of the Arp2/3 complex to initiate two major cellular events.

Proteins of the formin family, which are characterized by the presence of a formin homology domain - FH -, rather induce the formation of linear unbranched filaments. In contrast to Arp2/3, they do not possess any actin-like domain. How formins mechanistically induce the formation of new actin filaments remains unclear, but *in vitro* studies suggest that they interact with and stabilize actin dimers and trimers through a dimerization via their FH domains (Zigmond et al., 2003). Another intriguing property of formins is their ability to remain associated – or to undergo rapid cycles of association and dissociation – with the barbed end of the growing filament while promoting rapid monomer incorporation (Zigmond et al., 2003; Kozlov and Bershadsky, 2004). In other words, formins act as a processive elongator of actin filaments additionally to their nucleation property. Formins might be of high importance in cell processes based on the formation of long unbranched filaments. Besides formins, other nucleators of unbranched filaments, such as cordon-bleu or spire, exist but are recently identified and relatively less studied (Renault et al., 2008).

B. Elaboration of complex specialized domains

As discussed earlier, the intracellular compartmentalization of different functionally specialized domains is crucial to maximize their efficiency. Many of these specialized structures are designed by networks of actin filaments, which exert mechanical force on the membrane.

A few biophysical parameters on the actin cystoskeleton.

Diverse cellular processes – e.g. motility, membrane deformation and scission - rely, for a large part, on the ability of actin cytoskeleton to generate mechanical forces coupled with a surface. Early experimental studies have proposed that mechanical forces generated by actin polymerization could account for the formation of the acrosomal process, a long linear cell extension emanating from spermatozoids of certain ectoderms during fertilization (Tilney et al., 1973). The formal demonstration that actin polymerization alone could provide forces capable of triggering a cellular process came from the understanding of the actin-based propulsion of enteropathogens (*Listeria monocytogenes* and *Shigella flexneri*), and subsequent reconstitution of actin-based motility in a cell-free system (Theriot et al., 1992; Loisel et al., 1999).

An order of magnitude of the force yielded by actin polymerization can be estimated from measurements *in vitro* which indicate that the formin-induced insertion of one actin monomer at the barbed end produces a force around 1 pN (Kovar and Pollard, 2004; Berro et al., 2007). For actin filament polymerization to exert a force on a load, a mechanical coupling between these two parameters is required. From this statement, two important points can be raised: How can filament elongate if butting a surface? In addition, polymerizing filament would require to be anchored to a substratum; otherwise polymerization force would result in a pushing of the filament rearward. An elegant theoretical answer for these problems consists on the elastic Brownian ratchet model in which the actin filament, as well as the load, is considered to undergo constant oscillations due to thermal energy (Peskin et al., 1993; Mogilner and Oster, 1996). When filament intermittently bends, free space is made available for a monomer to insert thereby lengthening the filament. The restoring force of the filament then pushes the load forward, converting actin polymerization into net movement. However, actin polymerization alone is not sufficient to account for the diversity of actin-based cellular processes, each of them requiring different levels of stabilization and regulation. For instance, this is the case for membrane deformations which require very stiff counterpoises to overcome the high resistance of the membrane. Mechanical properties allow the cytoskeleton to generate scaffolds supporting specialized actin-based structures. Their analysis reveals two main types of actin organization.

Dendritic arrays of actin filaments: the example of the lamellipodium.

Lamellipodia at the front of migrating cells is the main illustration of a specialized domain based on an extensive branched organization. This structure consists on a large membrane extension driven by an intense actin polymerization **(Figure 4)** (Wang, 1985; Svitkina et al., 1997). The lamellipodium plays major role in cell migration, even though its absence appears to be compensated by other migratory structures (Suraneni et al., 2012; Wu et al., 2012). Electron microcopy studies revealed the elaborate network of actin filaments, constituted by two areas showing different actin organizations. Close to the leading edge (1-3 µm), a preponderant intricate meshwork of short branched actin filaments generates a dendritic-like organization (Svitkina et al., 1997; Svitkina and Borisy, 1999). These filaments are of uniform polarity with barbed ends facing the migrating edge (Svitkina et al., 1997).The existence of branched actin filaments within lamellipodia has been subject to intense debates, but is now universally accepted (Small et al., 1994; Resch et al., 2002; Koestler et al., 2008; Urban et al., 2010; Vinzenz

et al., 2012). A few micrometers away from the leading edge, a less dense organization in long linear filaments predominates (Svitkina et al., 1997). Experiments revealed that the lamellipodium is indeed constituted by two distinct cytoskeletal networks differing in their dynamics: an actin network showing a rapid actin retrograde flow close to the membrane and a more stable network behind (Ponti et al., 2004). The dendritic organization that prevails in lamellipodia suggests that it arises from an Arp2/3-mediated actin nucleation. Accordingly, lamellipodial structure entirely depends on the presence of the nucleator Arp2/3 which initiates and maintains the structure in a branched organization (Suraneni et al., 2012; Vinzenz et al., 2012; Wu et al., 2012). The meshwork of actin branches is furthermore stabilized by filamin which binds high angle orthogonal filaments (Flanagan et al., 2001; Stossel et al., 2001). Proteins from the tropomyosin family also indirectly stabilize actin filaments by preventing binding of several actin regulatory proteins.

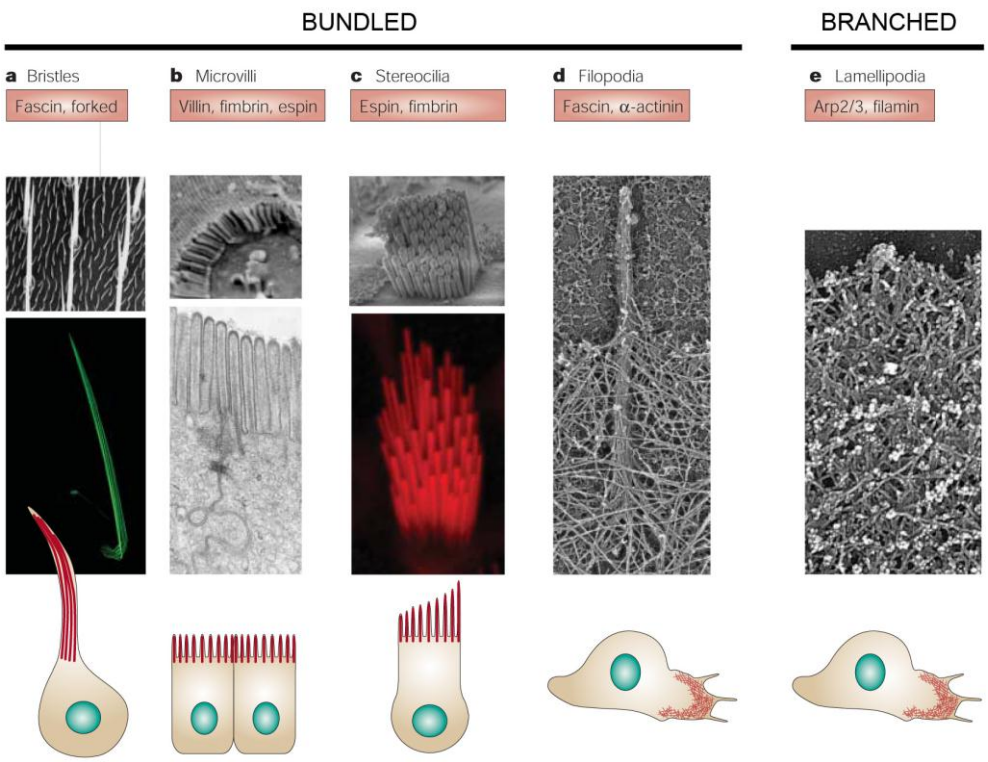

Figure 4: The different types of actin networks building specialized cellular domains
Two types of actin architecture support specialized membrane domains: The bundled network (a: bristles, b: intestinal microvilli, and c: stereocilia) and branched network (e: lamellipodia). Filopodia (d) are supported by an actin bundle but seem to arise from a branched network. The main proteins organizing the actin networks are indicated in the red boxes. Bristles: A micrograph obtained by scanning electron microscopy and a phalloidin staining are shown. Intestinal microvilli: Micrographs from scanning and transmission electron microscopy. Stereocilia: A micrograph obtained by scanning electron microscopy and a phalloidin staining are shown. Filopodia and lamellipodia: micrographs from transmission electron microscopy are shown. Adapted from Revenu et al., 2004.

To explain lamellipodium generation and maintenance, a model proposed by Pollard and Borisy is shown in **Figure 5**. In this model, Arp2/3 activation close to the membrane nucleates branched filaments that push against the membrane. The dendritic network of actin filaments originates as a result of Arp2/3 mediated nucleation. Capping proteins stop barbed ends elongation and prevent uncontrolled growth. Replenishment of the pool of monomers in ensured by ATP hydrolysis altogether with ADF/cofilin which induces dissociation of "aged" monomers and/or severs filaments. The coordinated action of profilin and thymosin β4 furthermore regulates the rate of monomers ready to elongate uncapped barbed ends.

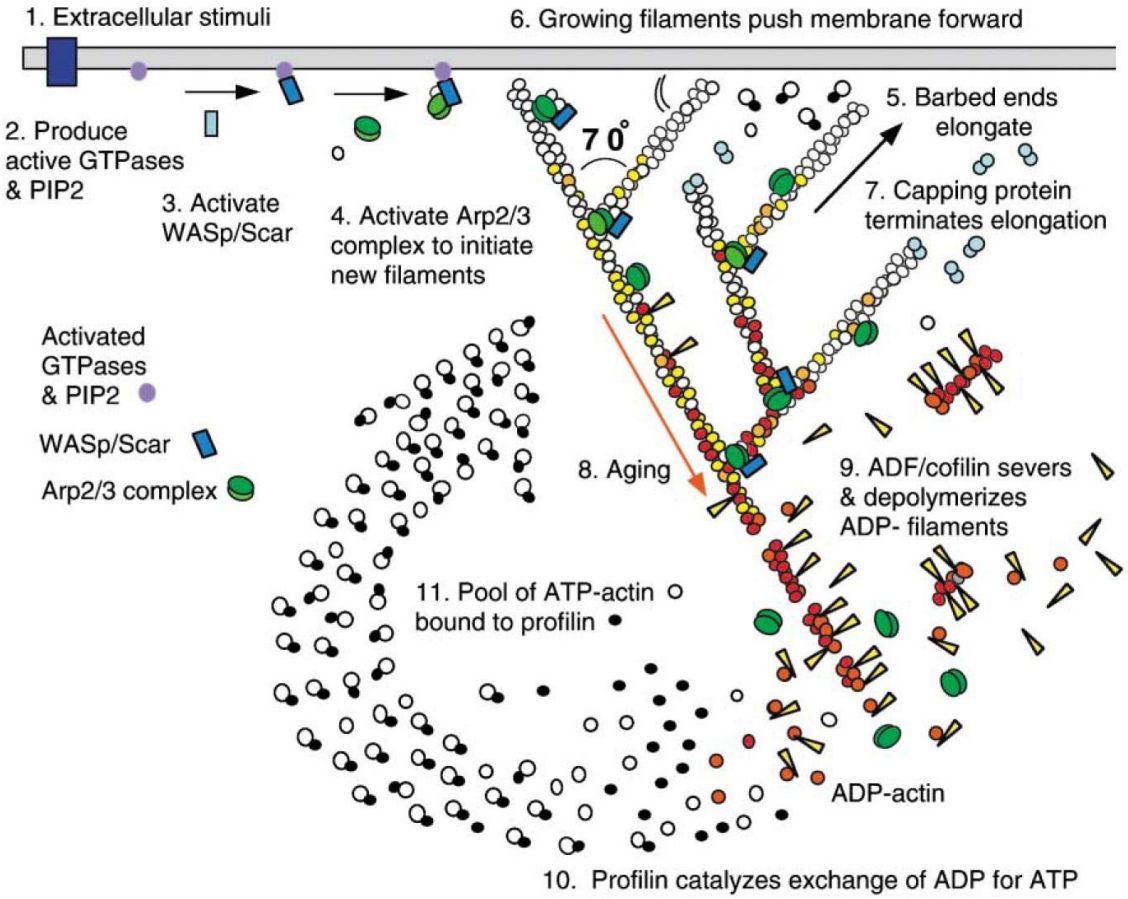

Figure 5: Model for nucleation and treadmilling at the lamellipodium
1-6: Activation of Arp2/3 at the membrane leads to the generation of a dendritic network of actin filaments, which pushes the membrane and drives the membrane extension. **7**: Capping proteins prevent the uncontrolled elongation of the filaments. **8-9**: The rear of the network disassembles efficiently due to natural "ageing" of filaments and severing and/or facilitated depolymerization by ADF/cofilin. **10-11**: Actin depolymerization releases numerous actin monomers. Profilin catalyzes ADP to ATP exchange thus regulating the pool of monomers ready to "feed" actin assembly. Adapted from Pollard and Borisy, 2003.

The lamellipodium is certainly the most widely studied organelle showing a dendritic organization, which seems also to be found in the immunological synapse, a large structure between an antigen presenting cell and a T lymphocyte (Billadeau and Burkhardt, 2006).

Networks of parallel filaments.

At the leading edge of motile cells, a second motility organelle is often generated: the filopodium. Filopodia also extend from the growth cone of developing neurons. Filopodia are highly dynamic finger-like membrane protrusions of several micrometers long emerging from the lamellipodium sheet. They are thought to function as directional sensors but experimental proof is still lacking. These proje**c**tions contain long linear filaments of uniform polarity; their growing ends oriented towards the structure tip **(Figure 4)** (Lewis and Bridgman, 1992; Svitkina et al., 1997). Since EM analyses showed that filopodia from motile cells systematically arise from the lamellipodial dendritic network, an attracting hypothesis concerning their initiation proposes that reorganization of the lamellipodial network allows the emergence of filopodia (Svitkina et al., 2003; Vignjevic et al., 2003). This possibility could be experimentally demonstrated *in vitro*: a reduction of capping proteins concentration leads to the formation of filopodia-like structures from a dendritic network (Vignjevic et al., 2003). Formins, in particular mDia2, localized at the filopodia tips may drive their initiation from the lamellipodia by protecting barbed ends from capping proteins and/or through nucleation and processive elongation (Zigmond et al., 2003; Yang et al., 2007). Also localized at the filopodia tips, proteins from the Ena/VASP might favor elongation owing to their ability to compete with capping proteins for barbed end binding (Bachmann et al., 1999). The importance of lamellipodia / filopodia interface highlights the possibility of intermediate state between purely dendritic and parallel filaments. Nevertheless, this model cannot be taken as a general rule for filopodial initiation. In this regard, fibroblasts devoid of Arp2/3, which cannot form a lamellipodium, present an increase in number of filopodia that seems to compensate for the loss of lamellipodium to ensure motility (Suraneni et al., 2012; Wu et al., 2012).

In filopodia as well as other types of slender actin-based membrane protrusions, the long linear filaments of uniform polarity are tightly packed together by diverse actin bundling proteins which organize the filaments in a bundle. Biophysical studies have proposed that such bundled organization provides stiffness to the actin network to avoid its buckling due to the opposite membrane tension (Mogilner and Rubinstein, 2005; Atilgan et al., 2006; Claessens et al., 2006; Bathe et al., 2008). The actin bundling proteins are a subset of actin cross-linking proteins, which bind several filaments to create an undefined network. The actin-bundling proteins additionally organize filaments in a regular, tight, parallel array to form a bundle; the latter can only be demonstrated by electron microscopy. The ability to bundle can be conferred by the presence of two F-actin binding motifs or by dimerization of a protein containing a unique F-actin binding

region. Actin filaments within filopodia are bundled by the actin binding proteins fascin, and T-plastin **(Figure 4)**. Fascin depletion results in a dramatic decrease in the number of filopodia, highlighting the importance of the bundled organization to initiate and sustain membrane protrusions (Kureishy et al., 2002; Vignjevic et al., 2006).

Another example of long membrane protrusion is the bristle from drosophila. Contrarily to the other membrane protrusion, each drosophila cell extends only one bristle. Bristles are long membrane deformations of around 400 µm and serve as sensory organelles **(Figure 4)**. A bristle is composed by long 11 actin bundles that are constituted by overlapping short actin filaments packed by the actin bundling proteins forked and fascin (Tilney et al., 1995; Guild et al., 2003).

Stereocilia are shorter apical membrane protrusions. Stereocilia, present on the apex of inner ear cells, allow mechanosensory transduction elicited by sound pressure. They display an organization that resembles a staircase of three rows **(Figure 4)** (Tilney et al., 1992). Each stereocilium of 1.5 – 5.5 µm long contains numerous actin filaments – until 900 – bundled by the actin bundling proteins T-plastin and espin (Tilney et al., 1988; Zheng et al., 2000). Their characteristic differential length renders stereocilia an excellent system to study the contribution of actin regulatory proteins to shape determination. In particular, several actin binding that regulate stereocilia length have been identified (Boëda et al., 2002; Belyantseva et al., 2005). They are differentially expressed between stereocilia rows but all localize to the stereocilia tips, illustrating the importance of this structure in morphogenesis of actin-based membrane protrusions. Nevertheless, a recent study following protein turnover in stereocilia revealed that these organelles might be much less dynamic than previously thought, as no actin treadmilling could be detected in the core of the protrusion (Zhang et al., 2012).

Microvilli are another typical example of short membrane protrusions supported by a central core of actin filaments. These structures are present on the surface of most of the cells, irrespective of their origin. Nevertheless, they are generally relatively short (<500 nm) and highly unstable (Gorelik et al., 2003), thus preventing any specialization. The inherent dynamics of these short-lived membrane projections combined to their ability to generate structures of higher order, suggest that they act as “elementary blocks” to assemble highly specialized structures on the cell surface (Gorelik et al., 2003). Indeed, various stable specialized domains seems to initially form by the aggregation of tiny membrane protrusions resembling microvilli; this is the case for the inner ear stereocilia and the drosophila bristle (DeRosier and Tilney, 2000). During the first stage of bristle formation, actin bundles are initiated from microvillus tip-

like structures at the cell surface. Their subsequent aggregation and organization by the actin bundling proteins forked and fascin generate a mature bristle (Tilney et al., 1996, 1998). Early in development, the surface of inner ear cells is covered by microvilli (Tilney and DeRosier, 1986). The stereocilia develop by the elongation and lateral addition of actin bundles from this microvilli precursors (Tilney and DeRosier, 1986). On the intestinal epithelium these short-lived structures also aggregate into stable highly ordered structures **(Figure 4)**. Thus, as proposed Tilney and DeRosier, microvilli might represent the "archetypal factory of F-actin bundles" (DeRosier and Tilney, 2000).

C. The epithelia: a polarized interface

The cytoskeleton has a central role in a broad range of cellular processes, which allow the generation of elaborated structures like the one found in epithelial cells. Epithelia ensure protection and concomitantly perform numerous exchanges with the external milieu. Accordingly, epithelial cells are designed to efficiently accomplish these functions **(Figure 6)**. Epithelial cells are polarized; they display two distinct membrane domains: the apical pole facing the lumen and the basolateral pole in contact with the neighboring cells and with the basal lamina. Each domain presents a proper protein and lipid composition. This property results in the formation of two functionally distinct membrane domains. For instance, on the absorptive intestinal cells, the apical pole is highly enriched in numerous digestive enzymes and peptides transporters, whereas their basolateral surface contains mainly canals to allow nutrients passage in the blood. Lipid composition also varies in epithelial cells, the epithelial pole being enriched in cholesterol and sphingolipids whereas the basolateral pole is rather composed of phosphatydilcholine (van Meer and Simons, 1988). In addition to the functional discrepancies between the membrane domains, polarity can also be structural as exemplified in the apical pole of absorptive epithelia covered with numerous microscopic membrane extensions: the microvilli. In vertebrates, the apical and basal poles are physically separated by a molecular complex: the tight junctions, or zonula occludens, a type of highly adhesive cell-cell junction essentially impermeable to fluid. In addition, these intimate cell-cell contacts link together the cytoskeleton of adjacent cells. Tight junctions thus guarantee the cohesion of the tissue, ensure the barrier function of tight epithelia and help to maintain cellular polarity. Located in a more basal manner, adherens junctions and desmosomes represent the anchoring junctional complexes. These types

of junctions are important for transmission of mechanical forces along the epithelium; they interconnect cytoskeletal elements of the neighboring cells. Indeed adherens junctions are tethered to apical cortical actin, a belt of actin filaments oriented in a parallel fashion to the apical pole. Desmosomes indirectly link together intermediate filaments from the neighboring cells **(Figure 6)**.

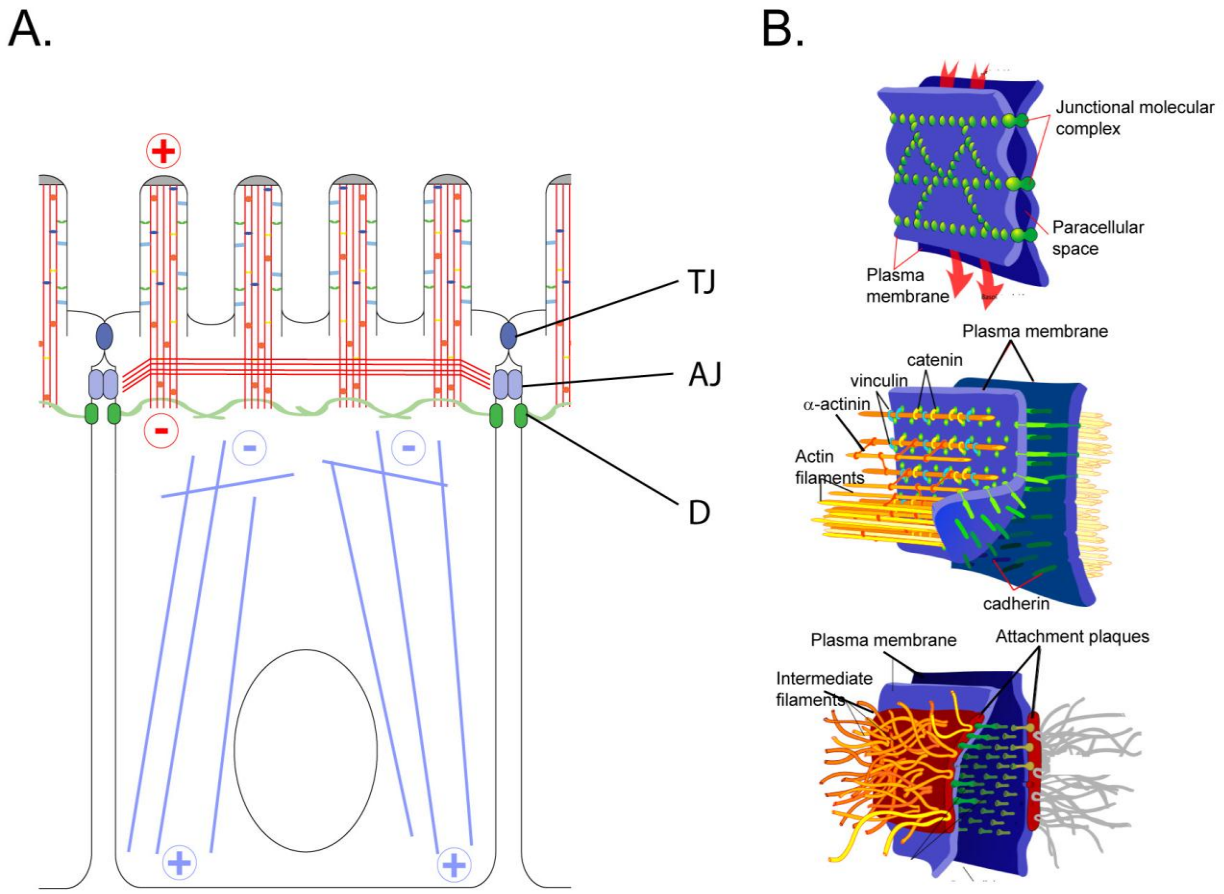

Figure 6: Intracellular organization of an epithelial cell
A. Schematic illustration of the major characteristics of an epithelial cell with a focus on the apical pole. The cytoskeletal elements actin, microtubules and intermediate filaments are depicted in red, light blue and light green, respectively. Polarities of actin filaments and microtubules are indicated. Tight junctions (TJ) seal the epithelium. Note the transversal actin belt emanating from the adherens junctions (AJ). Intermediate filaments are linked to the desmosomes (D). Adapted from Ubelmann et al., 2011. **B.** Detailed organization of the elements of the junctional complexes. From top to bottom: tight junctions, adherens junctions and desmosomes are depicted. Adapted from Wikipedia (http://www.wikipedia.org).

Polarized cells are endowed with the characteristics required to perform the epithelial functions; generation of an appropriate polarity is hence fundamental to epithelia. How polarity is established has fascinated numerous scientists since decades and is still not fully understood. It is however currently established that it requires the concerted action of the cytoskeleton, vesicular sorting, specific lipids synthesis, signaling molecules and polarity complexes.

Organization of polarized trafficking in epithelia.

Establishment of polarity results in an asymmetrical distribution of proteins and lipids on the apical and basolateral domains. This discrepancy is maintained by specific sorting of cargoes at the level of the Golgi apparatus or later on in post-Golgi endocytic compartments. How is polarized trafficking organized in epithelia?

Polarized trafficking includes sorting of proteins towards the apical or the basolateral membranes via vesicular or tubular structures and their final insertion at the membrane of destination by vesicle fusion. Polarized trafficking has been conceptually divided in different routes. In the biosynthetic route, the newly synthesized proteins can be directly delivered to their final destination - apical or basolateral - by early sorting. Alternatively, certain proteins follow an indirect pathway, or transcytosis; in other words, they first reach the basolateral membrane and are subsequently re-addressed to the apical pole, with or without endocytic intermediate. Polarized trafficking also relies for an important part on endocytic routes which allow protein recycling and exchanges between apical and basal poles **(Figure 7)**.

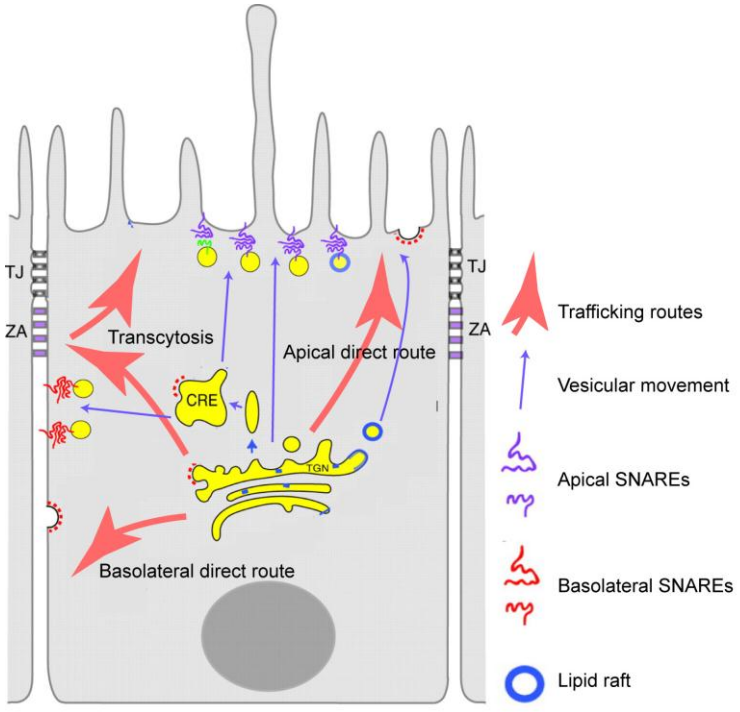

Figure 7: Vesicular trafficking in epithelia
Scheme depicting the main biosynthetic trafficking routes in epithelia. Post-Golgi vesicles are sorted and follow direct routes or transcystosis (red arrows). Vesicles movement is shown in blue arrows. Vesicles either reach directly their destination or traverse endocytic intermediates such as the common recycling endosome – CRE –. Some proteins are sorted apically accordingly to their lipid raft affinity. Fusion at the membrane usually involves SNAREs proteins. Adapted from Weisz and Rodriguez-Boulan, 2009.

The fate of delivery is governed by an important diversity of signals; I will try to summarize the most relevant for epithelial intestinal cells. The sorting machinery recognizes and interacts with these signals, which are generally harbored by the proteins.

Basolateral and apical sorting signals.

Glycosylation and GPI anchoring represent the two most well understood apical targeting determinants. The earliest identified apical sorting signal is certainly the addition of a glycosylphosphatidylinositol – GPI – lipid to a newly synthesized protein as a post-translational modification (Lisanti et al., 1989). Indeed, recombinant addition of a GPI anchor to a normally basolateral destined protein leads to its readdressing at the apical pole (Brown et al., 1989; Lisanti et al., 1989). Glycosylation also plays important role in polarized trafficking: on certain apical proteins, proper insertion of N- and O- glycans are essential for apical targeting (Scheiffele et al., 1995; Yeaman et al., 1997). Nevertheless N- and O- glycosylation of basolateral proteins is also relatively common, indicating that N- and O- linked glycans signals might be recessive relative to basolateral determinants (Rodriguez-Boulan et al., 2005).

The proposal of the existence of lipid rafts represents an important breakthrough in the field of polarized trafficking, as they have been proposed to function as a major sorting platform for apical exocytosis (van Meer and Simons, 1988; Brown and Rose, 1992; Simons and Ikonen, 1997). Albeit still controversial, the lipid raft hypothesis is strongly supported by a whole set of experimental data (Munro, 2003; Rodriguez-Boulan et al., 2005). Lipid rafts are membrane-associated cholesterol- and sphyngomyelin- rich microdomains which are initially assembled in the Golgi complex. They are biochemically defined as membrane resistant to detergent extraction (Brown and Rose, 1992). The lipid raft hypothesis states that raft-dependent proteins are sorted apically due to their affinity for lipid microdomains generated at the Golgi complex. The lipid microdomains and their associated proteins are subsequently delivered to the apical surface through the apical transport machinery **(Figure 7)**. The raft-proteins complex might be further stabilized by lectin proteins while reaching the apical membrane. In particular, galectin 4 has a prominent role in the apical delivery of several raft associated glycoproteins, likely by its virtue to form stable lattices constituted of glycolipids and glycoproteins (Braccia et al., 2003; Stechly et al., 2009).

Critical role of the cytoskeleton and regulators of vesicular trafficking.

Sorting and trafficking involve a coordinated action between the cytoskeleton and organizers of membrane trafficking.

The integrity of microtubule and actin networks is of prime importance to direct intracellular trafficking. For instance, cargoes exit the trans-Golgi network as long tubular structures or vesicles, both of them moving along microtubules (Kreitzer et al., 2003; Polishchuk et al., 2004). Interfering with the microtubule molecular motors dyneins causes a failure for proteins to reach the apical pole (Tai et al., 1999; Noda et al., 2001). This result altogether with dynamic imaging of vesicular movement demonstrate that microtubules are used as tracks for protein delivery (Toomre et al., 1999; Kreitzer et al., 2000). In enterocytes, a selective chemical perturbation of microtubules abrogates apical delivery of membrane proteins. Interestingly, enterocyte apico-basal polarity is also abolished following such treatment (Pavelka et al., 1983; Achler et al., 1989). An intact microtubule network is thus required to establish and maintain the polarity itself; presumably through delivery of polarity determinants. The actin cytoskeleton is also critical at different steps of polarized trafficking. Perturbing actin cytoskeleton generally disrupts proper targeting of basolateral and apical proteins. Actin cytoskeleton reorganization at the Golgi membrane provides the force to allow the budding of vesicular structures (Almeida et al., 2011). F-actin is additionally used as tracks for myosin motors-based movement of vesicular structures as revealed by time-lapse imaging (Jacob et al., 2003). Since the participation of the actin cytoskeleton to apical trafficking in enterocyte is an important part of this study, this specific aspect will be further discussed later on.

Vesicular trafficking is overall coordinated by a large family of small GTPases: the rab proteins. They are critical throughout the whole trafficking pathway, from vesicle budding, to vesicular movement and fusion at the membrane. For instance, rab6 mediates intra-Golgi trafficking (Olkkonen and Stenmark, 1997). Rab8 is another example of rab protein of high importance during polarized trafficking. Rab8 genetic ablation in mouse leads to a global impairment of apical trafficking in intestinal cells. Interestingly, this trafficking failure is coupled with a severe defect in apical membrane functional and structural specialization, providing an additional illustration of the tight interplay between membrane trafficking and polarization (Sato et al., 2007). The case of rab8 furthermore exemplifies the difficulty to define the functions of trafficking regulators among experimental models as it was previously shown to regulate basolateral trafficking in cultured cells from kidney epithelium (Huber et al., 1993).

Following intracellular movement, vesicles fuse at the membrane. An important mediator of this process is represented by the SNARE proteins. SNARE proteins are localized at the vesicle or at the target membrane, and accordingly named v-SNARE or t-SNARE. Interaction between v- and t-SNARE promotes the vesicle docking at the membrane **(Figure 7)**. Specific t-SNAREs are localized at each poles, but both apical and basolateral vesicle fusions involve SNARE proteins (Nejsum and Nelson, 2009).

D. The intestine: a specialized organ

Cellular specialization achieved by polarity is beautifully exemplified in the model we used in this study: the intestine, an organ dedicated to digestion and absorption. These two complementary processes ensure the nutritive function. Following ingestion of aliments, they are reduced – or digested - in simpler elements that can readily be assimilated by the organism after their absorption. Digestion of food is achieved by mechanical and enzymatic processes whereas absorption relies on cellular transport. In most of the animals, the nutritive function is performed in the digestive tract. In mammals, this tract extends from the stomach to the anus. The upper part of the tract is composed of the esophagus and the stomach. The lower part comprehends the small and large intestines.

The stomach fulfills an important part of the digestion by mechanical and enzymatic actions. It mashes the masticated food and secretes abundant quantities of digestive enzymes. The digestive process is further pursued in the small intestine, organ constituted by highly specialized intestinal cells, which harbor and secrete digestive enzymes. The vast majority of intestinal cells is represented by the enterocytes, a cell type specialized in absorption. This cell type absorbs peptides, amino acids and nutrients either passively through diffusion or actively via the expression of channels and transporters. The last part of the lower digestive tract, the colon, allows water re-absorption. Since these tissues are continuously exposed to ingested food, they are often confronted to noxious agents. To avoid deleterious effects to the organism, intestinal cells display a high level of cellular plasticity. In this PhD work, we investigated two important aspects of the biology of the cells that constitutes the intestines: how their functionality is established and how they rapidly adapt in a stress context.

Histo-Anatomical considerations on the large and small intestines.

As an epithelium, the intestinal mucosa separates the organism from the external milieu and ensures the integrity of the organism while performing numerous exchanges with the environment. The two latter processes are achieved by the formation of a virtually impermeable tissue and a spatial segregation of specific functions within the intestinal cell. These properties are characteristic from polarized epithelial cells. The intestine is constituted by a tubular structure covered by a simple polarized columnar mucosal epithelium organized around a lumen. The small intestine is sub-divided in three portions sharing relatively similar anatomical and gross functional properties: the duodenum, jejunum and ileum. Nevertheless, the protein composition slightly differs in these three parts, according to their respective specializations. Epithelial cells from the duodenum are particularly enriched in digestive enzymes. The jejunum is more specialized in absorption of luminal nutrients; jejunal cells express particularly high levels of transporters. Ileum preferentially absorbs vitamins and bile salts and accordingly ileal cells express high level of vitamins transporters.

Histologically, the intestinal tissue, made up of epithelial cells, lays on top of a connective tissue, the lamina propria. An organization around multiple levels of folds is a histological feature characteristic of the intestinal epithelium. The tissue itself is arranged in large folds, which themselves are formed by numerous finger-like extensions of the mucosa called the villi. An obvious advantage conferred by this architecture is the maximization of the surface contact with the lumen, a particularity well adapted to the specialization of this organ **(Figure 8)**. The epithelial tissue is constituted by several cell types which arise from the stem cells and differentiate. A cell compartmentation exists along the villi axis: the differentiated cells lining the villi are luminally exposed whereas the stem cells located at the inter-villi invaginations – the crypts - are relatively hidden and protected **(Figure 8)**. On the other hand, the global organization of the colonic tissue is slightly different as no villi structure exists. Instead the tissue is shaped around larger folds**.**

The intestinal mucosa is a highly dynamic tissue. Indeed the entire epithelium is renewed each three to five days due to the fast and continuous cycling of the stem cells which reside in the crypts. As a result, cells originating from the crypt continuously flow toward the villi. While reaching the crypt/villi frontier, cells engage their differentiation programs. Finally, differentiated cells undergo apoptosis when reaching the tips of the villi and are subsequently expelled in the lumen **(Figure 8)**.

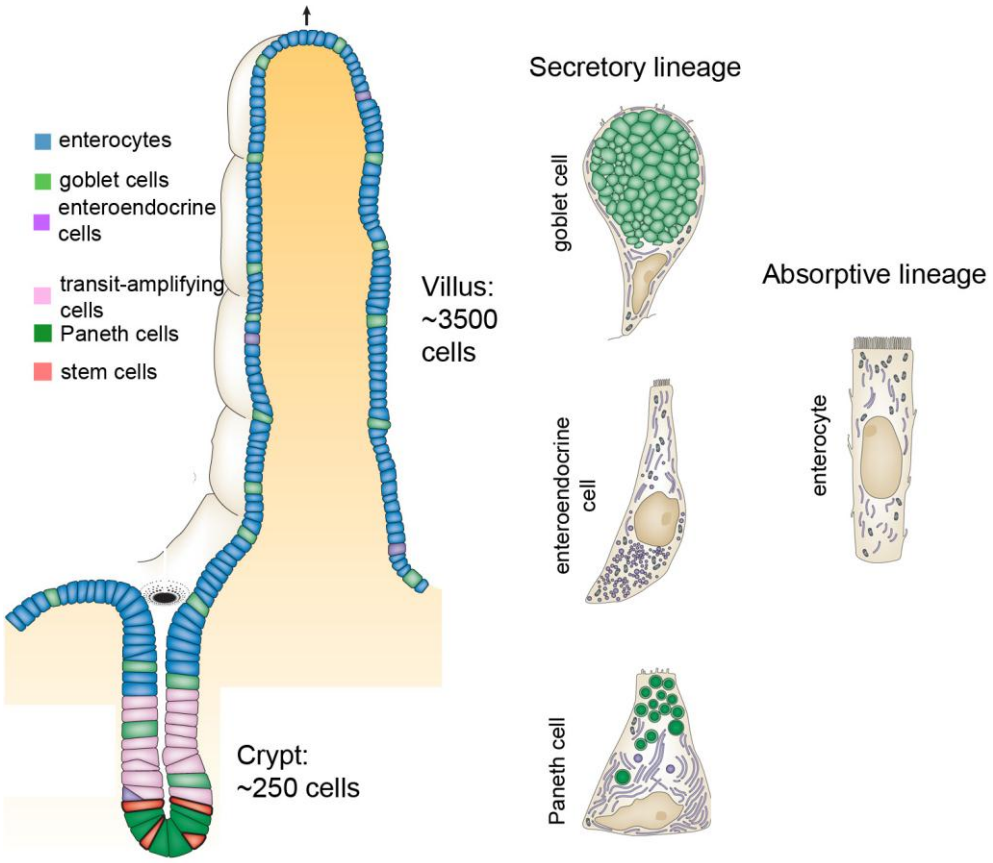

Figure 8: Organization of the intestinal epithelium
Organization of the intestinal epithelium around the crypt-villus axis. Daughter cells arising from the stem cells migrate towards the villus and differentiate into five differentiated cell types belonging to the secretory and absorptive lineages: Paneth cells, enteroendocrine cells, goblet cells, tuft cells (not represented) and enterocytes. Adapted from Crosnier et al., 2006.

The different cell types that constitute the intestinal epithelium

Stem cells: The stem cells, "buried" deeply in the crypts and continuously dividing, ensure the rapid renewal of the epithelium. Their "stemness" property has been assessed by the capacity of their progeny to differentiate into the different cell types and by their ability to retain DNA labeling. Moreover, these stem cells are able to generate organoids *in vitro* that closely resemble the structure of the organ (Sato et al., 2009). Up to now, two populations of stem cells characterized by expression of signatures genes have been identified. The Lgr5 positive stem cells were originally identified by the group of Hans Clevers, and the Bmi1 positive cells in the laboratory of Mario Capecchi (Barker et al., 2007; Sangiorgi and Capecchi, 2008). Lgr5 and Bmi1 cells present different spatial distribution in the crypt: cells positive for Lgr5 lay at the base of the crypts and Bmi1 cells localize in a slightly upper position. A hierarchy between stem

cells populations seems to exist, illustrated by the fact that Bmi1 positive cells might give rise to Lgr5 positive cells. The presence of two pools of potential stem cells could be of high importance to compensate the loss of one population in case of injury (Tian et al., 2011).

The differentiated intestinal cell types: The immediate progeny of the stem cells, the transit-amplifying cells, undergoes a limited round of divisions and, while migrating in the villus, differentiates in two lineages: absorptive and secretory. The lineages are constituted by five types of differentiated cell, identified so far.

The secretory lineage comprises the Paneth cells, the enteroendocrine cells, the goblet cells and the recently characterized tuft cells **(Figure 8)**. As the functions of these cells do not directly relate with this study, only a short description will be provided. The enteroendocrine cells locate in the intestinal villi and secrete various hormones which mostly regulate energy homeostasis. The Goblet cells are also present in villi and secrete mucus that covers the epithelium surface. Mucus provides a physical barrier, adding another level of protection against deleterious luminal agents. The tuft cells are under-represented in intestinal villi. Their exact functions remain less clear as they were recently characterized (Gerbe et al., 2011). They secrete opioids, synthesize prostaglandins and trefoil peptides. Interestingly, trefoil peptides have been shown to be essential for injury repair in the colon (Mashimo et al., 1996). In contrast, the Paneth cells reside in the crypts where they intercalate between stem cells. Functionally, they release several anti-microbial compounds in the lumen. They also participate in generating the appropriate microenvironment – or niche – for stem cells: a set of secreted molecules that ensures stem cells homeostasis.

Finally the absorptive lineage is represented by the enterocytes **(Figure 8)**. Enterocytes are, by far, the most abundant cell type in the intestinal epithelium, representing more than 80% of the total cell population. The enterocyte is a polarized cell highly specialized in absorption, orienting its apical pole towards the lumen. On the apex, the functional specialization is provided by the membrane composition combined with a specific structural organization, which further enhances the efficiency of this epithelium. Indeed the enterocyte apex is covered by an organized array of regular microvilli increasing cell size by 30-40 fold: the brush border (Brown, 1962). Microvilli are highly enriched in numerous digestive enzymes, channels and peptide transporters promoting the absorptive capacity. In human, the brush border covering each intestinal enterocytes consists of around 1700 microvilli measuring 1-2 μm in length and 0.1 μm in diameter (Brown 1962). Each microvillus is supported by 20-30 uniformly polarized actin

filaments organized in a bundle by three actin bundling proteins: villin, espin and plastin-1 **(Figures 6** and **9)** (Bretscher and Weber, 1979, 1980a; Tilney and Mooseker, 1971; Zheng et al., 2000). Brush borders are also found in colonocytes and cells from the kidney proximal tubule.

E. How is the cytoskeleton structuring the brush border organized?

Within microvilli.

Actin represents the major element composing microvilli (Tilney and Mooseker, 1971). In most of the organisms, genome encodes for several actin isoforms, which present only slight variation in their amino acid sequences but, in some case, perform specific functions (Dugina et al., 2009; Perrin and Ervasti, 2010). In *C. elegans*, the actin isoform ACT5 specifically localizes to microvilli and is required for their biogenesis (MacQueen et al., 2005). The mammalian genome encodes three classes of actin isoforms: alpha, beta and gamma (Vandekerckhove and Weber, 1978). Two studies have documented the existence of an actin isoform specific to mammalian microvilli (Sawtell et al., 1988; Hartman et al., 1989); this isoform was however never characterized. In polarized cells in culture, gamma-actin localizes apically whereas beta-actin distributes along the basolateral membrane (Dugina et al., 2009). Nevertheless, mice knocked-out for the gamma-actin gene display normal microvilli (Belyantseva et al., 2009). An eventual specific actin isoform building microvilli thus remains to be identified in mammalian.

The exceptional homogeneity of microvilli implies the existence of numerous actin binding proteins that tightly control actin assembly and organization. Within microvilli, the actin filaments are organized in a bundle, a structure characteristic of finger-like membrane protrusions. In intestinal microvilli, three actin bundling proteins have been identified: villin, espin and plastin-1 **(Figure 9)** (Bartles, 2000). The generated bundle presents a helical arrangement (Ohta et al., 2012). The bundled organization is believed to provide the stiffness required to overcome the membrane resistance (Atilgan et al., 2006; Claessens et al., 2006). Another remarkable feature of the microvilli cytoskeleton is the presence of regular cross-bridges made of myosin-1a and calmodulin, arranged in a spiral, linking the actin bundle to the plasma membrane along the protrusion (Mukherjee and Staehelin, 1971; Mooseker and Tilney, 1975; Matsudaira and Burgess, 1979, 1982a; Howe and Mooseker, 1983; Conzelman and Mooseker, 1987). Myosin-1a-mediated membrane adhesions may avoid coalescence of adjacent

microvilli through generation of membrane tension (Nambiar et al., 2009). In addition, this plus end directed myosin motor may participate in the very late steps of apical trafficking in the microvilli (Tyska and Mooseker, 2004; Tyska et al., 2005). The actin binding protein ezrin may also provide adhesion of the actin bundle to the membrane by virtue of its ability to bind F-actin and plasma membrane (Algrain et al., 1993; Berryman et al., 1993).

In the bundle, the actin filaments are uniformly polarized and present their barbed ends toward the distal part of the microvilli where they associate to the "tip complex", a plaque that appears electron dense when visualized by electron microscopy (Mooseker et al., 1982). Such tip complex structures, where actin polymerization takes place, are widely distributed in actin based membrane protrusions – microvilli, filopodia, stereocilia, bristles - and likely have a key function in the shape regulation of these structures (Mooseker et al., 1982; Svitkina et al., 2003; Tilney et al., 2004; Lin et al., 2005). In particular, recent biophysical experiments propose a prominent role of this complex in converting filaments polymerization rate into efficient membrane deformation (Footer et al., 2007; Brangbour et al., 2011).

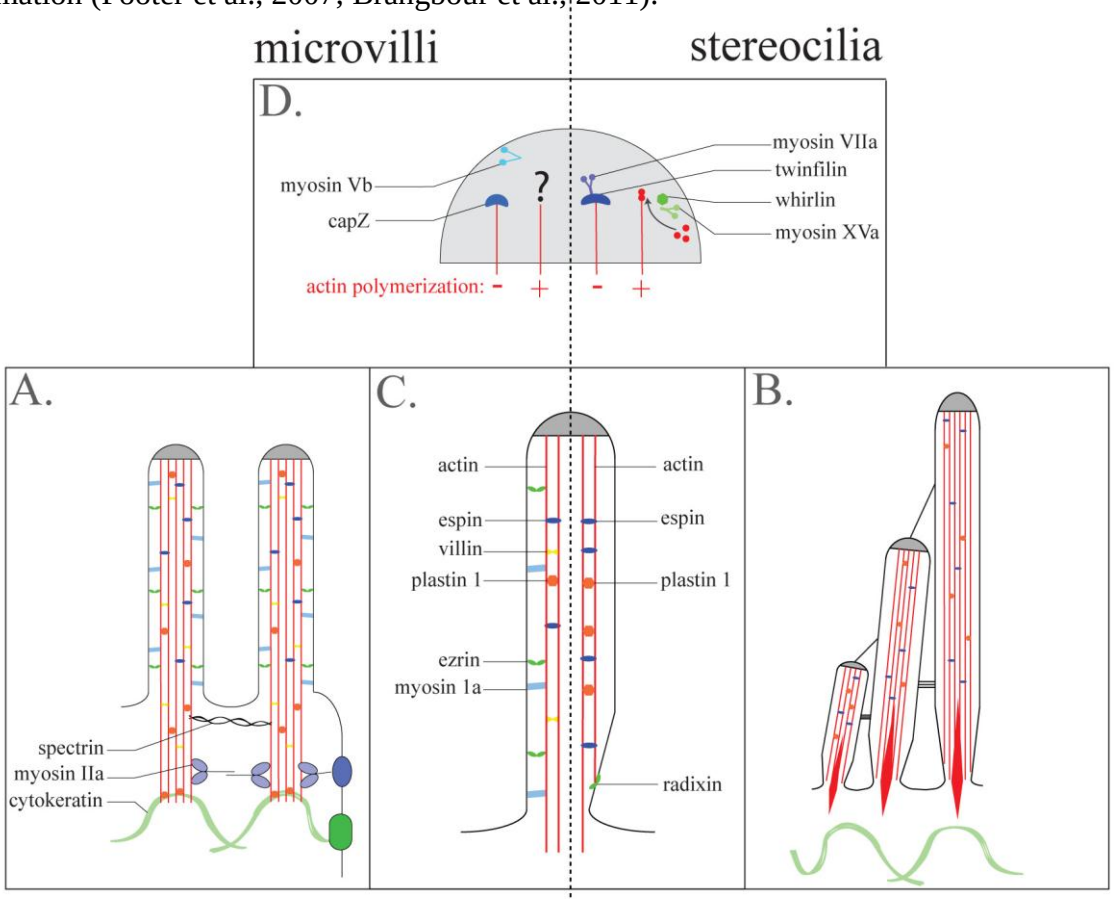

Figure 9: Description of the different molecular components involved in the shape regulation of intestinal microvilli (right) and stereocilia (left).
A, B: General aspect of brush border domains made of (a) microvilli found on intestinal cells apices and (b) stereocilia found on inner ear cells apices. **C:** Different proteins organize the parallel actin bundles that support microvilli and stereocilia structures. **D:** Highlight on the tips of microvilli structures where major regulation of actin polymerization is ensured by protein complexes identified in stereocilia. Such complexes remain to be found on intestinal microvilli.Adapted from Ubelmann et al., 2011

The terminal web.

The actin bundle further extends in a sub-apical zone - the terminal web - where it is referred as the rootlet of the microvillus. The terminal web consists of a dense fibrilar meshwork of intermediate filaments and actomyosin filaments oriented perpendicularly to the actin bundles (Hirokawa and Heuser, 1981; Louvard et al., 1992). Likely due to its density, intracellular organelles are excluded from the terminal web (Overton and Shoup, 1964). The actin bundle within the terminal web is bound to tropomyosins, which span seven actin subunits and therefore stabilize the structure. Rootlets are furthermore interconnected by a network of thin fibrils that comprise two types of filaments. Proteins of the spectrin family, originally identified as TW260/240 in chicken and, later on, termed fodrin in mouse, constitute the most thinner fibrillar structures linking adjacent rootlets (Drenckhahn et al., 1980; Hirokawa et al., 1983a; Pearl et al., 1984). Myosin II, which represents the second population of fibrils, is supposed to act as a long-range cross-linker of rootlets (Drenckhahn et al., 1980; Hirokawa et al., 1982). Myosin II and actin filaments constitute a circumferential belt that crosses the terminal web and emanates from the adherens junctional complex **(Figures 6** and **9)** (Drenckhahn and Dermietzel, 1988). This actomyosin ring endows the enterocyte with a contractile ability. Contraction – experimentally induced by ATP addition, for instance - causes microvilli to vesiculate and spread apart; thus providing a first hint of the physical cohesion between microvilli and the terminal web (Mooseker, 1976; Hirokawa et al., 1983b). Located more basally, intermediate filaments attached to the desmosomes are mainly constituted by cytokeratins types 8, 19, and the gastro-intestinal epithelium specific isoform 20 **(Figures 6** and **9)** (Moll et al., 1990; Quaroni et al., 1991). Interestingly their relative abundance depends on the differentiation status of the enterocytes (Quaroni et al., 1991).

The importance of the terminal web to shape the apical pole is highlighted by phenotypic observations resulting from diverse knockout approaches. Genetic loss of an intermediate filament protein – keratin 8 in mouse - or an IF organizer – IFO1 in *Caenorhabditis elegans* – result in a similar phenotype: shorter microvilli (Salas et al., 1997; Ameen et al., 2001; Carberry et al., 2012). These results show the implication of the intermediate filament network of the terminal web in the proper assembly of the apical pole. This implication is likely structural as loss of keratin filaments attachment to desmosome observed in desmoplakin knockout mice shortens microvilli as well (Sumigray and Lechler, 2012) This possibility is additionally supported by a physical interaction between plastin-1 and keratin 19 that could possibly provide an anchorage of the microvilli cytoskeleton into the terminal web. Consequently, plastin-1

genetic ablation results in a defective terminal web lacking its typical components (Grimm-Günter et al., 2009). Moreover, microvilli in absence of plastin-1 are shorter (Grimm-Günter et al., 2009). Altogether these results bring to light the cohesion conferred to the apex by the interplay between the microvilli actin bundle and the underlying terminal web. This dense intertwining between the different cytoskeletal elements has been most impressively visualized by quick freeze deep etch electron microscopy (Hirokawa and Heuser, 1981; Hirokawa et al., 1982).

How to traffic into microvilli?

Microvilli are structures of high hindrance and simultaneously highly enriched in specific proteins suited for their function. How the late steps of apical trafficking are organized in these crowded structures?

En route to the microvilli, trafficking vesicles encounter a first obstacle represented by the dense meshwork of the terminal web. Ultra-structural observations of the terminal web revealed the presence of vesicular structures linked to the microvilli rootlets, leading to the proposition that they could serve as "tracks" for the final delivery of apical proteins (Hirokawa et al., 1983a; Pearl et al., 1984). Owing to its motor activity, a myosin could power the movement of vesicles towards the microvillus allowing vesicles fusion at the membrane (Apodaca, 2001; Tyska and Mooseker, 2004). This hypothesis is strengthened by mislocalization of several microvillar digestive enzymes observed in presence of a non-functional myosin-1a (Tyska and Mooseker, 2004; Tyska et al., 2005). This myosin has also been detected on the outer membrane of the terminal web associated vesicles (Drenckhahn and Dermietzel, 1988; Fath and Burgess, 1993; Jacob et al., 2003). In addition, myosin-1a generates sufficient force to induce a plus end-directed translation of apical membrane along the actin bundle (McConnell and Tyska, 2007). However, a rootlet-mediated delivery of apical vesicles has been questioned as in polarized human intestinal cells, a GFP-myosin-1a construct does not label any moving vesicle (Tyska and Mooseker, 2004). In addition, the rootlets are coated with tropomyosins (Bretscher and Weber, 1978), which inhibit activity of myosin-1a (Fanning et al., 1994) and other class I myosins (Tang and Ostap, 2001). The presence of another motor: myosin VI could be detected in the terminal web (Heintzelman et al., 1994). Myosin VI, as a minus end directed motor, is rather involved in endocytosis events at the brush border, considering the microfilaments polarity (Ameen and Apodaca, 2007).

Alternatively, contraction of the actomyosin ring could power vesicle advance through the terminal web. In fact, this possibility has been proposed during the rapid microvilli insertion of the GLUT2 glucose transporter following glucose intake (Mace et al., 2007).

The composition itself of intestinal microvilli, particularly enriched in lipid raft, facilitates the proper insertion of digestive enzymes, as a majority of them are raft associated and glycosylated (Danielsen, 1995). Following their insertion into microvilli, apical proteins are confronted to opposing flows: endocytosis and actin treadmilling. Constitutive endocytosis, even though at a mild rate, occurs in microvilli (Hansen et al., 2009). Nevertheless, digestive enzymes, as determined for sucrase-isomaltase and dipeptidyl peptidase-4, show very slow rate of endocytosis and are excluded from the constitutive basal endocytosis (Matter et al., 1990; Klumperman et al., 1991; Hansen et al., 2009). The constant actin retrograde flow, due to treadmilling, also impedes stability of proteins linked to the microvillar bundle. Therefore, stable molecular scaffolds should exist to increase microvilli residence time of apical proteins. Myosin-1a has been proposed to stabilize lipid raft associated proteins in microvilli through its ability to link membrane to the cytoskeleton (Tyska and Mooseker, 2004; Tyska et al., 2005). A similar role has been described for the PDZ domain containing proteins NHERF1/2 that act as scaffolds to organize macromolecular complexes containing the exchanger Na+/H+ NHE3 to limit its lateral diffusion at the plasma membrane (Cha et al., 2004) despite their high dynamic state (Garbett and Bretscher, 2012).

Brush border biogenesis during adult lifehood and development.

Due to the dynamic nature of the intestine epithelium, enterocytes emerging from the crypts generate a brush border structure while differentiating. The non-differentiated crypt cells exhibit a poorly organized brush border containing short microvilli. As cells differentiate along the crypt villus axis, microvilli number and length increase to reach a normal mature brush border organization on fully differentiated cells (Fath et al., 1990).

To better describe how the brush border is structured, it is interesting to refer to the biogenesis of the brush border during intestine development, which has been well documented on chicken embryo. In particular, the associated changes in morphology, protein expression and localization could be precisely determined. From day 5 to day 10, some irregularly shaped membrane protrusions containing a filamentous meshwork expand from the apical pole. Villin

apically concentrates around day 8, rapidly followed – one day later - by an increase in membrane projections number and homogeneity (Shibayama et al., 1987). Interestingly, the latter observation correlates with the progressive elaboration of an aligned organization of the microfilaments, while plastin concentrates at the apex. Complete alignment of the actin filaments within each microvillus is achieved at day 11 (Overton and Shoup, 1964). Nevertheless, the microvilli lack an overall organization in a brush border. At this stage the electron dense tip is distinguishable (Chambers and Grey, 1979). Prior to hatching, the brush border acquires its final organization characterized by a perfectly parallel array of microvilli. Then, microvilli undergo a process of lengthening that persists until one week post-hatching when microvilli reach their final length **(Figure 10)** (Stidwill and Burgess, 1986). Myosin-1a localizes apically during hatching concomitantly to a decrease in diameter of the actin bundle, likely indicating that the myosin cross-bridges are critical for proper actin bundle organization **(Figure 10)** (Overton and Shoup, 1964; Shibayama et al., 1987). This apical localization is also concomitant to the differentiation of the apical membrane, suggesting a possible role for this myosin in trafficking, as discussed earlier (Shibayama et al., 1987).

Therefore, actin bundling proteins sequentially accumulate in the maturing microvilli **(Figure 10)**: villin first localizes to the nascent poorly organized microvilli, followed by T-plastin (Shibayama et al., 1987; Chafel et al., 1995). This transiently expressed isoform is replaced by the microvillar isoform plastin-1 few days later (Chafel et al., 1995). Espin concentrates apically later on during development, on a largely organized core bundle, and has been proposed to "lock" the actin organization (Bartles et al., 1998).

Terminal web elaboration during development.

The rootlets structures start to be detected by day 10 during chicken development. At day 13, only short filaments made of spectrin and myosin II interconnecting the rootlets are observed in the terminal web region, whereas the meshwork of intermediate filaments appears well developed (Takemura et al., 1988). The network of inter-rootlets filaments evolves to become denser and reaches an almost mature organization by day 21. The last morphological event occurs at day 3 post-hatching and consists on the stratification of the different cytoskeletal networks. Then, the terminal web shows its mature organization: located more apically, the actomyosin belt links the adherens junctions, whereas, located below, the meshwork of intermediate filaments connects the desmosomes.

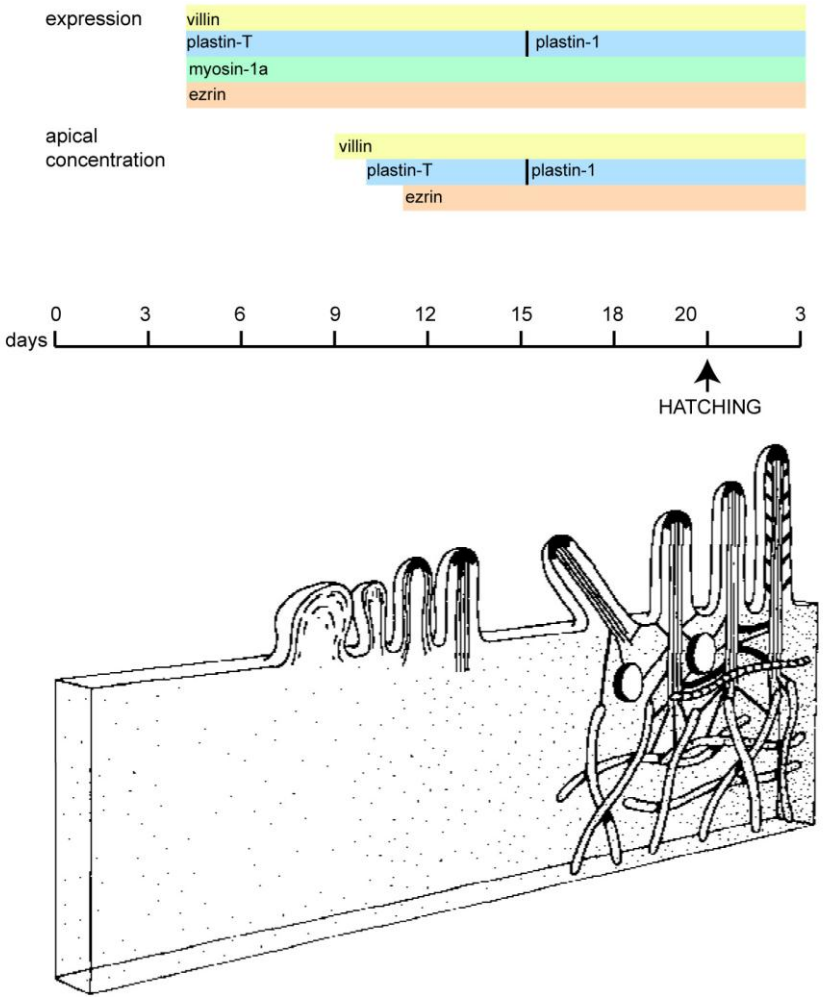

Figure 10: Brush border morphogenesis during embryo development
A. Diagram recapitulating the apical localization of different microvillar proteins during the brush border development in chicken. **B.** Drawing depicting the structural changes associated with microvilli development. Adapted from Louvard et al., 1992.

How microvilli are initiated?

The extensive description of brush border morphogenesis is insufficient to identify which upstream signaling factors induce microvilli biogenesis. Few molecules controlling the very initial steps of microvilli biogenesis have been documented. The Lkb1 kinase – the mammalian homolog of the polarity regulator Par4 from *Drosophila* and *C. elegans* – seems to play a major role. Indeed, experimental Lkb1 activation results in brush border formation in a single epithelial cell from intestinal origin. Moreover apical and basolateral proteins are well localized in this single cell, indicating a full polarization, even in absence of cell-cell contact (Baas et al., 2004). This microvilli biogenesis has been linked to ezrin phosphorylation by a downstream effector of the Lkb1 pathway (ten Klooster et al., 2009). Indeed, in cell culture ezrin phosphorylation

induces formation of tufts of microvilli (Bretscher, 1989; Gautreau et al., 2000) whereas its inactivation leads to microvilli breakdown (Kondo 2000). *In vivo*, the situation is more complicated as absence of ezrin in the mouse severely affects shape of microvilli but does not abrogate their biogenesis (Saotome et al., 2004; Casaletto et al., 2011).

How does actin initiate and shape microvilli?

The actin machinery that initiates microvillus protrusion is still not completely elucidated. It is interesting to refer to an early work, which documents the different steps of microvilli re-assembly following their disruption by hydrostatic pressure (Tilney and Cardell, 1970). After pressure relapse, Tilney and Cardell observed foci of electron dense material at the flattened apical surface. From these foci, nascent filaments arise correlating with extension of newly formed microvilli, thus strongly suggesting that these electron-dense structures nucleate actin filaments to control microvillus growth (Tilney and Cardell, 1970). This tip complex should play prominent role in microvilli shaping and initiation. Whereas the molecular composition of the tip complex has reached an advanced stage in stereocilia or filopodia, it remains quite obscure in microvilli. It is thus informative to compare experimental data obtained in these different systems **(Figure 9)**.

Actin polymerization is spatially restricted at the microvilli tips (Mooseker et al., 1982; Stidwill et al., 1984). This result has been confirmed by FRAP experiments showing that monomer addition occurs exclusively at the microvilli tips (Tyska and Mooseker, 2002) inducing a treadmilling process along the structure. Such actin cycling along the protrusion shaft is observed in microvilli (Tyska and Mooseker, 2002) and filopodia (Mallavarapu and Mitchison, 1999) but remains controversial in sterocilia (Schneider et al., 2002; Zhang et al., 2012). In the case of microvilli, their length remains constant despite a continuous actin polymerization at the tip complex. This observation implies the existence of a precise equilibrium, arising from regulation between polymerization at the tip and depolymerization at the rootlets. The actin depolymerization rate is directly affected by the composition in actin bundling proteins, as over-expression of espin results in a slower depolymerization rate of microvilli (Loomis et al., 2003; Lenz et al., 2010). The disassembly rate nevertheless appears not to be dynamically regulated. Indeed, in filopodia neuronal growth cone, the length of the membrane protrusions is dictated by the actin assembly rate, which varies accordingly to the filopodium extension and retraction whereas actin disassembly stays relatively constant (Mallavarapu and Mitchison, 1999). The rate

of actin polymerization reflects the concentration of free actin monomers available for polymerization (Pollard and Mooseker, 1981; Mooseker et al., 1982). In line with this idea, microvilli lengthening during development associates with a reversible increase in G-actin concentration that shifts back when elongation is complete (Stidwill and Burgess, 1986). The capping protein CapZ, present in the tip complex of microvilli caps growing ends and thus might be a critical regulator of actin monomer concentration **(Figure 9)** (Schafer et al., 1992). Antagonistic interplay between cappers and proteins from the Ena/VASP family may additionally finely tune microvilli length, as already described for filopodia (Bear et al., 2002; Schirenbeck et al., 2005).

Owing to their staircase organization, stereocilia represent the perfect system to study how the cell counts and measures. In fact, several protein complexes regulating stereocilia length have been identified. They all reside in the electron dense tip **(Figure 9)**. A tip concentration of the capping protein twinfilin-2 has been reported in the shorter row of stereocilia only (Peng et al., 2009). Interaction of twinfilin-2 with myosin IIIa is essential for its proper localization (Rzadzinska et al., 2009). A second complex composed of myosin XVa and whirlin has been detected on stereocilia tips, independently of their length (Rzadzinska et al., 2009). The function of this complex remains unclear, but lack of either one or the other component results in very short stereocilia without disturbing the staircase organization (Probst et al., 1998; Mburu et al., 2003). In summary, the myosin XVa/whirlin complex promotes actin assembly, whereas myosinIIIa/twinfilin-2 inhibits it. The interplay between these determinants likely determines the length gradation of stereocilia organization. In microvilli, similar regulatory molecular complexes, if existing, remain to be identified. In filopodia a myosin motor also concentrates at the growing extremities: myosin X (Berg and Cheney, 2002). Its overexpression increases filopodia numbers and length (Berg and Cheney, 2002). Myosin X transports Mena/VASP, a protein from the Ena/VASP family, at the filopodia tips and in turn favors elongation (Tokuo and Ikebe, 2004). The examples of filopodia and stereocilia underline the importance of specific myosin motors to direct actin regulatory complexes at the tip. In microvilli, myosin VIIa and Vb display a distal localization (Heintzelman et al., 1994; Wolfrum et al., 1998). A class I myosin, myosin 1d was recently been shown to localize to the terminal web and to discrete punctae at the microvilli tips (Benesh et al., 2010). Their contribution during elongation has still to be explored in microvilli.

A set of proteins from the eps8 family is also detected at the microvilli and filopodia tips (Croce et al., 2004; Zwaenepoel et al., 2012). Eps8 proteins cap and weakly bundle actin

filaments (Disanza et al., 2004, 2006; Hertzog et al., 2010). In *C. elegans* loss of eps8 results in longer microvilli, a result typical of loss of a capping protein (Croce et al., 2004). In the mouse, the situation becomes more complex as knocking out eps8 induces shorter microvilli (Tocchetti et al., 2010). This result might be explained by the existence in mammals of several eps8 isoforms, which show distinct properties towards actin dynamics (Zwaenepoel et al., 2012). Indeed, in association with ezrin and depending of its isoform, eps8 proteins have been shown to finely tune microvilli length by distinct capping and weak bundling activities (Hertzog et al., 2010; Zwaenepoel et al., 2012).

The actin organization conferred by actin binding proteins also critically shapes membrane protrusions. As seen in the general introduction, actin filaments supporting membrane protrusions are indeed constantly associated with several actin bundling proteins. It is widely accepted that these structural proteins provide the stiffness required for the actin network to overcome membrane resistance thereby allowing extension and maintenance of a straight protrusion.

Objectives

During the course of this study, I became interested in two complementary aspects of the role of the actin cytoskeleton supporting intestinal microvilli: the importance of the bundled architecture to microvillus biology and the events of microvillar actin reoganization that associate with cell migration. These two projects were unequally advanced when I joined the lab.

In the first part of this PhD work, we wondered to which extent the actin bundling proteins contribute to microvilli morphogenesis and functionality. The role of the microvillar actin bundling proteins has been a long-standing question in our laboratory as well as in some others. Their function is thought to be only structural: to endow the actin filaments with an organization allowing the membrane to protrude. To answer this question, our laboratory used a general mouse knockout approach to generate mice lacking the three microvillar actin bundling proteins. Indeed, the question of a possible compensation came naturally as it was already known that none of these proteins is individually required to enable microvilli protrusions (Ferrary et al., 1999; Grimm-Günter et al., 2009). At the time of my arrival, the mice were already obtained and the extensive electron microscopy analysis of the intestinal mucosa had already been accomplished. The investigations that I pursued on these animals allowed us to draw our major conclusions that are detailed in the next section.

The second aspect, which was in fact initially the main project of my PhD, consisted of investigating microvilli reorganization during cell migration. It is assumed that microvilli disassemble at the onset of cell migration, even though dynamic data is lacking (Nusrat et al., 1992; Albers et al., 1995). The aim was to obtain dynamic insights of this event to understand which mechanisms control it and to determine if it has any physiological relevance in the animal. Our working hypothesis postulates that villin severs microvillar F-actin leading to the collapse of the microvilli upon epithelial cell migration. This idea is not completely new as it has been suggested since several years in different reports (Glenney et al., 1981c; Nusrat et al., 1992; Albers et al., 1995; Ferrary et al., 1999), but has never been experimentally demonstrated. When I took charge of the project, the animal models were being generated at the transgenesis platform. These models allowed me to follow an *in vivo* approach that I could complement with cell culture experiments.

I/ An unexpected role for the actin architecture in retention of membrane proteins in microvilli

A. Actin bundling proteins and morphogenesis of actin-based protrusions

The three actin bundling proteins of microvilli

Microvilli concentrate three actin bundling proteins: villin is a 95 kDa actin binding protein mainly expressed in the absorptive cells of the intestine, colon and in the kidney proximal tubule (Bretscher and Weber, 1979, 1980b; Robine et al., 1985). In these polarized epithelia, villin localizes in the brush border (Bretscher and Weber, 1979; Matsudaira and Burgess, 1979) where it represents the most abundant microvillar protein, besides actin (Bretscher and Weber, 1979). Villin belongs to the gelsolin protein family and is organized around six repetitions of a conserved domain shared by all members of this family (Arpin et al., 1988). In addition, villin displays an extra carboxy terminal domain: the headpiece (Arpin et al., 1988). *In vitro*, villin bundles, caps, nucleates and severs actin filaments in a calcium dependent manner (Bretscher and Weber, 1980b; Glenney and Weber, 1981; Glenney et al., 1981a). Between the two first repetitions of the modulus, a calcium dependent actin binding domain has been identified (de Arruda et al., 1992). This site is responsible for villin-mediated actin severing (Matsudaira et al., 1985; Janmey and Matsudaira, 1988). A second F-actin binding site in the headpiece endows it with bundling property (Glenney et al., 1981a). Bundling involves a conserved motif of 4 charged amino acids – KKEK – crucial for actin binding and bundling (Friederich et al., 1992). Villin binding to F-actin seems to be governed by its phosphorylation status (Zhai et al., 2001, 2002). A dimerization site, located near the amino terminal sequence, was recently reported to account for villin bundling activity (George et al., 2007). Nevertheless, a 3D structure model of villin bound to F-actin determined by electron microscopy tomography is incompatible with a dimerization of the protein (Hampton et al., 2008), suggesting that the reported villin dimerization is artefactual.

Plastin-1, formerly I-fimbrin, is a 68 kDa actin bundling protein localized on microvilli, membrane ruffles and stereocilia (Matsudaira and Burgess, 1979; Bretscher and Weber, 1980a;

Bretscher, 1981). Three plastin isoforms exist and the isoform 1 has an expression pattern similar to villin (Lin et al., 1994). Plastin-1 belongs to the calponin homology (CH) domain family of actin binding proteins. Plastin-1 exhibits one N-terminal calcium binding domain and a repetition of two CH domains, each of them represents an F-actin binding domain (Revenu et al., 2004). Thus, plastin-1 is a monomeric actin bundling protein which organizes F-actin into tight bundles in a calcium dependent manner (Glenney et al., 1981b).

Espin is the third identified microvillar actin bundling protein. In intestinal tissue, alternate splicing produces a smaller espin weighing around 30 kDa (Bartles et al., 1998). In microvilli, espin appears to be 10-20 fold less abundant than villin and plastin-1 (Bartles et al., 1998). Espin is additionally expressed in kidney proximal tubule and is the major actin bundling protein of stereocilia (Zheng et al., 2000). On the contrary to vilin and plastin-1, espin bundling property is insensitive to calcium concentration. By sequence comparison with long espin and deletion mutagenesis a minimal region of 116 amino acids appears to be sufficient to bundle actin. At least two actin binding domains are presumably present in this region as espin bundles actin in a monomeric state (Bartles et al., 1998).

Due to their structural diversities, the different bundlers design F-actin networks of different mechanical properties (Claessens et al., 2006; Shin et al., 2009). For instance, espin produces identical bundles regardless of espin-actin ratio, thereby possibly facilitating reproducible mechanotransduction of sound along the stereocilium (Shin et al., 2009). In contrast, the structure of fascin-bundled networks is sensitive to the actin-fascin ratio, a property that could be particularly suited for the dynamic filopodia (Shin et al., 2009). Cooperation between actin bundling proteins is illustrated in the case of the bristles in which forked and fascin sequentially localize to drive the transition from a loosely to a highly organized actin network (Tilney et al., 1995). Thus cooperation between the bundlers might finely tunes the actin network to generate a framework adapted to the specific functions of the different protrusions.

Actin bundling proteins: essential players in protrusions morphogenesis?

Considering their ubiquitous presence in actin-based protrusions and their accepted role in building actin frameworks, actin bundling proteins should play major role during protrusion morphogenesis. Accordingly, fascin depletion results in a drastic decrease of filopodia number and the remaining ones are short and bent, running nearly parallel to the membrane (Vignjevic et

al., 2006). Conversely, overexpression of fascin or transfection of a constitutively active mutant produces numerous long filopodia (Yamashiro et al., 1998). In *Drosophila melanogaster*, mutants lacking forked or fascin present severe defects of bristles morphogenesis (Tilney et al., 1998). Jerker mice harbor a frameshift mutation in the espin C-terminal region that affects the stability of the protein leading to virtually espin null animals (Grüneberg et al., 1941; Zheng et al., 2000). In these mice, the absence of espin destabilizes sterocilia and ultimately causes their degeneration (Zheng et al., 2000).

Concerning microvilli, espin transfection in the epithelial cell line LLC-PK1, from kidney proximal tubule origin, results in a dramatic lengthening of existing microvilli (Loomis et al., 2003). Over-expression of T-plastin in the same cell line causes a mild increase in microvilli density and length (Arpin et al., 1994). The morphogenetic effect of intestinal isoform plastin-1 has not been investigated yet. Villin role in microvilli morphogenesis could be analyzed by a knock down approach. A cDNA encoding a villin antisense RNA was used to obtain a selected clone from the colonic transformed cell line Caco-2 resulting in a major down-regulation of the protein. Following polarization, only few dispersed microvilli lacking an organized actin core could be detected, in contrast to the well-developed brush border of original Caco-2 cells (Costa de Beauregard et al., 1995). Microinjection of purified villin in fibloblastic NIH-3T3 cells inversely results in the growth of surface microvilli and redistribution of F-actin from the stress fibers towards the apical pole (Franck et al., 1990). Villin ectopic expression in the fibroblastic cell line CV1 induces similar results. Moreover, this morphogenetic effect requires the presence of the conserved KKEK motif, suggesting that the actin bundling property is critical for microvilli morphogenesis (Friederich et al., 1992). In addition, preventing actin polymerization by treatment with cytochalasin D reverts the microvilli induction by villin (Friederich et al., 1993). From these different results actin bundling proteins contribution appears to be critical in the establishment of microvilli. This expectation is further reinforced by the sequential apical accumulation of the microvillar actin bundling proteins which correlates with precise morphological changes during development. To clarify the precise contributions *in vivo* of each actin bundling protein during apex morphological design, a set of single knockout mouse models was generated and characterized.

In light of the particularly detailed results concerning villin function in cell culture and its early localization during brush border development, villin appears to be the principal candidate to regulate microvilli morphogenesis and biogenesis. To confirm villin role *in vivo*, two teams independently generated villin null ($V^{-/-}$) mouse models. Surprisingly, these mice are perfectly

viable and fertile. Extensive characterization of their intestinal and colonic microvilli by electron microscopy does not reveal any defect neither in their morphology nor in their organization into a brush border **(Figure 11)** (Pinson et al., 1998; Ferrary et al., 1999). Only minor ultra-structural disorganization of the F-actin core is detected in transversal section of microvilli (Pinson et al., 1998). Further physiological experiments indicate that lack of villin does not affect absorption of water, salts and glucose (Athman et al., 2002). In contrast to its proposed role in cell culture, villin is thus dispensable for proper microvilli morphogenesis and function *in vivo*.

Jerker mice ($E^{-/-}$) that harbor a spontaneous autosomal recessive mutation located on the espin C-terminal region present normal espin mRNA level, but do not accumulate espin proteins, neither long espin nor the microvillar small espin (Grüneberg et al., 1941; Zheng et al., 2000). These mice are deaf, hyperactive and move erratically as a result of inner ear stereocilia degeneration. In collaboration with J. Bartles, the group of Sylvie Robine carefully analyzed the ultrastructure of intestinal cells from espin null mice: in absence of espin, no morphological defect is detected in intestinal brush border **(Figure 11)**.

Finally, mice devoid of plastin-1 ($P^{-/-}$) do not present any overt phenotype. Only minor ultra-structural defects of the enterocyte apical pole is reported (Grimm-Günter et al., 2009). Microvilli size is slightly reduced when compared to wild type animals **(Figure 11)**. On microvilli transversal sections, the actin filaments organization appears less precise. More strikingly, rootlet structures are lacking, correlating with more profound defects of the terminal web: myosin II, spectrin and tropomyosin are absent from the sub-apical structure, which is nonfunctional. Nevertheless, polarity is maintained and microvilli extend straight and organize into a regular brush border.

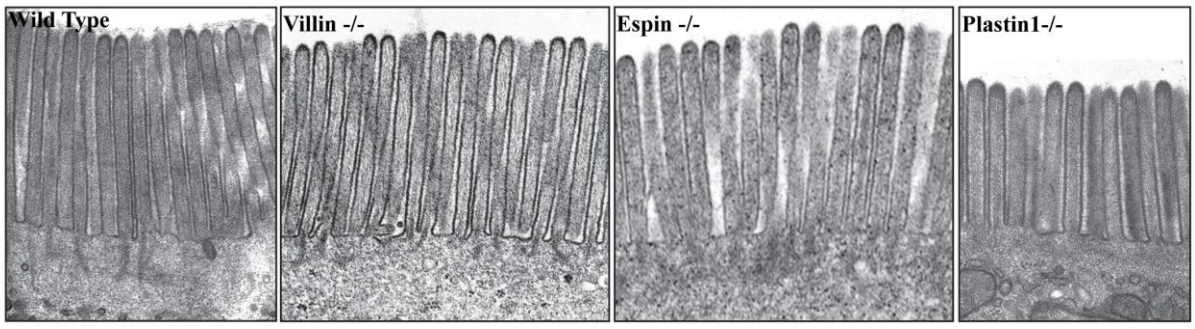

Figure 11: Brush border morphology in absence of the major microvillar proteins
Villin$^{-/-}$ and espin$^{-/-}$ microvilli do not present any morphological defect as compared to wild type microvilli. Plastin 1$^{-/-}$ microvilli are shorter; note the absence of rootlets. Adapted from Ubelmann et al., 2011.

These results demonstrate that none of the actin bundling protein is individually required for microvilli biogenesis and brush border organization. To explain this lack of strong phenotype the loss of one bundler could be compensated by the other actin bundling proteins. Detailed analysis of the microvillar protein content of $V^{-/-}$ and $P^{-/-}$ mice could not reveal any change of expression level of the remaining actin bundling proteins (Ferrary et al., 1999; Grimm-Günter et al., 2009). It is nevertheless conceivable that their basal expression level is sufficient to rescue the loss of one bundler. To address this question, intercross of the different mouse models presented above were performed in order to characterize mice lacking the three microvillar actin bundling proteins.

B. Results

Villin/espin/plastin-1 triple KO mice show growth defects.

To investigate redundancy among the three actin-bundling proteins of enterocytic microvilli — villin, plastin-1 and espin — the corresponding single KO were crossed before I joined the lab (Ferrary et al., 1999; Zheng et al., 2000; Grimm-Günter et al., 2009) to obtain all four possible combinations: villin/espin, villin/plastin-1, and espin/plastin-1 double KO mice ($VE^{-/-}$, $VP^{-/-}$, and $EP^{-/-}$ mice, respectively) and villin/espin/plastin-1 ($VEP^{-/-}$) triple KO mice. All these mice are viable and fertile. The double KO animals appear normal with the exception of mice lacking espin, which have behavioral defects, as described previously (Grüneberg et al., 1941). The VEP−/− mice demonstrated a smaller body size compared with wild-type (WT) animals **(Figure 12A)**. VEP−/− mice consistently showed a statistically significant growth delay during their first 60 days of life for both males and females compared with their triple heterozygote ($VEP^{+/-}$) half-sibling and double KO $VP^{-/-}$ controls. No significant difference in the growth of $VEP^{+/-}$ and $VP^{-/-}$ mice was found **(Figure 12B)**. The growth delay of $VEP^{-/-}$ mice became more pronounced at ∼20–25 days, which corresponds to the weaning period **(Figure 12B)**. Thus $VEP^{-/-}$ mice suffer from growth retardation for the duration of their first 60 days of growth.

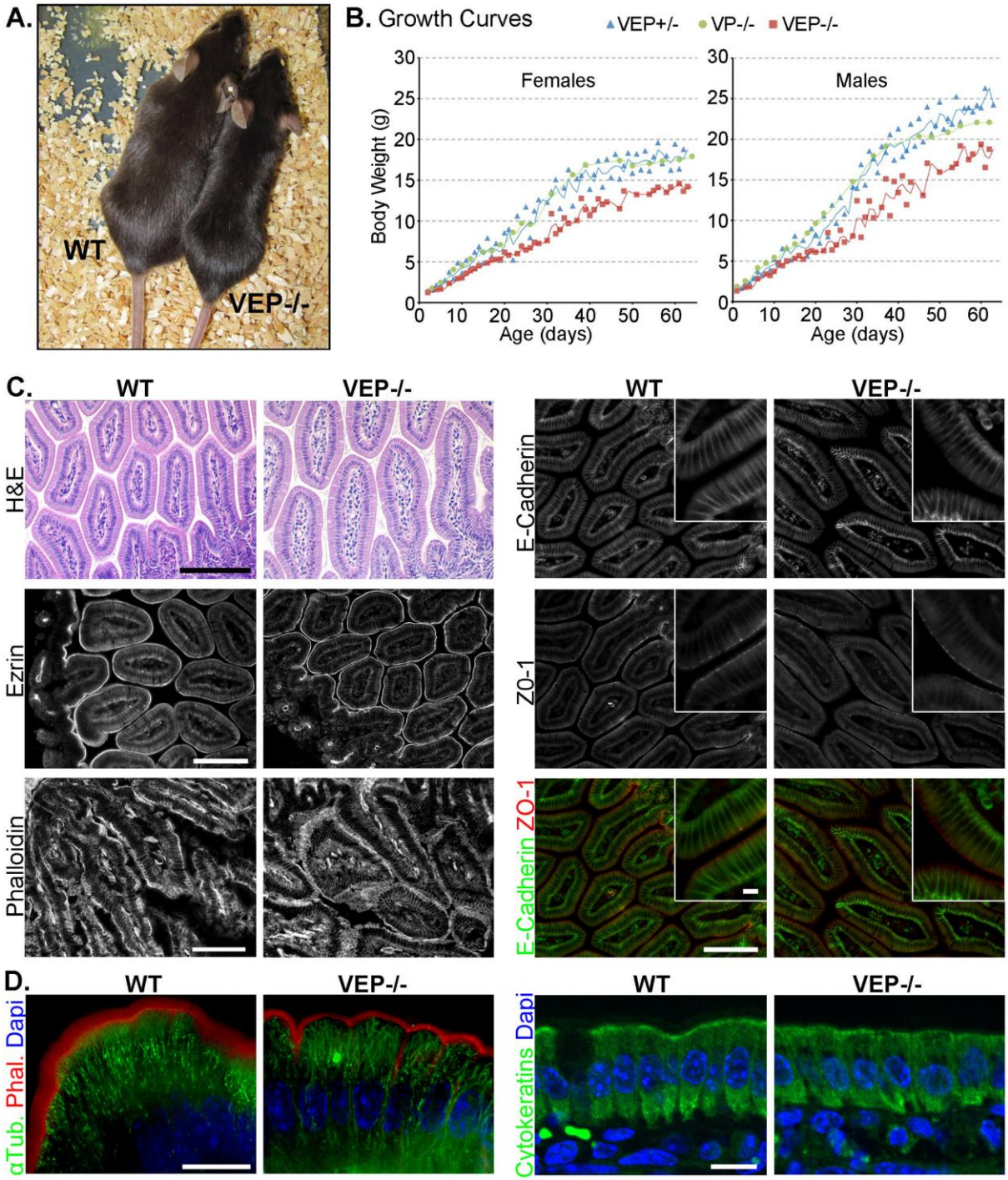

Figure 12: The VEP$^{-/-}$ mice have growth defects, but the morphology of their intestinal epithelium looks normal.

A. Picture of a triple KO VEP$^{-/-}$ animal next to a WT animal of the same age. **B.** Growth curves plotting the average weight of 35 triple heterozygotes (VEP$^{+/-}$), 16 villin/plastin-1 double KO (VP$^{-/-}$), and 35 triple KO (VEP$^{-/-}$) mice according to their age. Males and females were analyzed separately. **C** and **D.** Histological sections of jejunum from WT and triple KO (VEP$^{-/-}$) animals. **C.** H&E shows a hematoxilin and eosin staining (scale bar: 200 μm), phalloidin labels F-actin (scale bar: 100 μm). Immunostaining for ezrin, E-cadherin, and ZO-1 is shown. Scale bars: 100 μm; insets: 10 μm. **D.** The global cellular organization of the cytoskeletal elements is presented. Microtubules and F-actin are revealed by immunostaining against α-tubulin (α-Tub., green) and phalloidin labeling (Phal., red). Cytokeratins are labeled with a pancytokeratin antibody (green); dapi labels nuclei (blue). Scale bars: 10 μm.

The global organization of the enterocytes of VEP$^{-/-}$ mice is preserved.

A gross histological characterization of the mice was undertaken by Sylvie Robine and Céline Revenu. Despite displaying a growth retardation phenotype, the global crypt–villus organization of the intestinal epithelium of VEP$^{-/-}$ mice does not show any overt defects, as was revealed by hematoxilin-eosin staining **(Figure 12C)**. Intestinal sections from VEP$^{-/-}$ mice demonstrated normal apical concentrations of ezrin and F-actin compared with WT sections **(Figure 12C)**. The lateral and apical-lateral junctional markers E-cadherin and ZO-1 also retained their expected localizations in the VEP$^{-/-}$ enterocytes. Therefore, even in the absence of all three actin-bundling proteins, the intestinal epithelial organization and polarity appeared normal at the tissue level. We then investigated the distribution of the main cytoskeletal elements at the cellular level **(Figure 12D)**. In the VEP$^{-/-}$ enterocytes, microtubules showed the classical, mainly apico-basal orientation, and keratin filaments presented a normal diffuse pattern with a slight concentration in the terminal web as in enterocytes from WT mice. At this cellular resolution, the strong brush border localization of actin filaments, although maintained, often appeared narrower in the VEP$^{-/-}$ compared with the WT mice, suggesting an alteration at the level of the microvilli **(Figure 12D)**. Therefore the growth delay present in VEP$^{-/-}$ mice does not seem to be caused by abnormalities in intestinal morphology or global polarity of enterocytes.

Intestinal microvilli form even in the absence of the three actin-bundling proteins.

The results, analyses and conclusions presented in this paragraph and in the next one were, for the vast majority of them, already established at the time I joined the lab. My experimental and analytical contributions on these two sections were thus only minor.

In light of the proposed role of actin-bundling proteins in the formation of membrane protrusions, in close collaboration with the electron microscopy service from the Institut Curie transmission electron microscopy (TEM) was used, to investigate the defects generated by the combined absence of two or three bundling proteins in intestinal microvilli morphogenesis. Unexpectedly, microvilli were present in all KO mice analyzed, even in the absence of the three bundlers **(Figure 13**, **A** and **B)**. Although TEM confirmed the global preservation of the apico-basal polarity of the enterocytes, with a well-defined brush border facing the lumen, the cytoplasm of the VEP$^{-/-}$ cells demonstrated a higher concentration of vesicles, vacuoles, and tubular structures, especially in the apical area, compared with WT enterocytes. This was

quantified by evaluating the number of vesicular structures per square micrometer in the first apical micron of cytoplasm below the microvilli (1.74 ± 0.94, n_{WT} = 5 cells; 7.63 ± 0.52, $n_{VEP-/-}$ = 6 cells; Mann-Whitney $p < 0.01$; **Figure 13A)**. No defect in the brush border of the $VE^{-/-}$ mice could be detected. The $VP^{-/-}$, $EP^{-/-}$, and $VEP^{-/-}$ mice showed defects similar to those reported for the plastin-1 KO mice ($P^{-/-}$) (Grimm-Günter et al., 2009), namely, very short or absent actin bundle rootlets and a strong reduction in the apical organelle free zone **(Figure 13B)**.

Although the bundlers appeared nonessential for the formation of microvilli *per se*, they did have an effect on microvillar length **(Figure 13C)**. Compared with microvilli of WT animals, the microvilli of $VP^{-/-}$ mice presented a reduction in length of ~20%, similar to the $P^{-/-}$ mice (1.03 ± 0.14 μm, $n_{VP-/-}$ = 14, and 1.01 ± 0.16 μm, $n_{P}^{-/-}$ = 194, compared with 1.25 ± 0.26 μm, n_{WT} = 86; *t* test $p < 0.0001$). The $EP^{-/-}$ and the $VEP^{-/-}$ mice showed a major decrease in length of around 40% of the length of WT microvilli (0.76 ± 0.15 μm, $n_{EP-/-}$ = 75, compared with WT, *t* test $p < 0.0001$; 0.72 ± 0.11 μm, $n_{VEP-/-}$ = 58, compared with WT, *t* test $p < 0.0001$). The $VEP^{-/-}$ and $EP^{-/-}$ microvilli were thus very similar, with an average length of 724 and 763 nm, respectively, against 1253 nm for WT microvilli. Nevertheless, $VEP^{-/-}$ microvilli appeared less homogeneous in length per cell and less straight compared with $EP^{-/-}$ and a fortiori to WT microvilli **(Figure 13**, **A** and **B)**. This was confirmed by the significantly increased coefficient of variation of the length of microvilli per cell in the $VEP^{-/-}$ compared with WT cells (2.54 ± 1.37%, n_{WT} = 7 cells, and 10.85 ± 4.90%, $n_{VEP-/-}$ = 7 cells; Mann-Whitney $p < 0.01$). In conclusion, the absence of the three known actin-bundling proteins reduces microvillar length but does not prevent microvillar protrusion.

Figure 13: Microvilli still form in the $VEP^{-/-}$ mice
A. Transmission electron micrographs of sections of jejunum from WT, $EP^{-/-}$, and $VEP^{-/-}$ presenting a general view of the enterocyte polarity. Arrows point at apical vesicles and vacuoles in the $VEP^{-/-}$ sample. Scale bars: 2 μm. **B.** Transmission electron micrographs of sections of jejunum from WT, the three double KO ($VE^{-/-}$, $VP^{-/-}$, $EP^{-/-}$) and the triple KO ($VEP^{-/-}$) mice illustrating the organization of the brush border. Scale bars: 500 nm.
C. Histograms illustrating the average lengths of the intestinal microvilli depending on the genotype. Values are 1.25 ± 0.26 μm, n_{WT} = 86; 1.01 ± 0.16 μm, $n_{P-/-}$ = 194; 1.03 ± 0.14 μm, $n_{VP-/-}$ = 14; 0.76 ± 0.15 μm, $n_{EP-/-}$ = 75; 0.72 ± 0.11 μm, $n_{VEP-/-}$ = 58. *** *t* test $p < 0.001$.

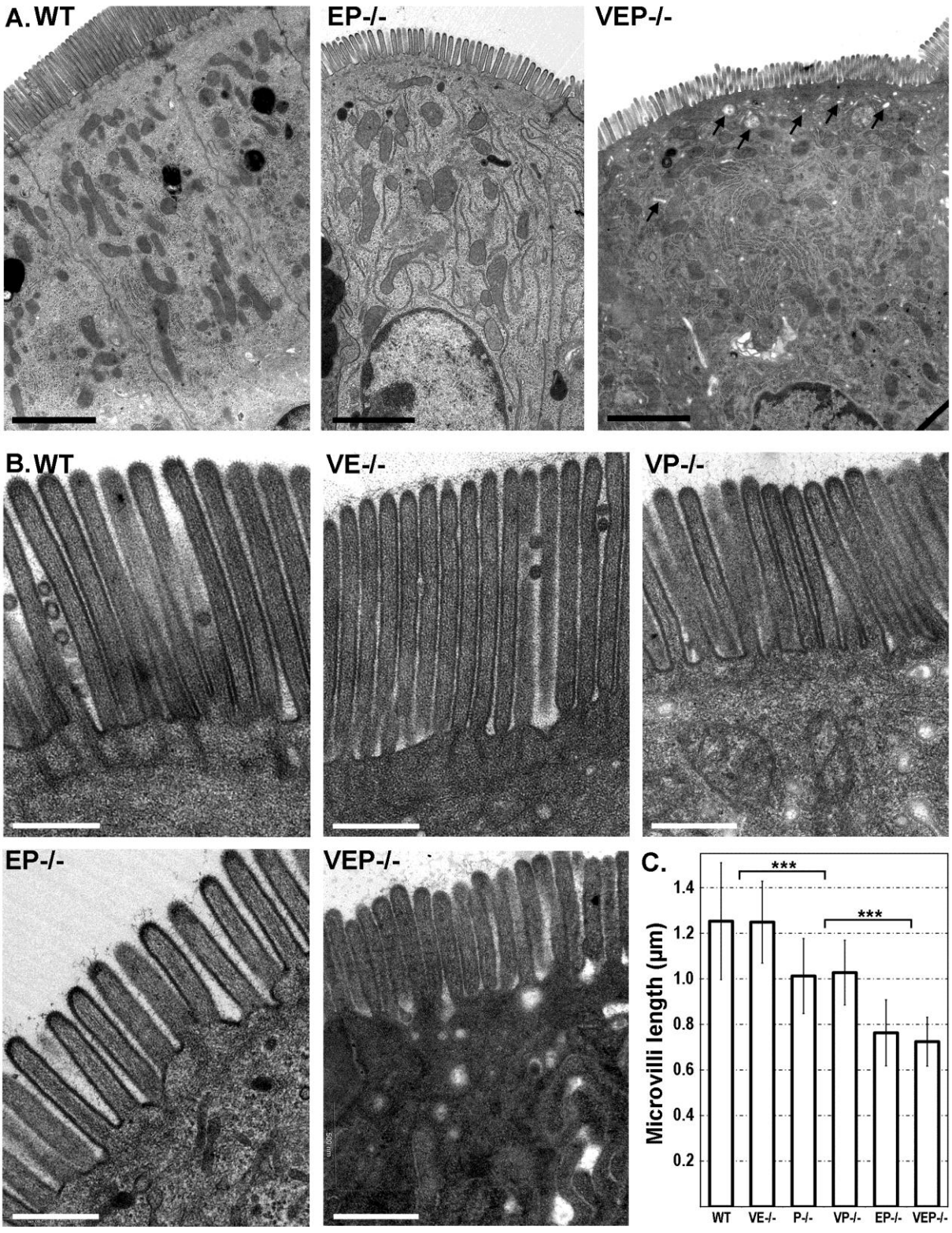
A. WT
EP-/-
VEP-/-
B. WT
VE-/-
VP-/-
EP-/-
VEP-/-
C.
Microvilli length (μm)
1.4
1.2
1.0
0.8
0.6
0.4
0.2
***
***
WT
VE-/-
P-/-
VP-/-
EP-/-
VEP-/-

The organization of F-actin into a bundle is lost in VEP$^{-/-}$ microvilli.

We next addressed the precise organization of actin filaments, which were detected in microvilli after phalloidin staining **(Figure 12D)**. The longitudinal striation due to the actin bundle was easily detectable by TEM in the double KO microvilli, whereas it was no longer distinguishable in the VEP$^{-/-}$ microvilli **(Figure 13B)**. TEM of transverse sections of WT microvilli demonstrated a sharp, electron-dense, dotted pattern that corresponded to transverse sections of individual actin filaments **(Figure 14A**, insets**)**. This pattern was absent in VEP$^{-/-}$ samples, which displayed only a few, indistinct darker areas that likely correspond to actin filaments **(Figure 14A)**. This prevented the quantification of the number of filaments in VEP$^{-/-}$ samples. Noticeably, although the reticular organization of microvilli was unaffected as measured by the angle between three adjacent microvilli (65.9 ± 9.7°, n_{WT} = 115; 62.4 ± 9.4°, $n_{VEP-/-}$ = 151), the transverse area of microvilli was strongly decreased in VEP$^{-/-}$ versus WT animals (5231.1 ± 836.7 nm^2, $n_{VEP-/-}$ = 91, and 8909.5 ± 1097.9 nm^2, n_{WT} = 137; *t* test $p < 0.0001$; **Figure 14B)**. As the number of filaments in the bundle influences the diameter of a protrusion (Tilney and Tilney, 1988), this could indicate a reduced number of filaments in the VEP$^{-/-}$ microvilli. In support of this hypothesis, western blotting revealed that the actin content of the purified brush borders was reduced in VEP$^{-/-}$ mice compared with WT controls, whereas the actin content of enterocytes remained unmodified between WT and VEP$^{-/-}$ total lysates **(Figure 14C)**.

To achieve better resolution of the actin filaments in microvilli, we performed TEM on isolated brush borders from WT and VEP$^{-/-}$ mice. This technique eliminates most of the background generated by the cytoplasmic elements, while the brush border actin cytoskeleton and its associated plasma membrane are preserved. As demonstrated by phalloidin staining, VEP$^{-/-}$ brush borders appeared thinner than WT brush borders and retained F-actin **(Figure 14**, **D** and **E**, insets**)**. TEM revealed that longitudinal actin filaments were still present in VEP$^{-/-}$ microvilli. However, they lost the normal bundled structure present in the WT situation **(**compare **Figure 14E** with **14D)**: the number of filaments seemed to be reduced, and their spacing was highly irregular. In some areas, actin filaments appeared compacted and indistinguishable from each other, or even interrupted, which could be due to wavy filaments going out of the section. In other areas, the spacing between two filaments was enlarged compared with the WT bundle. This disorganization explains the lack of sharp actin dots in the transverse sections **(Figure 14A)**. On the contrary, actin filaments in WT microvilli showed the expected highly regular bundle pattern resembling striae **(Figure 14D)**. The short or missing rootlets in VEP$^{-/-}$ mice look

similar to those reported for $P^{-/-}$ mice (Grimm-Günter et al., 2009). Actin-membrane bridges, known to be myosin-1a–based in WT animals, could still be detected in some VEP−/− samples **(Figure 14, D** and **E**, arrowheads**)**. These bridges cannot be detected in all sectioned microvilli, even in WT mice; therefore their number and arrangement cannot be reliably evaluated. Taken together, these data indicate that although actin filaments are still present in $VEP^{-/-}$ microvilli, they are sparse and no longer packed in parallel bundles.

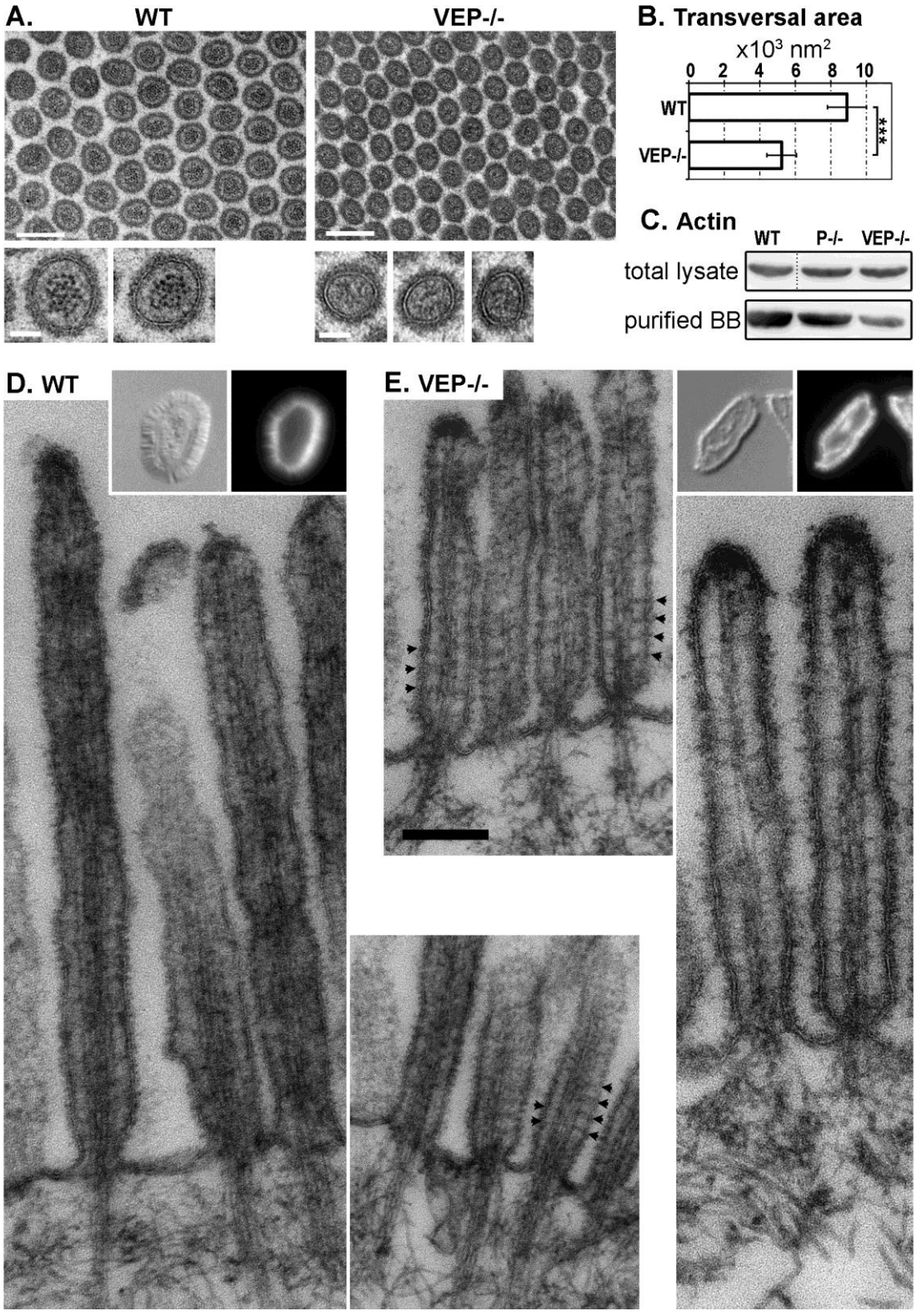

Figure 14: The organization of the actin bundle is affected in the VEP$^{-/-}$ microvilli
A. Transmission electron micrographs of transversal sections of the microvilli of WT and VEP$^{-/-}$ mice. Scale bars: 200 nm; insets: 50 nm. **B.** Histograms depicting the average area of transversal sections of microvilli depending on the genotype: 5231.1 ± 836.7 nm^2, $n_{VEP-/-}$ = 91 and 8909.5 ± 1097.9 nm^2, n_{WT} = 137. *** t test $p < 0.001$. **C.** Western blotting against actin on total lysates or lysates from isolated brush borders (loaded for equal total protein). **D** and **E.** Transmission electron micrographs of isolated brush borders from **D.** WT and **E.** VEP$^{-/-}$ mice. Typical isolated brush borders are shown in insets (left: Nomarski; right, phalloidin staining). Arrowheads highlight actin-membrane bridges. Scale bars: 200 nm.

The loss of the three bundlers appears not to be compensated.

I took the project in charge at this point, most of the results, analyses and conclusions presented above being already established. The three known actin bundling proteins of the microvilli thus seemed dispensable to maintain microvilli protrusions. In order to broaden this conclusion, I elected a proteomic approach to determine whether a fourth, unknown actin-bundling protein or a protein compensating the absence of the three bundlers could account for the protrusion of microvilli in the VEP$^{-/-}$ enterocytes. Alternatively, providing that no additional actin-bundling protein compensates for the triple KO, it would appear the bundled organization is not required for membrane protrusion. I performed mass spectrometric analysis of the total protein content of WT and VEP$^{-/-}$ isolated brush borders. The list of actin-related proteins found in the analysis of WT brush borders is presented in Table 1 (see page 65). All the additional proteins found in the analysis of VEP$^{-/-}$ brush borders are listed in Table 2 (see page 66). I furthermore performed various immunostainings and western blots to investigate the interesting hits. The potential actin cross-linkers harmonin and eps8 could be detected in WT and VEP$^{-/-}$ brush borders. However, only the short harmonin isoform, harmonin a, which lacks the actin cross-linking region (Verpy et al., 2000), but not the cross-linking isoform b (Boëda et al., 2002), could be detected in WT and VEP$^{-/-}$ brush borders by western blot analysis using a pan-harmonin antibody **(Figure 15B)**. The capping protein eps8 has also been recently proposed to have cross-linking activity *in vitro* that is enhanced by binding to IRSp53 (Disanza et al., 2006; Hertzog et al., 2010). IRSp53 was absent from both WT and VEP$^{-/-}$ brush borders, as it could neither be found it in the proteomic data nor be detected by western blotting **(Figure 15A)**. Moreover, eps8 expression levels were unchanged between WT and VEP$^{-/-}$ brush borders and, importantly, eps8 was strictly localized at the very tip, as expected, and did not extend along the shaft of the microvilli in the VEP$^{-/-}$ samples **(Figure 15A)**. Eps8 is thus not ectopically recruited and does not compensate for the loss of the actin-bundling proteins of VEP$^{-/-}$ intestinal microvilli. No extra actin-bundling or cross-linking proteins could be detected in the VEP$^{-/-}$

brush borders compared with WT (Table 2, see page 66). Thus the formation of microvilli in VEP$^{-/-}$ mice does not appear to be due to the compensatory recruitment of a fourth bundler but is more likely explained by the presence of the remaining actin-binding proteins normally present in microvilli.

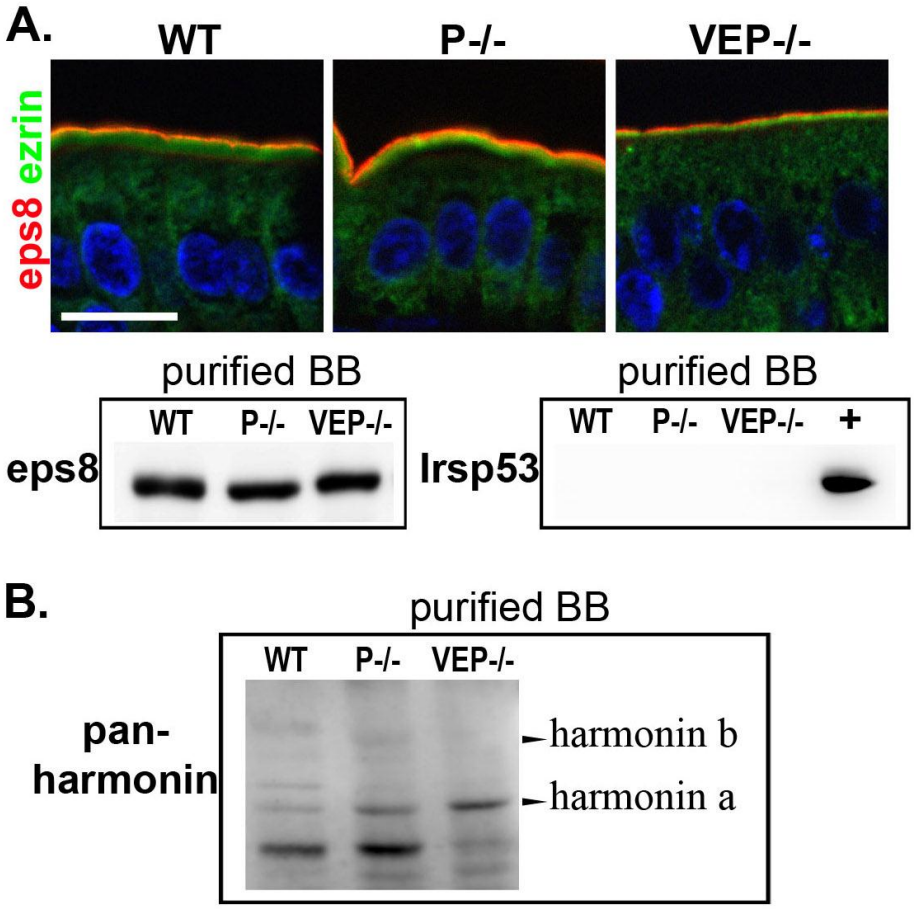

Figure 15: Distribution of potential actors of microvilli morphogenesis identified by proteomics analysis
Immunostainings and western blots on WT, P$^{-/-}$ and VEP$^{-/-}$ samples.
A. Eps8 localisation at the tips of microvilli analysed by immunostainings and counterstained for the microvillus protein ezrin (top). Scale bar 10 μm. Detection of Eps8 and IRSp53 by immunoblots performed on isolated brush border lysates loaded for equal protein content (bottom). For IRSp53, a lysate of caco-2 cells has been used as positive control (+). **B.** Immunoblots using a pan-harmonin antibody performed on isolated brush border lysates. The expected sizes of isoforms a and b are highlighted.

The EM analyses thus revealed a weaker phenotype than expected. In order to better describe the animal model we nevertheless decided to investigate the growth retardation reported as a physiological impact of the actin bundle organization was never described. As $VEP^{-/-}$ mice have reduced microvillar transverse area and length, their intestine absorptive surface could be significantly compromised and have an impact on growth. On the basis of the measured length, area, and density of microvilli in WT, $EP^{-/-}$, and $VEP^{-/-}$ intestine, we calculated the respective brush border membrane surfaces per square micrometer of apical domain, approximating microvilli to cylinders ($S_{WT} = 24.8 \pm 6.9\ \mu m^2$, $S_{EP-/-} = 12.0 \pm 2.5\ \mu m^2$, $S_{VEP-/-} = 14.4 \pm 2.8\ \mu m^2$; maximal SDs were calculated according to the Gaussian error-propagation law). The brush border membrane surface was strongly reduced in $VEP^{-/-}$ enterocytes compared with WT, but not $EP^{-/-}$, enterocytes. As the $EP^{-/-}$ and $VEP^{-/-}$ absorptive surfaces are similar, the effect of smaller microvilli on the $VEP^{-/-}$ growth retardation phenotype can be ruled out. The growth delay of $VEP^{-/-}$ mice is thus not due to a reduction in the absorptive surface of the epithelium but could be linked to a defect in actin bundle organization.

Digestive enzymes do not properly localize in the apical domain.

One important step toward understanding the phenotype of the $VEP^{-/-}$ mice is to define how the disorganization of the actin network accounts for growth retardation. Defects in the localization of the numerous digestive enzymes, transporters and canals expressed by the enterocytes could explain the growth defect. Trafficking toward the basolateral domain nevertheless did not appear to be affected, as illustrated by the basolateral localization of the Na^+/K^+-ATPase in $VEP^{-/-}$ enterocytes **(Figure 16B)**. I therefore analyzed the localization of digestive enzymes that are targeted to the apical surface of the enterocytes using a variety of apical trafficking routes. As the $VEP^{-/-}$ mouse demonstrates the major terminal web defects previously reported in the plastin-1 KO (Grimm-Günter et al., 2009), and as we need to unravel the specificity of the $VEP^{-/-}$ samples, both WT and $P^{-/-}$ samples were used as routine controls in this study **(Figure 18)**. The lipid raft–associated aminopeptidase N (APN) still localized properly in the $VEP^{-/-}$ brush border **(Figure 16A)**. Nevertheless, several enzymes presented an impressive sub-apical accumulation in the $VEP^{-/-}$ enterocytes, with a reduced signal left in the microvilli **(Figure 18A**, stars **and D)**. This was the case for raft-independent lactase phlorizin hydrolase (LPH), raft-associated sucrase-isomaltase (SI), and peptide transporter protein PepT1. Moreover, western blot analyses performed on lysates from purified brush borders showed that

the amount of these enzymes that still localized to the microvilli was reduced in the VEP$^{-/-}$ compared with the WT or P$^{-/-}$ samples **(Figure 18B),** thus confirming the reduced level observed by immunostainings. These observations appeared to be specific to VEP$^{-/-}$ mice as only minor LPH sub-apical accumulations could be seen in a few areas of the plastin-1 KO **(Figure 18A)** and its combinations **(Figure 17)**. Additionally, in the VP$^{-/-}$ enterocytes, SI also appeared delocalized and PepT1 showed some slight sub-apical accumulation but much less strikingly than in the VEP$^{-/-}$ samples **(Figure 17)**.

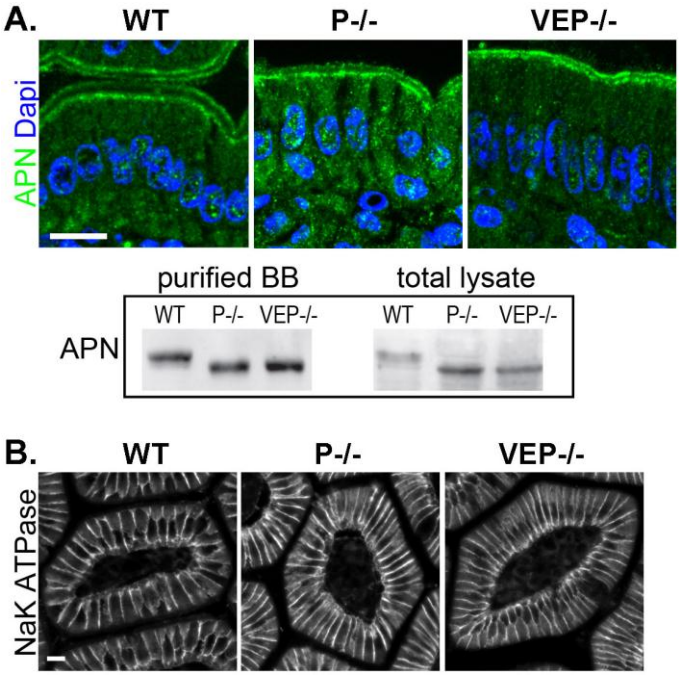

Figure 16: Not all polarity markers are affected in VEP$^{-/-}$ mice
A. Western blots and immunostainings against the apical enzyme aminopeptidase N (APN, green) on WT, P$^{-/-}$ and VEP$^{-/-}$ samples. Dapi labels nuclei (blue). Immunoblots are performed on total and isolated brush border lysates. **B.** Immunostainings for the basolateral pump Na+/K+ ATPase. Scale bars 10 µm.

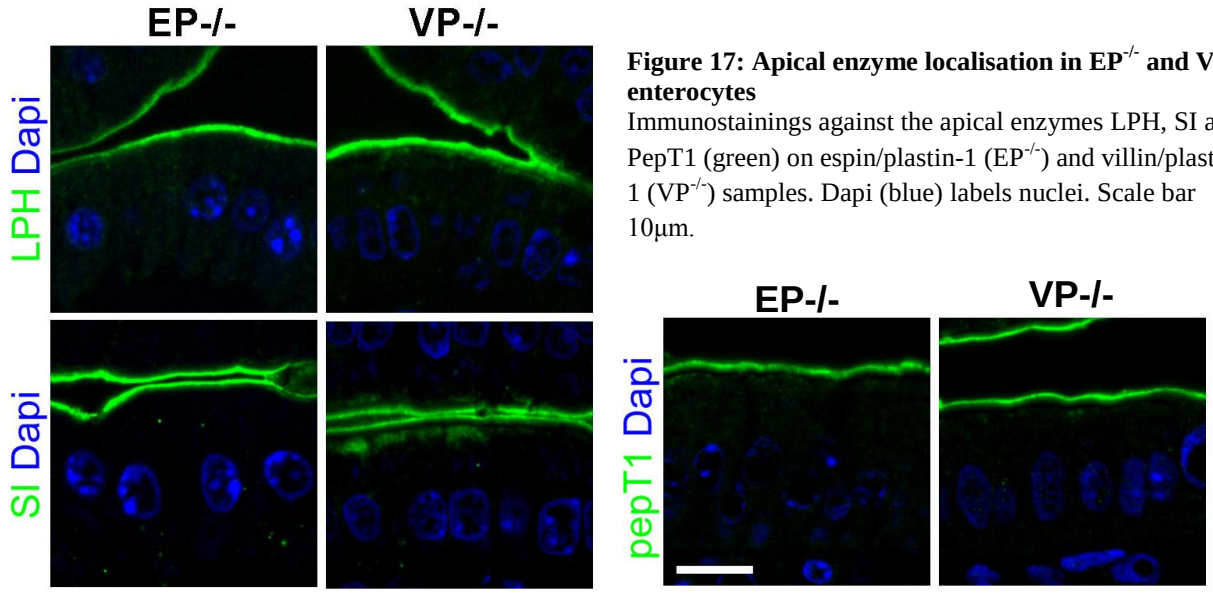

Figure 17: Apical enzyme localisation in EP$^{-/-}$ and VP$^{-/-}$ enterocytes
Immunostainings against the apical enzymes LPH, SI and PepT1 (green) on espin/plastin-1 (EP$^{-/-}$) and villin/plastin-1 (VP$^{-/-}$) samples. Dapi (blue) labels nuclei. Scale bar 10µm.

The amount of dipeptidylpeptidase IV (DPPIV), an enzyme following a transcytotic pathway, was strongly reduced in the $VEP^{-/-}$ microvilli, as demonstrated both by western blotting **(Figure 18B)** and immunostaining **(Figure 18A**, circle**)**, but contrarily to LPH, SI and pepT1, DPPIV did not show the intense sub-apical accumulations reported above. Finally, the glycosylphosphatidylinositol-anchored intestinal alkaline phosphatase (IAP) presented both a very strong decrease in the $VEP^{-/-}$ brush border, observed by western blotting and immunostaining, and a significant sub-apical accumulation **(Figure 18, A,** star and circle, and **B)**. The sub-apical accumulations reported by immunofluorescence were in agreement with the high vesicular content of the $VEP^{-/-}$ cytoplasm detected by TEM **(Figure 13)**. In support of this idea, SI immunostainings on thinner sections (3µm) revealed the presence of vesicular structures **(Figure 18D).** Compared with the WT cell and brush border lysates, a reproducible shift in the size of the bands detected by western blotting occurred for LPH, SI, DPPIV, and APN in the $P^{-/-}$ and $VEP^{-/-}$ samples **(Figures 18A and 16A)**. This shift could be suppressed by treating the samples with glycosidases and therefore reflects a difference in the glycosylation pattern (not shown). This unexpected phenomenon is not responsible for the phenotype of the $VEP^{-/-}$ mice, because it already occurs in the $P^{-/-}$ samples and thus must be due solely to the loss of plastin-1.

To obtain an insight into the intestinal physiology, I directly assess absorption in the $VEP^{-/-}$ mice by measuring the kinetics of glucose absorption of fasted WT, $P^{-/-}$, and $VEP^{-/-}$ mice following oral glucose load. The glucose absorptive capacity of $VEP^{-/-}$ intestine was strongly and significantly reduced compared with both WT and $P^{-/-}$ animals, as depicted by the measurements of glucose blood level plotted against time after gavage **(Figure 18C)**. Interestingly, the blood glucose level in $VEP^{-/-}$ mice was significantly reduced by 75% at 30 min. Such an early time point directly represents an alteration of the glucose absorption capacity of the enterocytes, as the adaptive physiological response to high glycaemia has not occurred yet.

The study of the triple KO enterocytes therefore reveals a major disruption in apical delivery and/or retention of enzymes at the apical membrane associated with malabsorption and subsequent growth delay that develops predominantly after weaning in the $VEP^{-/-}$ mice. The slight apical localization defects observed in the $VP^{-/-}$ samples are not sufficient to cause such a growth delay in these mice **(Figure 12B)**.

Figure 18: $VEP^{-/-}$ mice show apical localization defects of major digestive and absorptive brush border components

A. Histological sections of jejunum from WT, $P^{-/-}$ and $VEP^{-/-}$ animals immunostained for LPH, SI, PepT1, DPPIV, and IAP (green). DAPI (blue) labels nuclei. Scale bars: 10 µm. **B.** Western blots against LPH, SI, PepT1, DPPIV, and IAP were performed on total or isolated brush borders lysates (loaded for equal total protein). **C.** Blood glucose concentrations plotted over time during oral glucose tolerance test in mice fasted overnight ($n_{VEP+/-}$ = 3; $n_{P-/-}$ = 5; $n_{VEP-/-}$ = 3; Mann-Whitney: **, $p < 0.01$, *, $p < 0.05$). **D.** Thin histological sections (3µm) of jejunum from VEP-/- mice stained for SI observed by confocal microscopy (optical section: 0.5 µm). Bar: 10 µm.

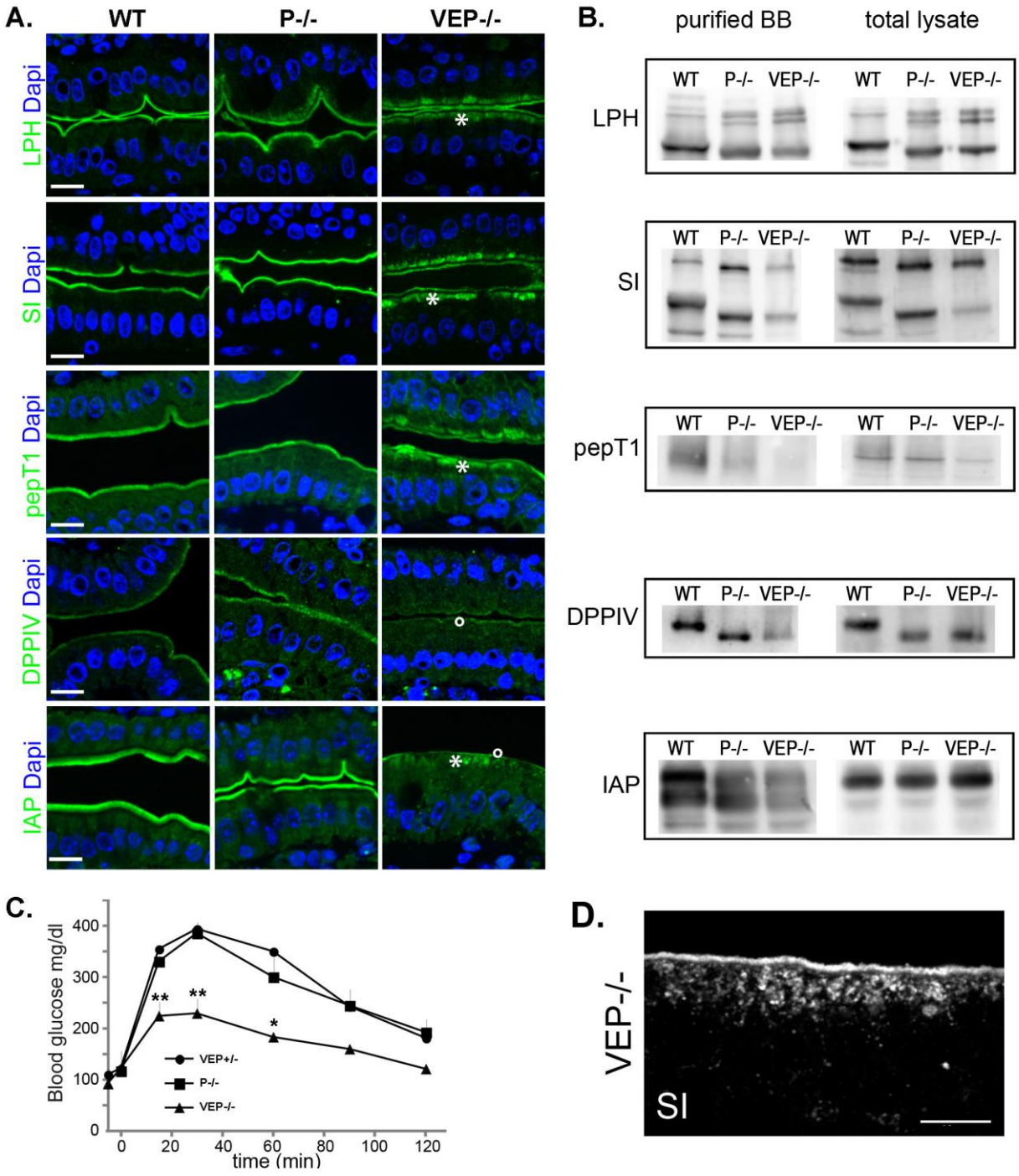

Apical membrane retention is deficient and myosin-1a is mislocalized.

To decipher the apical transport or anchorage mechanisms that are defective in the VEP$^{-/-}$ mice, I chose several molecular players involved in apical targeting and delivery in enterocytes and analyzed their subcellular localization. The organization of the Golgi was not affected in the VEP$^{-/-}$ enterocytes, as the Golgi marker giantin and the GTP-binding protein rab6, which is implicated in intra-Golgi transport, retained the localization observed in WT enterocytes **(Figure 19A)**. The Golgi apparatus appeared morphologically unaltered, suggesting

that a later step in the apical transport could be defective. In enterocytes, cargoes are known to traverse rab11- and rab8-positive compartments *en route* to the apical pole. Although the sub-nuclear localization of rab11 was not affected in the VEP$^{-/-}$ animals **(Figure 19A)**, rab8 sub-apical concentration looked slightly decreased when observed by immunofluorescence **(Figure 19B)**. However, this reduced rab8 apical localization could not be confirmed by western blotting **(Figure 19B)**. Whereas the apical delivery route did not appear affected, the early endosomal marker EEA1 interestingly exhibited an enlarged sub-apical localization in the VEP$^{-/-}$ enterocytes **(Figure 20A),** which strongly colocalized with the accumulation of apical markers, as shown for SI **(Figure 20B)**. These results suggest that endocytosis, rather than apical delivery, is responsible for the mislocalization of apical enzymes and transporters in the VEP$^{-/-}$ mice. Is endocytosis therefore enhanced in the absence of a proper actin bundle or are these apical components more prone to endocytosis? To discriminate between these two possibilities, I compared *in vivo* the kinetics of global endocytosis using the vital membrane stain FM dye as an endocytic probe perfused in the intestinal lumens of WT and VEP$^{-/-}$ mice, an approach successfully used in the past (Hansen et al., 2009). A modification in the internalization of the dye in the KO enterocytes could not be detected at any of the time points analyzed from 5 to 90 min **(Figure 20C)**. The global endocytosis rate is therefore not increased in the VEP$^{-/-}$ enterocytes, and the accumulation of apical digestive components in EEA1-positive compartments is most likely due to their deficient stabilization at the apical membrane.

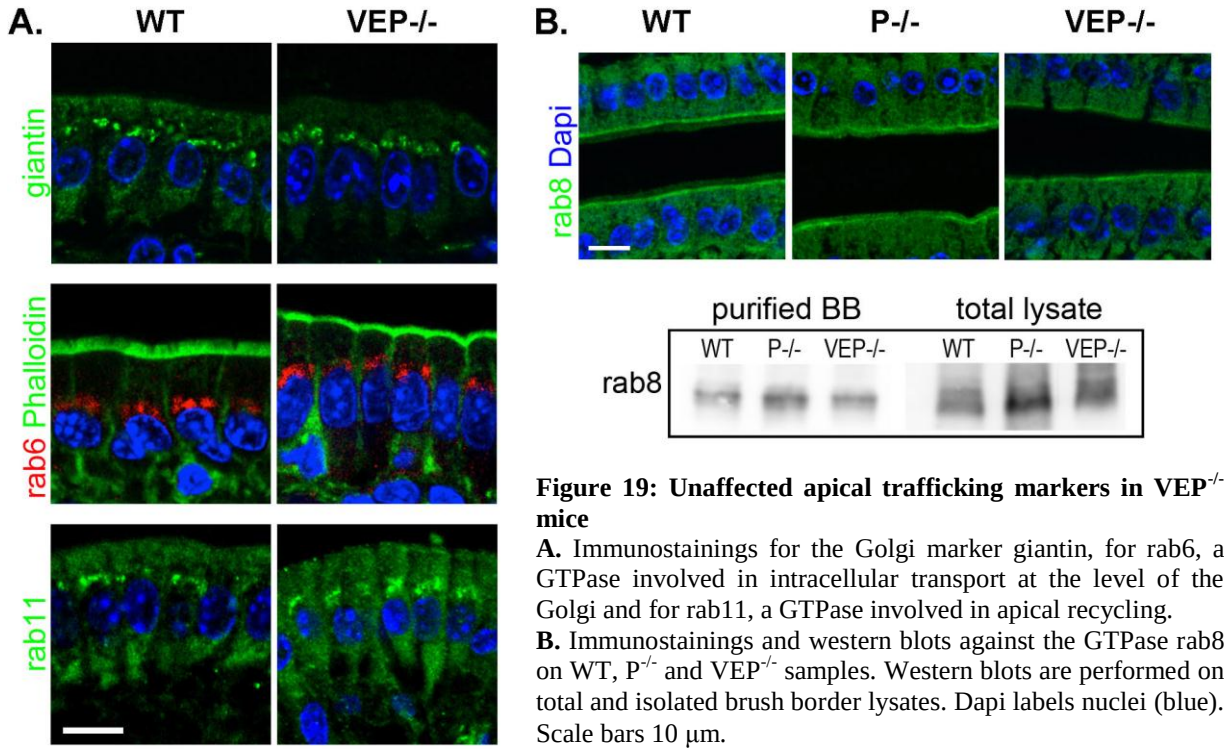

Figure 19: Unaffected apical trafficking markers in VEP$^{-/-}$ mice
A. Immunostainings for the Golgi marker giantin, for rab6, a GTPase involved in intracellular transport at the level of the Golgi and for rab11, a GTPase involved in apical recycling.
B. Immunostainings and western blots against the GTPase rab8 on WT, P$^{-/-}$ and VEP$^{-/-}$ samples. Western blots are performed on total and isolated brush border lysates. Dapi labels nuclei (blue). Scale bars 10 µm.

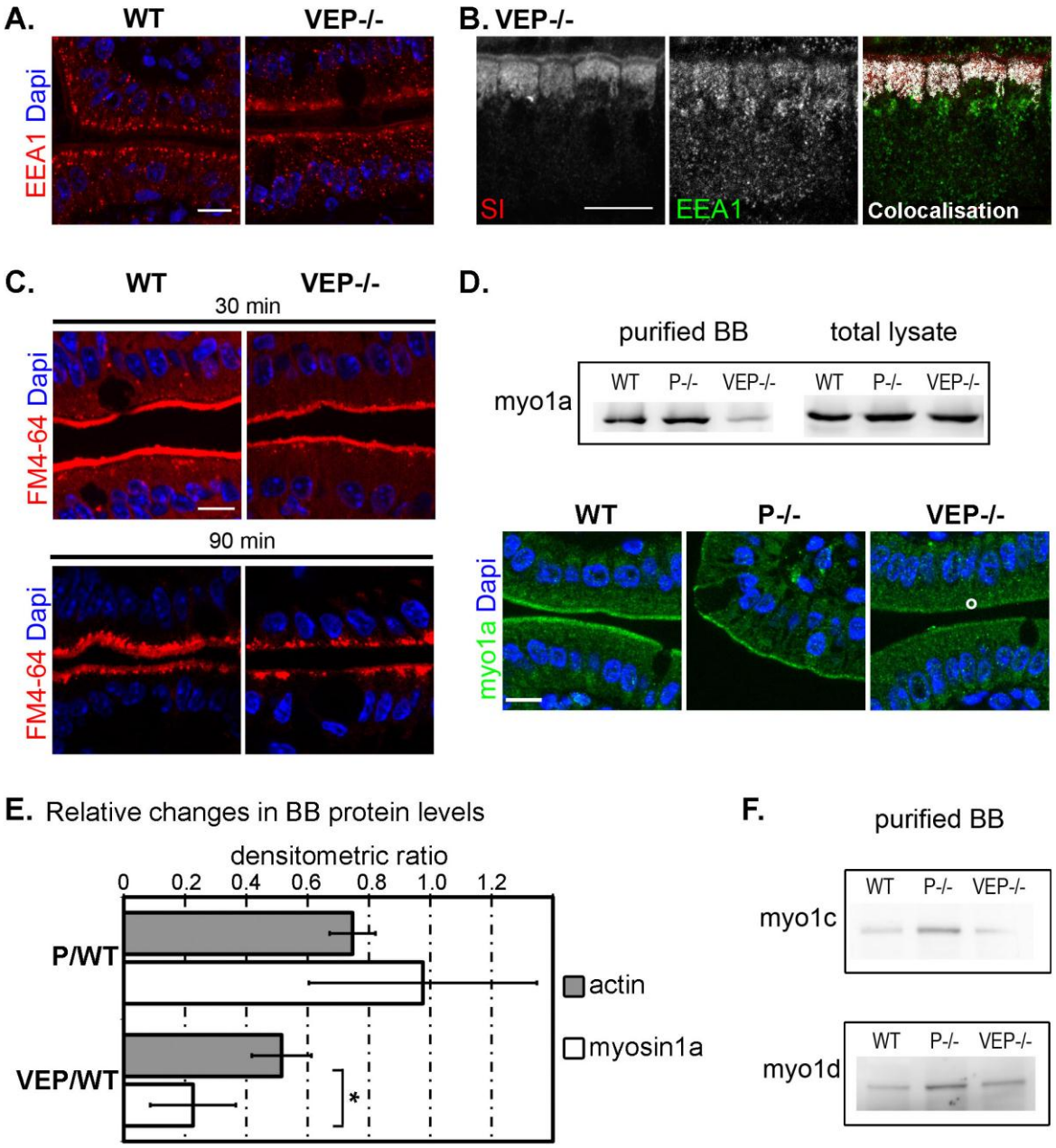

Figure 20: The apical domain retention machinery is affected in VEP$^{-/-}$ mice
A. Immunostaining against the early endosomal marker EEA1 in WT and VEP$^{-/-}$ enterocytes. **B.** Colocalization (white) of EEA1 (green) with the subapical accumulations of the enzyme SI (red) by immunostaining**. C.** Unchanged global endocytosis rate analyzed by the internalization of the vital membrane dye FM4-64 (red), shown at 30- and 90-min time points. **D.** Western blots and immunostaining against myosin-1a on WT, P$^{-/-}$, and VEP$^{-/-}$ samples. Western blot analysis was performed on total and isolated brush border lysates. DAPI labels nuclei (blue). Scale bars: 10 µm. **E.** Histograms depicting the relative changes of actin and myosin-1a protein content between P$^{-/-}$ or VEP$^{-/-}$ and WT brush borders (P/WT and VEP/WT, respectively). Values are densitometric ratios of western blotting performed on brush border lysates (P/WT: 0.98 ± 0.37, n_{myo1a} = 3, and 0.75 ± 0.07, n_{actin} = 5; VEP/WT: 0.23 ± 0.14, n_{myo1a} = 3, and 0.52 ± 0.10, n_{actin} = 5). *Wilcoxon two-sample test $p < 0.05$. **F.** Western blotting performed on isolated brush border lysates against myosins-1c and -1d on WT, P$^{-/-}$, and VEP$^{-/-}$ samples showing that the decrease in myosin-1a is not accompanied by their compensatory recruitment to the brush borders.

The mechanisms allowing membrane retention of apical enzymes and transporters in enterocytes are widely unknown. To date, only the actin motor myosin-1a, a brush border myosin, has been implicated in the anchorage of some apical enzymes (Tyska and Mooseker, 2004). Remarkably, whereas it is properly concentrated in the microvilli of WT and $P^{-/-}$ enterocytes, myosin-1a was substantially lost in $VEP^{-/-}$ microvilli, as detected by western blotting on isolated brush border lysates and by immunofluorescence **(Figure 20D)**. As the actin content was also diminished in $VEP^{-/-}$ brush borders **(Figure 14C)**, the reduction in myosin-1a could be due to the loss of the actin-bundling proteins or could solely reflects the lower actin content. Densitometric analysis of western blots allowed to quantify the relative changes in actin and myosin-1a content between WT and $P^{-/-}$ or $VEP^{-/-}$ brush borders **(Figure 20E)**. The densitometric ratio of $P^{-/-}$ over WT brush border samples was not significantly different between actin and myosin-1a (0.98 ± 0.37, $n_{myo1a} = 3$, and 0.75 ± 0.07, $n_{actin} = 5$, $p \leq 0.8$). In contrast, the densitometric ratio of $VEP^{-/-}$ over WT brush border samples was significantly reduced for myosin-1a compared with actin (0.23 ± 0.14, $n_{myo1a} = 3$, and 0.52 ± 0.10, $n_{actin} = 5$; Mann-Whitney $p < 0.05$). This demonstrates that $VEP^{-/-}$ brush borders lost approximately two times more myosin-1a than actin and that the decrease in myosin-1a was not merely due to a decrease in brush border actin. Although myosin-1a brush border level was strongly decreased, it was not completely absent. We could still detect some myosin-1a bridges by TEM **(Figure 14E)**, and the myosin-1a–based extrusion of vesicular membranes (McConnell and Tyska, 2007) was still detected upon ATP-induced myosin activation on isolated $VEP^{-/-}$ brush borders **(Figure 21)**. The KO of myosin-1a in mouse enterocytes does not cause defects at the whole-animal level (Tyska et al., 2005). This lack of phenotype has been accounted for by the compensatory recruitment of at least two other myosins, myosin-1c and -1d, in the brush border (Tyska et al., 2005; Benesh et al., 2010). I therefore used western blotting to analyze the brush border content of these class I myosins in our samples. The level of these two myosins did not increase between $VEP^{-/-}$ and WT brush borders **(Figure 20F)**. Neither of them became ectopically recruited to the microvilli in the absence of the three actin-bundling proteins, although myosin-1a was almost absent from $VEP^{-/-}$ microvilli. Thus the absence of the three actin-bundling proteins is associated with defects in the brush border localization of at least one player in apical enzyme retention, myosin-1a.

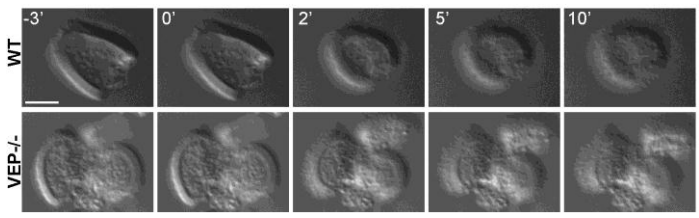

Figure 21: Vesicular membrane extrusion is preserved in brush borders of $VEP^{-/-}$ mice

DIC time-lapse series of WT and $VEP^{-/-}$ isolated brush borders before (-3') and after (0 to 10') addition of 200µM ATP showing the apical shedding of vesicles in both conditions. Bar 5µm.

Table 1: Actin binding proteins identified in WT isolated brush borders

Tables show identifier (NCBI protein accession number), description (NCBI protein definition), matching peptides (number of peptides identified per experiment), MW (molecular weight in Daltons), coverage (% of sequence coverage identified from MS/MS data) of the proteins identified by mass spectrometry. Showed is the best experiment.

Identifier	Description	Matching peptides	MW	Cover-age
Bundling				
gi|85986577	Plastin 1	43	70,4	46,5
gi|148667910	V illin 1	38	92,9	42,6
gi|46877084	Espin isoform 6	5	28,1	28,9
Cross linking				
gi|11230802	Actinin alpha 4	43	105	43,9
gi|61097906	Actinin alpha 1	16	103,1	20,7
gi|7304855	Actinin alpha 3	6	103	8,3
gi|38257404	Filamin B	14	277,8	8,3
gi|38257560	Filamin A	5	281,2	2,8
Capping				
gi|2833214	Eps8, EGF receptor kinase substrate 8	14	91,7	26,1
gi|83649737	Capping protein, muscle Z-line, beta isoform a	7	31,3	26
gi|6671672	Capping protein, muscle Z-line, alpha 2	5	33	25,5
gi|161086971	F-actin capping protein alpha-1 subunit	5	33	25,5
Nucleation				
gi|23956222	ARP3 actin-related protein 3 homolog	7	47,4	18,4
gi|148708705	Cordon-bleu, isoform CRA_b	4	146	3,5
gi|6681183	Diaphanous homolog 1	2	139,3	2,2
Myosins				
gi|71151983	Myosin heavy chain 14, NMHC II-C	151	228,6	54
gi|124487037	Myosin IA	54	118,7	37,8
gi|114326446	Myosin, heavy polypeptide 9, non-muscle isoform 1	51	226,4	27,3
gi|148694488	Myosin-VI	26	146,3	22,9
gi|148664634	Myosin VIIb,isoform CRA_b	22	241	11,8
gi|118026911	Myosin ID	19	116,1	18,4
gi|50510675	Myosin-11 isoform	18	228,3	9,1
gi|123262062	Myosin XVB	13	258,7	7,5
gi|17986258	Myosin light chain 6, smooth muscle and non-muscle	12	16,9	57
gi|13432181	Myosin-Ib	8	128,5	7
gi|148677575	Myosin Vb, isoform CRA_a	7	213,4	4
gi|56205559	Myosin, heavy polypeptide 10, non muscle	6	232,5	2,5
gi|15809016	Myosin regulatory light chain MRCL2	5	19,8	35,5
gi|124494242	Myosin IC isoform a	5	119,9	6,2
gi|125987842	Myosin-XVIIIa	6	232,8	5,4
gi|30410852	Myosin IE	5	126,8	5,3
Others				
gi|40849928	Plectin 1 isoform 11	112	517,3	28
gi|50881	Ezrin	17	69,3	30,9
gi|149251314	Cingulin	16	149,5	20,8
gi|41281802	Harmonin	10	102,3	15,1
gi|122890249	Coronin, actin binding protein 2A	8	61,7	10,5
gi|2851563	AΔseverin	8	80,3	21,1
gi|11127935	Epithelial protein lost in neoplasm-b, eplin	8	84,1	15,5
gi|149751320	Similar to tropomyosin 3 isoform 1	5	29	18,1
gi|11528490	Flightless I homolog	6	144,8	5,8
gi|148669742	Adducin 3, isoform CRA_c	3	83,5	5,5
	Dynamin 1-like, isoform CRA_c	3	83,3	3,9

Table 2: Proteins identified in VEP$^{-/-}$ but not in WT isolated brush borders

Tables show identifier (NCBI protein accession number), description (NCBI protein definition), matching peptides (number of peptides identified per experiment), MW (molecular weight in Daltons), coverage (% of sequence coverage identified from MS/MS data) of the proteins identified by mass spectrometry. Showed is the best experiment.

Identifier	Description	Matching peptides	MW	Cover-age
Actin binding				
gi|5031569	ARP1 actin related protein 1 homolog A, centractin alpha	3	42,6	12,8
Traffic				
gi|148704358	Adaptor protein complex AP-1, gamma 2 subunit, isoform CRA a	6	91,9	9,2
gi|48734610	Sec31a protein	6	98,2	9,5
gi|67906177	Sec23A	6	86,2	11,1
gi|148669551	Sec24 related gene family, member C, isoform CRA_a	4	118,6	4,7
gi|149254026	Sec31 like 1	4	144,1	5,7
gi|23956096	USO1 homolog, vesicle docking protein	3	107	3,4
gi|55670639	Chain M, Ap1 Clathrin Adaptor Core	3	48,5	5,4
Junction				
gi|148669535	V inculin, isoform CRA b	5	123,9	5
gi|156255171	Adducin 1 (alpha) isoform 1	4	80,6	7,6
Others				
gi|144922656	Lethal giant larvae homolog 2	3	114,3	3,7
gi|7106301	Microtubule associated protein, RP/EB family, member1	3	30	20,5

C.Discussion

The apico-basal polarity is preserved in absence of microvillar actin bundling proteins.

The overall cellular organization of the enterocytes in VEP$^{-/-}$ mice appears preserved as we can judge from our set of immunostainings. In particular, markers of specific compartments could not reveal any polarity defect in VEP$^{-/-}$ mice. As expected, F-actin strongly concentrates in the brush border. The other elements of the cytoskeleton, cytokeratins and tubulin orientates fairly normally as in a polarized cell. The microvilli structural protein ezrin, which localizes at the apex, only present a slightly narrower distribution, suggestive of microvilli shortening. E-cadherin delineates the basolateral cell boundaries and ZO-1 highlights the tight junctions, in an undistinguishable manner from WT mice. We conclude that enterocytes from VEP$^{-/-}$ mice retain their well-defined apico-basal polarity.

How to build microvilli without actin bundling proteins?

As discussed in the introduction, a whole set of experimental data supports the idea that actin bundling proteins are required to shape and maintain actin based membrane protrusions. Therefore it is surprising that mice devoid of the three microvillar actin bundling are still able to protrude and sustain microvilli. They only present a shorter size but organize in a regular brush border.

In light of this unexpected result, we will attempt to reexamine the initial data presented in the introduction to determine if the role of actin bundling proteins could be re-envisaged. An important part of the original rationale is based on comparisons between results obtained in different systems related to microvilli. In *Drosophila*, lack of forked or fascin results in major morphological defects of the bristles (Tilney et al., 1995, 1998). Bristles are however structurally very different from microvilli. In the apical pole of a sensory cell, only one bristle elongates, in a curved manner, to reach a much longer length compared to microvilli. The actin organization within bristles additionally largely differs from the one of intestinal apical protrusions. Indeed, each bristle is supported by numerous actin bundles, which are constructed from overlapping modules of short filaments (Tilney et al., 1996). In the mouse stereocilia, absence of espin induces their degeneration (Zheng et al., 2000). In contrast to microvilli, stereocilia are constituted by numerous actin bundles (Tilney et al., 1980; Rzadzinska et al., 2004). Moreover, recent protein turnover analyses in stereocilia unexpectedly revealed that actin treadmilling does not occur in the shaft of the stereocilia (Zhang et al., 2012). The actin cytoskeleton of these structures appears to be much more stable than previously thought. The points raised above demonstrate important structural discrepancies between these actin-based protrusions and microvilli. Therefore, comparisons between actin organizations of microvilli, stereocilia or bristles might not be appropriate. The other classical example of actin-based protrusion is represented by filopodia, which are structurally closer to microvilli as a unique actin bundle supports the protrusion. They are nevertheless more dynamic than microvilli. Altough fascin depletion leads to a dramatic reduction of filopodia number and length (Vignjevic et al., 2006), fascin bundling activity might not be required for filopodia protrusion. Indeed, a recently characterized fascin mutant for its actin bundling property could fully rescue filopodia formation in absence of endogenous fascin (Zanet et al., 2012). Thus, F-actin organization by the main bundler appears dispensable for proper filopodia formation. We should however not elude the fact that T-plastin additionally bundles actin filaments within filopodia (Bretscher and Weber, 1980a).

Several research teams specialized in biophysics have also questioned the pre-supposed role of actin bundlers. Theoretical studies have modeled that sole actin polymerization would produce the required force to overcome the membrane resistance to bending (Peskin et al., 1993; Mogilner and Rubinstein, 2005). The resistance force produced by membrane bending and tension is estimated as 10-20 pN for a cylinder of near microvilli size (Peskin et al., 1993). Formin-mediated actin polymerization of one filament generates a force in the range of 1 pN (Kovar and Pollard, 2004), thus the polymerization of 20-30 actin filaments, as observed in microvilli, is likely sufficient to overcome membrane resistance. Accordingly, in giant unilamellar vesicle containing actin monomers and no actin binding protein, induction of actin polymerization is sufficient to drive the formation of long slender membrane deformations resembling filopodia (Janmey et al., 1992; Miyata et al., 1999). As actin filaments are flexible, the force they generate after reaching a critical protrusion length is limited by their buckling that occurs in response to the membrane resilience force. This critical length is dependent on the number of filaments and on their rigidity, the latter being increased by their physical bundling (Mogilner and Rubinstein, 2005; Atilgan et al., 2006; Claessens et al., 2006; Bathe et al., 2008). In fact, for a membrane protrusion supported by 30 weakly bundled actin filaments, as found in microvilli, the critical length has been modeled to be near 0.4 µm (Mogilner and Rubinstein, 2005). This value is actually close to the mean length of microvilli from mice lacking villin, espin and plastin-1. Therefore, extension of microvilli protrusions of minimal size might not require a bundled organization.

Influence of actin bundling proteins on microvilli shape.

Biophysical models, as mentioned above, show that physical bundling of actin filaments increases their resistance to buckling thereby allowing longer protrusions. Indeed, we show that the actin bundling proteins cooperatively participate in the process of microvilli lengthening *in vivo*. Loss of the sole plastin-1 decreases microvilli length *in vivo* (Grimm-Günter et al., 2009). In contrast to its reported role in LLC-PK1 cells (Loomis et al., 2003), we show that espin positively regulates microvillar length only in the absence of plastin-1. On the other hand, additional loss of villin in double ($EP^{-/-}$) or single ($E^{-/-}$ or $P^{-/-}$) knockout mice has no effect. The three bundlers therefore do not contribute equally to microvillar morphogenesis. Actin bundling proteins, depending on their structures, organize actin filaments into bundles of different elasticity and geometry (Claessens et al., 2006; Bathe et al., 2008; Hampton et al., 2008). Thus,

we can speculate that each of the three microvillar actin bundling proteins does not endow the actin bundle with an equivalent geometry and stiffness. In support of this idea, plastin-1 incubated with actin filaments generates actin bundles more compact and straight as compared to villin-induced bundles (Matsudaira et al., 1983). Structural models have indeed documented a higher filaments separation within villin-mediated bundles (Hampton et al., 2008). Interestingly, villin contribution to the bundle architecture seems to be minimal when plastin-1 is present (Hampton et al., 2008; Brown and McKnight, 2010). In addition, these two proteins do not compete for the same binding sites on F-actin (Hampton et al., 2008; Brown and McKnight, 2010). The cooperative contribution of villin and espin to the bundle structure is not reported in the literature. Nevertheless, the actin bundling proteins do cooperatively contribute to the paracrystalline, bundled organization of filaments, as indicated by its loss in the VEP−/− mice compared with the single or the double knockouts.

Since the actin bundling proteins are dispensable for microvilli extensions, which mechanisms could provide the actin network with the remaining organization observed in $VEP^{-/-}$ mice in order to maintain the protrusions? Within actin-based protrusions, it has been proposed that the tension arising from membrane deformation could participate in the parallel arrangement of actin filaments (Liu et al., 2008). The role of the tip complex might also be critical for the filaments arrangement. As discussed earlier, the molecular actors residing in the tip complex have been particularly well described in stereocilia and filopodia. In filopodia, which structurally resemble microvilli, Ena/VASP and the mDia2 formin cooperate to processively elongate actin filaments thereby participating in their organization in a parallel array (Tokuo and Ikebe, 2004; Pellegrin and Mellor, 2005). In agreement with this idea, we could detect the mDia1 formin in enriched brush border fraction. Unfortunately, lack of reliable antibody against this protein prevented us to determine its distribution. In intestinal microvilli, elucidation of the composition of the tip complex remains preliminary. The eps8 proteins have been shown to localize at the tip and to play major role in microvilli morphogenesis through their actin capping and weak bundling activities (Croce et al., 2004; Disanza et al., 2006; Hertzog et al., 2010; Tocchetti et al., 2010; Zwaenepoel et al., 2012). Eps8 restricted tip localization, which is retained in $VEP^{-/-}$ mice, make it a credible molecular bond between the polymerizing ends of actin filaments. Besides the tip complex, links between the membrane and the cytoskeleton is a characteristic of microvillar actin organization. The membrane-cytoskeleton linker myosin-1a, through its ability to generate membrane tension, would be important to avoid microvilli coalescence (Nambiar et al., 2009). Indeed, in absence of myosin-1a, murine intestinal microvilli exhibit important herniations

(Tyska et al., 2005). Although we observed a substantial loss of myosin-1a level in microvilli, the characteristic membrane-cytoskeleton crossbridges could still be identified by electron microscopy. Owing to their properties, the tip complex and the remaining myosin bridges linking actin filaments to the membrane might be sufficient to maintain the longitudinal filaments observed in $VEP^{-/-}$ microvilli.

In conclusion, we have shown that organization of the microvillar actin bundle by the actin bundling proteins is dispensable to allow the microvillus protrusion. Are these proteins completely dispensable or do they contribute to microvillus function through a previously unknown mechanism?

Defective apical retention and increased internalization of membrane proteins?

In contrast to single knockout animals, $VEP^{-/-}$ mice suffer from growth retardation. The reduced bodyweight could be correlated with a severe glucose malabsorption. Could the reduced epithelium surface area caused by microvilli shortening account for the aforementioned defects? It is unlikely the case as, in the rat, removal of 45% of the intestine does not result in impaired growth (Menge and Robinson, 1978). More convincingly, the non-growth retarded $EP^{-/-}$ mice develop microvilli of similar size as the growth retarded $VEP^{-/-}$ mice. Thus, influence of the luminally exposed area can be ruled out to explain the overt phenotype of $VEP^{-/-}$ mice. It is more likely due to defects in distribution of apical enzymes, and transporters which are required for the digestive and absorptive processes. Indeed, we could observe a reduction of apical signal intensity and strong sub-apical accumulations of the digestive enzymes lactase phlorizin hydrolases (LPH), sucrase-isomaltase (SI) and intestinal alkaline phosphatase (IAP). Similar defects are reported for the pepT1 peptides transporter. Finally, the amount of digestive enzyme dipeptydil peptidase IV (DPPIV) is reduced at the brush border. Trafficking is nevertheless not globally impaired as aminopeptidase N (ApN) and the Na/K ATPase reach normally the apical and basolateral membranes, respectively.

Which are the trafficking pathways associated with the delivery of these apical proteins?

SI and LPH are directly addressed to the cell apex, whereas ApN and DPPIV follow a transcytotic pathway (Le Bivic et al., 1990; Matter et al., 1990). Sucrase-isomaltase, DPPIV, IAP, APN and pepT1 associate with lipid raft (Danielsen, 1995; Nguyen et al., 2007). In contrast, LPH apical delivery is dependent of a non-raft pathway which associates galectin-3 (Danielsen, 1995; Delacour et al., 2006). Among these apical proteins IAP only is GPI anchored (Garcia 1993). The different proteins are highly N- and O- glycosylated; however only the apical delivery of SI and DPPIV requires their glycosylation (Alfalah et al., 1999, 2002; Naim et al., 1999). The well-described LPH and SI apical trafficking routes present major differences in intestinal cells. After TGN exit, SI and LPH are segregated into two different vesicle populations (Jacob and Naim, 2001), likely reflecting their differential association with lipid rafts. En route to the apex, vesicles containing LPH or SI follow distinct cytoskeletal tracks: whereas an intact microtubule network is critical for SI and LPH apical delivery, a selective perturbation of the actin cytoskeleton by cytochalasin D impairs SI apical delivery only (Jacob et al., 2003). Time lapse imaging further reveals individual movement of SI associated vesicles along actin (Jacob et al., 2003). It is also worth to notice that myosin-1a is found associated to SI associated vesicles (Jacob et al., 2003). Among the aforementioned apical proteins, only APN distribution is unaltered in $VEP^{-/-}$ mice. It is thus not possible to assign a general failure of a specific pathway that would explain the localization defects that we report. Instead, the mislocalization involves proteins, which present a wide variety of apical addressing pathways suggesting a broader defect.

How to explain the localization defects?

As seen in the introduction, microvilli rootlets have been proposed to serve as tracks for the late steps of apical cargoes delivery. Rootlets could not be observed in microvilli from $VEP^{-/-}$ mice. Loss of these structures is already observed in absence of plastin-1 (Grimm-Günter et al., 2009), but in these mice apical enzymes are properly localized. This defect in the very apical cytoskeleton thus cannot account for apical proteins mislocalization in $VEP^{-/-}$ animals.

On their way to the apex, vesicles sequentially traverse diverse endosomal compartments. In particular, SI and LPH associated vesicles cross rab8 and rab11 positives endosomes. They however never cross compartments positive for the early endocytic marker EEA1 before docking

at the membrane (Cramm-Behrens et al., 2008). Thus, in intestinal cells, EEA1 primarily highlights early endosomes containing internalized molecules. Whereas rab4 and rab11 distribute normally in VEP$^{-/-}$ mice, EEA1 aberrantly accumulates and co-localizes with SI in sub-apical compartments. This result strongly suggests that apical membrane proteins are internalized at high rate via the endocytic pathway. Digestive enzymes are normally highly stable at the apex, illustrated by a very low rate of basal endocytosis and recycling in the intestinal epithelium (Matter et al., 1990; Hansen et al., 2009). Would basal rate of endocytosis be increased in VEP$^{-/-}$ mice? Using vital membrane dye, we rule out this possibility. It is thus likely that defective retention at the membrane of apical proteins causes their high internalization.

Actin cytoskeleton and stabilization of proteins at the membrane.

In polarized cells, several examples of membrane stabilization by the actin cytoskeleton have been reported. At the basolateral pole, the adaptor protein ankyrin mediates attachment of Na/K ATPase to the spectrin-actin cytoskeleton ensuring stabilization of the pump in membrane sub-domains (Nelson and Veshnock, 1987; Morrow et al., 1989). At the cell apex, the scaffolding protein NHERF links membrane proteins with ezrin to provide an anchor in the actin cytoskeleton. In particular, this scaffold limits membrane diffusion of the Na/H exchanger (Cha et al., 2004), and enhances apical concentration of a spliced variant of the plasma membrane Ca^{2+} pump (Padányi et al., 2010). In an analog manner, by virtue of its ability to link the actin cytoskeleton to the plasma membrane, myosin-1a has been proposed to anchor SI molecules to the actin bundle thereby increasing their stability at the membrane. Interfering with myosin-1a indeed leads to a mislocalization of SI in cell culture and in the mouse (Tyska and Mooseker, 2004; Tyska et al., 2005). Myosin-1a strong mislocalization in the absence of a structured actin network provides good evidence of the general mechanism at the origin of the retention defects. However myosin-1a knockout animals grow normally and IAP localizes normally, indicating a milder phenotype as compared to VEP$^{-/-}$ mice (Tyska et al., 2005). This mild phenotype was explained by a compensatory recruitment of other class I myosins at the brush border, in particular the isoforms 1c and 1d (Tyska et al., 2005; Benesh et al., 2010). This ectopic recruitment, which occurs solely in complete absence of myosin 1a, could be associated to differential actin binding affinities and competition for actin binding sites (Tyska et al., 2005; Benesh et al., 2010). In VEP$^{-/-}$ mice, similar ectopic recruitment is not observed. Thus the substantial loss of myosin-1a from brush border does not appear to be compensated. This

discrepancy with myosin-1a $^{-/-}$ mice suggests that the abnormality that affects the recruitment of myosin-1a could be structural, residing in the disorganization of the actin network, and would hence also perturb the recruitment of any other possible compensatory class I myosins, causing the apical defects observed.

Role of the microvillar actin core architecture in efficient recruitment of proteins.

Compared with single and double KO microvilli, those of VEP−/− mice demonstrate an additional structural defect: the lack of detectable organization of actin filaments into a bundle. Could the actin architecture allow the selective binding of specific proteins? In the VEP$^{-/-}$ enterocytes, because myosin-1a is not efficiently recruited to the microvilli, myosins are of particular interest. Tropomyosins decorate certain portions of actin filaments and inhibit myosin activity (Fanning et al., 1994; Temm-Grove et al., 1998; Tang and Ostap, 2001; DesMarais et al., 2002). More directly, different classes of unconventional myosins select specific actin filaments subpopulation and thereby display distinct spatial distribution in the cell (Brawley and Rock, 2009). This has been linked in part to the inhibitory effect of some actin binding proteins (e.g. tropomyosins) and to the affinity of certain myosin isoforms for specific actin architecture (Brawley and Rock, 2009). In particular, the filopodium myosin X selects specifically bundled actin for processive movement (Nagy et al., 2008). Myosin X stepping pattern, which takes advantage of two close actin filaments, indeed appears particularly suited for movement on bundled actin (Ricca and Rock, 2010). The structure of the head and tail regions of myosin X likely governs this selectivity (Nagy and Rock, 2010). The authors of this study furthermore speculated that, due to the difficulty to predict such structures, other actin architecture-selective myosins are yet to be discovered. Another non-exclusive possible explanation could reside in the fact that the architecture and dynamics of the bundle regulate the differential concentration of actin-binding molecules in the bundle (Naoz et al., 2008). Indeed, the presence of actin bundling proteins strongly influences the stability of the actin proteins present in the bundle (Zigmond et al., 1992; Tilney et al., 2003; Prost et al., 2007). Loss of such bundle stabilization is therefore likely to modify the localization of myosins and other associated molecules (Naoz et al., 2008).

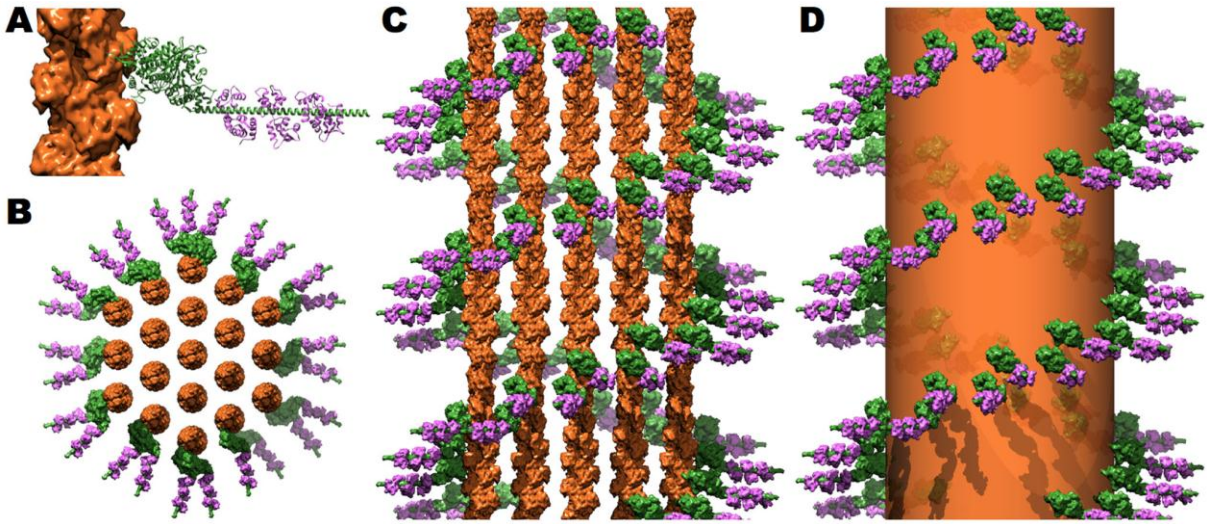

Figure 22: Structure of the myosin-1a / calmodulin cross-bridges.
A. Diagram of brush border myosin (green) with its three associated calmodulin light chains (purple) bound to actin (orange surface). B. When viewed down the long axis, the cross-bridges radially extend out from each outer filament in the core bundle. **C. and D**. When viewed from the side one may appreciate the barber-pole like motif of the cross-bridges about the actin core bundle (depicted as orange molecular surfaces in **C** and as a transparent orange cylinder in **D**. Adapted from Brown and McKnight, 2010.

Finally, the radial "barber pole" distribution of myosin-1a seems inherent to the microvillar bundle architecture. Indeed, *in vitro* addition of purified myosin-1a to actin bundles formed in presence of actin, villin, and plastin-1 results in a myosin-1a spiraling distribution comparable to that of lateral cross-bridges *in vivo* (Coluccio and Bretscher, 1989). Moreover, a 3D structural modeling of the microvillar cytoskeleton could strikingly reveal that the precise axial alignment of each microfilament together with their inherent helical arrangement lead to the regular exposition along the microvillus axis of spiraling myosin-1a binding sites towards the membrane (Brown and McKnight, 2010). Hindrance caused by the actin bundling proteins prevents myosin-1a binding to all other positions **(Figure 22)** (Brown and McKnight, 2010). Thus, myosin-1a precise distribution along the microvillar axis relies on the precise paracrystalline hexagonal arrangement of actin filaments together with the sterical hindrance generated by the bundlers.

In light of our results and these observations, we conclude that the function of actin-bundling proteins is not to power the morphogenesis of microvilli *per se* but rather to grant the actin network a precise architecture that allows the selective recruitment of proteins implicated in apical retention.

D.Limits and perspectives

The three actin bundling proteins are thus dispensable for the microvilli protrusions. However, we cannot totally exclude the possibility that a fourth, previously unidentified or unknown, actin bundling protein could provide the remaining organization found in the microvillar cores of VEP$^{-/-}$ mice. In particular, shortly after finishing the reviewing process, actin bundling properties in histone H2A-H2B and eukaryotic elongation factor 1 alpha (eEF1A) were reported (Doyle et al., 2011). Interestingly, in our extensive proteomic study we could detect a significant amount of peptides belonging to these two proteins. Thus, the possibility of additional actin bundlers in microvilli remains an open question that will require further experimental work.

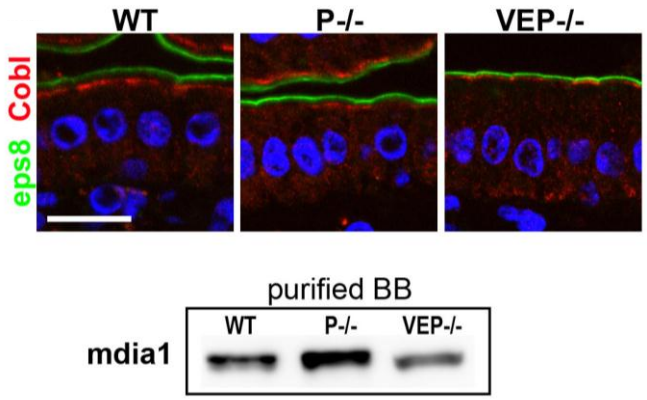

Figure 23: Identification of two actin nucleators in the brush border fraction
Immunostainings and western blots on WT, P$^{-/-}$ and VEP$^{-/-}$ samples.
Analysis of the nucleators of parallel actin networks detected by mass spectrometry in WT, P$^{-/-}$ and VEP$^{-/-}$ enterocytes. Immunostainings for cordon-bleu (Cobl) counterstained with Eps8 to identify microvilli tips (top) show a terminal web localisation of the nucleator in all samples. Scale bar 10µm. Immunoblots against mDia1 performed on isolated brush border lysates loaded for equal protein content (bottom) confirming its presence in the brush borders of the 3 samples.

Another intriguing outcome of this study consists of the proteomic identification of two nucleators of linear actin filaments in the brush border fraction: cordon-bleu and diaphanous homologue 1 (mDia1) **(Table 1 page 65, Figure 23)**. To date, the nucleation process that initiates microvilli assembly is unknown. By immunohistochemistry I could notice that cordon-bleu localized to the terminal web region and not to the tips of microvilli **(Figure 23)**, indicating that this protein is unlikely to have a role in initiating the actin filaments that support the microvilli protrusion. The presence of the formin diaphanous homologue 1, mDia1, could be confirmed by western blotting **(Figure 23)**, but the lack of antibodies suitable for immunofluorescence prevented from addressing its localization. Owing to its ability to nucleate and subsequently processively elongate actin filaments (Campellone and Welch, 2010), mDia1 thus appears to be a good candidate to initiate microvillar actin filaments. Recently, the adenomatous polyposis coli protein – APC – has been demonstrated to display on its C-terminal domain a potent actin nucleation property, which interestingly synergizes with mDia1 (Okada et al., 2010; Breitsprecher et al., 2012). In mouse colonic epithelium and in cultivated polarized

cells, APC seems to concentrate at the apex (Reinacher-Schick and Gumbiner, 2001; Rosin-Arbesfeld et al., 2001; Hughes et al., 2002; Marshall et al., 2011), albeit conflicting results exist (Näthke et al., 1996; Brocardo et al., 2005). At this point, we should also mention that APC peptides could not be detected by mass spectrometry in our analysis. Thus, mDia1, possibly in synergy with APC – if both present in the tip complex – conceivably could be important players in microvilli biogenesis.

The recent identification of a novel family of factors generating membrane curvature provided new insights on the initiation of membrane deformations: the Bin-amphiphysin-Rvs - BAR – proteins. The family has been divided in two subclasses depending on the orientation of the resulting curvature owing to their respective structural geometry, F-BAR proteins induce invagination of the membrane whereas I-BAR proteins generate membrane extrusions (Zhao et al., 2011). I-BAR proteins are thus particularly good candidates to initiate the early steps of deformation for the plasma membrane to protrude. I-BAR domains proteins are furthermore critical to organize scaffolds at the protrusions tips, allowing tight regulation of actin assembly (Ahmed et al., 2010). We could identify three I-BAR proteins from our mass spectrometry analyses performed on enriched brush border fraction: MIM, IRSp53 and IRTKS. Missing-in-metastasis – MIM - is essential for epithelial integrity in the kidney (Saarikangas et al., 2011). Lack of MIM indeed induces profound defects in intercellular junctions. Brush border is however unaffected in the proximal tubule cells (Saarikangas et al., 2011). The insulin receptor tyrosine kinase substrate p53 - IRSp53 - has prominent role during filopodia formation (Krugmann et al., 2001). We could not confirm the expression of IRSp53 in the small intestine by western blot. On the other hand, IRSp53 is expressed in the colon and concentrates in the brush border. In collaboration with the laboratory of Giorgio Scita we could have access to tissues from IRSp53 null mice. A preliminary electron microscopy analysis of the colonic tissue in absence of IRSp53 did not reveal any obvious defect of the apical microvilli. Therefore, MIM and IRSp53 unlikely play prominent role in the initiation of intestinal microvilli. Finally, the IRSp53-like insulin receptor tyrosine kinase substrate - IRTKS - has been less extensively characterized in the literature (Millard et al., 2007). As Giorgio Scita gratefully provided us with antibodies against IRTKS, an initial expression and localization study is planned.

Concerning the physiological defect, we were able to link the growth retardation phenotype to defective localization of various digestive and absorptive components and more directly to impaired glucose absorption. We could however not identify a defect in the distribution of a membrane bound glucose transporter.

Finally, we conclude our study proposing that in $VEP^{-/-}$ mice, apical membrane hydrolases and transporters are internalized at higher rates via normal endocytic pathway. This still needs formal demonstration using, for instance, biotinylation of exposed protein to monitor their internalization.

II/ Villin and cell plasticity

A. Villin, a multifunctional actin-binding protein

The second aim of this PhD work consists on investigating another important aspect of intestinal microvilli: their plasticity. Indeed, microvilli plasticity is associated with diverse stress contexts in the intestinal epithelium and likely depends on actin regulation by actin binding proteins. In contrast with the other actin bundling proteins, villin exhibits additional actin related properties: capping, nucleating and severing. In view of these unique properties, villin appears as a strong candidate to exert various regulatory functions within microvilli, besides a structural role. *In vitro*, villin preferentially bundles actin filaments at very low calcium concentration - below 10^{-7} M -, nucleates and caps filaments above 1 µM and finally acts as a F-actin severing protein when Ca^{2+} reaches 100 µM **(Figure 24)** (Bretscher and Weber, 1980b; Glenney et al., 1980; Walsh et al., 1984). Maximal severing efficiency is achieved at 400 µM (Northrop et al., 1986). In addition, phosphorylation on tyrosine residues changes villin conformation leading to inhibition of actin bundling and activation of its severing property at nanomolar Ca^{2+} concentration (Zhai et al., 2001; Kumar and Khurana, 2004). Villin also binds to phosphatidylinositol 4,5-bisphosphate (PIP_2) and this interaction favors actin bundling and inhibits the severing property (Kumar et al., 2004). Thus, various intracellular signals tightly regulate villin functions.

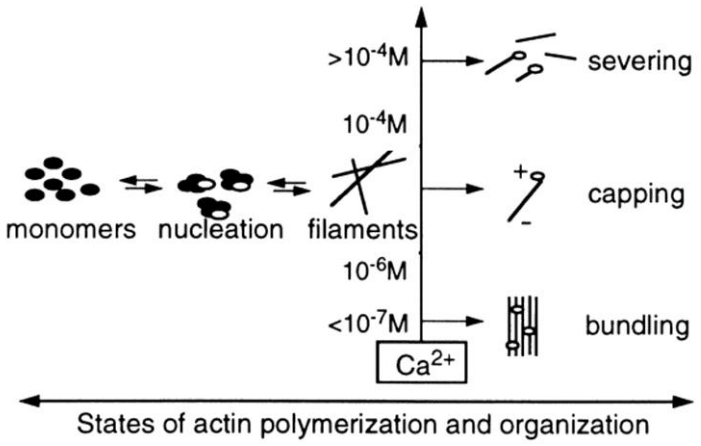

Figure 24: Calcium concentration regulates villin activities
Adapted from Ferrary et al., 1999.

The identification of the Ca^{2+} dependent actin severing property raised numerous interrogations concerning villin potential implication in microvilli cytoskeleton dynamics. In particular, villin has early been proposed to regulate microvilli assembly and disassembly (Glenney et al., 1981c). On demembranated microvilli cytoskeleton, rise in calcium concentration in the micromolar range results in the rapid collapse of the actin bundle (Glenney et al., 1980; Howe et al., 1980; Mooseker et al., 1980; Burgess and Prum, 1982). Villin was later on proposed to mediate this actin bundle breakdown by its actin severing activity (Matsudaira and Burgess, 1982b). The bundle loss leads to the destruction of the overall microvillus structure, which vesiculates (Burgess and Prum, 1982; Matsudaira and Burgess, 1982b). The presence in high amount of the calcium binding protein calmodulin, as part of the myosin-1a based cross bridges, was proposed to buffer free calcium ions within the microvilli thereby protecting the actin bundle from uncontrolled villin severing activity (Glenney et al., 1980; Glenney and Glenney, 1985). In response to Ca^{2+} signaling, villin might govern microvilli fate during physiological events. Indeed, although static in appearance, microvilli are highly dynamic structures, which rapidly retract, or even completely disassemble upon various intestinal stresses (nutrition, pathogen infection, mechanical stress....) (Tilney and Cardell, 1970; Rosenshine et al., 1996; Ferrary et al., 1999). Such cell shape changes could be important to grant intestinal cells with a certain plasticity. For instance, it has been speculated that microvilli disassembly could allow shuttling of short actin filaments within the cell (Glenney et al., 1981c).

Villin increases cellular dynamics.

Extensive analysis of villin null mice provided the first evidences supporting a role for villin severing activity during microvilli shape changes. The absence of detectable brush border structural defect in these mice clearly indicates that loss of villin bundling activity *in vivo* is dispensable or at least compensated (Pinson et al., 1998; Ferrary et al., 1999). Is it the case for villin severing activity? In contrast to brush borders isolated from wild type mice which show rapid disruption upon addition of Ca^{2+}, morphology of brush borders from villin null mice remain unchanged after Ca^{2+} stimulation (Ferrary et al., 1999). Our group hypothesized that villin severing property has a physiological relevance in the living animal. To investigate this possibility, different pharmaceutical and physiological strategies to increase Ca^{2+} concentration were used. In particular, treatment with the acetylcholine agonist carbachol causes a rapid rise in intracellular Ca^{2+} (Edelman et al., 1994) and results in villin tyrosine phosphorylation (Kumar

and Khurana, 2004). Carbachol basolateral infusion of isolated jejunal loops from anesthetized wild type mice leads to a substantial loss of brush border phalloidin labeling seen on histological sections, strongly suggesting microvilli disruption (Ferrary et al., 1999). Conversely, apical phalloidin labeling on sections from treated villin null mice remains unchanged. This result could be reproduced using other drugs rising Ca^{2+} concentration such as the Ca^{2+} ionophore A23187 or thapsigargin, a blocker of the endoplasmic reticulum Ca^{2+} ATPase (Ferrary et al., 1999). Nutritional stresses, e.g. fasting/refeeding, similarly induce increase in intracellular Ca^{2+} concentration presumably through the indirect action of catecholamines and digestive hormones (Ferrary et al., 1999). Accordingly, phalloidin staining on sections from fasted/refeeded villin null mice is unaffected whereas an important loss of the broad apical is observed on wild type mice (Ferrary et al., 1999). In conclusion, artificial or physiological rise in intracellular calcium possibly associated with villin phosphorylation induce microvillar F-actin severing resulting in major reorganization of the cell apices.

To further describe the villin null mice phenotype in relation to intestinal stress, our laboratory investigated the contribution of this protein during an experimental colitis induced by dextran sodium sulfate (DSS), an abrasive agent. The severity of the ulceration was directly linked to the phenotype: villin null mice show a higher sensitivity to DSS treatment as compared to wild type animals. Their poor survival rate correlates with higher mucosal destruction suggesting that villin is involved in cell injury and/or in epithelial repair (Ferrary et al., 1999). In light of these results and knowing that orchestrated movement of cells plays major role during wound healing in tissues (King and Newmark, 2012), villin was hypothesized to be a major factor involved in cell reorganization associated with cell motility. This hypothesis was however put into question as a recent study reported an increase of apoptosis in DSS treated villin null mice leading to the proposal of an anti-apoptotic role for villin (Wang et al., 2008a). The experimental procedure that was applied in these two studies nevertheless precluded discriminating whether villin influences tissue injury, as proposed by Wang and colleagues or rather repair, as suggested by Ferrary and colleagues.

B. Villin and cellular motion

Villin severing property enhances actin based motility.

Although villin potential role in cell survival has to be taken in consideration, the results presented above suggest that villin plays a key function during cell reorganization and migration on account of its F-actin severing property. A common experimental setup to study the contributions of actin binding proteins on migration consists on reconstituted systems of actin-based motility, which mostly recapitulate the *in vivo* machinery. These minimal systems are based on a core of proteins that ensure actin-based propulsion of enteropathogens, for example *Shigella flexneri*. During the infection process, *S. flexneri* subverts the host actin machinery to initiate its movement based on actin dynamics (Theriot et al., 1992). Indeed, the bacterium is propelled by an actin comet tail and propagates into adjacent enterocytes (Bernardini et al., 1989). On the outer membrane of the bacterium, the bacterial protein IcsA, binds to and recruit the Arp2/3 activator N-WASP. Thus, *S. flexneri* exploits the host protein Arp2/3 to generate a network of short branched filaments that polymerize at the bacterium surface thus providing the force required for its motion (Egile et al., 1999; Gouin et al., 1999). Success in reconstituting actin based movement *in vitro* using beads and a minimal set of pure proteins (Arp2/3, an activator of Arp2/3, a capping protein, actin and ADF) has been a major breakthrough (Loisel et al., 1999; van der Gucht et al., 2005). Indeed, the mechanistic similarities in terms of nucleation, actin dynamics and motility between lamellipodia and actin comet tails have proven these systems to be valuable tools to explore actin based motility. In particular, this system has been used to determine the contribution to actin dynamics of diverse actin binding proteins, including villin (Revenu et al., 2007). This system is particularly relevant since in newborn villin null mice, *S. flexneri* entrance and propagation is strongly reduced as compared to wild type animals. As a result, wild type mice die rapidly whereas villin null mice resist the infection (Athman et al., 2005). Interestingly, villin is recruited at the comet tail and its absence reduces the velocity of the bacterium (Athman et al., 2005). These results suggest a positive role of villin in actin dynamics. Could villin sever actin filaments within the comet tails thereby increasing actin dynamics?

To investigate the contribution of villin severing property, a loss of function approach was chosen. A set of mutations was designed resulting in a strong reduction of villin ability to sever F-actin. Most importantly, other actin related activities (i.e. capping, nucleating and bundling)

are preserved in the villin severing mutant, referred hereafter as villinΔsev. As a result, when expressed in cells, villinΔsev retains its morphogenetic effect; inducing a dense tuft of long microvilli on the dorsal cellular surface.

Actin based movement of S. flexneri revealed that the severing mutant abolishes the gain of bacteria velocity provided by villin. Furthermore, when villin replaces the capper on a reconstituted *in vitro* actin based movement assay, the severing activity enhances the velocity of the bead and reduces the actin density on the comet tail. These results suggest that villin severs F-actin and subsequently caps the newly formed barbed ends, thereby increasing the actin monomers available for polymerization (Revenu et al., 2007). In agreement with this hypothesis, *in vitro*, villin caps barbed ends released by F-actin severing, a process that favors actin depolymerization (Northrop et al., 1986). Could it be conceivable to transpose these findings in a migrating cell? Prior to discuss this aspect we will briefly depict how cellular movement is achieved.

How do cells generate movement?

We will here focus on the classical migration on 2D substrate as a monolayer constitutes the intestinal epithelium. The cellular processes driving cell migration in response to external cues have been reasonably well described.

The breakup of cellular symmetry and the subsequent generation of a front-rear polarity initiate the movement. At the cell front, the leading edge is characterized by the presence of a dynamic large membrane protrusion attached to the substrate: the lamellipodium. In the lamellipodium, the dynamics of the actin cytoskeleton, organized in a dendritic network, provide the mechanical force required to extend the cell front. This represents the first step of movement **(Figure 25)**. Arp2/3-mediated nucleation of new actin filaments ensures the recurrent extensions of the lamellipodium. In fact, the overall migratory edge, often abusively termed lamellipodium, is divided into two regions presenting different actin organization and dynamics: the lamellipodium and lamellum. The more distal part of the leading edge, referred as the lamellipodium, is predominantly composed of a dense 2D meshwork of branched actin filaments and presents high retrograde flow (Svitkina et al., 1997; Svitkina and Borisy, 1999; Ponti et al., 2004). Located a few micrometers backward, the lamellum is constituted by less organized actin filaments characterized by a slower actin retrograde flow (Svitkina et al., 1997; Svitkina and

Borisy, 1999; Ponti et al., 2004). Lamellum features stronger and more mature adhesions (Geiger et al., 2009). As we largely discussed the lamellipodium structure in the introduction, we will not give further details on this aspect herein.

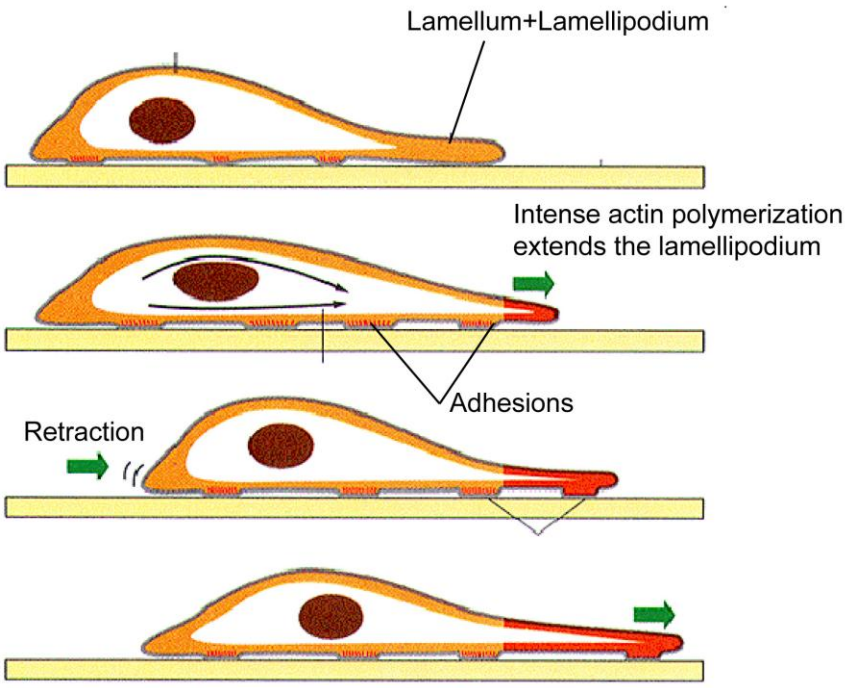

Figure 25: Cell migration is a stepwise process
Intense actin polymerization ensures the lamellipodium extension. New adhesions are formed at the leading edge. In the second step, rear adhesions disassemble allowing the cell translocation by contraction. Adapted from Ridley et al., 2003.

The second step of cell movement requires the formation of adhesions to anchor the cell to the substratum. At the cell leading edge, the lamellum couples the actin network with strong adhesions to the substrate, on which the cell pulls to move forward, owing to myosin II contractility **(Figure 25)** (Ponti et al., 2004). As movement occurs, the cell rear retracts to avoid cell disruption due to membrane tension. If front adhesions are too weak, cell contraction will cause the lamellipodium to bend upwards, detaching the leading edge from the substrate surface. This results in ruffling and transient retraction of the lamellipodium. Globally, adhesions assemble at the front and disassemble at the rear of the cells (Vicente-Manzanares et al., 2005). The precise coordination between lamellipodium extension and adhesion dynamics altogether with cell contraction orchestrate cell movement **(Figure 25)**.

Movement arises from cell shape changes dictated by cytoskeleton reorganization.

The actin cytoskeleton reorganization plays central role in migration since this process relies on cell shape changes and formation of actin-based membrane protrusions. The extensive cytoskeleton remodeling is largely governed by the rho family of small GTPases, which includes rho, rac and cdc42 (Nobes and Hall, 1995; Hall, 1998). Schematically, rho regulates stress fibers and adhesion assembly, while rac regulates lamellipodia protrusions and cdc42 triggers filopodia (Nobes and Hall, 1995; Hall, 1998, 2005). Their concerted regulation of cytoskeleton dynamics induces cell movement. Epithelial cells, due to the intrinsic nature of epithelia, move in a collective fashion, retaining cell-cell adhesions with their neighbors (Fenteany et al., 2000). Rho GTPases central role in epithelial cells movement has been reasonably well documented. Indeed, in intestinal cells, the requirement of rac- and rho-mediated cytoskeletal changes to drive efficient migration has been nicely described (Santos et al., 1997; Fenteany et al., 2000; Cetin et al., 2004; Dise et al., 2008). Cdc42 has a critical role in the directional polarization of moving intestinal cells, in accordance to what has been reported in other cell types (Stowers et al., 1995; Koch et al., 2009). Nevertheless, only rac inhibition abolishes cell movement while rho and cdc42 are accessory (Fenteany et al., 2000). A common major downstream effector of rho and rac is the actin depolymerizing/severing protein cofilin, which is critical to elicit actin reorganization (Carlier et al., 1997; Lawler, 1999; Mouneimne et al., 2006; Hopkins et al., 2007).

How to study intestinal cell migration *in vitro*?

The difficulty to follow migration *in vivo* in a dynamic fashion in an unexposed organ such as the gut prevents detailed functional analysis. To overcome this limitation, a widely used technique is represented by the wound healing assay, which consists on scratching a monolayer of cultivated cells to mimic tissue injury. Interestingly, in such system cell proliferation plays little role in migration, the closure of wounds instead relies solely on migration (Farooqui and Fenteany, 2005; Poujade et al., 2007). Furthermore, characterization of the migration profile revealed that movement of the monolayer does not occur uniformly, but rather involves very active “leader” cells, which develop a large lamellipodium and precede a small cohort of cells, thus forming extrusions – or “fingers” - of cells breaking the regular border. In addition, “leader cells” present a highly remodeled shape (Poujade et al., 2007). The progression of the “fingers” is entirely dependent on the leader cells (Reffay et al., 2011). Nevertheless, cells behind the margin, even located far away, extend cryptic lamellipodia towards the wound edge below the

front cells (Farooqui and Fenteany, 2005). Moreover, rac inhibition in the first row of cells is not sufficient to abrogate cell movement (Fenteany et al., 2000). These results suggest an overall participation of the cells that constitute the monolayer to the wound closure process. Cell migration associates with major cell shape changes: cells in front extend lamellipodia while undergoing apical pole reorganization. In particular, several proteins that concentrate on the cell apex are delocalized as the cell migrates (Nusrat et al., 1992; Lotz et al., 2000; Hopkins et al., 2007; Seltana et al., 2010; Chandhoke and Mooseker, 2012). Interestingly, a major disassembly of microvilli occurs on intestinal migrating cells, correlating with a substantial loss of apical F-actin (Nusrat et al., 1992; Chandhoke and Mooseker, 2012). At the lamellipodium, villin and actin concentrate, an observation that suggests a possible role for villin in actin dynamics within these structures (Nusrat et al., 1992; Athman et al., 2003).

Villin positively regulates cell migration in response to stimuli, in cell culture.

The original finding of the increased sensitivity to intestinal injuries in villin null mice was particularly intriguing and led to further investigate villin potential implication in cell migration. In isolated murine enterocytes and in canine renal MDCK cells, villin increases migration efficiency in response to hepatocyte growth factor (HGF) (Athman et al., 2003). HGF, which binds to the c-Met receptor, was originally identified as scatter factor and reported to disrupt epithelial cell-cell interaction leading to individual cell scattering (Gherardi et al., 1989; Bottaro et al., 1991). c-Met activation leads to PLC_{γ} hydrolysis of phosphoinositides, which ultimately raises intracellular Ca^{2+} (Mine et al., 1991; Gual et al., 2000). Interestingly, upon HGF stimulation villin expressing MDCK cells present a higher G/F actin ratio at the leading edge as compared to MDCK wild type cells (Athman et al., 2003). In contrast to HGF-induced cell migration, most of the epithelial cells, including the intestinal tissue, retain cell-cell contact when migrating. On this aspect, villin positive role in cell migration could be confirmed on more relevant wound healing assays induced by monolayer scratches (Tomar et al., 2004, 2006; Wang et al., 2007; Mathew et al., 2008).

Regarding the biochemistry of signaling governing villin role in cell migration, an important contribution was provided by the laboratory of Seema Khurana leading to the following model presented in **Figure 26**: at steady state, villin would bind to the plasma membrane and preferentially bundle F-actin by virtue of its strong affinity for PIP_2 (Kumar et al., 2004). Villin would furthermore sequester PIP_2 from its natural ligand $PLC_{\gamma}1$ as villin presents a higher

affinity for PIP_2 than $PLC_\gamma1$ (Kumar et al., 2004). In response to external stimuli (e.g. binding of HGF or EGF to their receptor) villin would be tyrosine phosphorylated, possibly by the c-Src kinase, favoring its actin severing property (Zhai et al., 2002; Tomar et al., 2004; Khurana and George, 2008; Mathew et al., 2008). Villin phosphorylation additionally reduces its affinity for PIP_2 and triggers its association with the SH2 domain of $PLC_\gamma1$ resulting in the catalytic activation of the phospholipase (Panebra et al., 2001; Kumar et al., 2004; Tomar et al., 2006; Wang et al., 2007). These biochemical properties would induce $PLC_\gamma1$ competitive binding to PIP_2 at the plasma membrane. Activated $PLC_\gamma1$ catalyzes the formation of diacylglycerol (DAG) and inositol 1,4,5-trisphosphate (IP_3) from PIP_2, which results in calcium release from the endoplasmic reticulum thus further enhancing villin-mediated F-actin severing. Overall, F-actin severing close to the plasma membrane would generate an abundant supply of barbed ends thereby favoring the intense actin polymerization required for lamellipodium generation and ultimately cell migration. This spatial control of actin dynamics would allow the generation of motility organelles in the direction of the movement thus promoting a crucial property of cell migration: the ability of the cells to move in a directional fashion. Thus, if the aforementioned model is correct, one would expect that loss of villin would abrogate epithelial cell ability to move or at least severely impede directional migration. Experimental data argue against this proposal as villin depletion in the human colorectal Caco-2 and in the porcine proximal kidney LLC-PK1 cell lines results in modest decrease of migration efficiency (Wang et al., 2007; Mathew et al., 2008). Furthermore, villin depleted cells still extend lamellipodia and data showing directionality defects has never been reported.

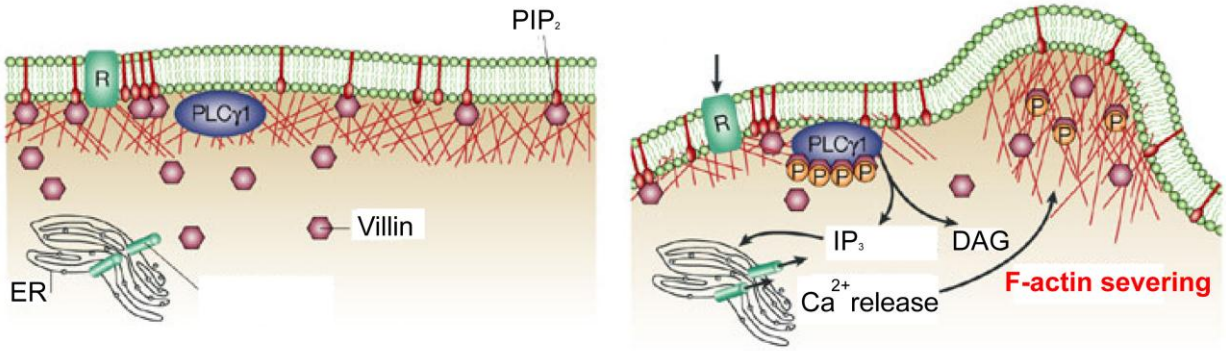

Figure 26: Model of villin regulation in actin remodeling at the membrane
The left diagram focuses on the membrane of a resting cell. A pool of villin associates with PIP_2 at the membrane. Following stimulation of membrane receptors (R) some villin molecules are tyrosine phosphorylated and associate with phospholipase C1 ($PLC_\gamma1$), leading to its activation. Villin phosphorylation favors its severing activity. Activated $PLC_\gamma1$ cleaves PIP_2 into DAG and IP_3, which in turn induces Ca^{2+} release from stores in the endoplasmic reticulum (ER). The increase in intracellular Ca^{2+} concentration additionally favors villin F-actin severing activity (right diagram. Adapted from Revenu et al., 2004.

Villin expression is mainly restricted to cells harboring a brush border (Robine et al., 1985). In addition, the vast majority of villin molecules are concentrated in the apical microvilli, which do not face the direction of the movement. Villin specific localization and its role in microvilli shape regulation associated with stress events raise the possibility of an additional function for villin at the apical pole during cell migration besides its hypothesized role in the cellular motility machinery. We propose that villin participates in the apical pole remodeling associated with cell migration.

Epithelia in motion.

If our hypothesis is correct, it implies that similar cell reorganization occur in the intestinal cells in movement. Migration in response to injury is fundamental to the intestinal epithelium. This tissue is indeed continuously subject to numerous restricted injuries induced by toxic luminal substances, inflammation, infections or oxidative stress, which overwhelm the barrier function (Blikslager et al., 2007; Sturm, 2008; Iizuka and Konno, 2011). Following injury, intestinal repair is ensured by a balance of migration and proliferation that takes place in a precise coordination of sequential event. Immediately after the injury, the whole villi structure contracts to limit exposure to noxious luminal content (Moore et al., 1989b; Grootjans et al., 2011). Villi contraction appears to result from myosin II activation, by the myosin light chain kinase, in the muscle fibers of the basement membrane (Grootjans et al., 2011). Within minutes, the lesion-adjacent cells migrate to cover the denuded area in a process referred as restitution (Moore et al., 1989a; Albers et al., 1995, 1996). When the two sheets converge, the tight junctions reassemble to terminate epithelium resealing and to restore the protective barrier function of the organ (Gookin et al., 2003). At longer term, increased cell proliferation allows the regeneration of the tissue.

How to study wound healing in the gut? Despite its difficult access, several *in vivo* approaches have been developed. The more classically used is based on the abrasive agent dextran sodium sulfate (DSS), which induces ample ulceration of the colonic mucosa mimicking colitis. Recently, an endoscopic system adapted to small animals has proven to be a valuable tool to study the biology of colon-healing. Indeed, this apparatus allows to generate tissular injuries in the colon using biopsy forceps and to dynamically monitor the healing process (Pickert et al., 2009; Seno et al., 2009). In these models of injuries, the importance of lesions and the experimental time scale however restrain detailed analysis of the early cell restitution. Finally,

restricted injuries limited to a few cells at the villi tips, can be induced by luminal infusion of detergents or bile salts (Moore et al., 1989a; Masuda et al., 2003) allowing to study the cell restitution process. Since few functional data are available, our comprehension of this early event is limited. On the other hand, the morphological changes of the epithelium in restitution have been well documented. Indeed, within minutes injury-adjacent cells progressively lose their columnar phenotype and flatten (Moore et al., 1989a). This cell shape change strikingly correlates with deep structural alterations at the apex as shown by loss of several apical markers (Albers et al., 1995, 1996). In fact, these apical markers - F-actin, sucrase-isomaltase, villin - are specifically concentrated in microvilli; their exclusion from the apex suggests microvilli disassembly. Indeed, electron microscopy reveals an almost complete collapse of microvilli on migrating enterocytes (Albers et al., 1995; Masuda et al., 2003). These observations strikingly resemble the apical reorganization reported during cell migration in culture. Within a few hours the villi structures are completely recovered by intestinal cells (Moore et al., 1989a). As expected, the actin cytoskeleton plays major role during these processes. Indeed, on injured intestine treated with cytochalasin D, the migrating enterocytes do not present the aforementioned shape changes and the resealing of the epithelium is abolished (Albers et al., 1996). In view of these observations, the terms of de-differentiation or epithelial-to-mesenchymal transition (EMT) have been proposed to characterize this loss of defined apico-basal polarity. The words differentiation and EMT often imply changes in genes expression. Considering the short time scale of these changes it is very likely that the cell to become motile rather re-distributes already synthesized cellular components instead of relying on *de novo* protein synthesis. In addition, due to their intrinsic nature, epithelial cells retain cell-cell adhesion while migrating, differing in that from a true EMT process. We would prefer to nomenclature this migrating process as an adoption of a motile phenotype.

Movement of intestinal cells in response to a wound thus involves a major apex remodeling, which interestingly seems not to be specific to intestinal tissues. For instance, on their apical surface, respiratory, corneal and retinal pigment polarized epithelia display numerous short microvilli that are disassembled on cells migrating in response to injury (Haik and Zimny, 1977; Oganesian et al., 1997; Sacco et al., 2004). Since apical reorganization appears to be a hallmark of polarized epithelia in motion, it suggests that such cell reorganization promote migration. Molecules that execute apical pole remodeling thus likely play critical role in migration of polarized epithelial cells, which have to quickly evolve from an apico-basal to a front-rear polarity. Considering the different points raised above, we hypothesized that villin mediates

microvilli effacement thereby promoting migration. Although this idea was suggested in several studies in the past, the lack of functional tools precluded any formal demonstration. Taking advantage of the villin severing mutant previously described, we were able to directly address this issue, using cell culture and animal models. In the material and methods section, I will first briefly depict the procedures that were followed to complete the experimental work before describing the results that I obtained.

C.Material and methods

Mice generation

The mice were generated by Speedy Mouse® Technology (Nucleis, France) to produce a single copy transgene insertion at the *hprt* locus. The villin sequences were cloned into the pCAGloxCATlox transgenesis vector under the ubiquitous cytomegalovirus immediate-early enhancer chicken β-actin hybrid (CAG) promoter (D. Vignjevic) **(Figure 27)**. The transgene was then transferred by the Gateway technology into a destination vector pDEST-HPRT (Nucleis) carrying two homologous arms of the *hprt* gene. The vector was linearized using PvuI and electroporated into *hprt*-deficient BPES-embryonic stem (ES) cells by standard methods. The targeting construct contained the missing sequences in BPES-ES cells and two regions of homology of the *hprt* gene, which allowed insertion of the transgene at this locus. The targeted ES clones were efficiently selected, thanks to the restoration of the ability to grow in hypoxanthine-aminopterin-thymidine (HAT) medium through a correct homologous recombination. Genotyping of HAT-resistant ES clones was performed by PCR analysis of genomic DNA using a forward primer from the eCFP gene, 181CFP.F 5′-CTCGTGACCACCTTCGGCT-3′ and a reverse primer from the poly(A) sequence, SV40polyA_45pb.m 5′-GTTTCAGGTTCAGGGGGAGG-3′. Samples were amplified for 30 cycles, each consisting of denaturation at 94 °C for 40 s, annealing at 60 °C for 40 s, and elongation at 72 °C for 40 s. Targeted ES cells were injected into C57BL/6-derived blastocysts that were then transplanted into the uteri of recipient females. Resulting chimeric males were bred with C57BL/6 females.

Tamoxifen injection

Plasmid recombination was induced by chronic tamoxifen injections. Briefly mice, including controls were injected were injected intraperitonally with tamoxifen (50 μg/g of animal body weight) for 2 consecutive days/week for a total of 4 weeks.

Genotyping

Mice genotypes were determined by PCR on genomic DNA extracted from mouse tail tips. Villin knockout was assessed using the following oligonucleotides: 5’ GGA AAC CCG ATA GTA TCC TG 3’ and 5’ GAC TAC ATA GCA GTC ACC ATC G 3 amplifying a fragment of the villin knockout allele’; 5’ CGA ATT CGC CAA TGA CAA GAC 3’ and 5’ GAC TAC ATA GCA GTC ACC ATC G 3 amplifying a fragment of villin wild type allele. A fragment of the mCherry-villin plasmid was amplified with : 5’ CCA GAC CGT TCA GCT GGA TAT TAC GGC CTT 3’ and 5’ CCT GAA TCG CCA GCG GCA TCA GCA 3’ Finally, pvillin-creERT2 transgene was determined using the following oligonucleotides: 5’ CAA GCC TGG CTC GAC GGC C 3’ and 5’ CGC GAA CAT CTT CAG GTT CT 3’.

Image analysis

All images were processed and pseudocolored using ImageJ (National Institutes of Health). Measurements and analyses were performed using the same software. Images comparing different genotypes or experimental conditions were acquired and post-processed with identical parameters.

Tissue cell lysis and western blotting

The intestine of adult mice was isolated and divided into three parts of identical length corresponding to the duodenum, jejunum, and ileum. For particular experiments, the colon was isolated and divided in two parts of identical length corresponding to proximal and distal colon. Frozen jejunal or colonic tissues were homogenized with a Dounce homogenizer in a solution containing 50 mM Tris- HCl (pH 7.5), 150 mM NaCl, 20 mM MgCl2, 5 mM EDTA, 1% Triton X-100, 1% NP-40, 0.5% SDS, and protease inhibitor cocktail (Sigma-Aldrich, St. Louis, MO).

Cells grown at confluence were lysed in the same lysis solution. Proteins were extracted after centrifugation at 15,000 × g for 10 min at 4°C. Thirty micrograms of total protein was used for electrophoresis on 7.5% SDS-polyacrylamide gels under reducing conditions, and transferred to a nitrocellulose membrane using standard procedures. Immunogens were visualized using the enhanced chemiluminescence method (Thermo Scientific, Lafayette, CO). Densitometry measurements were carried out using the software ImageJ and normalized to the loading controls. The antibodies used in this study are: anti-ezrin (from M. Arpin), anti-sucrase-isomaltase (B. Nichols), anti-villin (from our laboratory), anti-tubulin (Santa-Cruz), anti-βactin (Cell Signaling), anti-Ecadherin (BD Biosciences), anti-cleaved caspase 3 (Cell Signaling).

Sampling and preparation of the tissues for histological analyses

Short pieces of intestinal or colonic samples were washed with phosphate-buffered saline (PBS). To prepare tissue for paraffin sectioning, tissues were fixed in 4% paraformaldehyde (PFA) or in Carnoy solution (60% ethanol, 30% chloroform and 10% acetic acid), 2 h at room temperature or overnight at 4°C. The samples were then ethanol dehydrated and embedded in paraffin. For frozen sections, tissues were fixed for 2 h in PFA 4% and incubated overnight in a 30% glucose solution diluted in PBS, or snap frozen in 2methylbutane precooled by liquid nitrogen. They were then embedded in optimal cutting temperature medium (OCT) and frozen at −80°C.

Immunohistochemistry

Histological sections of 5 or 8 μm were prepared from paraffin- or OCT-embedded tissues depending on the experiment. For paraffin sections, paraffin was removed by two 5 min washes in xylene. Sections were then hydrated with ethanol solutions of decreasing concentrations. Unmasking of the epitopes was performed by boiling for 20 min in Antigen Unmasking Solution (Vector Laboratories, Burlingame, CA). For frozen sections, OCT was removed by several PBS washes. OCT-embedded snap frozen tissues were post-fixed in 4% PFA for 20 min. Sections were incubated for 45 min at room temperature in blocking buffer (3% fetal calf serum [FCS] in PBS) and then overnight at 4°C with primary antibody (see above) diluted in 3% FCS or Phalloidin-Alexa488 (Invitrogen) diluted in PBS alone. After several washes, secondary fluorescent antibody was added for 90 min. Representative images from immunostainings were

acquired using an Apotome system with a 10× or 63× water Plan-Apochromat lens (Zeiss, Jena, Germany) or CM60 epifluorescence microscope (Leica) or an inverted confocal spinning disk microscope Eclipse Ti Roper/Nikon, all coupled to a Coolsnap HQ2 camera (Photometrics).

In vivo experiments

Experiments were carried out on sex-matched mice (for the transgenic mice) of similar age. For living animal experiments, anesthesias were performed by injection of a ketamine/xylazine mix (100 mg/ml each) diluted in 150 mM NaCl. Mice were killed at the end of experiments by cervical dislocation.

Carbachol treatment

After mouse anesthesia, a jejunum loop was in situ isolated, taking care not to injure the local vasculature. The loop was carefully placed in a Petri dish containing 10 μM carbachol (Sigma Chemical Co.) solution diluted in PBS plus Ca^{2+} (10 mM) for 20 min to achieve a basolateral infusion of the drug. After mouse sacrifice, small samples of treated tissue were washed and snap frozen in precooled 2methylbutane. Experiment was repeated at least in three different animals per genotype. For a more detailed protocol, see Ferrary et al., 1999.

Procedure for biopsy induced injury and mouse endoscopy.

A straight-type rigid miniature endoscope Coloview mouse endoscopic system (Karl-Storz) linked to an Archos 48 tablet (Archos) for video acquisition was used to visualize mouse colon. Images were extracted from acquired videos using VLC software (VideoLAN). After mouse anesthesia, the endoscope probe was introduced to the mid-descending colon. Then, a flexible 3-French biopsy forceps was inserted and used to remove an area of the entire mucosa and submucosa avoiding penetration of the muscularis propria. Particular care was taken to generate lesions of comparable size. Tissue healing was then monitored by endoscopy at day 3 and 7 post-injury. Tissue healing process was quantified by measuring the wounded area using ImageJ on extracted images. The images were very cautiously chosen to show similar viewpoints in term of endoscopy camera orientation and distance from the injury. For tissue analysis, injured area was

localized with the endoscopic probe on sacrificed mice. Corresponding colon segment was then sampled and processed for immunohistochemistry. The number of mice analyzed is described in the results.

Bile salt induced injuries

Following mouse anesthesia, a small incision was performed to allow access to the small intestine. Two knots were made using surgical suture thread to isolate a small intestinal segment. Particular caution was taken to avoid any damage to local vasculature. The intestinal loop was then filled with a sodium deoxycholate (DOC) solution diluted in PBS at 20mM and incubated at room temperature for 5min. After several washes with PBS, the segment was filled with Dulbecco's modified eagle's medium (DMEM) supplemented with 20% fetal bovine serum (FBS). Suture thread was then removed. Intestinal loop was carefully replaced inside the mouse and cell restitution was allowed for 30min. Treated tissue was then vigorously washed in PBS, fixed in Carboy solution and subsequently processed for immunohistochemistry. The number of mice analyzed is described in the results.

Plasmids

The mCherry-villin plasmids used in this study were described previously in Revenu et al, 2007. Actin-EYFP plasmid was obtained from Clontech. PA-GFP-actin plasmid developed in the Lippincott-Schwartz laboratory was given by D. Vignjevic. For endogenous villin depletion, plKO vector (Addgene) was used. Short hairpin RNA (shRNA) sequences specific for endogenous porcine villin were cloned inside the multiple cloning site and verified by sequencing. Two different hairpin sequences were used: shRNA1: Forward oligonucleotide :5' CCG GAA CCA GGC ACT GAA CTT TAT CCT CGA GGA TAA AGT TCA GTG CCT GGT TTT TTT G 3; reverse oligonucleotide: 5' AAT TCA AAA AAA CCA GGG CAC TGA ACT TTA TCC TCG AGG ATA AAG TTC AGT GCC TGG TT 3'. shRNA2: Forward oligonucleotide: 5' CCG GAA GCC AGC CAG GAT GAA ATC ACT CGA GTG ATT TCA TCC TGG CTG GCT TTT TTT G 3'; reverse oligonucleotide: 5' AAT TCA AAA AAA GCC AGC CAG GAT GAA ATC ACT CGA GTG ATT TCA TCC TGG CTG CTT 3'.

Cell culture and transfection

LLC-PK1 cells (CCL 101; American Type Culture Collection, Manassas, VA) were given by M. Arpin and grown in DMEM (Invitrogen) containing 10% fetal bovine serum. LLC-PK1 cells were transiently transfected by electroporation. The stable LLC-PK1 cell line expressing actin-EYFP was obtained through a clonal approach using cloning rings after selection by G418 (Invitrogen). This cell line was subsequently used to obtain cell lines depleted for endogenous villin and enriched in mCherry-villinWT or mCherry-villinΔsev expressing cells by fluorescence-activated cytometry cell sorting. Lentiviral particles were obtained by transfection of HEK293T cells with lentiviral vector in addition to pVSVG and pgag by Polyethylenimine (PEI) in a biosafety level 3 compliant laboratory. Medium containing viral particles was collected 48hrs post-transfection and filtrated using 0.44 µm sterile filters. One ml of medium containing viral particles was then added to $25*10^4$ LLC-PK1 cells seeded in 6 well plates. Following 24hrs of infection cells were vigorously washed and selected using Puromycin (Invitrogen). G418 was used at 500 µg/ml. Puromycin was used at 1µg/ml.

Wound healing assays

In all time lapse experiments further described cells were kept at 37° C and in a 5% $C0_2$ atmosphere during acquisition. For quantification of cell migration, $36*10^5$ cells were seeded and grown at confluence overnight in Ibidi small culture inserts (Ibidi) placed on glass bottom dishes. Cells were serum starved for 90 min with DMEM/F12 (without phenol red) medium and culture inserts were removed to induce cell migration. Medium was then replaced by DMEM/F12 (without phenol red) supplemented with 20% FBS. Then, wound healing process was monitored by time lapse video microscopy using a 10x CFI PLAN objective of an Eclipse Ti inverted widefield microscope allowing multipositional acquisitions (Nikon) coupled to a Coolsnap HQ2 camera (Photometrics). Wounded area colonized by the monolayer was carefully quantified at the different time points using ImageJ. All quantifications were carried out on data obtained in a same experiment including the different experimental conditions to be compared. For wound healing monitored at high resolution, cells were seeded and grown at confluence ($1*10^6$ cells) overnight in glass bottom dishes. Cells were serum starved with DMEM/F12 medium. Wounds were induced by scratching the cell monolayer with a 0.6g needle. After washing with medium, medium was replaced by DMEM/F12 (without phenol red) supplemented with 20% FBS. Then, time lapse image acquisition was performed using the 60x/1,4 OIL N2 PL

APO VC objective of an inverted confocal spinning disk microscope Eclipse Ti Roper/Nikon coupled to a Coolsnap HQ2 camera. Stacks of were acquired with a Z interval of 0.6 um. All experiments aforedescribed were performed at least three times.

Photo-activation experiments

LLC-PK1 cells depleted for endogenous villin (shRNA2) were co-transfected with PAGFP-actin and mCherry-VillinWT or mCherry-VillinΔsev plasmids. Following cells recovery, they were seeded at confluence (1*106 cells) in glass bottom dishes and grown overnight. Scratching assay was then performed as described earlier. Experiments were carried out using the 40x/1,3 OIL DICII PL APO objective of an inverted Laser Scanning Confocal LSM710NLO (Carl Zeiss) coupled with a Mai Tai 2 photon laser (Newport). Using the ZEN software (Carl Zeiss) a small region in the dorsal face of the cell was selected. Caution was taken to select regions of similar size in the different cells analyzed. A single pulse of 2 photon laser at 810nm wavelength (2*405nm) was burst in the region of interest to photo-activate PAGFP. Time lapse acquisition was performed using confocal mode with stacks of 1 µm Z interval. Acquired images were identically post-processed and denoised using the Copernic Denoising software (J. Boulanger).

D. Results

Generation and characterization of mCherry-villin transgenic mouse models.

To study at the cellular level the contribution of F-actin severing by villin during wound healing *in vivo* fluorescently tagged villin wild-type or mutated proteins was expressed in mouse enterocytes. Inducible transgenesis targeting vectors containing floxed mCherry-villin wild type (mCherry-villinWT) or a previously described mCherry-villin selectively mutated for its F-actin severing property (mCherry-villinΔsev) (Revenu et al., 2007) under a CAG ubiquitous promoter were constructed by Céline Revenu before my arrival **(Figure 27)**. Using Speedy Mouse® technology, mouse models carrying a single copy of the transgene inserted in the *hprt* locus were generated. By successive crosses with villin-creERT2 mice (el Marjou et al., 2004) in a villin null background, I generated mice carrying either villinWT and villin-creERT2 transgenes or villinΔsev and villin-creERT2 transgenes (referred to as tgvillinWT or tgvillinΔsev, respectively), allowing to study the function of villin and its severing mutant in absence of endogenous villin.

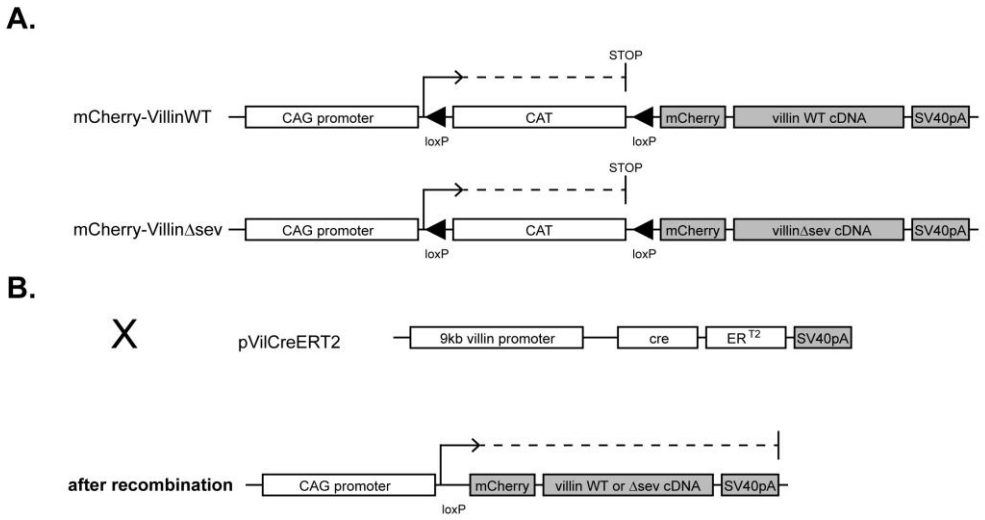

Figure 27: Schematic representation of the transgenesis plasmids

A. Schematic representation of the transgenesis plasmids. The mCherry-villin constructs are inserted into the multiple cloning site of the pCAGloxCATlox transgenesis plasmid driven by the CAG promoter (D. Vignjevic). Without recombination, the stop codon in the CAT sequence prevents transcription of the inserted constructs. **B.** Mice harboring the plasmids are crossed with mice expressing creERT2 under the villin promoter. Upon tamoxifen injection, recombination occurs in tissues where villin is expressed, leading to expression of the constructs.

The first important point consisted of describing these animal models. After tamoxifen induction, protein expressions were determined on protein extracts from jejunal and colonic tissues, revealing a single band of around 120 kDa in the total cell extracts, with comparable levels for both tgvillinWT and tgvillinΔsev mice **(Figure 28A)**. This molecular weight corresponds to villin (92.5 kDa) fused to the mCherry protein (around 30 kDa). A slight decrease of villin amount when compared to endogenous villin expression could be noticed **(Figure 27A)**. To evaluate the cellular distribution of both transgenic proteins, we analyzed the mCherry fluorescence on frozen histological sections that revealed a homogeneous signal along the villi axis in the small intestine and in the colonic tissues **(Figure 28B)**. This distribution is similar to the distribution of endogenous villin **(Figure 28B)**. At higher magnification, we observed a strong concentration of the mCherry-fused proteins at the apices of the enterocytes co-localizing with the intense apical F-actin brush border signal, as expected for villin **(Figure 28C)**. The two mouse models thus recapitulate expression and localization of the endogenous protein.

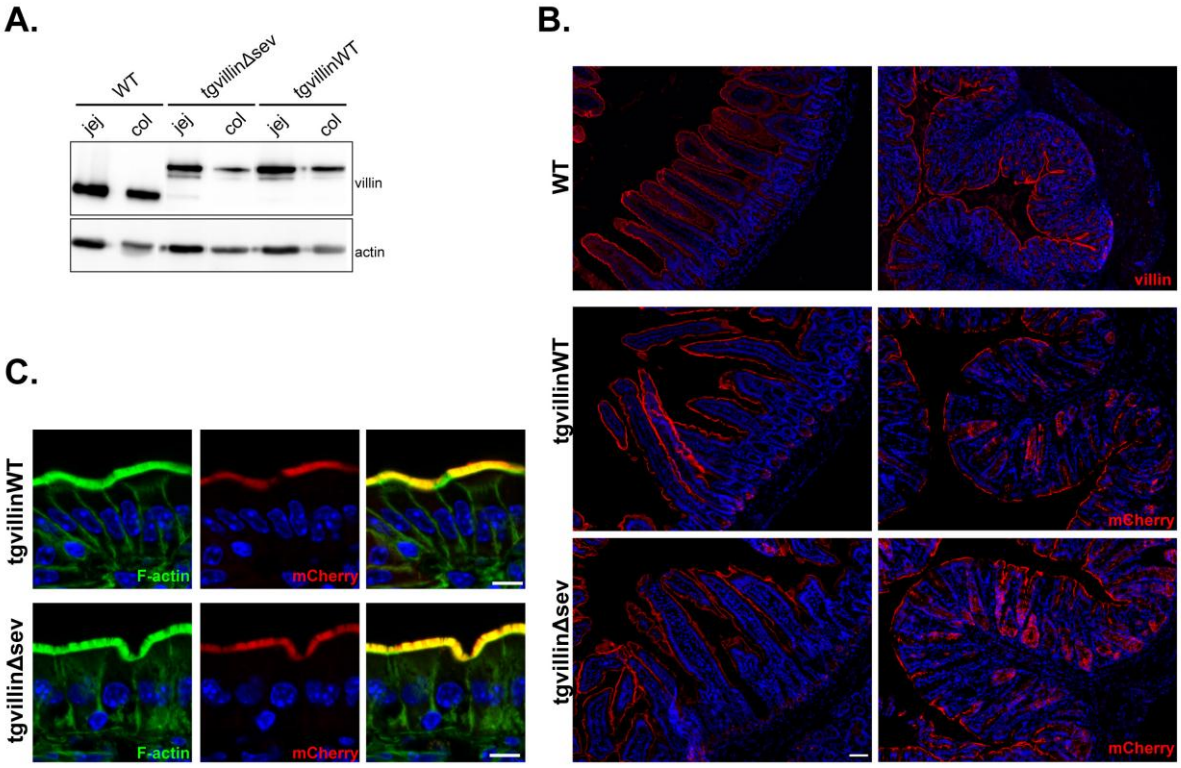

Figure 28: The transgenic mouse models recapitulate endogenous villin expression and distribution

A. Western blot against villin and actin on total extract from jejunum or colon of wild type (WT), villin knockout expressing transgenic wild type villin (tgvillinWT) or villin knockout expressing transgenic severing mutant villin (tgvillinΔsev) mice. The shift in villin molecular weight is due to the mCherry tag. **B.** Histological paraffin sections from jejunum stained for villin (red). Histological frozen sections from jejunum showing villin-mCherry fluorescence (red). DAPI labels nuclei (blue). Scale bar: 100 µm. **C.** Higher magnification of histological frozen sections of jejunum stained for F-actin by phalloidin (green). mCherry-villin fluorescence is shown (red). DAPI labels nuclei (blue). Scale bar: 10 µm.

mCherry-villin proteins are functional and villin-mediated F-actin severing is required for microvilli disassembly *in vivo*.

To assess *in vivo* the functionality of the transgenic proteins, basolateral infusion of carbachol was performed on isolated intestinal segments and F-actin distribution in enterocytes was analyzed on corresponding histological sections. This procedure increases intracellular calcium and induces the loss of the microvillar F-actin in a villin dependant manner (Ferrary et al., 1999). As previously described (Ferrary et al., 1999), the broad F-actin apical labeling of enterocytes was essentially lost on carbachol treated wild type animals, likely indicating a disruption of the brush border **(Figure 29A** and **C)**. Accordingly, apical actin staining width was strongly reduced on treated animals (2.28 ± 0.08 µm versus 0.54 ± 0.07 µm, t-test $p<0.001$). The remaining apical F-actin staining corresponds to the terminal web and junctional actin belt region. In contrast, the broad apical F-actin labeling was preserved on treated villin knockout animals (2.34 ± 0.07 µm versus 2.20 ± 0.10 µm, t-test $p>0.5$**) (Figure 29A** and **C)**. Importantly, carbachol exposure of tgvillinWT intestinal segments led to a striking reduction of the apical F-actin width (2.10 ± 0.09 µm versus 0.68 ± 0.05 µm, t-test $p<0.001$), restoring the wild-type behavior **(Figure 29B and C)**. Thus, mCherry-villinWT is functional *in vivo* and rescues the loss of endogenous villin. Conversely, carbachol-treated tgvillinΔsev mice did not present any alteration of apical phalloidin staining of enterocytes (2.08 ± 0.08 µm versus 1.92 ± 0.15 µm, t-test $p>0.5$) **(Figure 29B and C)**. These results therefore validate the functionality of the transgenes in the newly generated mouse models and demonstrate that *in vivo*, villin mediates carbachol induced microvillar F-actin disassembly through its severing property.

Efficient wound healing in the mouse colon requires F-actin severing by villin.

Villin has been proposed to be involved in cellular plasticity and survival following DSS induced lesions (Ferrary et al., 1999; Wang et al., 2008b). The high level of apoptosis in this system however hinders a precise analysis of epithelial restitution. To unambiguously clarify whether villin participates in gut wound healing beside an anti-apoptotic role, mechanical injuries were performed on the colonic mucosa in order to minimize potential biological side effects of DSS injuries. With the help of M. Chamaillard who owns such an apparatus, a biopsy forceps linked to an endoscopic system dedicated to small animal was used to create a discrete round-shaped millimeter-size injury in the distal part of the colon. This allows evaluation of the mucosal repair and its quantification by careful measurement of the injured area.

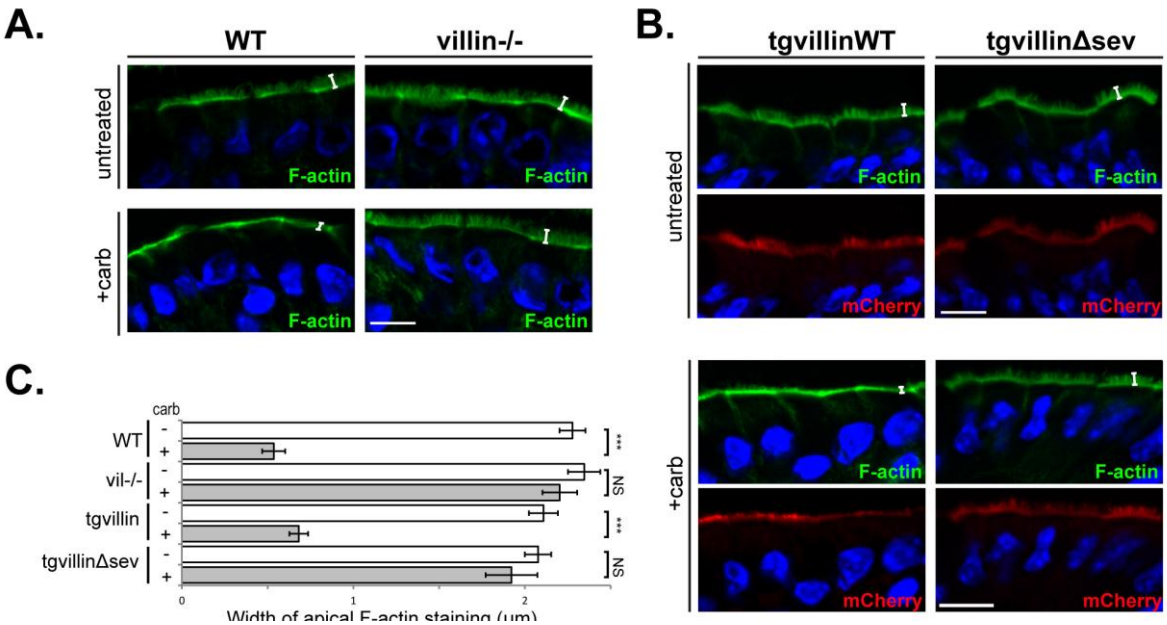

Figure 29: Transgenic villin proteins are functional and villin severing activity is required for brush border dissasembly upon carbachol treatment *in vivo*

A. and B. Histological frozen sections from untreated or carbachol treated (+carb) small intestines stained for F-actin by phalloidin (green). DAPI labels nuclei (blue). White brackets highlight the width of the F-actin concentration at the apex of the enterocytes. Scale bar: 10 µm. A. Sections from WT or villin-/- mice. B. Sections from tgvillinWT or tgvillinΔsev mice. mCherry-villin fluorescence is shown (red). **C.** Histogram depicting the width of the apical F-actin concentration of WT, vil-/-, tgvillinWT or tgvillinΔsev mice untreated or treated with carbachol. Width values (in µm) are: WT=2.28 ± 0.08; WT_{+carb}=0.54 ± 0.07; villin-/-=2.35 ± 0.09; villin-/-$_{+carb}$=2.20 ± 0,10; tgvillinWT= 2.10 ± 0,09; tgvillinWT$_{+carb}$= 0.68 ± 0.05; tgvillinΔsev=2.08 ± 0.08; tgvillinΔsev$_{+carb}$=1.92 ± 0.15. Numbers of measurements are: WT untreated=15; WT_{+carb}=15; villin-/- untreated=8; villin-/-$_{+carb}$=16; tgvillinWT=11; tgvillinWT$_{+carb}$=44; tgvillinΔsev=15; tgvillinΔsev$_{+carb}$=45. *** t test $p < 0.001$. NS: non-significant p value>0.05.

Wild type mice consistently showed an important reduction of the ulcered area at day 3 (not shown). By day 7, the colon surface appeared regular, making the original lesion hardly distinguishable **(Figure 30A)**. In contrast, colonic repair in villin null mice was slightly delayed at day 3 (not shown). More strikingly, the irregular and depressed appearance of the tissue indicated an incomplete repair at day 7 **(Figure 30A)**. Quantifications confirmed a significantly slower reduction of the injured surface area as compared to wild type animals (69 ± 7 % versus 55 ± 10 % at day 3, and 56 ± 9 % versus 18 ± 3 % at day 7; t-test $p<0.01$ at day 7) **(Figure 30B)**. Thus, *in vivo*, efficient colonic wound healing requires villin.

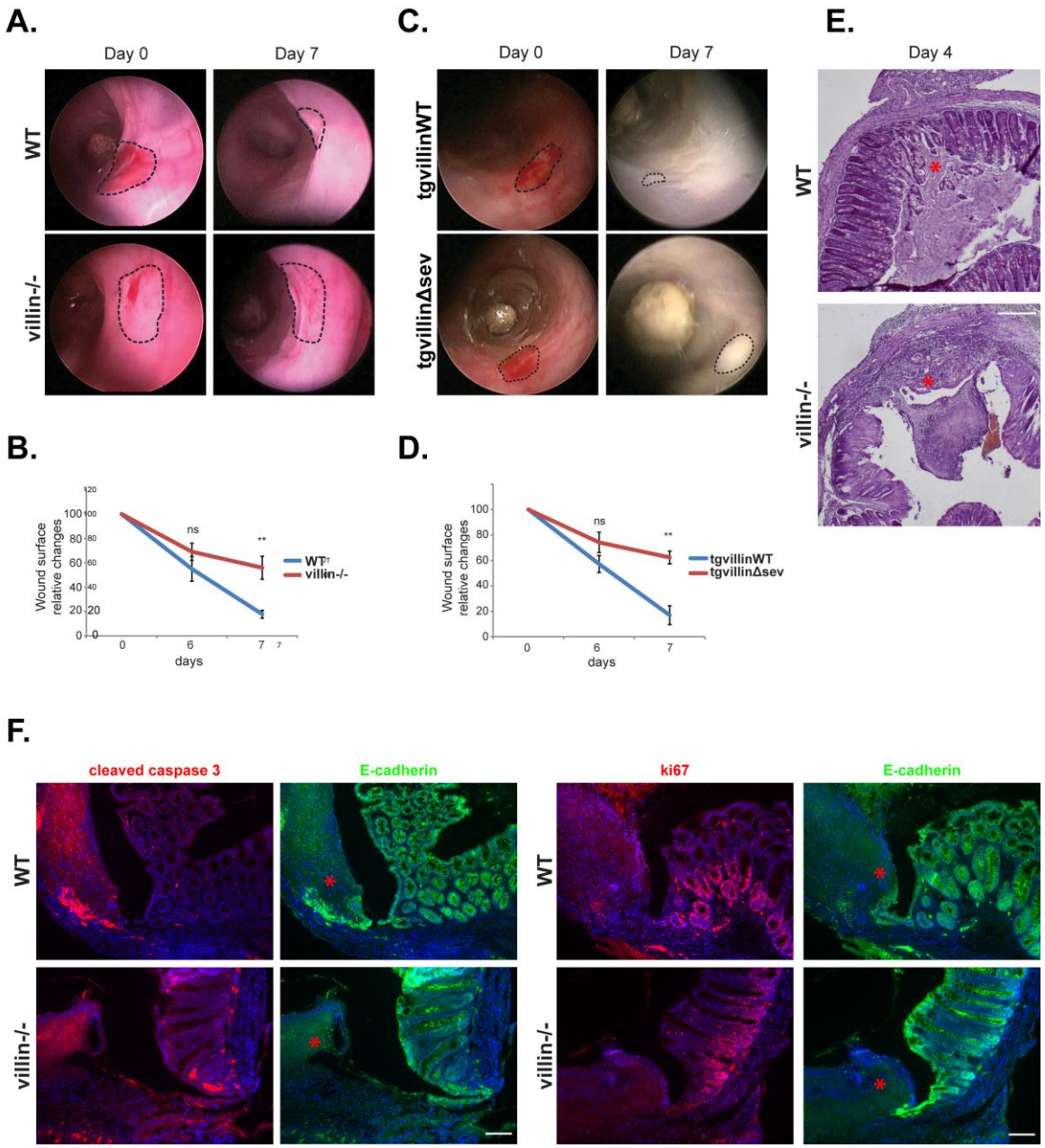

Figure 30: Efficient colonic wound healing requires villin through its actin severing property

A. and C. Serial endoscopic snapshots showing the site of biopsy-induced injury in mouse colon of the indicated genotypes at day 0 and 7 post-wounding. Images are representative of at least 4 animals per genotype. Dashed lines delineate the wounded area. **B. and D.** Plot of the average wounded area changes overtime for mice of the indicated genotype, normalized to the original lesion size at day 0. Values are for WT and villin-/-, respectively: day 3: 54 ± 10 % versus 69 ± 7 %; day 7: 17 ± 3 % versus 56 ± 9 %. Number of animals are: n_{WT}=6; $n_{villin-/-}$=4. Values are for tgvillinWT and tgvillinΔsev, respectively: day 3: 57 ± 6 % versus 74 ± 8 %; day 7: 17 ± 8 % versus 62 ± 5. Number of animals are: $n_{tgvillinWT}$=4; $n_{tgvillinΔsev}$=5. ** t-test $p < 0.01$; ns: non-significant p value>0.05. **E.** Hematoxylin-eosin staining of histological sections from the mucosal injured area at day 4 post-wounding in WT and villin-/- mice. Red asterisks highlight the injured area. Scale bar: 200 µm. **F.** Histological sections from WT and villin-/- mice, at day 4 post-injury, stained for cleaved caspase 3 (left panel, red) or ki67 (right panel, red) and E-cadherin (green). Dapi stains nuclei (blue). Red asterisks highlight the injured area. Scale bars: 100µm.

To better document the healing process, histological studies were carried out on colonic paraffin sections corresponding to the injuries previously identified by colonoscopy at day 4, when significant difference arises between wild type and villin null animals **(Figure 30E)**. To exclude an implication of cell proliferation and apoptosis in the differences of tissue healing, these cellular processes were evaluated by immunostainings (**Figure 30F**). Co-stainings for E-cadherin and the proliferative cell marker Ki67 did not reveal any major difference in terms of proliferation. Considering apoptosis, the number of cells co-labeled with E-cadherin and cleaved caspase 3 was not increased between wild type animals and the inefficiently repairing villin null mice. Thus, an eventual role of this protein in cell survival or proliferation can be excluded to explain the repair defect reported in absence of villin in this context. We next wondered whether the actin severing property is important to regulate colonic tissue healing. For this purpose injury repair in tgvillinΔsev and in tgvillinWT mice was compared. In tgvillinWT animals, most of the original wound was repaired by day 7 **(Figure 30C)**, mimicking wild type mice. On the contrary, injuries induced on tgvillinΔsev mice failed to heal properly at day 3 and 7 **(Figure 30C)**. We confirmed these observations by measuring the injured surface area over time of tgvillinΔsev versus tgvillinWT mice (74 ± 8 % versus 57 ± 6 % at day 3, and 62 ± 5 % versus 17 ± 7 % at day 7, t-test $p<0.01$ for day 7) **(Figure 30D)**. Altogether, these results demonstrate *in vivo* the critical role of villin-mediated F-actin severing during colonic injury repair independently of its anti-apoptotic function. Given the known impact of villin in cell migration, we decided to look more in details at the migratory properties of the epithelial cells.

Figure 31: Villin positively regulates cell migration through its actin severing property

A. Western blot against villin and tubulin performed against LLCPK-1 cells infected with lentiviral particles of shRNA empty plasmid or containing shRNA sequences directed against porcine villin. Two different shRNA were used. Tubulin represents the loading controls. **B.** Left panel: Quantification of the colonized area by the LLCPK-1 monolayer at 10h post wounding, normalized to 100 for the fastest cells. Values are: shRNA1: 72.6 ± 5.5 %; shRNA2: 71 ± 5.6 %; t-test *** p value<0.001; ns non-significant p value>0.05 Right panel: Serial micrographs from transmission light microscopy time-lapses of wound healing assays on a monolayer of LLCPK-1 cells in the different conditions. Scale bar: 100 µm. **C.** Western blot against villin and actin performed on LLCPK-1 cells infected with lentiviral particles of shRNA empty plasmid or containing shRNA sequences directed against porcine villin and reexpressing wild type (villinWT) or severing mutant (villinΔsev) human villin. **D.** Left panel: Quantification of the colonized area by the LLCPK-1 monolayer at 10h post wounding, normalized to 100 for the fastest cells. Values are: shRNA2: 60 ± 3 %; villinΔsev: 71 ± 5 %. Right panel: Serial micrographs from transmission light microscopy time lapses of wound healing assays on a monolayer of LLCPK-1 cells in the different conditions. Scale bar: 100 µm. **E.** Relative number of lamellipodia formation per field over time in villinWT or villinΔsev expressing cells. Values are normalized to the number of lamellipodia at 20 min post-injury determined in villinWT expressing cells.

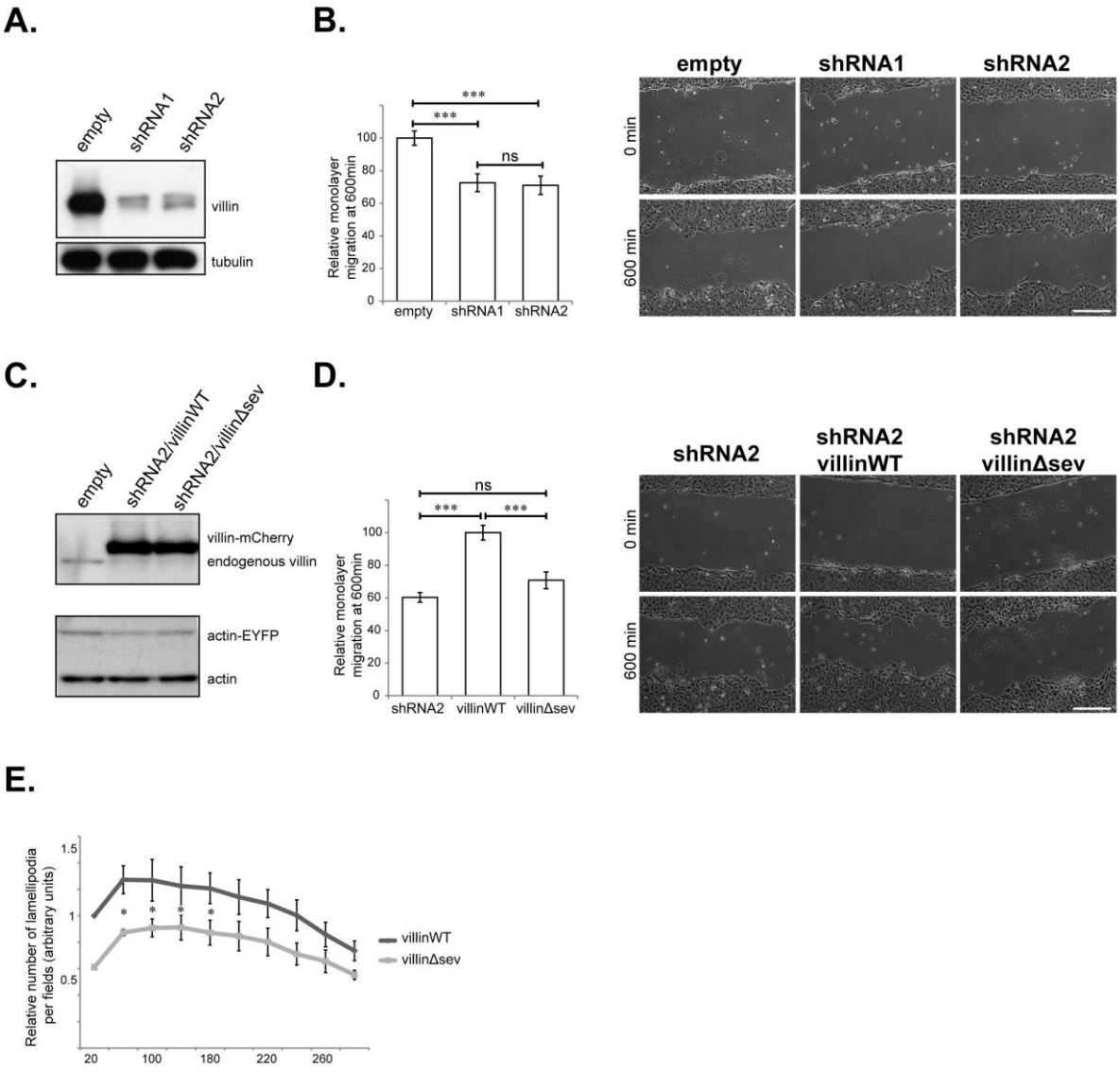

Villin severing activity is required for efficient wound healing of LLC-PK1 cells.

To analyze at the cellular level the dynamics of the healing process, wound healing models in cell culture were chosen to overcome limitations intrinsic to *in vivo* systems. The cell culture model chosen should closely recapitulate the apico-basal polarization and differentiation of enterocytes *in vivo*. The non-transformed porcine epithelial LLC-PK1 cell line derived from kidney proximal tubule is classically used to study microvillus biology and expresses villin endogenously. A stable cell line expressing an actin-EYFP construct through a clonal approach was generated, resulting in a nearly 100 % homogeneity. Endogenous villin was afterward depleted in these cells by two different shRNA, resulting in a depletion of nearly 80 % with both shRNA on confluent cells **(Figure 31A)**. One shRNA was randomly chosen to pursue the experiments and express the mCherry-villin constructs. Following transfection, mCherry-

villinWT or mCherry-villinΔsev expressing cells were sorted by FACS. The FACS-sorted cells showed comparable expression levels as seen by western blot, which furthermore confirmed endogenous villin depletion **(Figure 31C)**. The cellular distribution of the transfected proteins revealed an important co-localization of the mCherry-fused proteins and EYFP-actin in the apical microvilli of confluent unwounded LLC-PK1 sorted cells **(Figure 32)**. In addition, expression of the two villin constructs resulted in a similar marked increase in microvilli size as compared to non-transfected cells depleted for endogenous villin **(Figure 32)**. Thus and as previously reported (Revenu et al., 2007), the mCherry-villin proteins retain their correct sub-cellular localization and their morphogenetic effect in LLCPK-1 cells.

To evaluate the previously reported role of villin during cell migration and validate the cell culture system, small culture insert dedicated to 2D wound healing assays were used, allowing robust quantification in different experimental conditions. Time lapse multi-position microscopy revealed a modest but significant reduction of the relative area colonized by the monolayer of villin depleted LLC-PK1 cells at 10 h normalized to cells expressing the empty vector (72 ± 5 % and 71 ± 5 % for shRNA1 and shRNA2, respectively; t-test $p<0.001$ for each) indicating an inefficient migration in absence of villin **(Figure 31B)**. Wild-type villin re-expression significantly enhanced normalized cell migration (100 ± 4.5 % versus 60 ± 3 %, for villin depleted cells re-expressing villin WT and villin depleted cells, respectively; t-test $p<0.001$), thus rescuing the depletion of endogenous villin **(Figure 31D)**. In contrast, cells re-expressing villin severing mutant did not show any significant difference in their migratory property as compared to villin depleted cells (70 ± 5 % versus 60 ± 3 %; t-test $p>0.05$) **(Figure 31D)**. These results confirm that villin improves the efficiency of *in vitro* wound closure and demonstrate that it is due to its F-actin severing property.

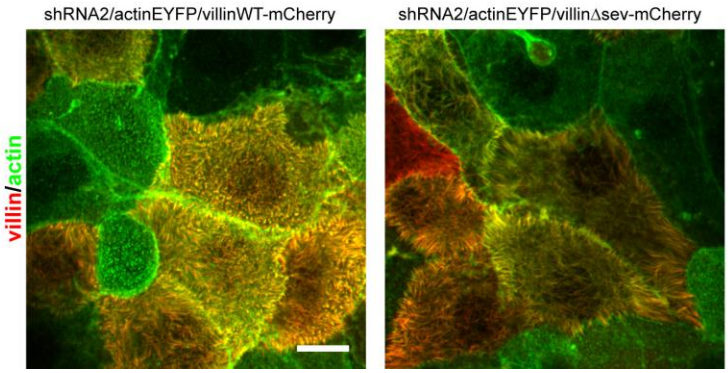

Figure 32: VillinΔsev protein retains its microvillar distribution and its morphogenetic effect

Total projections of Z stacks acquired by spinning disk microscopy. Micrographs represent overlays of EYFP-actin (green) and villinWT- or villinΔsev-mCherry (red). Note the presence of cells untransfected for villin. Scale bar: 10 um.

Villin severing activity is required for efficient microvilli disassembly upon cell migration.

Epithelial cells are able to migrate in the absence of villin. Villin must then have a function specialized in cells developing microvilli. To get further insights, at the sub-cellular level, into villin regulation of cell reorganization during migration, the wound healing process was inspected by time lapse imaging using high resolution spinning disk confocal microscopy. Cell migration was induced by scratching assays on monolayers of the previously described sorted cells. As reported in the past, lamellipodia displayed a marked concentration of mCherry-villin, which overlapped with the narrow intense actin-EYFP signal (Athman et al., 2003). Villin devoid of its F-actin severing property also showed lamellipodial recruitment, thus providing another indication of its functionality. In cells re-expressing wild type mCherry-villin, an important apical pole remodeling was consistently observed, concomitantly to lamellipodium extension. Indeed, a rapid disassembly of EYFP-actin and mCherry-villinWT positive microvilli could be observed on the x,y plane of the migrating cells and confirmed on the x,z reconstruction **(**see arrows on **Figure 33A** and **B; Movies S1 and S2)**. This type of image treatment furthermore allowed to quantify the relative apical fluorescence intensities during cell migration by selecting a region of interest corresponding to the very upper part of the cell on the x,z representations. Accordingly, a rapid conspicuous decrease of actin and villin apical fluorescence relative intensities could be reported **(Figure 33C)**. In the presence of villin, microvilli are thus rapidly disassembled upon migration. In contrast, in most of migrating villinΔsev positive LLC-PK1 cells, the apical microvilli appeared strikingly more stable, showing no apparent disassembly (see arrows on **Figure 33A** and **B; Movies S3 and S4)**. Consequently, the decreases of apical relative fluorescence intensities were significantly impeded compared to the previous condition **(Figure 33C)**. To confirm this phenotype, the presence or absence of apical microvilli, revealed by the mCherry-villin proteins, was quantified on cells fixed at 30 min post-wounding. On migrating cells characterized by the presence of a lamellipodium, careful examination of the presence of mCherry positive apical microvilli structures revealed that whereas a majority of migrating cells re-expressing wild type villin were devoid of microvilli, this number was significantly reduced when expressing villinΔsev (62.5 % vs. 43.4% for villinWT and villinΔsev, respectively; $P<0.01$) **(Figure 33D)**. Altogether, these results clearly demonstrate that villin is required to efficiently sever microvillar actin filaments resulting in brush border disassembly at the onset of cell migration.

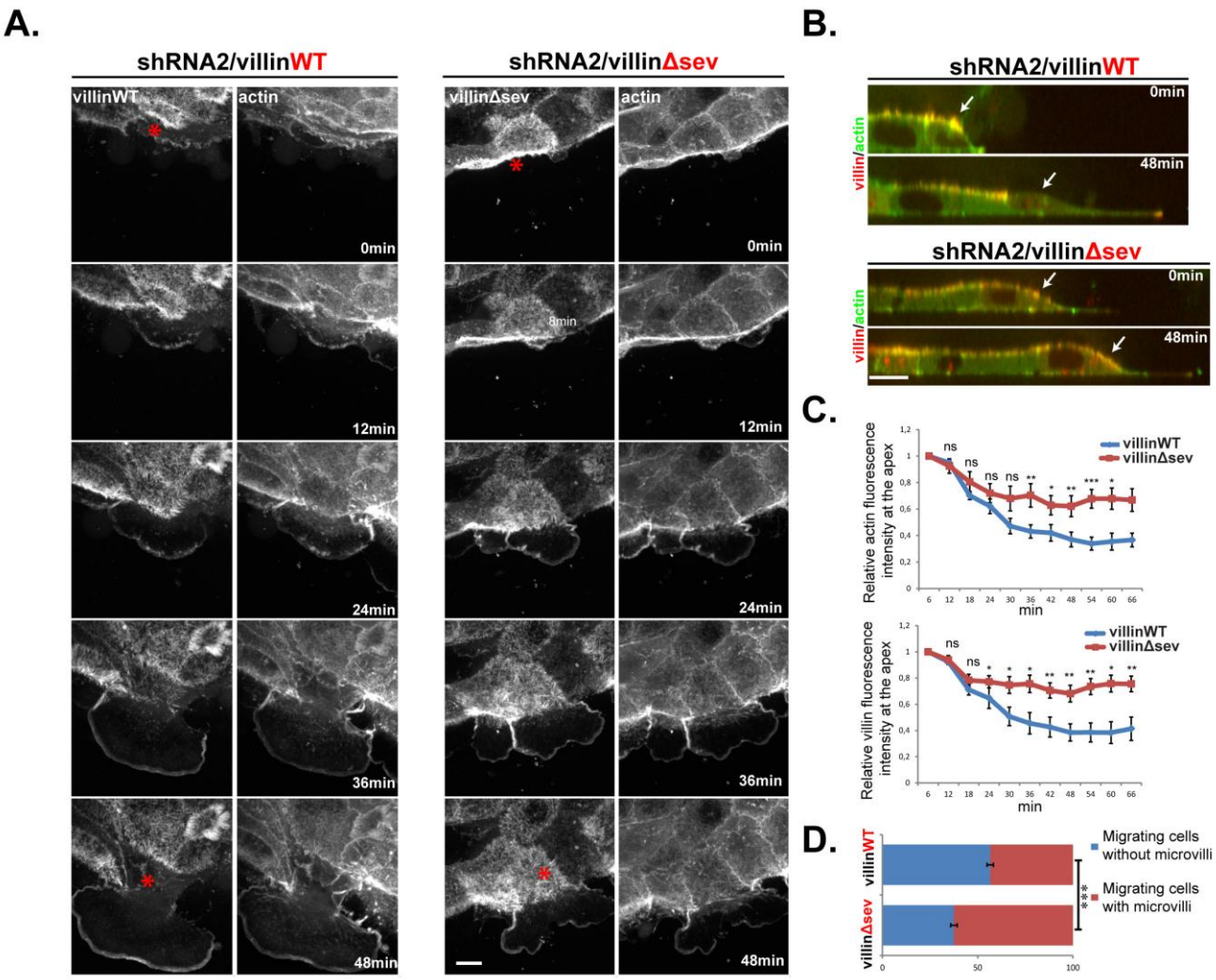

Figure 33: Microvilli disassemble upon cell migration via villin severing activity

A. Migration of LLCPK-1 cells depleted for endogenous porcine villin (shRNA2) expressing EYFP-actin and mCherry- villinWT or villinΔsevvisualized by spinning disk time-lapse microscopy. EYFP and mCherry channels are shown. Images are maximal projections of the acquired Z stacks. Serial images are shown at 12min interval. Red asterisks highlight the migrating cells analyzed. Scale bar: 10 µm. **B.** Z reconstructions of the migrating cells highlighted in A at 0 min and 48 min. Overlays of EYFP-actin (green) and mCherry-villin (red) is shown. White arrows point at the dorsal face of the migrating cell. Scale bar: 10 µm. **C.** Plots depicting the villin and actin fluorescence intensities at the dorsal face of the cells transfected for mCherry- villinWT or villinΔsev overtime quantified from images acquired by spinning disk time-lapse microscopy. Number of cells analyzed: $n_{villinwt}$=10; $n_{villin\Delta sev}$=19. **D.** Histogram representing the penetrance of the phenotype illustrated by the presence or the absence of apical microvilli, positive for mCherry-villin, on migrating cells transfected for mCherry-villinWT or villinΔsev at 30 min post-injury on fixed cells. Values are: 62.5 ± 1.7 % and 43.4 ± 1.7 % for villinWT and villinΔsev, respectively. T-test *** p value < 0.001. Number of cells analyzed: $n_{villinwt}$ =121; $n_{villin\Delta sev}$ =95.

Microvillar actin is rapidly integrated at the lamellipodium upon migration.

Since the enhancement of epithelial cell migration induced by villin severing activity correlates with the disassembly of apical microvilli, we hypothesized that the lack of apical pole disassembly could hinder the repolarization of the cells towards a migratory organization. In agreement with this idea, a precise quantification of the scratch wound assays demonstrated a significant decrease in the rate of lamellipodia formed in villinΔsev expressing cells compared to villinWT at the onset of migration **(Figure 31E)**. Could the microvillar actin be required for this lamellipodia formation by being directly and rapidly engaged in migratory structures?

The intracellular dynamics of microvillar actin in migrating cells was followed using a photo-activable green fluorescent protein (PAGFP-actin) in confluent LLC-PK1 cells depleted for endogenous villin and expressing villinWT or villinΔsev. Actin molecules were specifically photo-activated locally at the apex of early-migrating LLC-PK1 cells **(Figure 34A)** following monolayer scratch. A rapid and consequent recruitment of PAGFP-actin could be observed at the lamellipodium of cells expressing wild type villin **(Figure 34B; Movie S5)**. In contrast, the recruitment of photoactivated PAGFP molecules was lower in cells expressing villinΔsev **(Figure 34B; Movie S5)**. Accordingly, quantifications of the ratio of photoactived actin molecules recruited at the lamellipodium revealed a prompt redistribution of microvillar actin towards the lamellipodium of cells expressing wild type villin whereas recruitment was significantly reduced in cells expressing villinΔsev (17 ± 7 % versus 4 ± 0.8 % at 6min post-photoactivation; t-test $p<0.05$) **(Figure 34C)**. To exclude a bias caused by an eventual difference in the actin exchange and/or assembly at the lamellipodium of cells expressing villinWT or villinΔsev, PAGFP-actin molecules were photo-activated in a region positioned slightly away from the lamellipodium leading edge, in the lamellum, and monitored integration at the lamellipodium. Importantly, quantifications could not reveal any influence of villin F-actin severing on the rate of lamellar actin integration at the lamellipodium **(Figure 34D)**. Due to the fast actin treadmilling in microvilli (Tyska and Mooseker, 2002; Waharte et al., 2005), the PAGFP-actin is not expected to remain stable at the apex of the cells even in the absence of villin severing activity. A slight but not significant increase in PAGFP-actin stability was nevertheless detected in cells expressing vilinlΔsev **(Figure 34E)**. These results thus show that actin molecules resulting from microvilli disassembly mediated by villin F-actin severing property are rapidly integrated at the nascent lamellipodium, without the lamellipodium actin polymerization rate to be modified.

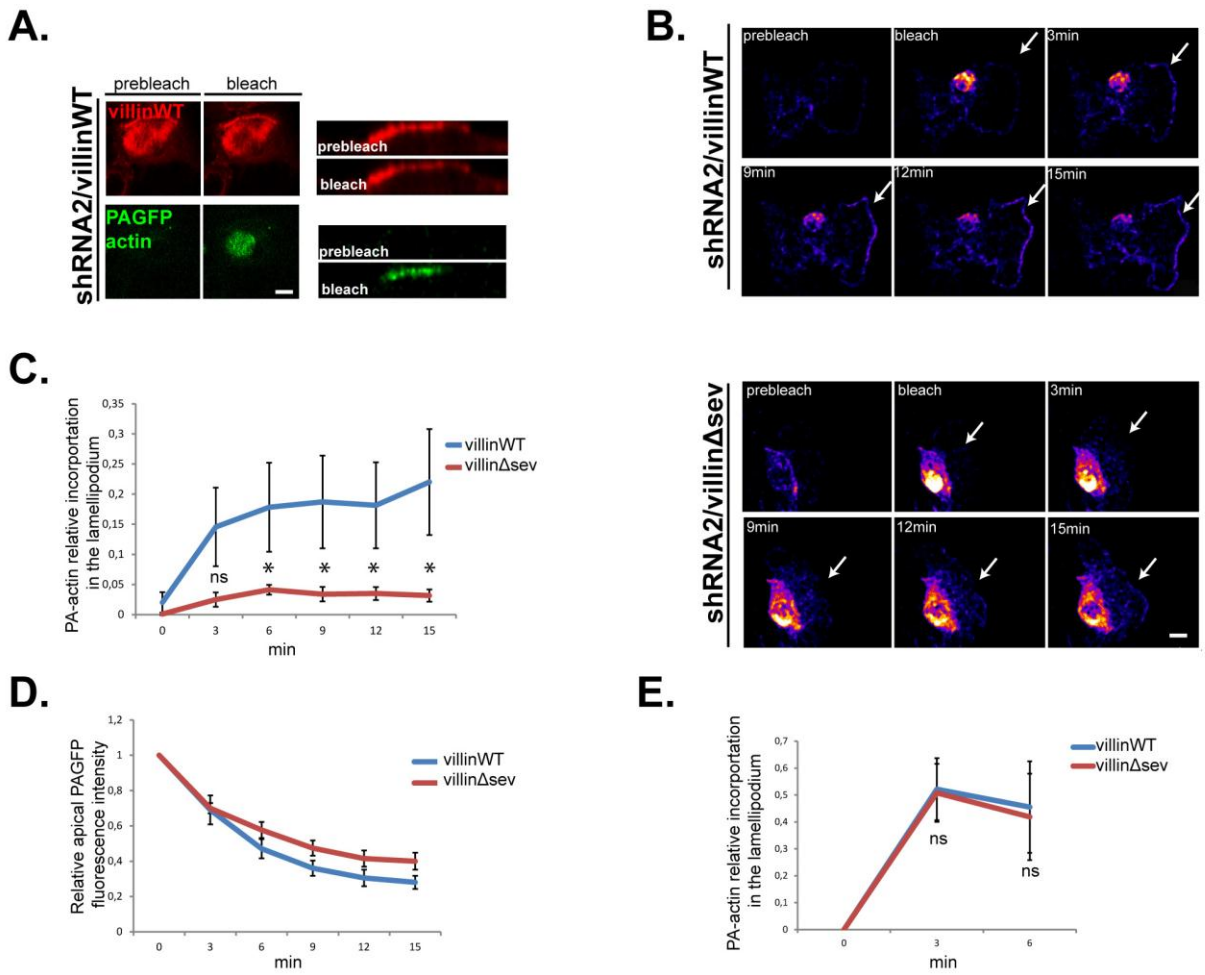

Figure 34: Microvillar actin is rapidly integrated at the lamellipodium following microvillus disassembly

A. Biphotonic laser photo-activation of PAGFP-actin at the apical face of a confluent monolayer of LLC-PK1 cells depleted for endogenous villin and expressing villinWT-mCherry and PAGFP-actin. Left panel: Total projections of the Z stacks before and immediately after photo-activation. Right inset: Z reconstruction of the Z stacks before and immediately after photo-activation. Scale bar: 10 µm. **B.** Serial micrographs of total Z projections pseudo-colored with the fire lookup table. Biphotonic laser photo-activation at the dorsal face of an early migrating cell depleted for endogenous villin and expressing villinWT-mCherry (upper panel) and villinΔsev (lower panel). White arrows point at the lamellipodium edge. Scale bars: 10 µm. **C.** Plot of the proportion of apically photo-activated actin incorporated in the lamellipodia overtime. Number of cells analyzed: $n_{villinWT}$=10; $n_{villin\Delta sev}$=16. T-test NS: p value > 0.05; * p value < 0.01. **D.** Plot depicting the proportion of incorporation at the lamellipodia overtime of photo-activated actin slightly away from the lamellipodial edge. Number of cells analyzed: $n_{villinWT}$ = 4; $n_{villin\Delta sev}$ = 4. **E.** Plot depicting the relative photo-activated actin intensity at the apical face of the cells for cells expressing villinWT or villinΔsev. Number of cells analyzed: $n_{villinWT}$ = 10; $n_{villin\Delta sev}$ = 16.

Villin is essential for microvilli disassembly upon cell migration *in vivo*.

These results, obtained using a wound healing model in cell culture, provide dynamic description and quantification of the important apical domain remodeling induced by villin severing property at the onset of cell migration. To assess the relevance of this newly demonstrated function of villin in physiological situations, we wondered whether similar rapid cell reorganization occurs during intestinal wound healing *in vivo*. The extent of the biopsy induced injury **(Figure 30)** and the subsequent time scale of the healing process however prevented the use of this technique to evaluate such prompt cell response. A strategy inducing milder chemical lesions by the bile acid sodium deoxycholate was rather chosed (DOC), which produces sharp lesions of the epithelial cells on the upper part of the intestinal villi, as observed on histological paraffin sections of the injured tissue **(Figure 35A**, upper panels**)**. E-cadherin immunostaining, which delineates basolateral boundaries of the cells, revealed that the enterocytes immediately adjacent to the wound conserved a columnar shape. They also retained the exclusion of E-cadherin from the apical domain, as expected for a polarized epithelium. Importantly, the digestive enzyme sucrase-isomaltase maintained a strict apical sub-cellular distribution on these cells. Thus apico-basal polarity is preserved on the enterocytes immediately following adjacent cell injury. No obvious difference could be detected after bile acid injuries on the epithelia of wild type and villin null mice **(Figure 35A**, upper panels**)**. DOC was subsequently washed out to allow cell restitution to take place. After 30 minutes, dramatic cell reorganization of the wound adjacent enterocytes could be detected in wild type mice, revealing a progressive flattening of the epithelial cells as seen with the E-cadherin staining **(Figure 35A**, lower panels**)**. E-cadherin was no longer excluded from the apex, suggesting an alteration of apicobasal polarity. Strikingly, on most of the wild type cells was noticed a complete loss of the apical localization of sucrase-isomaltase and ezrin, two microvilli markers, indicating microvillus disassembly (**Figure 35A** and **B)**. These observations closely resemble the cell remodeling associated with cell migration in culture **(Figure 33)**. In contrast, in villin null mice, most of the cells in contact with the injury conserved an intense SI and ezrin apical staining, thus indicating a strongly impaired efficiency of microvillus disassembly **(Figure 35A and B)**. To exclude the possibility that the observed cell reorganizations are due to an eventual apoptotic program, cleaved caspase-3 staining revealed very few apoptotic enterocytes adjacent to the wound, independently of the two genotypes **(Figure 35C** and quantification in **D)**. These results lead to the conclusion that villin is essential for the disassembly of microvilli and for apical domain remodeling elicited by wound healing *in vivo*.

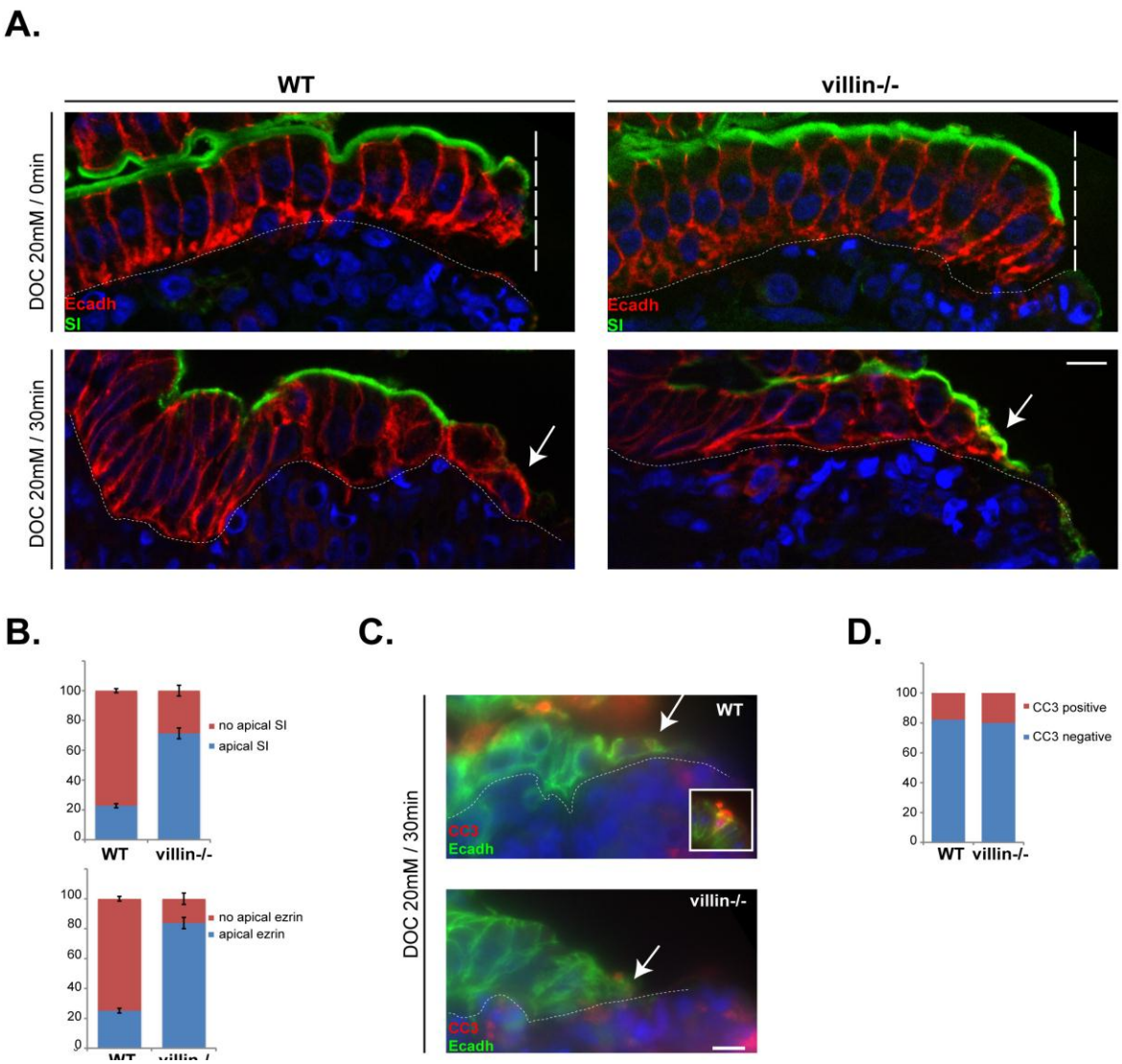

Figure 35: Villin is essential for brush border disassembly upon cell migration *in vivo*.

A. Histological paraffin sections of small intestine of wild type (WT) or villin null (villin-/-) mice luminally treated with sodium deoxycholate (DOC) just after washout (upper panel) or 30 min after washout (lower panel) stained for E-cadherin (Ecadh, red) and sucrase-isomaltase (SI, green). DAPI labels nuclei (blue). Vertical dashed lines highlight the injured area; basal dashed lines delineate the lamina propria; arrows indicate the injury-adjacent enterocytes. **B.** Histograms depicting the presence or the absence of apical staining of SI or ezrin quantified on histological paraffin sections of small intestine of WT or villin-/- treated with DOC, 30 min after washout. Values are: WT, 22 ± 1 % and villin-/-, 71 ± 3 % for apical SI. WT, 25 ± 1.6 % and villin-/-, 84 ± 4 % for apical ezrin. SI: n_{WT}=84 cells analyzed from 8 animals; $n_{villin-/-}$=147 cells analyzed from 12 animals. Ezrin: n_{WT}=45 cells analyzed from 6 animals; $n_{vil-/-}$=26 cells analyzed from 3 animals. **C.** Histological paraffin sections of small intestine of WT or villin-/- mice luminally treated with DOC, 30min after washout, stained for E-cadherin (green) and cleaved-capsase 3 (red). DAPI labels nuclei (blue). A positive control is shown in the inset, which represents an apoptotic enterocyte at a villus tip. Basal dashed lines delineate the lamina propria; arrows indicate the injury-adjacent enterocytes. **D.** Histogram of the ratio of enterocytes at the wound edge positive for cleaved caspase 3, quantified from histological paraffin sections of small intestine stained for cleaved caspase 3 from WT or villin-/- mice treated with DOC, 30min after washout. Values are: WT: 82 % and villin-/-: 80 % of non-apoptotic cells.

E. Discussion

In this study, we definitively demonstrate that villin directly participates in apical pole remodeling of migrating cells to promote wound healing. We show that villin severs F-actin within microvilli to initiate their disassembly thereby promoting cell migration. We moreover provide direct evidence that villin mediated F-actin severing enhances the rapid integration of this newly released actin pool at the lamellipodium, suggesting that apical domain disruption, illustrated by microvilli disassembly, releases substantial amount of cellular components that stimulate motility. Most importantly, we also demonstrate *in vivo* the physiological and biological relevance of these functions during injury healing in the gut, an organ subject to various lesions that can be deleterious in the absence of an efficient tissue repair process.

Villin severing activity mediates rapid microvillus disassembly.

Villin has been shown to promote epithelial cell migration in diverse cell lines (Athman et al., 2003; Tomar et al., 2004; Wang et al., 2007; Mathew et al., 2008). How could villin regulate cell motility? As discussed in the introduction, villin localizes to the lamellipodium and participates in the extension of the structure, presumably by enhancing actin dynamics as suggested by *in vitro* actin based motility assays (Athman et al., 2003; Revenu et al., 2012). Villin is thus likely involved directly in the motility machinery of epithelial cells. However, no reports have investigated, during cell migration, a possible function of this protein in microvilli, the specialized domain where it concentrates. We used LLC-PK1 cells, from porcine proximal kidney origin, which are epithelial cells closely resembling to intestinal cells and classically used to study the biology of the microvilli (Tyska and Mooseker, 2002; Loomis et al., 2006; Zwaenepoel et al., 2012). In agreement with our initial hypothesis, we could not only provide dynamic insights on the occurrence of a sudden microvilli disassembly that associates with migration but furthermore demonstrate that such apical pole remodeling is driven essentially by villin F-actin severing. However, in our experimental setup, expression of a villin severing mutant did not completely abolish microvilli disassembly on migrating cells. How to explain this relatively mild phenotype we report? First, to avoid a complete detachment of the monolayer following the scratch we used only partially differentiated confluent cells, which display not fully mature microvilli. These pre-mature microvilli could be less stable and more prone to

disassembly, a possibility that could be supported by the description of increased actin turnover rates assessed in non-confluent LLC-PK1 cells (Tyska and Mooseker, 2002). Secondly, the mutations introduced in the villin cDNA result in a drastic reduction of its ability to sever F-actin but do not abrogate it (Revenu et al., 2007). Indeed, *in vitro* depolymerization assays indicate that Δsev mutations lead to a reduction of villin severing activity to 16% of its normal value (Revenu et al., 2007). Finally, actin severing and/or depolymerization by ADF/cofilin was proposed to account for the reported collapse of microvilli from kidney proximal tubule following ischemia/reperfusion *in vivo* (Schwartz et al., 1999; Ashworth et al., 2001). This type of injury appears to induce ADF activation and relocalization to the apical domain (Schwartz et al., 1999; Ashworth et al., 2001). Since LLC-PK1 cells used in this study are from renal origin, it is conceivable that villin and ADF/cofilin act in concert to mediate microvilli disassembly in these cells.

Most importantly, we were able to confirm that similar apex remodeling occurs *in vivo*, following mild injury of the intestinal epithelium. These types of experimental injuries have been widely used to study the restitution process in the intestine (Moore et al., 1989a; Albers et al., 1995, 1996; Masuda et al., 2003). On wild type enterocytes adjacent to the injury, we observed a striking loss of apical ezrin and sucrase-isomaltase (SI) stainings. As these two proteins illustrate microvilli structure and functionality, their loss likely reflects microvilli disassembly. In support of this possibility, loss of apical sucrase-isomaltase staining, following similar type of injuries, correlates with microvilli disruption as determined by electron microscopy (Albers et al., 1995). In contrast, we did not observe such cell reorganization in enterocytes from villin null mice: the apical pole of migrating enterocytes appears more stable and conserves strict apical distributions of ezrin and SI. Of notice, this *in vivo* phenotype caused by the loss of villin is highly penetrant. Altogether, these results strongly suggest that intestinal microvilli disassembly is induced mainly by villin, which severs microvillar actin filaments. We conclude that, in a migratory context *in vivo*, villin is a direct effector of enterocyte apical pole remodeling.

Advantages of F-actin severing versus capping proteins in cytoskeleton remodeling.

In a study depicting a structural model of the microvilli, it was suggested that, as a structural element of the actin core, villin cannot simultaneously bind membrane PIP_2 and actin (Brown and McKnight, 2010). Therefore activation of the severing property by dynamic dissociation from PIP_2 could not account for microvilli disassembly. It was instead proposed that reversible

interaction between villin and PIP_2, sterically allowed at the microvillus tip only, could lead to filaments capping by villin, which, when considering the actin treadmilling rate, would progressively extinguish the microvillus within 20 minutes (Brown and McKnight, 2010). While filaments capping alone could possibly induce microvillus collapse, we clearly demonstrate the impact of villin severing property on this morphological process. In addition, the time scale of the abrupt microvilli destruction – typically occurring within 6-12 minutes - that we report would be incompatible with a progressive depolymerization of the bundle. Thus, villin severing activity within the microvillus shaft most likely constitutes the driving force for its rapid disassembly upon stress conditions.

Proteins in charge of cytoskeleton reorganization are definitely not specific of microvilli. Among other examples, in the highly dynamic filopodia, cofilin efficiently severs F-actin and is dynamically targeted to the shaft during stalling and retraction of the protrusions, suggesting a key role in these processes (Breitsprecher et al., 2011). This result elegantly illustrates the advantage of molecules executing actin cytoskeleton breakup to allow rapid shape remodeling of organelles.

Role of the apical pole remodeling induced by cell migration.

As seen earlier, apex reorganization is not specific to migrating intestinal cells. It rather widely occurs in different organs and thus seems inherent to the migratory phenotype of epithelial polarized cells. Why would apical pole destruction be important for cell migration? To attempt to answer this question several biological and biophysical points can be raised.

Precise regulation of plasma membrane tension is critical for efficient migration. Membrane in the front of motile cells is constantly pushed by the actin cytoskeleton resulting in increased membrane tension. In non-apico-basally polarized cells, tension is uniformly distributed along the membrane as local application of force generates membrane tension that rapidly propagates and equilibrates within milliseconds (Kozlov and Mogilner, 2007). Interestingly, artificially rising membrane tension by hyperosmotic swelling impairs lamellipodium efficiency (Raucher and Sheetz, 2000), presumably by affecting the rate of polymerization. Indeed, the molecular Brownian ratchet model stipulates that thermal fluctuations of the polymerizing actin filaments abutting a membrane surface allow insertion of actin monomers. Subsequent collision of the fluctuating filament with the membrane generates pushing force against the membrane. Thus, a

higher membrane tension would affect membrane pushing. Variation of membrane tension may also regulate endo- and exocytosis, two processes important for cell extension (Gauthier et al., 2011). In the case of epithelial polarized cells, membrane tension is higher on the apical than on the basolateral pole (Dai and Sheetz, 1999). This discrepancy is due to the physical separation by tight junctions generating domains of distinct lipid composition and is likely additionally reinforced by the presence of numerous membrane protrusions: the microvilli (Nambiar et al., 2009; Boulant et al., 2011). Their disassembly might thus alleviate membrane tension and thereby indirectly favor migration.

Secondly, microvilli employ important quantities of diverse cellular components. For instance, owing to their number, apical microvilli occupy a large amount of plasma membrane. Rapid cell surface changes such as reported during lamellipodium extensions require net membrane addition at the leading edge as plasma membrane is basically inextensible (Morris and Homann, 2001). This aspect is reflecting the plasma membrane low tensile properties. We can speculate that microvilli disassembly releases important amount of plasma membrane, in a close manner to caveolae, which act as a membrane reservoir allowing rapid cell surface extension (Sinha et al., 2011).

Analogously, microvilli concentrate high amount of actin. We calculated that apex concentrates more than 50% of the total phalloidin fluorescence signal in the mouse enterocyte. Thus, its disruption would release numerous free barbed ends that upon capping by villin would depolymerize into free G-actin (Northrop et al., 1986). In support of this idea, we could observe a prompt integration of microvilli-released actin at the lamellipodium on villin positive cells. Conversely, the recruitment is decreased on cells expressing villin severing mutant. Villin thus increases the release of microvillar actin and its insertion at the lamellipodium, a mechanism that likely favors lamellipodium efficiency and results in increased cell motility. Two published observations, which are based on the fact that cytoplasmic G-actin concentration largely determines the magnitude of the cell extension (Kiuchi et al., 2011), argue in favor of this possibility: (I) ADF/cofilin mediated F-actin severing has been proposed to indirectly increase lamellipodium efficiency by supplying an abundant pool of actin monomers (Kiuchi et al., 2007). (II) Myosin II contributes to actin network disassembly at the rear of the cell thereby promoting a treadmilling-like process to sustain cell motility: F-actin is disassembled at the rear and reinserted at the polymerizing leading edge (Wilson et al., 2010). Interfering with this cell-scale treadmilling impedes cell migration and thus highlights the importance of local F-actin network disassembly to sustain a spatially distinct actin polymerization (Wilson et al., 2010). In

complement of its structural role, villin may thus have a comparable function in the actin-rich apical microvilli. As a matter of comparison, ischemia/reperfusion in the kidney induces important cytoskeletal reorganization including microvilli collapse. Following microvilli disassembly, intense F-actin patches are detected within the cytoplasm of injured cells (Golenhofen et al., 1995). This observation fits well with our hypothesis concerning a remobilization of disassembled microvillar F-actin within the cell.

How to envisage actin transport to the lamellipodium in the case of a migrating epithelial cell? Interestingly, such rapid long range transport of actin within a migrating cell has already been reported. Indeed, using photobleaching experiments Zicha and collaborators could document the delivery of actin from the rear of the cell to the protruding lamellipodium at speeds exceeding 5µm/s, a value compatible with the timescale of our observations (Zicha et al., 2003). This rate of motion implies active transport that may rely on an intracellular fluid flow involving myosin II (Keren et al., 2009) or myosin-1c (Fan et al., 2012).

Villin severing property is responsible for efficient tissue healing.

In light of the arguments raised above, it appears likely that villin-induced apical reorganization could promote cell migration. To investigate this possibility, we performed wound healing assays on monolayers of epithelial polarized LLC-PK1cells depleted for endogenous villin only or additionally re-expressing the villin severing mutant. In these cells, wound closure was affected as a result of inefficient migration. The latter result was expected as villin-severing activity has previously been shown to enhance actin-based motility (Revenu et al., 2007). We could however notice that the impairment of microvillus disassembly in the presence of the villin severing mutant is associated with a reduction of the number of cells developing lamellipodia, that is to say of cells having efficiently repolarized into a migratory organization. This observation reinforces the hypothesis that apex disassembly provides cellular materials to stimulate migration, as discussed above. Enterocytes hence require microvillus F-actin severing by villin to efficiently acquire a migratory phenotype.

In the intestine, an organ highly subjected to lesions, villin function in cell migration might be important to restore tissue homeostasis following a lesion. This idea is actually reinforced by our results showing villin-mediated apex remodeling *in vivo*. As largely discussed previously, two studies have described a positive role for villin during mucosal injury in the mouse colon,

although divergent explanations were provided (Ferrary et al., 1999; Wang et al., 2008b). In fact, the experimental procedure that was applied precluded any conclusion on whether villin influences tissue injury or rather repair. To exclude similar types of biological outcome due to the method of injury we instead produced localized instantaneous mechanical lesions on the mouse colonic mucosa, using an endoscopic system (Pickert et al., 2009; Seno et al., 2009). We could then unequivocally demonstrate the critical role of villin during wound healing in the colon. Furthermore, we were able to determine that villin function in tissue healing largely depends on its severing property. Indeed, villin null and villinΔsev mice heal in an undistinguishable manner.

Tissue repair in the colon and other organs involves a precise coordination between cell proliferation and cell migration (Sturm, 2008; Friedl and Gilmour, 2009; Seno et al., 2009; Normand et al., 2011). Importantly, a first set of immunostainings that we recently performed revealed no difference of epithelial cell proliferation associated with tissue healing in the presence or absence of villin. In view of the extent of overall tissue remodeling, cell survival additionally likely contributes to colon repair, even if not documented on mechanical injuries. Likewise, cell survival is unaffected by the loss of villin. Then, a possible contribution of these cellular processes is unlikely to explain our results.

To better understand wound healing in the colon it is interesting to refer to the work of the group of Thaddeus Stappenbeck, which gives a detailed insight of the different cellular responses associated with tissue repair following mechanical injury (Seno et al., 2009). Within hours, fibrin and platelets are massively recruited to the wound bed presumably to allow clotting. By day 2, this cellular material is replaced by a monolayer of non-proliferative epithelial cells that cover the original wound. At the same timescale, a spatially defined increase in cell proliferation is detected in the wound adjacent crypts. The later phase involves important tissue remodeling and by day 6 the recovery of the injured area is nearly complete. The epithelial cells that early recover the wound bed by day 2 seem to arise from the adjacent crypts as determined by bromodeoxyuridine tracing. The tracing experiment further revealed a replacement within two days of these wound associated cells, demonstrating their rapid migration and turnover. Interestingly, these cells are characterized by a flattened morphology and an absence of apical villin staining, two observations that mostly resemble our description of migrating enterocytes in the small intestine. These observations additionally support the hypothesis that migratory defects caused by the absence of villin and its severing property are responsible of the inefficient colon tissue repair observed.

Which contribution for cell migration during wound healing in the gut?

Responses of the gut epithelium to injury have been mostly characterized using experimental models of large (e.g. DSS or biopsy induced lesion) or more restricted (e.g. induced by bile salts or detergent) injury. An overall comprehensive unified model is however lacking. Indeed, very few studies are available on the contribution of cell migration in large wounds and conversely of cell proliferation in restricted injuries, probably attributable to the experimental limitations inherent to *in vivo* models. The accepted model stipulates that migration of wound-adjacent cells within minutes allows re-epithelialization, independently of cell proliferation. Then, in a timescale of hours to days, increase in cell proliferation restores the cell pool (Sturm, 2008). As suggested by this model and our results, villin null mice should show defects of re-epithelialization following DOC injuries. Nevertheless, the unequal extents of the DOC induced injuries prevented us to estimate tissue recovery. Mechanical injuries in the colon allow such quantifications but produce lesions of higher importance. Sole cell restitution is insufficient to account for resealing of such large injuries, which rather involve a more complex interplay of simultaneous proliferation and fast migration (Seno et al., 2009). Given the fact that cell proliferation seems unaffected by the loss of villin, cell migration appears as the good candidate to explain our results, as we discussed above. In addition, our results in cell culture, which morphologically correlate the restituting enterocytes *in vivo*, suggest that an impaired migration is the main cause of inefficient wound healing of large lesions in the colon of villin null or villinΔsev mice. We could however not formally demonstrate this assertion as monitoring cell migration, a highly dynamic process, requires sequential observations at a cellular level, an approach not yet available in the mouse gut.

How could villin severing activity be regulated?

Our results indicate that, during intestinal cell migration, villin severing property is spatially and temporally activated leading to microvillus disassembly. This conclusion obviously raises questions about the spatiotemporal regulation of villin severing property. As largely discussed in the introduction, variation in calcium concentration regulates villin functions. Villin severing activity is favored at high calcium concentration (in the range of 100 µM) (Kumar and Khurana, 2004). On the other hand at low Ca^{2+}, villin is believed to fold into a compact auto-inhibited configuration, which would place the tail domain close to the F-actin binding site responsible for severing and consequently would inhibit actin severing and favor actin bundling (Burtnick et al.,

1997). Calcium binding would release this inhibition by a “hinge” mechanism (Choe et al., 2002). Since villin structure has not been solved, these structural conformations are inferred from comparison with gelsolin, its closest homolog (Finidori et al., 1992). Within a cell, the intracellular calcium concentration is typically in the hundred nM range, but increases in response to various stimuli. In resting cells, villin severing activity thus would be unfavorable. Conversely, injury on an epithelial monolayer produces an immediate rise in calcium concentration in the wound-adjacent cells that subsequently propagates in the monolayer (Klepeis et al., 2001). However, information concerning the range of calcium concentration reached in these circumstances is missing.

The high Ca^{2+} concentration required to activate villin severing property has been however considered as non-physiological (Kumar and Khurana, 2004). Nevertheless, several evidences document that calcium concentration can reach very high concentration locally – until several hundreds of µM -, in the so-called calcium microdomains (McCarron et al., 2006). These microdomains arise nearby specific channels that allow calcium influx through the membrane, in a process termed store-operated calcium entry (Parekh, 2008). Indeed, calcium depletion from the internal stores – e.g. the endoplasmic reticulum – induces calcium influx from the extracellular space through these store-operated channels (Targos et al., 2005). Members of the families of the L-type Ca2+ channels - Ca_V – and the transient receptor potential cation channel – TRPC - are among the best characterized store-operated channels (Targos et al., 2005; Parekh, 2008). Interestingly, $Ca_V1.3$ localizes to the apical pole of enterocytes (Morgan et al., 2006) and several members of TRPC have been identified in cells from intestinal origin (Rao et al., 2006). Furthermore, TRPC mediated Ca^{2+} influx promotes intestinal cell migration in wound healing assay (Rao et al., 2010). This calcium influx might be triggered by an interaction between the small GTPase rac - fundamental to cell movement in intestine – and $PLC_\gamma1$ leading to calcium store depletion (Rao et al., 2008). Overall, the store-operated calcium entry process fits particularly well with the current model of villin activation involving the PIP_2 hydrolysis pathway, described in the introduction. In addition, a direct role of calcium storage by the microvilli has been proposed by Klaus Lange. ATP-actin monomers indeed bind Ca^{2+} with high affinity by their divalent cation site. When assembled in filaments, the rate constant decreases, making the exchange of the bound cation unfavorable. Thus high levels of Ca^{2+} might be released upon disassembly of microvillar F-actin (Lange and Brandt, 1996; Lange et al., 1997).

Besides these considerations on local calcium signaling, phosphorylation of certain tyrosine residues inhibits actin bundling and activates villin severing properties, even in the absence of

high calcium concentration (Kumar and Khurana, 2004). Furthermore, various villin phosphorylation mutants revealed that villin regulation of cell motility seems to require its phosphorylation (Tomar et al., 2004). More specifically, ten phosphorylation sites have been identified on the villin sequence, four located near the N terminal domain and six towards the C-terminal sequence (Tomar et al., 2004, 2006). Combinations of phosphorylation mutants obtained by site-directed mutagenesis allowed functional dissection of the respective contributions of the two regions. Phosphorylation of the N-terminal tyrosines is critical for villin proper localization in the cell and association with actin, whereas phosphorylation of the C-terminal tyrosine residues regulates villin association with PLC_{γ} (Tomar et al., 2004, 2006). Nevertheless, phosphorylation of the entire core is required to enhance cell migration (Tomar et al., 2006). Most of the data regarding the contribution of villin phosphorylation has been obtained using a villin construct mutated for the ten phosphorylation sites. This construct does not locate properly within the cell and consequently results obtained using this mutant should be taken with caution (Tomar et al., 2004).

Overall, it is highly probable that coordination of calcium signaling and tyrosine phosphorylation enhances villin severing activity. Indeed, tyrosine phosphorylated villin interacts with and activates $PLC_{\gamma}1$ leading to Ca^{2+} release from the endoplasmic reticulum (Athman et al., 2003; Wang et al., 2007). In turn, store operated calcium entry would provide the necessary Ca^{2+} influx to sustain villin severing.

F. How to envision the role of villin in epithelial cell migration? Limits and perspectives

Considering that the vast majority of villin molecules concentrate in the apex at steady state, villin likely redistributes from the microvilli to the leading edge of lamellipodium from migrating cells. In this structure, villin might increase actin dynamics, likely through its severing activity. This process might favor lamellipodium extension (Athman et al., 2003). Alternatively villin may bundle actin in the lamellipodium to provide the necessary mechanical force, as proposed by George and colleagues (George et al., 2007). Our data showing similar migration efficiency on cells devoid of villin or re-expressing the severing mutant however argue against this latter possibility. Considering these previous results and our findings, villin might have a

dual role during epithelial cell migration: it could initiate apical microvilli disassembly thereby providing abundant free barbed ends and/or G-actin to stimulate motility and directly participates in lamellipodium extension. Our observation that lamellipodia formation rate is significantly impeded in absence of villin severing activity fits well with this proposal. Nevertheless, at this point, any definitive conclusion on this conceptual model linking villin contributions in the microvilli and in the lamellipodium would require a physical uncoupling between these two organelles.

III/ General conclusions

Microvilli: stable structures arising from tight regulation of a dynamic system.

The numerous microvilli that crowd the apices of intestinal cells perform the absorptive function of the intestine. To accomplish this vital function in a continuous fashion, microvilli are remarkably stable despite the highly dynamic nature inherent to actin-based protrusions. Microvilli are maintained in a dynamic equilibrium, which is thought to be ensured by a set of actin binding proteins that regulate actin assembly and its organization in a tightly packed bundle. In a first aspect of our work we could demonstrate that the primary function of the proteins organizing the actin filaments in a bundle - villin, espin and plastin-1 - is not to enable and sustain the membrane protrusion as previously assumed. Instead, they confer the specific actin architecture suited for the apical retention of membrane proteins essential for intestinal physiology. Our contribution is important in the sense that it represents a substantial change in the way we consider the function of these proteins. In addition, it is one of the few *in vivo* studies showing the intimate link between the actin architecture of the microvillus and its physiological functionality. Since the microvillus stability arises from the regulation of a dynamic system, slight changes in this equilibrium should allow rapid remodeling of the structure. Accordingly, we could bring into light the central role of villin in the fine tuning of this balance. Owing to its diverse actin related properties, villin would act as a functional switch dictating the microvillus fate in response to external stimuli. Although hypothesized by several previous studies, our work represents the first demonstration of such a role, illustrated in a pathological situation: the tissue injury.

Potential model of microvilli disassembly.

In light of our results, how can we integrate our conclusions to outline a putative updated model of the microvillus cytoskeleton? At steady state, microvilli proper shape and functionality would be controlled by the specific actin architecture. Microvilli would reach their maximal size owing to the dense bundled organization of actin filaments. The tightly controlled actin

treadmilling altogether with the bundled organization would ensure the shape of the structure **(Figure 36A)**. In addition, this local actin architecture would provide the appropriate framework for the apical retention of membrane proteins in charge of digestion and absorption thus establishing the functionality of the microvillus. In this context, the presence of villin, which exhibits an actin severing property, in the bundle would put the system in a precarious equilibrium. Nevertheless, at steady state microvilli are highly stable: villin severing activity would be minimal likely by reasons of a villin non-phosphorylated state and to a low free Ca^{2+} concentration ensured by the buffering action of calmodulin. In turn, upon intestinal stress, villin bundling activity would be inhibited and conversely the severing activity favored. Microvilli destruction would follow as a result of F-actin severing and free barbed ends capping by villin. Interestingly, the villin structure itself appears suited for this function: the 3D structure of villin bound to F-actin reveals the presence of multiple binding sites that only weakly interact with F-actin thereby allowing rapid change of conformation of the protein (Hampton et al., 2008). Increase in free Ca^{2+} would eventually inhibit plastin-1 actin bundling property thus additionally facilitating the bundle collapse. Indeed F-actin depolymerization is hindered by actin bundling proteins, which have to dissociate to allow further depolymerization (Loomis et al., 2003; Prost et al., 2007; Lenz et al., 2010). The relative low abundance of espin likely indicates a sporadic distribution on the bundle. Espin would thus have only minor consequences on actin depolymerization induced by filaments severing and capping (Brown and McKnight, 2010). Furthermore, microvilli disassembly has an important consequence: the release in the cytoplasm of microvillar elements illustrated in our study by the remobilization of microvillar actin towards motility structures, in a migratory context **(Figure 36B)**. In conclusion, the presence of three redundant actin bundling proteins are not required to enable and sustain the microvilli protrusion but participate in a critical manner in the establishment of microvillus functionality. At the same time the versatile villin embed the cytoskeleton with the machinery for rapid disassembly.

Microvilli disassembly: a common response to intestinal stresses?

Interestingly, microvilli collapse is not specific to migrating epithelial cells but is rather reported in a wide variety of stresses. For instance, mechanical pressure applied to the enterocytes, nutritional or calcium stresses, induce microvilli shortening or even complete disassembly (Tilney and Cardell, 1970; Ferrary et al., 1999). Similar observations are reported during various pathological situations, such as anoxia or ischemia (Yamamoto et al., 1980; Chen

et al., 1994), or infection by enteropathogens or virii (Moon et al., 1983; Brunet et al., 2000b).

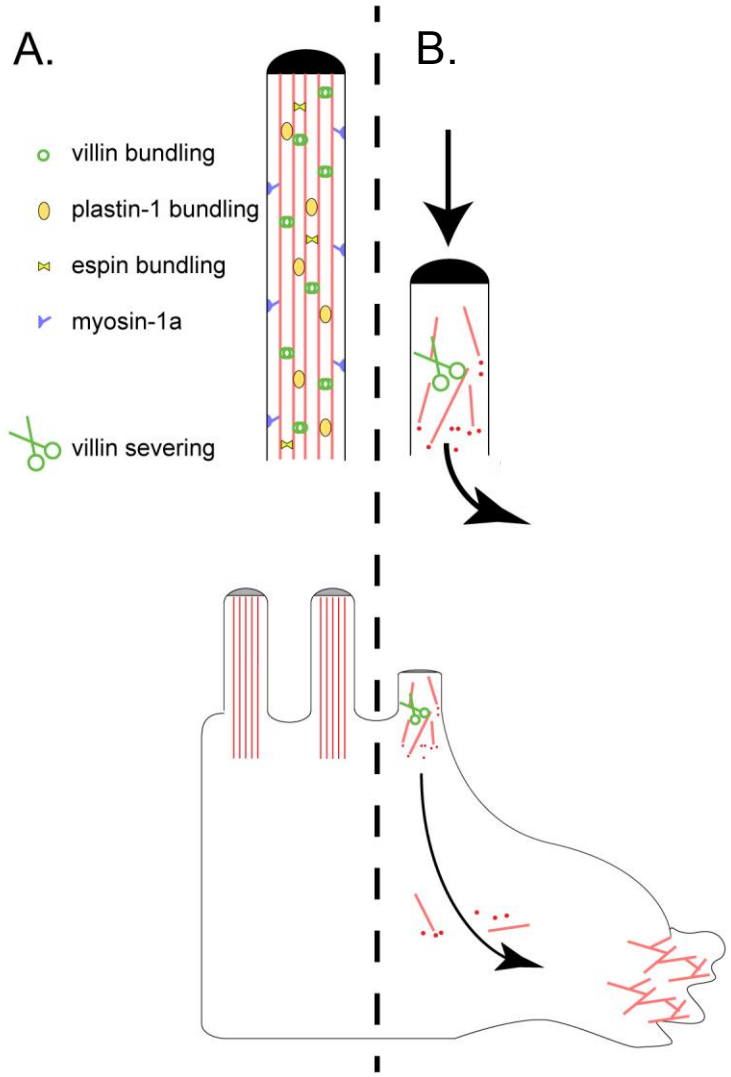

Figure 36: Model depicting an enterocyte adopting a motile phenotype
A. At resting state, the actin bundling proteins cooperatively ensure correct microvilli morphology and actin organization. **B.** During wound healing, the enterocyte become motile and undergo cell shape changes. Villin drives the disassembly of microvillar F-actin. Released actin molecules are incorporated at the lamellipodium. Actin is shown in red.

Villin and apical pole remodeling.

Microvilli disassembly following nutritional or calcium stresses indeed requires villin (Ferrary et al., 1999). We now demonstrate that their disassembly is induced by villin F-actin severing activity. Could we transpose this result to apex remodeling in other contexts?

Enterocyte infection by rotavirii and enteropathogenic E. coli (EPEC) leads to a severe microvilli disruption (Moon et al., 1983; Brunet et al., 2000b). Interestingly, the infection process is associated with an increase in Ca^{2+} concentration (Brunet et al., 2000a; Brown et al., 2008), raising the possibility of an activation of the villin severing property. EPEC-induced microvilli effacement seems to involve unbinding of myosin-1a to actin (Iizumi et al., 2007). Myosin-1a has been proposed to buffer Ca^{2+} in the microvilli via the bound calmodulins (Tyska et al., 2005; M. Mooseker, personal communication). It it thus conceivable that myosin-1a perturbation by EPEC indirectly leads to unregulated villin F-actin severing. The case of EPEC is particularly interesting as it additionally involves a dramatic apical actin cytoskeleton reorganization leading to the formation of a pedestal, on which the bacteria attach (Moon et al., 1983). This pedestal concentrates high amount of actin, suggesting a remobilization of microvillar actin following brush border effacement, in a conceptually close manner to what we show during epithelial cell migration.

Overall, this thesis documents the critical importance of regional actin architecture to ensure a proper biological function as exemplified in the intestinal microvilli. Simultaneously villin, one of the proteins in charge of the microvillar actin organization can induce local actin rearrangement leading to microvilli disassembly in stress contexts. Our experiments furthermore show for the first time that such microvilli reorganization seems to be of prime importance to sustain other cellular processes, documented in the case of a migrating cell. Even though regionally very restricted within the cell, villin-induced actin reorganization appears to have major consequences at the cell level, in agreement with systematic analysis documenting that very local actin dynamics can have cell scale morphological consequences and favor cell movement (Lacayo et al., 2007).

References

Achler, C., Filmer, D., Merte, C., and Drenckhahn, D. (1989). Role of microtubules in polarized delivery of apical membrane proteins to the brush border of the intestinal epithelium. J. Cell Biol. *109*, 179–189.

Ahmed, S., Goh, W.I., and Bu, W. (2010). I-BAR domains, IRSp53 and filopodium formation. Semin. Cell Dev. Biol. *21*, 350–356.

Albers, T.M., Lomakina, I., and Moore, R.P. (1995). Fate of polarized membrane components and evidence for microvillus disassembly on migrating enterocytes during repair of native intestinal epithelium. Lab. Invest. *73*, 139–148.

Albers, T.M., Lomakina, I., and Moore, R.P. (1996). Structural and functional roles of cytoskeletal proteins during repair of native guinea pig intestinal epithelium. Cell Biol. Int. *20*, 821–830.

Alfalah, M., Jacob, R., and Naim, H.Y. (2002). Intestinal dipeptidyl peptidase IV is efficiently sorted to the apical membrane through the concerted action of N- and O-glycans as well as association with lipid microdomains. J. Biol. Chem. *277*, 10683–10690.

Alfalah, M., Jacob, R., Preuss, U., Zimmer, K.P., Naim, H., and Naim, H.Y. (1999). O-linked glycans mediate apical sorting of human intestinal sucrase-isomaltase through association with lipid rafts. Curr. Biol. *9*, 593–596.

Algrain, M., Turunen, O., Vaheri, A., Louvard, D., and Arpin, M. (1993). Ezrin contains cytoskeleton and membrane binding domains accounting for its proposed role as a membrane-cytoskeletal linker. J. Cell Biol. *120*, 129–139.

Almeida, C.G., Yamada, A., Tenza, D., Louvard, D., Raposo, G., and Coudrier, E. (2011). Myosin 1b promotes the formation of post-Golgi carriers by regulating actin assembly and membrane remodelling at the trans-Golgi network. Nat. Cell Biol. *13*, 779–789.

Ameen, N., and Apodaca, G. (2007). Defective CFTR apical endocytosis and enterocyte brush border in myosin VI-deficient mice. Traffic *8*, 998–1006.

Ameen, N.A., Figueroa, Y., and Salas, P.J. (2001). Anomalous apical plasma membrane phenotype in CK8-deficient mice indicates a novel role for intermediate filaments in the polarization of simple epithelia. J. Cell. Sci. *114*, 563–575.

Apodaca, G. (2001). Endocytic traffic in polarized epithelial cells: role of the actin and microtubule cytoskeleton. Traffic *2*, 149–159.

Arpin, M., Friederich, E., Algrain, M., Vernel, F., and Louvard, D. (1994). Functional differences between L- and T-plastin isoforms. J. Cell Biol. *127*, 1995–2008.

Arpin, M., Pringault, E., Finidori, J., Garcia, A., Jeltsch, J.M., Vandekerckhove, J., and Louvard, D. (1988). Sequence of human villin: a large duplicated domain homologous with other actin-severing proteins and a unique small carboxy-terminal domain related to villin specificity. J. Cell Biol. *107*, 1759–1766.

de Arruda, M.V., Bazari, H., Wallek, M., and Matsudaira, P. (1992). An actin footprint on villin. Single site substitutions in a cluster of basic residues inhibit the actin severing but not capping activity of villin. J. Biol. Chem. *267*, 13079–13085.

Ashworth, S.L., Sandoval, R.M., Hosford, M., Bamburg, J.R., and Molitoris, B.A. (2001). Ischemic injury induces ADF relocalization to the apical domain of rat proximal tubule cells. Am. J. Physiol. Renal Physiol. *280*, F886–894.

Athman, R., Fernandez, M.-I., Gounon, P., Sansonetti, P., Louvard, D., Philpott, D., and Robine, S. (2005). Shigella flexneri infection is dependent on villin in the mouse intestine and in primary cultures of intestinal epithelial cells. Cell. Microbiol. *7*, 1109–1116.

Athman, R., Louvard, D., and Robine, S. (2003). Villin enhances hepatocyte growth factor-induced actin cytoskeleton remodeling in epithelial cells. Mol. Biol. Cell *14*, 4641–4653.

Athman, R., Tsocas, A., Presset, O., Robine, S., Rozé, C., and Ferrary, E. (2002). In vivo absorption of water and electrolytes in mouse intestine. Application to villin -/- mice. Am. J. Physiol. Gastrointest. Liver Physiol. *282*, G634–639.

Atilgan, E., Wirtz, D., and Sun, S.X. (2006). Mechanics and dynamics of actin-driven thin membrane protrusions. Biophys. J. *90*, 65–76.

Baas, A.F., Kuipers, J., van der Wel, N.N., Batlle, E., Koerten, H.K., Peters, P.J., and Clevers, H.C. (2004). Complete polarization of single intestinal epithelial cells upon activation of LKB1 by STRAD. Cell *116*, 457–466.

Bachmann, C., Fischer, L., Walter, U., and Reinhard, M. (1999). The EVH2 domain of the vasodilator-stimulated phosphoprotein mediates tetramerization, F-actin binding, and actin bundle formation. J. Biol. Chem. *274*, 23549–23557.

Barker, N., van Es, J.H., Kuipers, J., Kujala, P., van den Born, M., Cozijnsen, M., Haegebarth, A., Korving, J., Begthel, H., Peters, P.J., et al. (2007). Identification of stem cells in small intestine and colon by marker gene Lgr5. Nature *449*, 1003–1007.

Bartles, J.R. (2000). Parallel actin bundles and their multiple actin-bundling proteins. Curr. Opin. Cell Biol. *12*, 72–78.

Bartles, J.R., Zheng, L., Li, A., Wierda, A., and Chen, B. (1998). Small espin: a third actin-bundling protein and potential forked protein ortholog in brush border microvilli. J. Cell Biol. *143*, 107–119.

Bathe, M., Heussinger, C., Claessens, M.M.A.E., Bausch, A.R., and Frey, E. (2008). Cytoskeletal bundle mechanics. Biophys. J. *94*, 2955–2964.

Bear, J.E., Svitkina, T.M., Krause, M., Schafer, D.A., Loureiro, J.J., Strasser, G.A., Maly, I.V., Chaga, O.Y., Cooper, J.A., Borisy, G.G., et al. (2002). Antagonism between Ena/VASP proteins and actin filament capping regulates fibroblast motility. Cell *109*, 509–521.

Belyantseva, I.A., Boger, E.T., Naz, S., Frolenkov, G.I., Sellers, J.R., Ahmed, Z.M., Griffith, A.J., and Friedman, T.B. (2005). Myosin-XVa is required for tip localization of whirlin and differential elongation of hair-cell stereocilia. Nat. Cell Biol. *7*, 148–156.

Belyantseva, I.A., Perrin, B.J., Sonnemann, K.J., Zhu, M., Stepanyan, R., McGee, J., Frolenkov, G.I., Walsh, E.J., Friderici, K.H., Friedman, T.B., et al. (2009). Gamma-actin is required for cytoskeletal maintenance but not development. Proc. Natl. Acad. Sci. U.S.A. *106*, 9703–9708.

Benesh, A.E., Nambiar, R., McConnell, R.E., Mao, S., Tabb, D.L., and Tyska, M.J. (2010). Differential localization and dynamics of class I myosins in the enterocyte microvillus. Mol. Biol. Cell *21*, 970–978.

Berg, J.S., and Cheney, R.E. (2002). Myosin-X is an unconventional myosin that undergoes intrafilopodial motility. Nat. Cell Biol. *4*, 246–250.

Bernardini, M.L., Mounier, J., d' Hauteville, H., Coquis-Rondon, M., and Sansonetti, P.J. (1989). Identification of icsA, a plasmid locus of Shigella flexneri that governs bacterial intra- and intercellular spread through interaction with F-actin. Proc. Natl. Acad. Sci. U.S.A. *86*, 3867–3871.

Berro, J., Michelot, A., Blanchoin, L., Kovar, D.R., and Martiel, J.-L. (2007). Attachment conditions control actin filament buckling and the production of forces. Biophys. J. *92*, 2546–2558.

Berryman, M., Franck, Z., and Bretscher, A. (1993). Ezrin is concentrated in the apical microvilli of a wide variety of epithelial cells whereas moesin is found primarily in endothelial cells. J. Cell. Sci. *105 (Pt 4)*, 1025–1043.

Billadeau, D.D., and Burkhardt, J.K. (2006). Regulation of cytoskeletal dynamics at the immune synapse: new stars join the actin troupe. Traffic *7*, 1451–1460.

Le Bivic, A., Quaroni, A., Nichols, B., and Rodriguez-Boulan, E. (1990). Biogenetic pathways of plasma membrane proteins in Caco-2, a human intestinal epithelial cell line. J. Cell Biol. *111*, 1351–1361.

Blikslager, A.T., Moeser, A.J., Gookin, J.L., Jones, S.L., and Odle, J. (2007). Restoration of barrier function in injured intestinal mucosa. Physiol. Rev. *87*, 545–564.

Boëda, B., El-Amraoui, A., Bahloul, A., Goodyear, R., Daviet, L., Blanchard, S., Perfettini, I., Fath, K.R., Shorte, S., Reiners, J., et al. (2002). Myosin VIIa, harmonin and cadherin 23, three Usher I gene products that cooperate to shape the sensory hair cell bundle. EMBO J. *21*, 6689–6699.

Bottaro, D.P., Rubin, J.S., Faletto, D.L., Chan, A.M., Kmiecik, T.E., Vande Woude, G.F., and Aaronson, S.A. (1991). Identification of the Hepatocyte Growth Factor Receptor as the C-Met Proto-Oncogene Product. Science *251*, 802–804.

Boulant, S., Kural, C., Zeeh, J.-C., Ubelmann, F., and Kirchhausen, T. (2011). Actin dynamics counteract membrane tension during clathrin-mediated endocytosis. Nat. Cell Biol. *13*, 1124–1131.

Braccia, A., Villani, M., Immerdal, L., Niels-Christiansen, L.-L., Nystrøm, B.T., Hansen, G.H., and Danielsen, E.M. (2003). Microvillar membrane microdomains exist at physiological temperature. Role of galectin-4 as lipid raft stabilizer revealed by "superrafts."J. Biol. Chem. *278*, 15679–15684.

Brangbour, C., du Roure, O., Helfer, E., Démoulin, D., Mazurier, A., Fermigier, M., Carlier, M.-F., Bibette, J., and Baudry, J. (2011). Force-velocity measurements of a few growing actin filaments. PLoS Biol. *9*, e1000613.

Brawley, C.M., and Rock, R.S. (2009). Unconventional myosin traffic in cells reveals a selective actin cytoskeleton. Proc. Natl. Acad. Sci. U.S.A. *106*, 9685–9690.

Breitsprecher, D., Jaiswal, R., Bombardier, J.P., Gould, C.J., Gelles, J., and Goode, B.L. (2012). Rocket launcher mechanism of collaborative actin assembly defined by single-molecule imaging. Science *336*, 1164–1168.

Breitsprecher, D., Koestler, S.A., Chizhov, I., Nemethova, M., Mueller, J., Goode, B.L., Small, J.V., Rottner, K., and Faix, J. (2011). Cofilin cooperates with fascin to disassemble filopodial actin filaments. J. Cell. Sci. *124*, 3305–3318.

Bretscher, A. (1981). Fimbrin is a cytoskeletal protein that crosslinks F-actin in vitro. Proc. Natl. Acad. Sci. U.S.A. *78*, 6849–6853.

Bretscher, A. (1989). Rapid phosphorylation and reorganization of ezrin and spectrin accompany morphological changes induced in A-431 cells by epidermal growth factor. J. Cell Biol. *108*, 921–930.

Bretscher, A., and Weber, K. (1978). Localization of actin and microfilament-associated proteins in the microvilli and terminal web of the intestinal brush border by immunofluorescence microscopy. J. Cell Biol. *79*, 839–845.

Bretscher, A., and Weber, K. (1979). Villin: the major microfilament-associated protein of the intestinal microvillus. Proc. Natl. Acad. Sci. U.S.A. *76*, 2321–2325.

Bretscher, A., and Weber, K. (1980a). Fimbrin, a new microfilament-associated protein present in microvilli and other cell surface structures. J. Cell Biol. *86*, 335–340.

Bretscher, A., and Weber, K. (1980b). Villin is a major protein of the microvillus cytoskeleton which binds both G and F actin in a calcium-dependent manner. Cell *20*, 839–847.

Brocardo, M., Näthke, I.S., and Henderson, B.R. (2005). Redefining the subcellular location and transport of APC: new insights using a panel of antibodies. EMBO Rep. *6*, 184–190.

Brown, A.L., Jr (1962). Microvilli of the human jejunal epithelial cell. J. Cell Biol. *12*, 623–627.

Brown, D.A., Crise, B., and Rose, J.K. (1989). Mechanism of membrane anchoring affects polarized expression of two proteins in MDCK cells. Science *245*, 1499–1501.

Brown, D.A., and Rose, J.K. (1992). Sorting of GPI-anchored proteins to glycolipid-enriched membrane subdomains during transport to the apical cell surface. Cell *68*, 533–544.

Brown, J.W., and McKnight, C.J. (2010). Molecular model of the microvillar cytoskeleton and organization of the brush border. PLoS ONE *5*, e9406.

Brown, M.D., Bry, L., Li, Z., and Sacks, D.B. (2008). Actin pedestal formation by EPEC is regulated by IQGAP1, calcium and calmodulin. J. Biol. Chem. M803477200.

Brunet, J.P., Cotte-Laffitte, J., Linxe, C., Quero, A.M., Géniteau-Legendre, M., and Servin, A. (2000a). Rotavirus infection induces an increase in intracellular calcium concentration in human intestinal epithelial cells: role in microvillar actin alteration. J. Virol. *74*, 2323–2332.

Brunet, J.P., Jourdan, N., Cotte-Laffitte, J., Linxe, C., Géniteau-Legendre, M., Servin, A., and Quéro, A.M. (2000b). Rotavirus infection induces cytoskeleton disorganization in human intestinal epithelial cells: implication of an increase in intracellular calcium concentration. J. Virol. *74*, 10801–10806.

Burgess, D.R., and Prum, B.E. (1982). Reevaluation of brush border motility: calcium induces core filament solution and microvillar vesiculation. J. Cell Biol. *94*, 97–107.

Burtnick, L.D., Koepf, E.K., Grimes, J., Jones, E.Y., Stuart, D.I., McLaughlin, P.J., and Robinson, R.C. (1997). The crystal structure of plasma gelsolin: implications for actin severing, capping, and nucleation. Cell *90*, 661–670.

Campellone, K.G., and Welch, M.D. (2010). A nucleator arms race: cellular control of actin assembly. Nat. Rev. Mol. Cell Biol. *11*, 237–251.

Carberry, K., Wiesenfahrt, T., Geisler, F., Stöcker, S., Gerhardus, H., Überbach, D., Davis, W., Jorgensen, E.,

Leube, R.E., and Bossinger, O. (2012). The novel intestinal filament organizer IFO-1 contributes to epithelial integrity in concert with ERM-1 and DLG-1. Development *139*, 1851–1862.

Carlier, M.F., Laurent, V., Santolini, J., Melki, R., Didry, D., Xia, G.X., Hong, Y., Chua, N.H., and Pantaloni, D. (1997). Actin depolymerizing factor (ADF/cofilin) enhances the rate of filament turnover: implication in actin-based motility. J. Cell Biol. *136*, 1307–1322.

Casaletto, J.B., Saotome, I., Curto, M., and McClatchey, A.I. (2011). Ezrin-mediated apical integrity is required for intestinal homeostasis. Proc. Natl. Acad. Sci. U.S.A. *108*, 11924–11929.

Cetin, S., Ford, H.R., Sysko, L.R., Agarwal, C., Wang, J., Neal, M.D., Baty, C., Apodaca, G., and Hackam, D.J. (2004). Endotoxin inhibits intestinal epithelial restitution through activation of Rho-GTPase and increased focal adhesions. J. Biol. Chem. *279*, 24592–24600.

Cha, B., Kenworthy, A., Murtazina, R., and Donowitz, M. (2004). The lateral mobility of NHE3 on the apical membrane of renal epithelial OK cells is limited by the PDZ domain proteins NHERF1/2, but is dependent on an intact actin cytoskeleton as determined by FRAP. J. Cell. Sci. *117*, 3353–3365.

Chafel, M.M., Shen, W., and Matsudaira, P. (1995). Sequential expression and differential localization of I-, L-, and T-fimbrin during differentiation of the mouse intestine and yolk sac. Dev. Dyn. *203*, 141–151.

Chambers, C., and Grey, R.D. (1979). Development of the structural components of the brush border in absorptive cells of the chick intestine. Cell Tissue Res. *204*, 387–405.

Chandhoke, S.K., and Mooseker, M.S. (2012). A Role for Myosin IXb, a motor-Rho-GAP Chimera, in Epithelial Wound Healing and Tight Junction Regulation. Molecular Biology of the Cell.

Chen, J., Doctor, R.B., and Mandel, L.J. (1994). Cytoskeletal dissociation of ezrin during renal anoxia: role in microvillar injury. Am. J. Physiol. *267*, C784–795.

Choe, H., Burtnick, L.D., Mejillano, M., Yin, H.L., Robinson, R.C., and Choe, S. (2002). The calcium activation of gelsolin: insights from the 3A structure of the G4-G6/actin complex. J. Mol. Biol. *324*, 691–702.

Claessens, M.M.A.E., Bathe, M., Frey, E., and Bausch, A.R. (2006). Actin-binding proteins sensitively mediate F-actin bundle stiffness. Nat Mater *5*, 748–753.

Le Clainche, C., and Carlier, M.-F. (2008). Regulation of actin assembly associated with protrusion and adhesion in cell migration. Physiol. Rev. *88*, 489–513.

Coluccio, L.M., and Bretscher, A. (1989). Reassociation of microvillar core proteins: making a microvillar core in vitro. J. Cell Biol. *108*, 495–502.

Conzelman, K.A., and Mooseker, M.S. (1987). The 110-kD protein-calmodulin complex of the intestinal microvillus is an actin-activated MgATPase. J. Cell Biol. *105*, 313–324.

Cooper, J.A., and Schafer, D.A. (2000). Control of actin assembly and disassembly at filament ends. Curr. Opin. Cell Biol. *12*, 97–103.

Costa de Beauregard, M.A., Pringault, E., Robine, S., and Louvard, D. (1995). Suppression of villin expression by antisense RNA impairs brush border assembly in polarized epithelial intestinal cells. EMBO J. *14*, 409–421.

Cramm-Behrens, C.I., Dienst, M., and Jacob, R. (2008). Apical cargo traverses endosomal compartments on the passage to the cell surface. Traffic *9*, 2206–2220.

Croce, A., Cassata, G., Disanza, A., Gagliani, M.C., Tacchetti, C., Malabarba, M.G., Carlier, M.-F., Scita, G., Baumeister, R., and Di Fiore, P.P. (2004). A novel actin barbed-end-capping activity in EPS-8 regulates apical morphogenesis in intestinal cells of Caenorhabditis elegans. Nat. Cell Biol. *6*, 1173–1179.

Dai, J., and Sheetz, M.P. (1999). Membrane tether formation from blebbing cells. Biophys. J. *77*, 3363–3370.

Danielsen, E.M. (1995). Involvement of detergent-insoluble complexes in the intracellular transport of intestinal brush border enzymes. Biochemistry *34*, 1596–1605.

Delacour, D., Cramm-Behrens, C.I., Drobecq, H., Le Bivic, A., Naim, H.Y., and Jacob, R. (2006). Requirement for galectin-3 in apical protein sorting. Curr. Biol. *16*, 408–414.

Derivery, E., Sousa, C., Gautier, J.J., Lombard, B., Loew, D., and Gautreau, A. (2009). The Arp2/3 activator WASH controls the fission of endosomes through a large multiprotein complex. Dev. Cell *17*, 712–723.

DeRosier, D.J., and Tilney, L.G. (2000). F-Actin Bundles Are Derivatives of Microvilli What Does This Tell US About How Bundles Might Form? J Cell Biol *148*, 1–6.

DesMarais, V., Ichetovkin, I., Condeelis, J., and Hitchcock-DeGregori, S.E. (2002). Spatial regulation of actin dynamics: a tropomyosin-free, actin-rich compartment at the leading edge. J. Cell. Sci. *115*, 4649–4660.

Disanza, A., Carlier, M.-F., Stradal, T.E.B., Didry, D., Frittoli, E., Confalonieri, S., Croce, A., Wehland, J., Di Fiore, P.P., and Scita, G. (2004). Eps8 controls actin-based motility by capping the barbed ends of actin filaments. Nat. Cell Biol. *6*, 1180–1188.

Disanza, A., Mantoani, S., Hertzog, M., Gerboth, S., Frittoli, E., Steffen, A., Berhoerster, K., Kreienkamp, H.-J., Milanesi, F., Di Fiore, P.P., et al. (2006). Regulation of cell shape by Cdc42 is mediated by the synergic actin-bundling activity of the Eps8-IRSp53 complex. Nat. Cell Biol. *8*, 1337–1347.

Dise, R.S., Frey, M.R., Whitehead, R.H., and Polk, D.B. (2008). Epidermal Growth Factor Stimulates Rac Activation Through Src and Phosphatidylinositol 3-Kinase to Promote Colonic Epithelial Cell Migration. Am J Physiol Gastrointest Liver Physiol *294*, G276–G285.

Doyle, A., Crosby, S.R., Burton, D.R., Lilley, F., and Murphy, M.F. (2011). Actin bundling and polymerisation properties of eukaryotic elongation factor 1 alpha (eEF1A), histone H2A-H2B and lysozyme in vitro. J. Struct. Biol. *176*, 370–378.

Drenckhahn, D., and Dermietzel, R. (1988). Organization of the actin filament cytoskeleton in the intestinal brush border: a quantitative and qualitative immunoelectron microscope study. J. Cell Biol. *107*, 1037–1048.

Drenckhahn, D., Steffens, R., and Gröschel-Stewart, U. (1980). Immunocytochemical localization of myosin in the brush border region of the intestinal epithelium. Cell Tissue Res. *205*, 163–166.

Dugina, V., Zwaenepoel, I., Gabbiani, G., Clément, S., and Chaponnier, C. (2009). Beta and gamma-cytoplasmic actins display distinct distribution and functional diversity. J. Cell. Sci. *122*, 2980–2988.

Edelman, J.L., Kajimura, M., Woldemussie, E., and Sachs, G. (1994). Differential effects of carbachol on calcium entry and release in CHO cells expressing the m3 muscarinic receptor. Cell Calcium *16*, 181–193.

Egile, C., Loisel, T.P., Laurent, V., Li, R., Pantaloni, D., Sansonetti, P.J., and Carlier, M.F. (1999). Activation of the CDC42 effector N-WASP by the Shigella flexneri IcsA protein promotes actin nucleation by Arp2/3 complex and bacterial actin-based motility. J. Cell Biol. *146*, 1319–1332.

Fan, Y., Eswarappa, S.M., Hitomi, M., and Fox, P.L. (2012). Myo1c facilitates G-actin transport to the leading edge of migrating endothelial cells. J. Cell Biol. *198*, 47–55.

Fanning, A.S., Wolenski, J.S., Mooseker, M.S., and Izant, J.G. (1994). Differential regulation of skeletal muscle myosin-II and brush border myosin-I enzymology and mechanochemistry by bacterially produced tropomyosin isoforms. Cell Motil. Cytoskeleton *29*, 29–45.

Farooqui, R., and Fenteany, G. (2005). Multiple rows of cells behind an epithelial wound edge extend cryptic lamellipodia to collectively drive cell-sheet movement. J. Cell. Sci. *118*, 51–63.

Fath, K.R., and Burgess, D.R. (1993). Golgi-derived vesicles from developing epithelial cells bind actin filaments and possess myosin-I as a cytoplasmically oriented peripheral membrane protein. J. Cell Biol. *120*, 117–127.

Fath, K.R., Obenauf, S.D., and Burgess, D.R. (1990). Cytoskeletal protein and mRNA accumulation during brush border formation in adult chicken enterocytes. Development *109*, 449–459.

Fenteany, G., Janmey, P.A., and Stossel, T.P. (2000). Signaling pathways and cell mechanics involved in wound closure by epithelial cell sheets. Curr. Biol. *10*, 831–838.

Ferrary, E., Cohen-Tannoudji, M., Pehau-Arnaudet, G., Lapillonne, A., Athman, R., Ruiz, T., Boulouha, L., El Marjou, F., Doye, A., Fontaine, J.J., et al. (1999). In vivo, villin is required for Ca(2+)-dependent F-actin disruption in intestinal brush borders. J. Cell Biol. *146*, 819–830.

Finidori, J., Friederich, E., Kwiatkowski, D.J., and Louvard, D. (1992). In vivo analysis of functional domains from villin and gelsolin. J. Cell Biol. *116*, 1145–1155.

Flanagan, L.A., Chou, J., Falet, H., Neujahr, R., Hartwig, J.H., and Stossel, T.P. (2001). Filamin A, the Arp2/3 complex, and the morphology and function of cortical actin filaments in human melanoma cells. J. Cell Biol. *155*, 511–517.

Footer, M.J., Kerssemakers, J.W.J., Theriot, J.A., and Dogterom, M. (2007). Direct measurement of force generation by actin filament polymerization using an optical trap. Proc. Natl. Acad. Sci. U.S.A. *104*, 2181–2186.

Franck, Z., Footer, M., and Bretscher, A. (1990). Microinjection of villin into cultured cells induces rapid and

long-lasting changes in cell morphology but does not inhibit cytokinesis, cell motility, or membrane ruffling. J. Cell Biol. *111*, 2475–2485.

Friederich, E., Kreis, T.E., and Louvard, D. (1993). Villin-induced growth of microvilli is reversibly inhibited by cytochalasin D. J. Cell. Sci. *105 (Pt 3)*, 765–775.

Friederich, E., Vancompernolle, K., Huet, C., Goethals, M., Finidori, J., Vandekerckhove, J., and Louvard, D. (1992). An actin-binding site containing a conserved motif of charged amino acid residues is essential for the morphogenic effect of villin. Cell *70*, 81–92.

Friedl, P., and Gilmour, D. (2009). Collective cell migration in morphogenesis, regeneration and cancer. Nat. Rev. Mol. Cell Biol. *10*, 445–457.

Garbett, D., and Bretscher, A. (2012). PDZ interactions regulate rapid turnover of the scaffolding protein EBP50 in microvilli. The Journal of Cell Biology.

Gauthier, N.C., Fardin, M.A., Roca-Cusachs, P., and Sheetz, M.P. (2011). Temporary increase in plasma membrane tension coordinates the activation of exocytosis and contraction during cell spreading. Proc. Natl. Acad. Sci. U.S.A. *108*, 14467–14472.

Gautreau, A., Louvard, D., and Arpin, M. (2000). Morphogenic effects of ezrin require a phosphorylation-induced transition from oligomers to monomers at the plasma membrane. J. Cell Biol. *150*, 193–203.

Geiger, B., Spatz, J.P., and Bershadsky, A.D. (2009). Environmental sensing through focal adhesions. Nat. Rev. Mol. Cell Biol. *10*, 21–33.

George, S.P., Wang, Y., Mathew, S., Srinivasan, K., and Khurana, S. (2007). Dimerization and Actin-Bundling Properties of Villin and Its Role in the Assembly of Epithelial Cell Brush Borders. J. Biol. Chem. *282*, 26528–26541.

Gerbe, F., van Es, J.H., Makrini, L., Brulin, B., Mellitzer, G., Robine, S., Romagnolo, B., Shroyer, N.F., Bourgaux, J.-F., Pignodel, C., et al. (2011). Distinct ATOH1 and Neurog3 requirements define tuft cells as a new secretory cell type in the intestinal epithelium. J. Cell Biol. *192*, 767–780.

Gherardi, E., Gray, J., Stoker, M., Perryman, M., and Furlong, R. (1989). Purification of scatter factor, a fibroblast-derived basic protein that modulates epithelial interactions and movement. Proc. Natl. Acad. Sci. U.S.A. *86*, 5844–5848.

Glenney, J.R., Jr, Bretscher, A., and Weber, K. (1980). Calcium control of the intestinal microvillus cytoskeleton: its implications for the regulation of microfilament organizations. Proc. Natl. Acad. Sci. U.S.A. *77*, 6458–6462.

Glenney, J.R., Jr, Geisler, N., Kaulfus, P., and Weber, K. (1981a). Demonstration of at least two different actin-binding sites in villin, a calcium-regulated modulator of F-actin organization. J. Biol. Chem. *256*, 8156–8161.

Glenney, J.R., Jr, and Glenney, P. (1985). Comparison of Ca++-regulated events in the intestinal brush border. J. Cell Biol. *100*, 754–763.

Glenney, J.R., Jr, Kaulfus, P., Matsudaira, P., and Weber, K. (1981b). F-actin binding and bundling properties of fimbrin, a major cytoskeletal protein of microvillus core filaments. J. Biol. Chem. *256*, 9283–9288.

Glenney, J.R., Jr, Kaulfus, P., and Weber, K. (1981c). F actin assembly modulated by villin: Ca++-dependent nucleation and capping of the barbed end. Cell *24*, 471–480.

Glenney, J.R., Jr, and Weber, K. (1981). Calcium control of microfilaments: uncoupling of the F-actin-severing and -bundling activity of villin by limited proteolysis in vitro. Proc. Natl. Acad. Sci. U.S.A. *78*, 2810–2814.

Golenhofen, N., Doctor, R.B., Bacallao, R., and Mandel, L.J. (1995). Actin and villin compartmentation during ATP depletion and recovery in renal cultured cells. Kidney Int. *48*, 1837–1845.

Gookin, J.L., Galanko, J.A., Blikslager, A.T., and Argenzio, R.A. (2003). PG-mediated closure of paracellular pathway and not restitution is the primary determinant of barrier recovery in acutely injured porcine ileum. Am. J. Physiol. Gastrointest. Liver Physiol. *285*, G967–979.

Gorelik, J., Shevchuk, A.I., Frolenkov, G.I., Diakonov, I.A., Lab, M.J., Kros, C.J., Richardson, G.P., Vodyanoy, I., Edwards, C.R.W., Klenerman, D., et al. (2003). Dynamic Assembly of Surface Structures in Living Cells. PNAS *100*, 5819–5822.

Gouin, E., Gantelet, H., Egile, C., Lasa, I., Ohayon, H., Villiers, V., Gounon, P., Sansonetti, P.J., and Cossart, P. (1999). A comparative study of the actin-based motilities of the pathogenic bacteria Listeria monocytogenes,

Shigella flexneri and Rickettsia conorii. J. Cell. Sci. *112 (Pt 11)*, 1697–1708.

Grimm-Günter, E.-M.S., Revenu, C., Ramos, S., Hurbain, I., Smyth, N., Ferrary, E., Louvard, D., Robine, S., and Rivero, F. (2009). Plastin 1 binds to keratin and is required for terminal web assembly in the intestinal epithelium. Mol. Biol. Cell *20*, 2549–2562.

Grootjans, J., Thuijls, G., Derikx, J.P.M., van Dam, R.M., Dejong, C.H.C., and Buurman, W.A. (2011). Rapid lamina propria retraction and zipper-like constriction of the epithelium preserves the epithelial lining in human small intestine exposed to ischaemia-reperfusion. J. Pathol. *224*, 411–419.

Grüneberg, H., Burnett, J.B., and Snell, G.D. (1941). The Origin of Jerker, a New Gene Mutation of the House Mouse, and Linkage Studies Made with It. Proc. Natl. Acad. Sci. U.S.A. *27*, 562–565.

Gual, P., Giordano, S., Williams, T.A., Rocchi, S., Van Obberghen, E., and Comoglio, P.M. (2000). Sustained recruitment of phospholipase C-gamma to Gab1 is required for HGF-induced branching tubulogenesis. Oncogene *19*, 1509–1518.

van der Gucht, J., Paluch, E., Plastino, J., and Sykes, C. (2005). Stress release drives symmetry breaking for actin-based movement. Proc. Natl. Acad. Sci. U.S.A. *102*, 7847–7852.

Guild, G.M., Connelly, P.S., Ruggiero, L., Vranich, K.A., and Tilney, L.G. (2003). Long continuous actin bundles in Drosophila bristles are constructed by overlapping short filaments. J. Cell Biol. *162*, 1069–1077.

Haik, B.G., and Zimny, M.L. (1977). Scanning electron microscopy of corneal wound healing in the rabbit. Invest. Ophthalmol. Vis. Sci. *16*, 787–796.

Hall, A. (1998). Rho GTPases and the actin cytoskeleton. Science *279*, 509–514.

Hall, A. (2005). Rho GTPases and the control of cell behaviour. Biochem. Soc. Trans. *33*, 891–895.

Hampton, C.M., Liu, J., Taylor, D.W., DeRosier, D.J., and Taylor, K.A. (2008). The 3D structure of villin as an unusual F-Actin crosslinker. Structure *16*, 1882–1891.

Hansen, G.H., Rasmussen, K., Niels-Christiansen, L.-L., and Danielsen, E.M. (2009). Endocytic trafficking from the small intestinal brush border probed with FM dye. Am. J. Physiol. Gastrointest. Liver Physiol. *297*, G708–715.

Hartman, A.L., Sawtell, N.M., and Lessard, J.L. (1989). Expression of actin isoforms in developing rat intestinal epithelium. J. Histochem. Cytochem. *37*, 1225–1233.

Heintzelman, M.B., Hasson, T., and Mooseker, M.S. (1994). Multiple unconventional myosin domains of the intestinal brush border cytoskeleton. J. Cell. Sci. *107 (Pt 12)*, 3535–3543.

Hertzog, M., Milanesi, F., Hazelwood, L., Disanza, A., Liu, H., Perlade, E., Malabarba, M.G., Pasqualato, S., Maiolica, A., Confalonieri, S., et al. (2010). Molecular basis for the dual function of Eps8 on actin dynamics: bundling and capping. PLoS Biol. *8*, e1000387.

Hirokawa, N., Cheney, R.E., and Willard, M. (1983a). Location of a protein of the fodrin-spectrin-TW260/240 family in the mouse intestinal brush border. Cell *32*, 953–965.

Hirokawa, N., and Heuser, J.E. (1981). Quick-freeze, deep-etch visualization of the cytoskeleton beneath surface differentiations of intestinal epithelial cells. J. Cell Biol. *91*, 399–409.

Hirokawa, N., Keller, T.C., 3rd, Chasan, R., and Mooseker, M.S. (1983b). Mechanism of brush border contractility studied by the quick-freeze, deep-etch method. J. Cell Biol. *96*, 1325–1336.

Hirokawa, N., Tilney, L.G., Fujiwara, K., and Heuser, J.E. (1982). Organization of actin, myosin, and intermediate filaments in the brush border of intestinal epithelial cells. J. Cell Biol. *94*, 425–443.

Hopkins, A.M., Pineda, A.A., Winfree, L.M., Brown, G.T., Laukoetter, M.G., and Nusrat, A. (2007). Organized migration of epithelial cells requires control of adhesion and protrusion through Rho kinase effectors. Am. J. Physiol. Gastrointest. Liver Physiol. *292*, G806–817.

Howe, C.L., and Mooseker, M.S. (1983). Characterization of the 110-kdalton actin-calmodulin-, and membrane-binding protein from microvilli of intestinal epithelial cells. J. Cell Biol. *97*, 974–985.

Howe, C.L., Mooseker, M.S., and Graves, T.A. (1980). Brush-border calmodulin. A major component of the isolated microvillus core. J. Cell Biol. *85*, 916–923.

Huber, L.A., Pimplikar, S., Parton, R.G., Virta, H., Zerial, M., and Simons, K. (1993). Rab8, a small GTPase involved in vesicular traffic between the TGN and the basolateral plasma membrane. J. Cell Biol. *123*, 35–45.

Hughes, S.A., Carothers, A.M., Hunt, D.H., Moran, A.E., Mueller, J.D., and Bertagnolli, M.M. (2002). Adenomatous polyposis coli truncation alters cytoskeletal structure and microtubule stability in early intestinal tumorigenesis. J. Gastrointest. Surg. *6*, 868–874; discussion 875.

Iizuka, M., and Konno, S. (2011). Wound healing of intestinal epithelial cells. World J. Gastroenterol. *17*, 2161–2171.

Iizumi, Y., Sagara, H., Kabe, Y., Azuma, M., Kume, K., Ogawa, M., Nagai, T., Gillespie, P.G., Sasakawa, C., and Handa, H. (2007). The Enteropathogenic E. coli Effector EspB Facilitates Microvillus Effacing and Antiphagocytosis by Inhibiting Myosin Function. Cell Host & Microbe *2*, 383–392.

Jacob, R., Heine, M., Alfalah, M., and Naim, H.Y. (2003). Distinct cytoskeletal tracks direct individual vesicle populations to the apical membrane of epithelial cells. Curr. Biol. *13*, 607–612.

Jacob, R., and Naim, H.Y. (2001). Apical membrane proteins are transported in distinct vesicular carriers. Curr. Biol. *11*, 1444–1450.

Janmey, P.A., Cunningham C C, Oster G F, and Stossel T P (1992). Mechanics of Swelling. From Clays to Living Cells and Tissues. In Mechanics of Swelling. From Clays to Living Cells and Tissues, (Karalis TK (Springer, Berlin)), pp. pp 333–346.

Janmey, P.A., and Matsudaira, P.T. (1988). Functional comparison of villin and gelsolin. Effects of Ca2+, KCl, and polyphosphoinositides. J. Biol. Chem. *263*, 16738–16743.

Keren, K., Yam, P.T., Kinkhabwala, A., Mogilner, A., and Theriot, J.A. (2009). Intracellular fluid flow in rapidly moving cells. Nature Cell Biology *11*, 1219–1224.

Khurana, S., and George, S.P. (2008). Regulation of cell structure and function by actin-binding proteins: villin's perspective. FEBS Lett. *582*, 2128–2139.

King, R.S., and Newmark, P.A. (2012). The cell biology of regeneration. J. Cell Biol. *196*, 553–562.

Kiuchi, T., Nagai, T., Ohashi, K., and Mizuno, K. (2011). Measurements of spatiotemporal changes in G-actin concentration reveal its effect on stimulus-induced actin assembly and lamellipodium extension. J. Cell Biol. *193*, 365–380.

Kiuchi, T., Ohashi, K., Kurita, S., and Mizuno, K. (2007). Cofilin promotes stimulus-induced lamellipodium formation by generating an abundant supply of actin monomers. J. Cell Biol. *177*, 465–476.

Klepeis, V.E., Cornell-Bell, A., and Trinkaus-Randall, V. (2001). Growth factors but not gap junctions play a role in injury-induced Ca2+ waves in epithelial cells. J. Cell. Sci. *114*, 4185–4195.

ten Klooster, J.P., Jansen, M., Yuan, J., Oorschot, V., Begthel, H., Di Giacomo, V., Colland, F., de Koning, J., Maurice, M.M., Hornbeck, P., et al. (2009). Mst4 and Ezrin induce brush borders downstream of the Lkb1/Strad/Mo25 polarization complex. Dev. Cell *16*, 551–562.

Klumperman, J., Boekestijn, J.C., Mulder, A.M., Fransen, J.A., and Ginsel, L.A. (1991). Intracellular localization and endocytosis of brush border enzymes in the enterocyte-like cell line Caco-2. Eur. J. Cell Biol. *54*, 76–84.

Koch, S., Capaldo, C.T., Samarin, S., Nava, P., Neumaier, I., Skerra, A., Sacks, D.B., Parkos, C.A., and Nusrat, A. (2009). Dkk-1 inhibits intestinal epithelial cell migration by attenuating directional polarization of leading edge cells. Mol. Biol. Cell *20*, 4816–4825.

Koestler, S.A., Auinger, S., Vinzenz, M., Rottner, K., and Small, J.V. (2008). Differentially oriented populations of actin filaments generated in lamellipodia collaborate in pushing and pausing at the cell front. Nat. Cell Biol. *10*, 306–313.

Kovar, D.R., and Pollard, T.D. (2004). Insertional assembly of actin filament barbed ends in association with formins produces piconewton forces. Proc. Natl. Acad. Sci. U.S.A. *101*, 14725–14730.

Kozlov, M.M., and Bershadsky, A.D. (2004). Processive capping by formin suggests a force-driven mechanism of actin polymerization. J. Cell Biol. *167*, 1011–1017.

Kozlov, M.M., and Mogilner, A. (2007). Model of polarization and bistability of cell fragments. Biophys. J. *93*, 3811–3819.

Kreitzer, G., Marmorstein, A., Okamoto, P., Vallee, R., and Rodriguez-Boulan, E. (2000). Kinesin and dynamin are required for post-Golgi transport of a plasma-membrane protein. Nat. Cell Biol. *2*, 125–127.

Kreitzer, G., Schmoranzer, J., Low, S.H., Li, X., Gan, Y., Weimbs, T., Simon, S.M., and Rodriguez-Boulan, E. (2003). Three-dimensional analysis of post-Golgi carrier exocytosis in epithelial cells. Nat. Cell Biol. *5*, 126–136.

Krugmann, S., Jordens, I., Gevaert, K., Driessens, M., Vandekerckhove, J., and Hall, A. (2001). Cdc42 induces filopodia by promoting the formation of an IRSp53:Mena complex. Curr. Biol. *11*, 1645–1655.

Kumar, N., and Khurana, S. (2004). Identification of a functional switch for actin severing by cytoskeletal proteins. J. Biol. Chem. *279*, 24915–24918.

Kumar, N., Zhao, P., Tomar, A., Galea, C.A., and Khurana, S. (2004). Association of villin with phosphatidylinositol 4,5-bisphosphate regulates the actin cytoskeleton. J. Biol. Chem. *279*, 3096–3110.

Kureishy, N., Sapountzi, V., Prag, S., Anilkumar, N., and Adams, J.C. (2002). Fascins, and their roles in cell structure and function. Bioessays *24*, 350–361.

Lacayo, C.I., Pincus, Z., VanDuijn, M.M., Wilson, C.A., Fletcher, D.A., Gertler, F.B., Mogilner, A., and Theriot, J.A. (2007). Emergence of large-scale cell morphology and movement from local actin filament growth dynamics. PLoS Biol. *5*, e233.

Lange, J., Schlieps, K., Lange, K., and Knoll-Köhler, E. (1997). Activation of calcium signaling in isolated rat hepatocytes is accompanied by shape changes of microvilli. Exp. Cell Res. *234*, 486–497.

Lange, K., and Brandt, U. (1996). Calcium storage and release properties of F-actin: evidence for the involvement of F-actin in cellular calcium signaling. FEBS Lett. *395*, 137–142.

Lawler, S. (1999). Regulation of actin dynamics: The LIM kinase connection. Curr. Biol. *9*, R800–802.

Lenz, M., Prost, J., and Joanny, J.-F. (2010). Actin cross-linkers and the shape of stereocilia. Biophys. J. *99*, 2423–2433.

Lewis, A.K., and Bridgman, P.C. (1992). Nerve growth cone lamellipodia contain two populations of actin filaments that differ in organization and polarity. J. Cell Biol. *119*, 1219–1243.

Lin, C.S., Shen, W., Chen, Z.P., Tu, Y.H., and Matsudaira, P. (1994). Identification of I-plastin, a human fimbrin isoform expressed in intestine and kidney. Mol. Cell. Biol. *14*, 2457–2467.

Lin, H.W., Schneider, M.E., and Kachar, B. (2005). When size matters: the dynamic regulation of stereocilia lengths. Curr. Opin. Cell Biol. *17*, 55–61.

Lisanti, M.P., Caras, I.W., Davitz, M.A., and Rodriguez-Boulan, E. (1989). A glycophospholipid membrane anchor acts as an apical targeting signal in polarized epithelial cells. J. Cell Biol. *109*, 2145–2156.

Liu, A.P., Richmond, D.L., Maibaum, L., Pronk, S., Geissler, P.L., and Fletcher, D.A. (2008). Membrane-induced bundling of actin filaments. Nat Phys *4*, 789–793.

Loisel, T.P., Boujemaa, R., Pantaloni, D., and Carlier, M.F. (1999). Reconstitution of actin-based motility of Listeria and Shigella using pure proteins. Nature *401*, 613–616.

Loomis, P.A., Kelly, A.E., Zheng, L., Changyaleket, B., Sekerková, G., Mugnaini, E., Ferreira, A., Mullins, R.D., and Bartles, J.R. (2006). Targeted wild-type and jerker espins reveal a novel, WH2-domain-dependent way to make actin bundles in cells. J. Cell. Sci. *119*, 1655–1665.

Loomis, P.A., Zheng, L., Sekerková, G., Changyaleket, B., Mugnaini, E., and Bartles, J.R. (2003). Espin cross-links cause the elongation of microvillus-type parallel actin bundles in vivo. J. Cell Biol. *163*, 1045–1055.

Lotz, M.M., Rabinovitz, I., and Mercurio, A.M. (2000). Intestinal restitution: progression of actin cytoskeleton rearrangements and integrin function in a model of epithelial wound healing. Am. J. Pathol. *156*, 985–996.

Louvard, D., Kedinger, M., and Hauri, H.P. (1992). The differentiating intestinal epithelial cell: establishment and maintenance of functions through interactions between cellular structures. Annu. Rev. Cell Biol. *8*, 157–195.

Mace, O.J., Morgan, E.L., Affleck, J.A., Lister, N., and Kellett, G.L. (2007). Calcium absorption by Cav1.3 induces terminal web myosin II phosphorylation and apical GLUT2 insertion in rat intestine. J. Physiol. (Lond.) *580*, 605–616.

MacQueen, A.J., Baggett, J.J., Perumov, N., Bauer, R.A., Januszewski, T., Schriefer, L., and Waddle, J.A. (2005). ACT-5 Is an Essential Caenorhabditis elegans Actin Required for Intestinal Microvilli Formation. Mol. Biol. Cell *16*, 3247–3259.

Mallavarapu, A., and Mitchison, T. (1999). Regulated actin cytoskeleton assembly at filopodium tips controls their extension and retraction. J. Cell Biol. *146*, 1097–1106.

el Marjou, F., Janssen, K.-P., Chang, B.H.-J., Li, M., Hindie, V., Chan, L., Louvard, D., Chambon, P., Metzger, D., and Robine, S. (2004). Tissue-specific and inducible Cre-mediated recombination in the gut epithelium. Genesis *39*, 186–193.

Marshall, T.W., Lloyd, I.E., Delalande, J.M., Näthke, I., and Rosenblatt, J. (2011). The tumor suppressor adenomatous polyposis coli controls the direction in which a cell extrudes from an epithelium. Mol. Biol. Cell *22*, 3962–3970.

Mashimo, H., Wu, D.C., Podolsky, D.K., and Fishman, M.C. (1996). Impaired defense of intestinal mucosa in mice lacking intestinal trefoil factor. Science *274*, 262–265.

Masuda, K., Ikeda, H., Kasai, K., Fukuzawa, Y., Nishimaki, H., Takeo, T., and Itoh, G. (2003). Diversity of restitution after deoxycholic acid-induced small intestinal mucosal injury in the rat. Dig. Dis. Sci. *48*, 2108–2115.

Mathew, S., George, S.P., Wang, Y., Siddiqui, M.R., Srinivasan, K., Tan, L., and Khurana, S. (2008). Potential Molecular Mechanism for C-Src Kinase-Mediated Regulation of Intestinal Cell Migration. J. Biol. Chem. *283*, 22709–22722.

Matsudaira, P., Jakes, R., and Walker, J.E. (1985). A gelsolin-like Ca2+-dependent actin-binding domain in villin. Nature *315*, 248–250.

Matsudaira, P., Mandelkow, E., Renner, W., Hesterberg, L.K., and Weber, K. (1983). Role of fimbrin and villin in determining the interfilament distances of actin bundles. Nature *301*, 209–214.

Matsudaira, P.T., and Burgess, D.R. (1979). Identification and organization of the components in the isolated microvillus cytoskeleton. J. Cell Biol. *83*, 667–673.

Matsudaira, P.T., and Burgess, D.R. (1982a). Organization of the cross-filaments in intestinal microvilli. J. Cell Biol. *92*, 657–664.

Matsudaira, P.T., and Burgess, D.R. (1982b). Partial reconstruction of the microvillus core bundle: characterization of villin as a Ca++-dependent, actin-bundling/depolymerizing protein. J. Cell Biol. *92*, 648–656.

Matter, K., Stieger, B., Klumperman, J., Ginsel, L., and Hauri, H.P. (1990). Endocytosis, recycling, and lysosomal delivery of brush border hydrolases in cultured human intestinal epithelial cells (Caco-2). J. Biol. Chem. *265*, 3503–3512.

Mburu, P., Mustapha, M., Varela, A., Weil, D., El-Amraoui, A., Holme, R.H., Rump, A., Hardisty, R.E., Blanchard, S., Coimbra, R.S., et al. (2003). Defects in whirlin, a PDZ domain molecule involved in stereocilia elongation, cause deafness in the whirler mouse and families with DFNB31. Nat. Genet. *34*, 421–428.

McCarron, J.G., Chalmers, S., Bradley, K.N., MacMillan, D., and Muir, T.C. (2006). Ca2+ microdomains in smooth muscle. Cell Calcium *40*, 461–493.

McConnell, R.E., and Tyska, M.J. (2007). Myosin-1a powers the sliding of apical membrane along microvillar actin bundles. J. Cell Biol. *177*, 671–681.

van Meer, G., and Simons, K. (1988). Lipid polarity and sorting in epithelial cells. J. Cell. Biochem. *36*, 51–58.

Menge, H., and Robinson, J.W. (1978). The relationship between the functional and structural alterations in the rat small intestine following proximal resection of varying extents. Res Exp Med (Berl) *173*, 41–53.

Millard, T.H., Dawson, J., and Machesky, L.M. (2007). Characterisation of IRTKS, a novel IRSp53/MIM family actin regulator with distinct filament bundling properties. J. Cell. Sci. *120*, 1663–1672.

Mine, T., Kojima, I., Ogata, E., and Nakamura, T. (1991). Comparison of effects of HGF and EGF on cellular calcium in rat hepatocytes. Biochem. Biophys. Res. Commun. *181*, 1173–1180.

Miyata, H., Nishiyama, S., Akashi, K., and Kinosita, K., Jr (1999). Protrusive growth from giant liposomes driven by actin polymerization. Proc. Natl. Acad. Sci. U.S.A. *96*, 2048–2053.

Mogilner, A., and Oster, G. (1996). Cell motility driven by actin polymerization. Biophys. J. *71*, 3030–3045.

Mogilner, A., and Rubinstein, B. (2005). The physics of filopodial protrusion. Biophys. J. *89*, 782–795.

Moll, R., Schiller, D.L., and Franke, W.W. (1990). Identification of protein IT of the intestinal cytoskeleton as a novel type I cytokeratin with unusual properties and expression patterns. J. Cell Biol. *111*, 567–580.

Moon, H.W., Whipp, S.C., Argenzio, R.A., Levine, M.M., and Giannella, R.A. (1983). Attaching and effacing activities of rabbit and human enteropathogenic Escherichia coli in pig and rabbit intestines. Infect. Immun. *41*, 1340–1351.

Moore, R., Carlson, S., and Madara, J.L. (1989a). Rapid barrier restitution in an in vitro model of intestinal epithelial injury. Lab. Invest. *60*, 237–244.

Moore, R., Carlson, S., and Madara, J.L. (1989b). Villus contraction aids repair of intestinal epithelium after injury. Am. J. Physiol. *257*, G274–283.

Mooseker, M.S. (1976). Brush border motility. Microvillar contraction in triton-treated brush borders isolated from intestinal epithelium. J. Cell Biol. *71*, 417–433.

Mooseker, M.S., Graves, T.A., Wharton, K.A., Falco, N., and Howe, C.L. (1980). Regulation of microvillus structure: calcium-dependent solation and cross-linking of actin filaments in the microvilli of intestinal epithelial cells. J. Cell Biol. *87*, 809–822.

Mooseker, M.S., Pollard, T.D., and Wharton, K.A. (1982). Nucleated polymerization of actin from the membrane-associated ends of microvillar filaments in the intestinal brush border. J. Cell Biol. *95*, 223–233.

Mooseker, M.S., and Tilney, L.G. (1975). Organization of an actin filament-membrane complex. Filament polarity and membrane attachment in the microvilli of intestinal epithelial cells. J. Cell Biol. *67*, 725–743.

Morgan, E.L., Mace, O.J., Affleck, J., and Kellett, G.L. (2006). Apical GLUT2 and Cav1.3: regulation of rat intestinal glucose and calcium absorption. The Journal of Physiology *580*, 593–604.

Morris, C.E., and Homann, U. (2001). Cell surface area regulation and membrane tension. J. Membr. Biol. *179*, 79–102.

Morrow, J.S., Cianci, C.D., Ardito, T., Mann, A.S., and Kashgarian, M. (1989). Ankyrin links fodrin to the alpha subunit of Na,K-ATPase in Madin-Darby canine kidney cells and in intact renal tubule cells. J. Cell Biol. *108*, 455–465.

Mouneimne, G., DesMarais, V., Sidani, M., Scemes, E., Wang, W., Song, X., Eddy, R., and Condeelis, J. (2006). Spatial and temporal control of cofilin activity is required for directional sensing during chemotaxis. Curr. Biol. *16*, 2193–2205.

Mukherjee, T.M., and Staehelin, L.A. (1971). The fine-structural organization of the brush border of intestinal epithelial cells. J. Cell. Sci. *8*, 573–599.

Munro, S. (2003). Lipid rafts: elusive or illusive? Cell *115*, 377–388.

Nagy, S., Ricca, B.L., Norstrom, M.F., Courson, D.S., Brawley, C.M., Smithback, P.A., and Rock, R.S. (2008). A myosin motor that selects bundled actin for motility. Proc. Natl. Acad. Sci. U.S.A. *105*, 9616–9620.

Nagy, S., and Rock, R.S. (2010). Structured post-IQ domain governs selectivity of myosin X for fascin-actin bundles. J. Biol. Chem. *285*, 26608–26617.

Naim, H.Y., Joberty, G., Alfalah, M., and Jacob, R. (1999). Temporal association of the N- and O-linked glycosylation events and their implication in the polarized sorting of intestinal brush border sucrase-isomaltase, aminopeptidase N, and dipeptidyl peptidase IV. J. Biol. Chem. *274*, 17961–17967.

Nambiar, R., McConnell, R.E., and Tyska, M.J. (2009). Control of cell membrane tension by myosin-I. Proc. Natl. Acad. Sci. U.S.A. *106*, 11972–11977.

Naoz, M., Manor, U., Sakaguchi, H., Kachar, B., and Gov, N.S. (2008). Protein localization by actin treadmilling and molecular motors regulates stereocilia shape and treadmilling rate. Biophys. J. *95*, 5706–5718.

Näthke, I.S., Adams, C.L., Polakis, P., Sellin, J.H., and Nelson, W.J. (1996). The adenomatous polyposis coli tumor suppressor protein localizes to plasma membrane sites involved in active cell migration. J. Cell Biol. *134*, 165–179.

Nejsum, L.N., and Nelson, W.J. (2009). Epithelial cell surface polarity: the early steps. Front. Biosci. *14*, 1088–1098.

Nelson, W.J., and Veshnock, P.J. (1987). Ankyrin binding to (Na+ + K+)ATPase and implications for the organization of membrane domains in polarized cells. Nature *328*, 533–536.

Nguyen, H.T.T., Charrier-Hisamuddin, L., Dalmasso, G., Hiol, A., Sitaraman, S., and Merlin, D. (2007). Association of PepT1 with lipid rafts differently modulates its transport activity in polarized and nonpolarized cells. Am. J. Physiol. Gastrointest. Liver Physiol. *293*, G1155–1165.

Nobes, C.D., and Hall, A. (1995). Rho, rac, and cdc42 GTPases regulate the assembly of multimolecular focal complexes associated with actin stress fibers, lamellipodia, and filopodia. Cell *81*, 53–62.

Noda, Y., Okada, Y., Saito, N., Setou, M., Xu, Y., Zhang, Z., and Hirokawa, N. (2001). KIFC3, a microtubule minus end-directed motor for the apical transport of annexin XIIIb-associated Triton-insoluble membranes. J. Cell Biol. *155*, 77–88.

Normand, S., Delanoye-Crespin, A., Bressenot, A., Huot, L., Grandjean, T., Peyrin-Biroulet, L., Lemoine, Y., Hot, D., and Chamaillard, M. (2011). Nod-like receptor pyrin domain-containing protein 6 (NLRP6) controls epithelial self-renewal and colorectal carcinogenesis upon injury. Proc. Natl. Acad. Sci. U.S.A. *108*, 9601–9606.

Northrop, J., Weber, A., Mooseker, M.S., Franzini-Armstrong, C., Bishop, M.F., Dubyak, G.R., Tucker, M., and Walsh, T.P. (1986). Different calcium dependence of the capping and cutting activities of villin. J. Biol. Chem. *261*, 9274–9281.

Nusrat, A., Delp, C., and Madara, J.L. (1992). Intestinal epithelial restitution. Characterization of a cell culture model and mapping of cytoskeletal elements in migrating cells. J. Clin. Invest. *89*, 1501–1511.

Oganesian, A., Bueno, E., Yan, Q., Spee, C., Black, J., Rao, N.A., and Lopez, P.F. (1997). Scanning and transmission electron microscopic findings during RPE wound healing in vivo. Int Ophthalmol *21*, 165–175.

Ohta, K., Higashi, R., Sawaguchi, A., and Nakamura, K. (2012). Helical arrangement of filaments in microvillar actin bundles. J. Struct. Biol. *177*, 513–519.

Okada, K., Bartolini, F., Deaconescu, A.M., Moseley, J.B., Dogic, Z., Grigorieff, N., Gundersen, G.G., and Goode, B.L. (2010). Adenomatous polyposis coli protein nucleates actin assembly and synergizes with the formin mDia1. J. Cell Biol. *189*, 1087–1096.

Olkkonen, V.M., and Stenmark, H. (1997). Role of Rab GTPases in membrane traffic. Int. Rev. Cytol. *176*, 1–85.

Overton, J., and Shoup, J. (1964). Fine structure of cell surface specialization in the maturing duodenal mucosa of the chick. J. Cell Biol. *21*, 75–85.

Padányi, R., Xiong, Y., Antalffy, G., Lór, K., Pászty, K., Strehler, E.E., and Enyedi, A. (2010). Apical scaffolding protein NHERF2 modulates the localization of alternatively spliced plasma membrane Ca2+ pump 2B variants in polarized epithelial cells. J. Biol. Chem. *285*, 31704–31712.

Panebra, A., Ma, S.-X., Zhai, L.-W., Wang, X.-T., Rhee, S.G., and Khurana, S. (2001). Regulation of Phospholipase C-Γ1 by the Actin-Regulatory Protein Villin. Am J Physiol Cell Physiol *281*, C1046–C1058.

Parekh, A.B. (2008). Ca2+ microdomains near plasma membrane Ca2+ channels: impact on cell function. J. Physiol. (Lond.) *586*, 3043–3054.

Pavelka, M., Ellinger, A., and Gangl, A. (1983). Effect of colchicine on rat small intestinal absorptive cells. I Formation of basolateral microvillus borders. J. Ultrastruct. Res. *85*, 249–259.

Pearl, M., Fishkind, D., Mooseker, M., Keene, D., and Keller, T., 3rd (1984). Studies on the spectrin-like protein from the intestinal brush border, TW 260/240, and characterization of its interaction with the cytoskeleton and actin. J. Cell Biol. *98*, 66–78.

Pellegrin, S., and Mellor, H. (2005). The Rho family GTPase Rif induces filopodia through mDia2. Curr. Biol. *15*, 129–133.

Peng, A.W., Belyantseva, I.A., Hsu, P.D., Friedman, T.B., and Heller, S. (2009). Twinfilin 2 regulates actin filament lengths in cochlear stereocilia. J. Neurosci. *29*, 15083–15088.

Perrin, B.J., and Ervasti, J.M. (2010). The actin gene family: function follows isoform. Cytoskeleton (Hoboken) *67*, 630–634.

Peskin, C.S., Odell, G.M., and Oster, G.F. (1993). Cellular motions and thermal fluctuations: the Brownian ratchet. Biophys. J. *65*, 316–324.

Pickert, G., Neufert, C., Leppkes, M., Zheng, Y., Wittkopf, N., Warntjen, M., Lehr, H.-A., Hirth, S., Weigmann, B., Wirtz, S., et al. (2009). STAT3 links IL-22 signaling in intestinal epithelial cells to mucosal wound healing. J. Exp. Med. *206*, 1465–1472.

Pinson, K.I., Dunbar, L., Samuelson, L., and Gumucio, D.L. (1998). Targeted disruption of the mouse villin gene does not impair the morphogenesis of microvilli. Dev. Dyn. *211*, 109–121.

Polishchuk, R., Di Pentima, A., and Lippincott-Schwartz, J. (2004). Delivery of raft-associated, GPI-anchored proteins to the apical surface of polarized MDCK cells by a transcytotic pathway. Nat. Cell Biol. *6*, 297–307.

Pollard, T.D., and Borisy, G.G. (2003). Cellular motility driven by assembly and disassembly of actin filaments. Cell *112*, 453–465.

Pollard, T.D., and Mooseker, M.S. (1981). Direct measurement of actin polymerization rate constants by electron microscopy of actin filaments nucleated by isolated microvillus cores. J. Cell Biol. *88*, 654–659.

Ponti, A., Machacek, M., Gupton, S.L., Waterman-Storer, C.M., and Danuser, G. (2004). Two distinct actin networks drive the protrusion of migrating cells. Science *305*, 1782–1786.

Poujade, M., Grasland-Mongrain, E., Hertzog, A., Jouanneau, J., Chavrier, P., Ladoux, B., Buguin, A., and Silberzan, P. (2007). Collective migration of an epithelial monolayer in response to a model wound. Proc. Natl. Acad. Sci. U.S.A. *104*, 15988–15993.

Probst, F.J., Fridell, R.A., Raphael, Y., Saunders, T.L., Wang, A., Liang, Y., Morell, R.J., Touchman, J.W., Lyons, R.H., Noben-Trauth, K., et al. (1998). Correction of deafness in shaker-2 mice by an unconventional myosin in a BAC transgene. Science *280*, 1444–1447.

Prost, J., Barbetta, C., and Joanny, J.-F. (2007). Dynamical Control of the Shape and Size of Stereocilia and Microvilli. Biophysical Journal *93*, 1124–1133.

Quaroni, A., Calnek, D., Quaroni, E., and Chandler, J.S. (1991). Keratin expression in rat intestinal crypt and villus cells. Analysis with a panel of monoclonal antibodies. J. Biol. Chem. *266*, 11923–11931.

Rao, J.N., Liu, S.V., Zou, T., Liu, L., Xiao, L., Zhang, X., Bellavance, E., Yuan, J.X.-J., and Wang, J.-Y. (2008). Rac1 promotes intestinal epithelial restitution by increasing Ca2+ influx through interaction with phospholipase C-(gamma)1 after wounding. Am. J. Physiol., Cell Physiol. *295*, C1499–1509.

Rao, J.N., Platoshyn, O., Golovina, V.A., Liu, L., Zou, T., Marasa, B.S., Turner, D.J., Yuan, J.X.-J., and Wang, J.-Y. (2006). TRPC1 functions as a store-operated Ca2+ channel in intestinal epithelial cells and regulates early mucosal restitution after wounding. Am. J. Physiol. Gastrointest. Liver Physiol. *290*, G782–792.

Rao, J.N., Rathor, N., Zou, T., Liu, L., Xiao, L., Yu, T.-X., Cui, Y.-H., and Wang, J.-Y. (2010). STIM1 translocation to the plasma membrane enhances intestinal epithelial restitution by inducing TRPC1-mediated Ca2+ signaling after wounding. Am. J. Physiol., Cell Physiol. *299*, C579–588.

Raucher, D., and Sheetz, M.P. (2000). Cell spreading and lamellipodial extension rate is regulated by membrane tension. J. Cell Biol. *148*, 127–136.

Reffay, M., Petitjean, L., Coscoy, S., Grasland-Mongrain, E., Amblard, F., Buguin, A., and Silberzan, P. (2011). Orientation and polarity in collectively migrating cell structures: statics and dynamics. Biophys. J. *100*, 2566–2575.

Reinacher-Schick, A., and Gumbiner, B.M. (2001). Apical membrane localization of the adenomatous polyposis coli tumor suppressor protein and subcellular distribution of the beta-catenin destruction complex in polarized epithelial cells. J. Cell Biol. *152*, 491–502.

Renault, L., Bugyi, B., and Carlier, M.-F. (2008). Spire and Cordon-bleu: multifunctional regulators of actin dynamics. Trends Cell Biol. *18*, 494–504.

Resch, G.P., Goldie, K.N., Krebs, A., Hoenger, A., and Small, J.V. (2002). Visualisation of the actin cytoskeleton by cryo-electron microscopy. J. Cell. Sci. *115*, 1877–1882.

Revenu, C., Athman, R., Robine, S., and Louvard, D. (2004). The co-workers of actin filaments: from cell structures to signals. Nat. Rev. Mol. Cell Biol. *5*, 635–646.

Revenu, C., Courtois, M., Michelot, A., Sykes, C., Louvard, D., and Robine, S. (2007). Villin severing activity enhances actin-based motility in vivo. Mol. Biol. Cell *18*, 827–838.

Revenu, C., Ubelmann, F., Hurbain, I., El-Marjou, F., Dingli, F., Loew, D., Delacour, D., Gilet, J., Brot-Laroche, E., Rivero, F., et al. (2012). A new role for the architecture of microvillar actin bundles in apical retention of membrane proteins. Mol. Biol. Cell *23*, 324–336.

Ricca, B.L., and Rock, R.S. (2010). The stepping pattern of myosin X is adapted for processive motility on bundled actin. Biophys. J. *99*, 1818–1826.

Robine, S., Huet, C., Moll, R., Sahuquillo-Merino, C., Coudrier, E., Zweibaum, A., and Louvard, D. (1985). Can villin be used to identify malignant and undifferentiated normal digestive epithelial cells? Proc. Natl. Acad. Sci. U.S.A. *82*, 8488–8492.

Rodriguez-Boulan, E., Kreitzer, G., and Müsch, A. (2005). Organization of vesicular trafficking in epithelia. Nat. Rev. Mol. Cell Biol. *6*, 233–247.

Rosenshine, I., Ruschkowski, S., and Finlay, B.B. (1996). Expression of attaching/effacing activity by enteropathogenic Escherichia coli depends on growth phase, temperature, and protein synthesis upon contact with epithelial cells. Infect. Immun. *64*, 966–973.

Rosin-Arbesfeld, R., Ihrke, G., and Bienz, M. (2001). Actin-dependent membrane association of the APC tumour suppressor in polarized mammalian epithelial cells. EMBO J. *20*, 5929–5939.

Rzadzinska, A.K., Nevalainen, E.M., Prosser, H.M., Lappalainen, P., and Steel, K.P. (2009). MyosinVIIa interacts with Twinfilin-2 at the tips of mechanosensory stereocilia in the inner ear. PLoS ONE *4*, e7097.

Rzadzinska, A.K., Schneider, M.E., Davies, C., Riordan, G.P., and Kachar, B. (2004). An actin molecular treadmill and myosins maintain stereocilia functional architecture and self-renewal. J. Cell Biol. *164*, 887–897.

Saarikangas, J., Mattila, P.K., Varjosalo, M., Bovellan, M., Hakanen, J., Calzada-Wack, J., Tost, M., Jennen, L., Rathkolb, B., Hans, W., et al. (2011). Missing-in-metastasis MIM/MTSS1 promotes actin assembly at intercellular junctions and is required for integrity of kidney epithelia. J. Cell. Sci. *124*, 1245–1255.

Sacco, O., Silvestri, M., Sabatini, F., Sale, R., Defilippi, A.-C., and Rossi, G.A. (2004). Epithelial cells and fibroblasts: structural repair and remodelling in the airways. Paediatr Respir Rev *5 Suppl A*, S35–40.

Salas, P.J., Rodriguez, M.L., Viciana, A.L., Vega-Salas, D.E., and Hauri, H.P. (1997). The apical submembrane cytoskeleton participates in the organization of the apical pole in epithelial cells. J. Cell Biol. *137*, 359–375.

Sangiorgi, E., and Capecchi, M.R. (2008). Bmi1 is expressed in vivo in intestinal stem cells. Nat. Genet. *40*, 915–920.

Santos, M.F., McCormack, S.A., Guo, Z., Okolicany, J., Zheng, Y., Johnson, L.R., and Tigyi, G. (1997). Rho proteins play a critical role in cell migration during the early phase of mucosal restitution. J. Clin. Invest. *100*, 216–225.

Saotome, I., Curto, M., and McClatchey, A.I. (2004). Ezrin is essential for epithelial organization and villus morphogenesis in the developing intestine. Dev. Cell *6*, 855–864.

Sato, T., Mushiake, S., Kato, Y., Sato, K., Sato, M., Takeda, N., Ozono, K., Miki, K., Kubo, Y., Tsuji, A., et al. (2007). The Rab8 GTPase regulates apical protein localization in intestinal cells. Nature *448*, 366–369.

Sato, T., Vries, R.G., Snippert, H.J., van de Wetering, M., Barker, N., Stange, D.E., van Es, J.H., Abo, A., Kujala, P., Peters, P.J., et al. (2009). Single Lgr5 stem cells build crypt-villus structures in vitro without a mesenchymal niche. Nature *459*, 262–265.

Sawtell, N.M., Hartman, A.L., and Lessard, J.L. (1988). Unique isoactins in the brush border of rat intestinal epithelial cells. Cell Motil. Cytoskeleton *11*, 318–325.

Schafer, D.A., Mooseker, M.S., and Cooper, J.A. (1992). Localization of capping protein in chicken epithelial cells by immunofluorescence and biochemical fractionation. J. Cell Biol. *118*, 335–346.

Scheiffele, P., Peränen, J., and Simons, K. (1995). N-glycans as apical sorting signals in epithelial cells. Nature *378*, 96–98.

Schirenbeck, A., Arasada, R., Bretschneider, T., Schleicher, M., and Faix, J. (2005). Formins and VASPs may co-operate in the formation of filopodia. Biochem. Soc. Trans. *33*, 1256–1259.

Schneider, M.E., Belyantseva, I.A., Azevedo, R.B., and Kachar, B. (2002). Rapid renewal of auditory hair bundles. Nature *418*, 837–838.

Schwartz, N., Hosford, M., Sandoval, R.M., Wagner, M.C., Atkinson, S.J., Bamburg, J., and Molitoris, B.A. (1999). Ischemia activates actin depolymerizing factor: role in proximal tubule microvillar actin alterations. Am. J. Physiol. *276*, F544–551.

Seltana, A., Basora, N., and Beaulieu, J.-F. (2010). Intestinal epithelial wound healing assay in an epithelial-mesenchymal co-culture system. Wound Repair Regen *18*, 114–122.

Seno, H., Miyoshi, H., Brown, S.L., Geske, M.J., Colonna, M., and Stappenbeck, T.S. (2009). Efficient colonic mucosal wound repair requires Trem2 signaling. Proc. Natl. Acad. Sci. U.S.A. *106*, 256–261.

Shibayama, T., Carboni, J.M., and Mooseker, M.S. (1987). Assembly of the intestinal brush border: appearance and redistribution of microvillar core proteins in developing chick enterocytes. J. Cell Biol. *105*, 335–344.

Shin, H., Purdy Drew, K.R., Bartles, J.R., Wong, G.C.L., and Grason, G.M. (2009). Cooperativity and frustration in protein-mediated parallel actin bundles. Phys. Rev. Lett. *103*, 238102.

Simons, K., and Ikonen, E. (1997). Functional rafts in cell membranes. Nature *387*, 569–572.

Sinha, B., Köster, D., Ruez, R., Gonnord, P., Bastiani, M., Abankwa, D., Stan, R.V., Butler-Browne, G., Vedie, B., Johannes, L., et al. (2011). Cells respond to mechanical stress by rapid disassembly of caveolae. Cell *144*, 402–413.

Small, J.V., Herzog, M., Häner, M., and Abei, U. (1994). Visualization of actin filaments in keratocyte lamellipodia: negative staining compared with freeze-drying. J. Struct. Biol. *113*, 135–141.

Stechly, L., Morelle, W., Dessein, A.-F., André, S., Grard, G., Trinel, D., Dejonghe, M.-J., Leteurtre, E., Drobecq, H., Trugnan, G., et al. (2009). Galectin-4-regulated delivery of glycoproteins to the brush border membrane of enterocyte-like cells. Traffic *10*, 438–450.

Stidwill, R.P., and Burgess, D.R. (1986). Regulation of intestinal brush border microvillus length during development by the G- to F-actin ratio. Dev. Biol. *114*, 381–388.

Stidwill, R.P., Wysolmerski, T., and Burgess, D.R. (1984). The brush border cytoskeleton is not static: in vivo turnover of proteins. J. Cell Biol. *98*, 641–645.

Stossel, T.P., Condeelis, J., Cooley, L., Hartwig, J.H., Noegel, A., Schleicher, M., and Shapiro, S.S. (2001). Filamins as integrators of cell mechanics and signalling. Nat. Rev. Mol. Cell Biol. *2*, 138–145.

Stowers, L., Yelon, D., Berg, L.J., and Chant, J. (1995). Regulation of the polarization of T cells toward antigen-presenting cells by Ras-related GTPase CDC42. Proc. Natl. Acad. Sci. U.S.A. *92*, 5027–5031.

Sturm, A. (2008). Epithelial restitution and wound healing in inflammatory bowel disease. World Journal of Gastroenterology *14*, 348.

Sumigray, K.D., and Lechler, T. (2012). Desmoplakin controls microvilli length but not cell adhesion or keratin organization in the intestinal epithelium. Mol. Biol. Cell *23*, 792–799.

Suraneni, P., Rubinstein, B., Unruh, J.R., Durnin, M., Hanein, D., and Li, R. (2012). The Arp2/3 complex is required for lamellipodia extension and directional fibroblast cell migration. J. Cell Biol. *197*, 239–251.

Svitkina, T.M., and Borisy, G.G. (1999). Arp2/3 complex and actin depolymerizing factor/cofilin in dendritic organization and treadmilling of actin filament array in lamellipodia. J. Cell Biol. *145*, 1009–1026.

Svitkina, T.M., Bulanova, E.A., Chaga, O.Y., Vignjevic, D.M., Kojima, S., Vasiliev, J.M., and Borisy, G.G. (2003). Mechanism of filopodia initiation by reorganization of a dendritic network. J. Cell Biol. *160*, 409–421.

Svitkina, T.M., Verkhovsky, A.B., McQuade, K.M., and Borisy, G.G. (1997). Analysis of the actin-myosin II system in fish epidermal keratocytes: mechanism of cell body translocation. J. Cell Biol. *139*, 397–415.

Tai, A.W., Chuang, J.Z., Bode, C., Wolfrum, U., and Sung, C.H. (1999). Rhodopsin's carboxy-terminal cytoplasmic tail acts as a membrane receptor for cytoplasmic dynein by binding to the dynein light chain Tctex-1. Cell *97*, 877–887.

Takemura, R., Masaki, T., and Hirokawa, N. (1988). Developmental organization of the intestinal brush-border cytoskeleton. Cell Motil. Cytoskeleton *9*, 299–311.

Tang, N., and Ostap, E.M. (2001). Motor domain-dependent localization of myo1b (myr-1). Curr. Biol. *11*, 1131–1135.

Targos, B., Barańska, J., and Pomorski, P. (2005). Store-operated calcium entry in physiology and pathology of mammalian cells. Acta Biochim. Pol. *52*, 397–409.

Temm-Grove, C.J., Jockusch, B.M., Weinberger, R.P., Schevzov, G., and Helfman, D.M. (1998). Distinct localizations of tropomyosin isoforms in LLC-PK1 epithelial cells suggests specialized function at cell-cell adhesions. Cell Motil. Cytoskeleton *40*, 393–407.

Theriot, J.A., Mitchison, T.J., Tilney, L.G., and Portnoy, D.A. (1992). The rate of actin-based motility of intracellular Listeria monocytogenes equals the rate of actin polymerization. Nature *357*, 257–260.

Tian, H., Biehs, B., Warming, S., Leong, K.G., Rangell, L., Klein, O.D., and de Sauvage, F.J. (2011). A reserve stem cell population in small intestine renders Lgr5-positive cells dispensable. Nature *478*, 255–259.

Tilney, L.G., and Cardell, R.R. (1970). Factors controlling the reassembly of the microvillous border of the small intestine of the salamander. J. Cell Biol. *47*, 408–422.

Tilney, L.G., Connelly, P., Smith, S., and Guild, G.M. (1996). F-Actin Bundles in Drosophila Bristles Are Assembled from Modules Composed of Short Filaments. J Cell Biol *135*, 1291–1308.

Tilney, L.G., Connelly, P.S., and Guild, G.M. (2004). Microvilli appear to represent the first step in actin bundle formation in Drosophila bristles. J. Cell. Sci. *117*, 3531–3538.

Tilney, L.G., Connelly, P.S., Ruggiero, L., Vranich, K.A., and Guild, G.M. (2003). Actin filament turnover regulated by cross-linking accounts for the size, shape, location, and number of actin bundles in Drosophila bristles. Mol. Biol. Cell *14*, 3953–3966.

Tilney, L.G., Connelly, P.S., Vranich, K.A., Shaw, M.K., and Guild, G.M. (1998). Why Are Two Different Cross-Linkers Necessary for Actin Bundle Formation In Vivo and What Does Each Cross-Link Contribute? J Cell Biol *143*, 121–133.

Tilney, L.G., Cotanche, D.A., and Tilney, M.S. (1992). Actin filaments, stereocilia and hair cells of the bird cochlea. VI. How the number and arrangement of stereocilia are determined. Development *116*, 213–226.

Tilney, L.G., and DeRosier, D.J. (1986). Actin filaments, stereocilia, and hair cells of the bird cochlea. IV. How the actin filaments become organized in developing stereocilia and in the cuticular plate. Dev. Biol. *116*, 119–129.

Tilney, L.G., Derosier, D.J., and Mulroy, M.J. (1980). The organization of actin filaments in the stereocilia of cochlear hair cells. J. Cell Biol. *86*, 244–259.

Tilney, L.G., Hatano, S., Ishikawa, H., and Mooseker, M.S. (1973). The polymerization of actin: its role in the generation of the acrosomal process of certain echinoderm sperm. J. Cell Biol. *59*, 109–126.

Tilney, L.G., and Mooseker, M. (1971). Actin in the brush-border of epithelial cells of the chicken intestine. Proc. Natl. Acad. Sci. U.S.A. *68*, 2611–2615.

Tilney, L.G., and Tilney, M.S. (1988). The actin filament content of hair cells of the bird cochlea is nearly constant even though the length, width, and number of stereocilia vary depending on the hair cell location. J. Cell Biol. *107*, 2563–2574.

Tilney, L.G., Tilney, M.S., and Cotanche, D.A. (1988). New observations on the stereocilia of hair cells of the chick cochlea. Hear. Res. *37*, 71–82.

Tilney, L.G., Tilney, M.S., and Guild, G.M. (1995). F actin bundles in Drosophila bristles. I. Two filament cross-links are involved in bundling. J. Cell Biol. *130*, 629–638.

Tocchetti, A., Soppo, C.B.E., Zani, F., Bianchi, F., Gagliani, M.C., Pozzi, B., Rozman, J., Elvert, R., Ehrhardt, N., Rathkolb, B., et al. (2010). Loss of the actin remodeler Eps8 causes intestinal defects and improved metabolic status in mice. PLoS ONE *5*, e9468.

Tokuo, H., and Ikebe, M. (2004). Myosin X transports Mena/VASP to the tip of filopodia. Biochem. Biophys. Res. Commun. *319*, 214–220.

Tomar, A., George, S., Kansal, P., Wang, Y., and Khurana, S. (2006). Interaction of Phospholipase C-Γ1 with Villin Regulates Epithelial Cell Migration. J. Biol. Chem. *281*, 31972–31986.

Tomar, A., Wang, Y., Kumar, N., George, S., Ceacareanu, B., Hassid, A., Chapman, K.E., Aryal, A.M., Waters, C.M., and Khurana, S. (2004). Regulation of Cell Motility by Tyrosine Phosphorylated Villin. Mol. Biol. Cell *15*, 4807–4817.

Toomre, D., Keller, P., White, J., Olivo, J.C., and Simons, K. (1999). Dual-color visualization of trans-Golgi network to plasma membrane traffic along microtubules in living cells. J. Cell. Sci. *112 (Pt 1)*, 21–33.

Tyska, M.J., Mackey, A.T., Huang, J.-D., Copeland, N.G., Jenkins, N.A., and Mooseker, M.S. (2005). Myosin-1a is critical for normal brush border structure and composition. Mol. Biol. Cell *16*, 2443–2457.

Tyska, M.J., and Mooseker, M.S. (2002). MYO1A (brush border myosin I) dynamics in the brush border of LLC-PK1-CL4 cells. Biophys. J. *82*, 1869–1883.

Tyska, M.J., and Mooseker, M.S. (2004). A role for myosin-1A in the localization of a brush border disaccharidase. J. Cell Biol. *165*, 395–405.

Urban, E., Jacob, S., Nemethova, M., Resch, G.P., and Small, J.V. (2010). Electron tomography reveals unbranched networks of actin filaments in lamellipodia. Nat. Cell Biol. *12*, 429–435.

Vandekerckhove, J., and Weber, K. (1978). At least six different actins are expressed in a higher mammal: an analysis based on the amino acid sequence of the amino-terminal tryptic peptide. J. Mol. Biol. *126*, 783–802.

Verpy, E., Leibovici, M., Zwaenepoel, I., Liu, X.Z., Gal, A., Salem, N., Mansour, A., Blanchard, S., Kobayashi, I., Keats, B.J., et al. (2000). A defect in harmonin, a PDZ domain-containing protein expressed in the inner ear

sensory hair cells, underlies Usher syndrome type 1C. Nat. Genet. *26*, 51–55.

Vicente-Manzanares, M., Webb, D.J., and Horwitz, A.R. (2005). Cell migration at a glance. J. Cell. Sci. *118*, 4917–4919.

Vignjevic, D., Kojima, S., Aratyn, Y., Danciu, O., Svitkina, T., and Borisy, G.G. (2006). Role of fascin in filopodial protrusion. J. Cell Biol. *174*, 863–875.

Vignjevic, D., Yarar, D., Welch, M.D., Peloquin, J., Svitkina, T., and Borisy, G.G. (2003). Formation of filopodia-like bundles in vitro from a dendritic network. J. Cell Biol. *160*, 951–962.

Vinzenz, M., Nemethova, M., Schur, F., Mueller, J., Narita, A., Urban, E., Winkler, C., Schmeiser, C., Koestler, S.A., Rottner, K., et al. (2012). Actin branching in the initiation and maintenance of lamellipodia. Journal of Cell Science.

Waharte, F., Brown, C.M., Coscoy, S., Coudrier, E., and Amblard, F. (2005). A two-photon FRAP analysis of the cytoskeleton dynamics in the microvilli of intestinal cells. Biophys. J. *88*, 1467–1478.

Walsh, T.P., Weber, A., Davis, K., Bonder, E., and Mooseker, M. (1984). Calcium dependence of villin-induced actin depolymerization. Biochemistry *23*, 6099–6102.

Wang, Y., Srinivasan, K., Siddiqui, M.R., George, S.P., Tomar, A., and Khurana, S. (2008a). A novel role for villin in intestinal epithelial cell survival and homeostasis. J. Biol. Chem. *283*, 9454–9464.

Wang, Y., Srinivasan, K., Siddiqui, M.R., George, S.P., Tomar, A., and Khurana, S. (2008b). A novel role for villin in intestinal epithelial cell survival and homeostasis. J. Biol. Chem. *283*, 9454–9464.

Wang, Y., Tomar, A., George, S.P., and Khurana, S. (2007). Obligatory Role for Phospholipase C-Γ1 in Villin-Induced Epithelial Cell Migration. Am J Physiol Cell Physiol *292*, C1775–C1786.

Wang, Y.L. (1985). Exchange of actin subunits at the leading edge of living fibroblasts: possible role of treadmilling. J. Cell Biol. *101*, 597–602.

Wilson, C.A., Tsuchida, M.A., Allen, G.M., Barnhart, E.L., Applegate, K.T., Yam, P.T., Ji, L., Keren, K., Danuser, G., and Theriot, J.A. (2010). Myosin II contributes to cell-scale actin network treadmilling through network disassembly. Nature *465*, 373–377.

Wolfrum, U., Liu, X., Schmitt, A., Udovichenko, I.P., and Williams, D.S. (1998). Myosin VIIa as a common component of cilia and microvilli. Cell Motil. Cytoskeleton *40*, 261–271.

Wu, C., Asokan, S.B., Berginski, M.E., Haynes, E.M., Sharpless, N.E., Griffith, J.D., Gomez, S.M., and Bear, J.E. (2012). Arp2/3 is critical for lamellipodia and response to extracellular matrix cues but is dispensable for chemotaxis. Cell *148*, 973–987.

Yamamoto, M., Plessow, B., Koch, H.K., and Oehlert, W. (1980). Electron microscopic studies on the small intestinal mucosa of rats after mechanical intestinal obstruction and ischemia. Virchows Arch., B, Cell Pathol. *32*, 157–164.

Yamashiro, S., Yamakita, Y., Ono, S., and Matsumura, F. (1998). Fascin, an actin-bundling protein, induces membrane protrusions and increases cell motility of epithelial cells. Mol. Biol. Cell *9*, 993–1006.

Yang, C., Czech, L., Gerboth, S., Kojima, S., Scita, G., and Svitkina, T. (2007). Novel roles of formin mDia2 in lamellipodia and filopodia formation in motile cells. PLoS Biol. *5*, e317.

Yarar, D., To, W., Abo, A., and Welch, M.D. (1999). The Wiskott-Aldrich syndrome protein directs actin-based motility by stimulating actin nucleation with the Arp2/3 complex. Curr. Biol. *9*, 555–558.

Yeaman, C., Le Gall, A.H., Baldwin, A.N., Monlauzeur, L., Le Bivic, A., and Rodriguez-Boulan, E. (1997). The O-glycosylated stalk domain is required for apical sorting of neurotrophin receptors in polarized MDCK cells. J. Cell Biol. *139*, 929–940.

Zanet, J., Jayo, A., Plaza, S., Millard, T., Parsons, M., and Stramer, B. (2012). Fascin promotes filopodia formation independent of its role in actin bundling. J. Cell Biol. *197*, 477–486.

Zhai, L., Kumar, N., Panebra, A., Zhao, P., Parrill, A.L., and Khurana, S. (2002). Regulation of actin dynamics by tyrosine phosphorylation: identification of tyrosine phosphorylation sites within the actin-severing domain of villin. Biochemistry *41*, 11750–11760.

Zhai, L., Zhao, P., Panebra, A., Guerrerio, A.L., and Khurana, S. (2001). Tyrosine phosphorylation of villin regulates the organization of the actin cytoskeleton. J. Biol. Chem. *276*, 36163–36167.

Zhang, D.-S., Piazza, V., Perrin, B.J., Rzadzinska, A.K., Poczatek, J.C., Wang, M., Prosser, H.M., Ervasti, J.M., Corey, D.P., and Lechene, C.P. (2012). Multi-isotope imaging mass spectrometry reveals slow protein turnover in hair-cell stereocilia. Nature *481*, 520–524.

Zhao, H., Pykäläinen, A., and Lappalainen, P. (2011). I-BAR domain proteins: linking actin and plasma membrane dynamics. Current Opinion in Cell Biology *23*, 14–21.

Zheng, L., Sekerková, G., Vranich, K., Tilney, L.G., Mugnaini, E., and Bartles, J.R. (2000). The deaf jerker mouse has a mutation in the gene encoding the espin actin-bundling proteins of hair cell stereocilia and lacks espins. Cell *102*, 377–385.

Zicha, D., Dobbie, I.M., Holt, M.R., Monypenny, J., Soong, D.Y.H., Gray, C., and Dunn, G.A. (2003). Rapid actin transport during cell protrusion. Science *300*, 142–145.

Zigmond, S.H., Evangelista, M., Boone, C., Yang, C., Dar, A.C., Sicheri, F., Forkey, J., and Pring, M. (2003). Formin leaky cap allows elongation in the presence of tight capping proteins. Curr. Biol. *13*, 1820–1823.

Zigmond, S.H., Furukawa, R., and Fechheimer, M. (1992). Inhibition of actin filament depolymerization by the Dictyostelium 30,000-D actin-bundling protein. J. Cell Biol. *119*, 559–567.

Zwaenepoel, I., Naba, A., Da Cunha, M.M.L., Del Maestro, L., Formstecher, E., Louvard, D., and Arpin, M. (2012). Ezrin regulates microvillus morphogenesis by promoting distinct activities of Eps8 proteins. Mol. Biol. Cell *23*, 1080–1094.

IV/ Appendix

A.: Publication I: A new role for the architecture of microvillar actin bundles in apical retention of membrane proteins. *MBoC, 2012*.

B.: Publication II: Actin dynamics counteract membrane tension during clathrin-mediated endocytosis. *NCB, 2011*.

C.: Publication III: Microvilli. *Cellular domains, 2011*.

A. Publication I

A new role for the architecture of microvillar actin bundles in apical retention of membrane proteins.

Revenu C*, Ubelmann F*, Hurbain I, El-Marjou F, Dingli F, Loew D, Delacour D, Gilet J, Brot-Laroche E, Rivero F, Louvard D, Robine S.

*: co first authors

Mol Biol Cell. 2012 Jan;23(2):324-36.

A new role for the architecture of microvillar actin bundles in apical retention of membrane proteins

Céline Revenu[a,*,†], Florent Ubelmann[a,*], Ilse Hurbain[a,b], Fatima El-Marjou[a], Florent Dingli[c], Damarys Loew[c], Delphine Delacour[d], Jules Gilet[e], Edith Brot-Laroche[e], Francisco Rivero[f], Daniel Louvard[a], and Sylvie Robine[a]

[a]Unité Mixte de Recherche 144, Centre National de la Recherche Scientifique, [b]Cell and Tissue Imaging Facility-IbiSA, and [c]Laboratory of Proteomic Mass Spectrometry, Institut Curie, 75248 Paris, Cedex 05, France; [d]Institut Jacques-Monod, CNRS-UMR7592, Paris 7 University, 75013 Paris, France; [e]Centre de Recherche des Cordeliers, Université Pierre et Marie Curie, UMR S 872, 75006 Paris, France; [f]Centre for Cardiovascular and Metabolic Research, The Hull York Medical School, and Department of Biological Sciences, University of Hull, Hull HU6 7RX, United Kingdom

ABSTRACT **Actin-bundling proteins are identified as key players in the morphogenesis of thin membrane protrusions. Until now, functional redundancy among the actin-bundling proteins villin, espin, and plastin-1 has prevented definitive conclusions regarding their role in intestinal microvilli. We report that triple knockout mice lacking these microvillar actin-bundling proteins suffer from growth delay but surprisingly still develop microvilli. However, the microvillar actin filaments are sparse and lack the characteristic organization of bundles. This correlates with a highly inefficient apical retention of enzymes and transporters that accumulate in subapical endocytic compartments. Myosin-1a, a motor involved in the anchorage of membrane proteins in microvilli, is also mislocalized. These findings illustrate, in vivo, a precise role for local actin filament architecture in the stabilization of apical cargoes into microvilli. Hence, the function of actin-bundling proteins is not to enable microvillar protrusion, as has been assumed, but to confer the appropriate actin organization for the apical retention of proteins essential for normal intestinal physiology.**

Monitoring Editor
Keith E. Mostov
University of California, San Francisco

Received: Sep 7, 2011
Revised: Oct 19, 2011
Accepted: Nov 16, 2011

This article was published online ahead of print in MBoC in Press (http://www.molbiolcell.org/cgi/doi/10.1091/mbc.E11-09-0765) on November 23, 2011.

*These authors contributed equally to this work.

†Present address: EMBL, 69126 Heidelberg, Germany.

Address correspondence to: Céline Revenu (revenu@embl.de) or Sylvie Robine (sylvie.robine@curie.fr).

Abbreviations used: APN, aminopeptidase N; DAPI, 4′,6-diamidino-2-phenylindole; DPPIV, dipeptidylpeptidase IV; DTT, dithiothreitol; EGTA, ethylene glycol tetraacetic acid; $EP^{-/-}$, espin/plastin-1 double KO mice; FCS, fetal calf serum; IAP, intestinal alkaline phosphatase; KO, knockout; LPH, lactase phlorizin hydrolase; OCT, optimal cutting temperature compound; $P^{-/-}$, plastin-1 KO mice; PBS, phosphate-buffered saline; PepT1, peptide transporter protein T1; PFA, paraformaldehyde; SI, sucrase-isomaltase; TEM, transmission electron microscopy; $VE^{-/-}$, villin/espin double KO mice; $VEP^{-/-}$, villin/espin/plastin-1 triple KO mice; $VP^{-/-}$, villin/plastin-1 double KO mice; WT, wild type.

INTRODUCTION

Epithelia constitute the interface between an organ or organism and its environment. This interface ensures a selective barrier that enables protection from external aggressions while allowing necessary exchanges with the surroundings. Most epithelia are indeed specialized in the secretion and/or absorption of various molecules. This functional interface requires a tight sealing of epithelial cells with their neighbors and an asymmetrical subcellular organization between the external (apical) and internal (basal) domains of the epithelial cell. The mechanisms responsible for this striking structural and functional separation between the apical and basal domains are beginning to be well understood. It is clear that complex sorting and cargo-trafficking machineries are essential for the establishment of epithelial cell polarity (Rodriguez-Boulan *et al*., 2005; Sato *et al*., 2007; Weisz and Rodriguez-Boulan, 2009).

The absorptive cells of the intestine, termed enterocytes, represent the archetype of apico-basal polarity in epithelial cells. Tight and adherens junctions separate a basolateral domain from the

brush border, a highly differentiated apical pole structure composed of a dense array of finger-like protrusions: the microvilli. The brush border considerably increases apical cell surface area for the exposure of membrane-bound hydrolases, which participate in the last step of extracellular digestion, and channels and transporters for nutrient uptake. Intestinal microvilli are supported by parallel arrays of actin filaments that create a paracrystalline arrangement: the actin bundle. Actin filaments are constantly polymerizing at the tip of each bundle, but the mechanism of nucleation of the actin network is still unknown. The actin network is linked to the plasma membrane via myosin-1a bridges (Coluccio and Bretscher, 1989), whereas its rootlets expand into the cytoplasm and are connected to the actin and intermediate filaments of the terminal web (Hirokawa *et al.*, 1982, 1983). The ERM protein ezrin participates in the organization of this terminal web region and in the proper shaping of microvilli (Saotome *et al.*, 2004). A capping and cross-linking protein present at the plus end of the filaments, Eps8, has also been implicated in the regulation of microvillar morphogenesis (Croce *et al.*, 2004). Three actin-bundling proteins, villin, plastin-1, and espin, are present in intestinal microvilli. Actin-bundling proteins represent a subset of actin cross-linking proteins, as they are able not only to bind several filaments to create an undefined network, but also to organize filaments in a regular, tight, parallel array to form a bundle; the latter can only be demonstrated by electron microscopy. We will therefore refer in this paper to actin-bundling proteins using this strict definition of proteins that build a paracrystalline bundle.

Stereocilia, bristles, and filopodia are, as microvilli, membrane protrusions supported by parallel bundles of actin filaments (reviewed in Revenu *et al.*, 2004). These actin-based structures all contain several actin-bundling proteins thought to be essential for the formation of the protrusions (Bartles, 2000). Indeed, the down-regulation of the bundler fascin induces a decrease of filopodia number and the remaining ones are short and bent, running nearly parallel to the membrane (Vignjevic *et al.*, 2006). Conversely, fascin overexpression and constitutive activation produce numerous filopodia (Yamashiro *et al.*, 1998; Vignjevic *et al.*, 2006). In *Drosophila melanogaster*, forked or fascin mutants strongly affect bristle morphogenesis (Tilney *et al.*, 1995, 1998). In the jerker mouse, the absence of espin destabilizes inner ear stereocilia, leading to their degeneration (Zheng *et al.*, 2000). Finally, in cells in culture, the ectopic expression of villin in a fibroblastic cell line induces the formation of microvillus-like protrusions (Friederich *et al.*, 1989; Franck *et al.*, 1990), whereas its down-regulation disrupts brush border maintenance in a polarized colonic cell line (Costa de Beauregard *et al.*, 1995). In light of these results, it was proposed that bundling proteins confer requisite stiffness for the actin network to deform the membrane and extend a straight protrusive structure.

However, knockout (KO) of the gene encoding villin in mice did not lead to any detectable morphological defect in the enterocyte brush border (Pinson *et al.*, 1998; Ferrary *et al.*, 1999). Similarly, we were unable to observe an alteration of the organization of intestinal microvilli in jerker mice lacking espins (unpublished data). The loss of plastin-1 predominantly affects the organization of the terminal web, although a slight reduction in the length of microvilli was reported (Grimm-Gunter *et al.*, 2009). Thus none of the three actin-bundling proteins is individually essential for the formation and maintenance of intestinal microvilli. Redundancy among the three actin-bundling proteins was proposed to account for the robustness of the system and therefore for the lack of phenotypes in all the single KO studied.

In the present study, we investigate the function of actin-bundling proteins in intestinal microvilli by circumventing these possible compensatory mechanisms through the analysis of double and triple KO of the three actin-bundling proteins of the intestinal brush border in mice. We demonstrate that the bundled architecture of actin filaments is not primarily necessary for microvilli morphogenesis but is essential for the proper recruitment of key players in the apical membrane anchorage of digestive and absorptive proteins.

RESULTS

Villin/espin/plastin-1 triple KO mice show growth defects

To investigate redundancy among the three actin-bundling proteins of enterocytic microvilli—villin, plastin-1 and espin—we crossed the corresponding single KO (Ferrary *et al.*, 1999; Zheng *et al.*, 2000; Grimm-Gunter *et al.*, 2009) to obtain all four possible combinations: villin/espin, villin/plastin-1, and espin/plastin-1 double KO mice ($VE^{-/-}$, $VP^{-/-}$, and $EP^{-/-}$ mice, respectively) and villin/espin/plastin-1 ($VEP^{-/-}$) triple KO mice. All these mice are viable and fertile. The double KO animals appear normal with the exception of mice lacking espin, which have behavioral defects, as described previously (Gruneberg *et al.*, 1941). The $VEP^{-/-}$ mice demonstrated a smaller body size compared with wild-type (WT) animals (Figure 1A). $VEP^{-/-}$ mice consistently showed a statistically significant growth delay during their first 60 d of life for both males and females compared with their triple heterozygote ($VEP^{+/-}$) half-sibling and double KO $VP^{-/-}$ controls. No significant difference in the growth of $VEP^{+/-}$ and $VP^{-/-}$ mice was found (Figure 1B). The growth delay of $VEP^{-/-}$ mice became more pronounced at ~20–25 d, which corresponds to the weaning period (Figure 1B). Thus $VEP^{-/-}$ mice suffer from growth retardation for the duration of their first 60 d of growth.

The global organization of the enterocytes of $VEP^{-/-}$ mice is preserved

Despite displaying a growth retardation phenotype, the global crypt–villus organization of the intestinal epithelium of $VEP^{-/-}$ mice does not show any overt defects, as was revealed by hematoxilin-eosin staining (Figure 1C). Intestinal sections from $VEP^{-/-}$ mice demonstrated normal apical concentrations of ezrin and F-actin compared with WT sections (Figure 1C). The lateral and apical-lateral junctional markers E-cadherin and ZO-1 also retained their expected localizations in the $VEP^{-/-}$ enterocytes. Therefore, even in the absence of all three actin-bundling proteins, the intestinal epithelial organization and polarity appeared normal at the tissue level. We then investigated the distribution of the main cytoskeletal elements at the cellular level (Figure 1D). In the $VEP^{-/-}$ enterocytes, microtubules showed the classical, mainly apico-basal orientation, and keratin filaments presented a normal diffuse pattern with a slight concentration in the terminal web as in enterocytes from WT mice. At this cellular resolution, the strong brush border localization of actin filaments, although maintained, often appeared narrower in the $VEP^{-/-}$ compared with the WT mice, suggesting an alteration at the level of the microvilli (Figure 1D). Therefore the growth delay present in $VEP^{-/-}$ mice does not seem to be caused by abnormalities in intestinal morphology or global polarity of enterocytes.

Intestinal microvilli form even in the absence of the three actin-bundling proteins

Given the proposed role of actin-bundling proteins in the formation of membrane protrusions, we used transmission electron microscopy (TEM) to investigate the defects generated by the combined absence of two or three bundling proteins in intestinal microvilli morphogenesis. Unexpectedly, microvilli were present in all KO mice analyzed, even in the absence of the three bundlers (Figure 2, A and B). Although TEM confirmed the global preservation of the

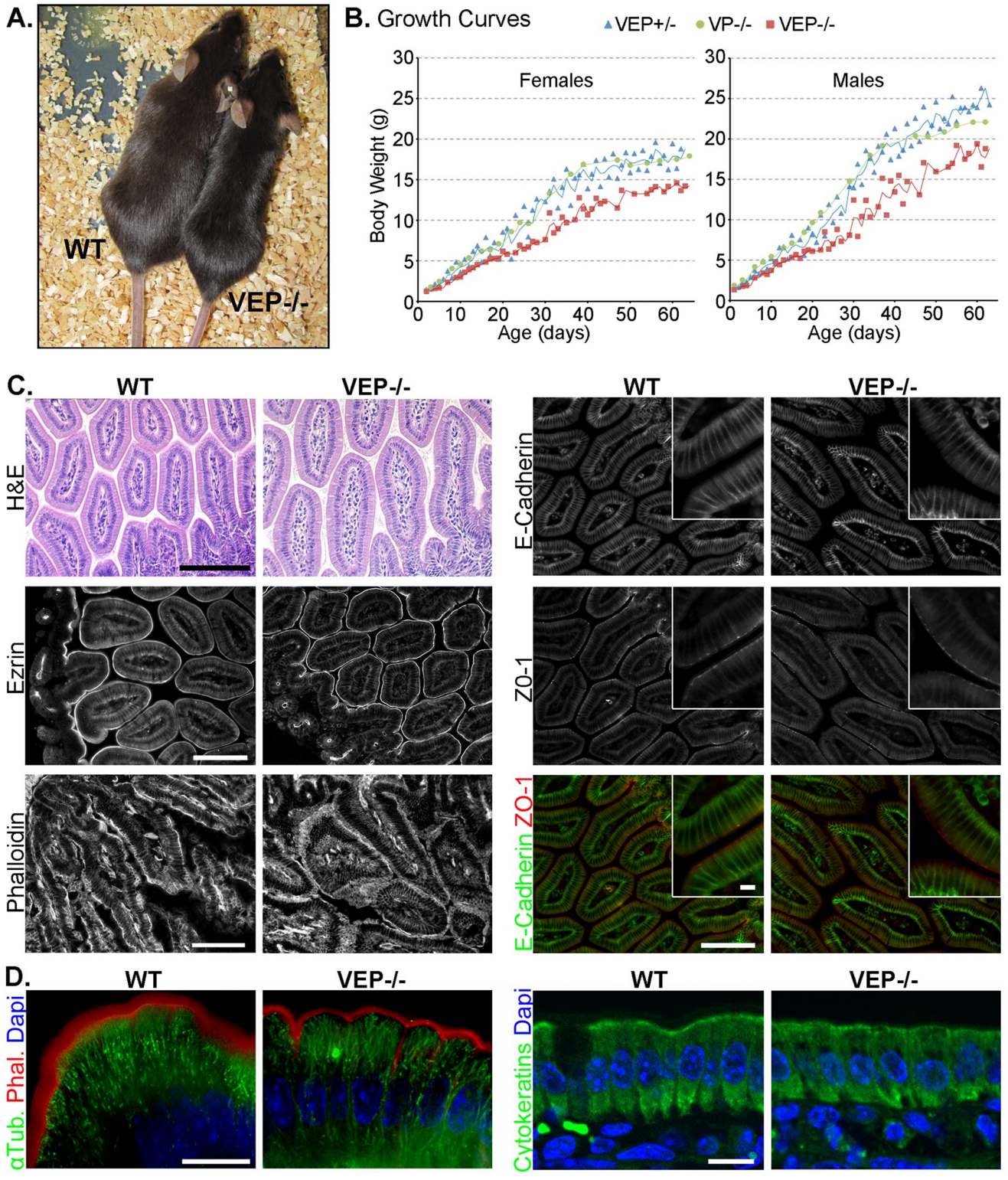

FIGURE 1: The VEP$^{-/-}$ mice have growth defects, but the morphology of their intestinal epithelium looks normal. (A) Picture of a triple KO VEP$^{-/-}$ animal next to a WT animal of the same age. (B) Growth curves plotting the average weight of 35 triple heterozygotes (VEP$^{+/-}$), 16 villin/plastin-1 double KO (VP$^{-/-}$), and 35 triple KO (VEP$^{-/-}$) mice according to their age. Males and females were analyzed separately. (C and D) Histological sections of jejunum from WT and triple KO (VEP$^{-/-}$) animals. (C) H&E shows a hematoxilin and eosin staining (scale bar: 200 μm), phalloidin labels F-actin (scale bar: 100 μm). Immunostaining for ezrin, E-cadherin, and ZO-1 is shown. Scale bars: 100 μm; insets: 10 μm. (D) The global cellular organization of the cytoskeletal elements is presented. Microtubules and F-actin are revealed by immunostaining against α-tubulin (α-Tub., green) and phalloidin labeling (Phal., red). Cytokeratins are labeled with a pancytokeratin antibody (green); 4′,6-diamidino-2-phenylindole (DAPI) labels nuclei (blue). Scale bars: 10 μm.

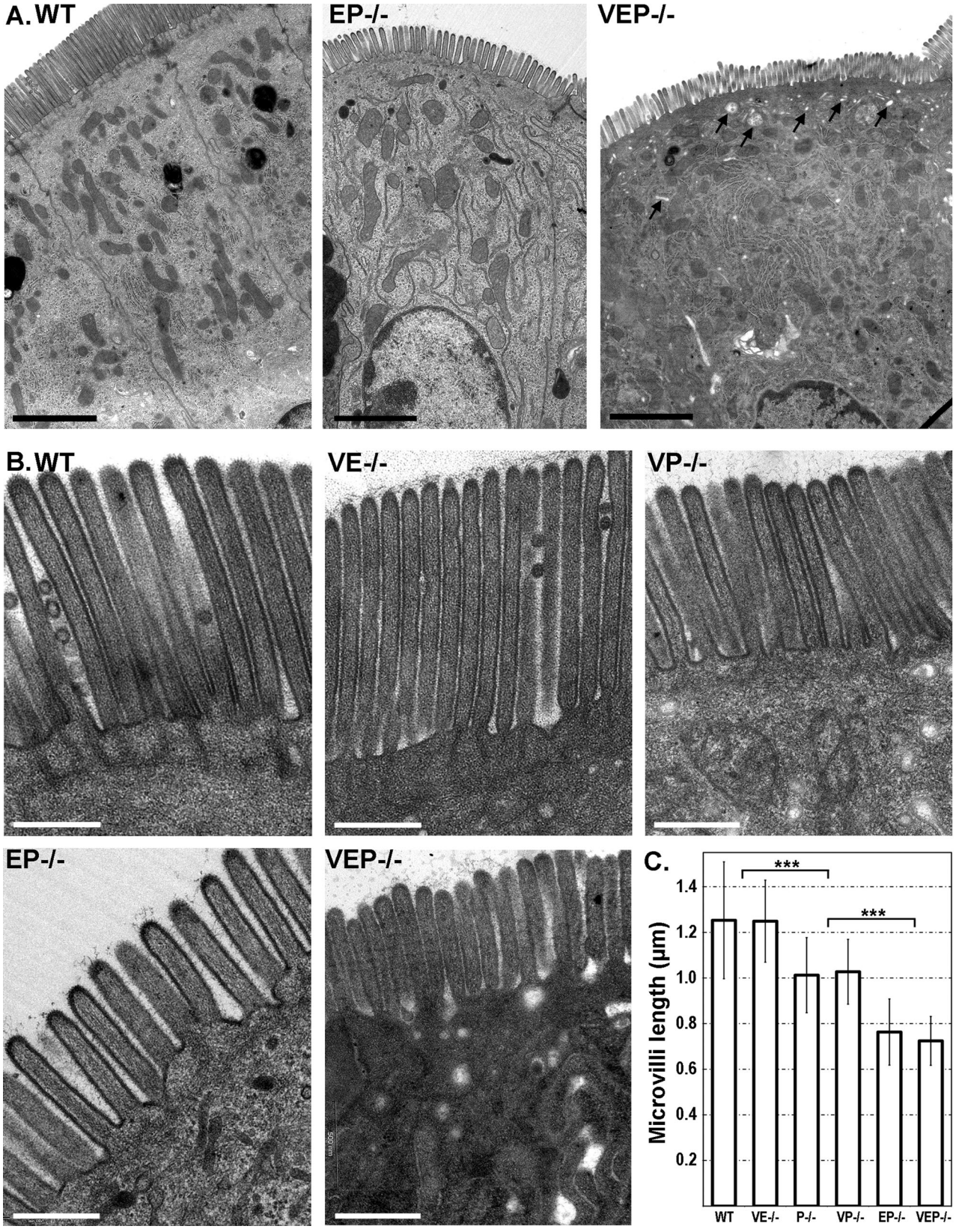

FIGURE 2: Microvilli still form in the VEP$^{-/-}$ mice. (A) Transmission electron micrographs of sections of jejunum from WT, EP$^{-/-}$, and VEP$^{-/-}$ presenting a general view of the enterocyte polarity. Arrows point at apical vesicles and vacuoles in the VEP$^{-/-}$ sample. Scale bars: 2 µm. (B) Transmission electron micrographs of sections of jejunum from WT, the three double KO (VE$^{-/-}$, VP$^{-/-}$, EP$^{-/-}$) and the triple KO (VEP$^{-/-}$) mice illustrating the organization of the brush border. Scale bars: 500 nm. (C) Histograms illustrating the average lengths of the intestinal microvilli depending on the genotype. Values are 1.25 ± 0.26 µm, n_{WT} = 86; 1.01 ± 0.16 µm, $n_{P-/-}$ = 194; 1.03 ± 0.14 µm, $n_{VP-/-}$ = 14; 0.76 ± 0.15 µm, $n_{EP-/-}$ = 75; 0.72 ± 0.11 µm, $n_{VEP-/-}$ = 58. *** *t* test $p < 0.001$.

apico-basal polarity of the enterocytes, with a well-defined brush border facing the lumen, the cytoplasm of the VEP$^{-/-}$ cells demonstrated a higher concentration of vesicles, vacuoles, and tubular structures, especially in the apical area, compared with WT enterocytes. This was quantified by evaluating the number of vesicular structures per square micrometer in the first apical micron of cytoplasm below the microvilli (1.74 ± 0.94, n_{WT} = 5 cells; 7.63 ± 0.52, $n_{VEP-/-}$ = 6 cells; Mann-Whitney $p < 0.01$; Figure 2A). We could not detect any defect in the brush border of the VE$^{-/-}$ mice. The VP$^{-/-}$, EP$^{-/-}$, and VEP$^{-/-}$ mice showed defects similar to those reported for the plastin-1 KO mice (P$^{-/-}$; Grimm-Gunter *et al.*, 2009), namely, very short or absent actin bundle rootlets and a strong reduction in the apical organelle free zone (Figure 2B).

Although the bundlers appeared nonessential for the formation of microvilli per se, they did have an effect on microvillar length (Figure 2C). Compared with microvilli of WT animals, the microvilli of VP$^{-/-}$ mice presented a reduction in length of ~20%, similar to the P$^{-/-}$ mice (1.03 ± 0.14 µm, $n_{VP-/-}$ = 14, and 1.01 ± 0.16 µm, $n_{P-/-}$ = 194, compared with 1.25 ± 0.26 µm, n_{WT} = 86; *t* test $p < 0.0001$). The EP$^{-/-}$ and the VEP$^{-/-}$ mice showed a major decrease in length of around 40% of the length of WT microvilli (0.76 ± 0.15 µm, $n_{EP-/-}$ = 75, compared with WT, *t* test $p < 0.0001$; 0.72 ± 0.11 µm, $n_{VEP-/-}$ = 58, compared with WT, *t* test $p < 0.0001$). The VEP$^{-/-}$ and EP$^{-/-}$ microvilli were thus very similar, with an average length of 724 and 763 nm, respectively, against 1253 nm for WT microvilli. Nevertheless, VEP$^{-/-}$ microvilli appeared less homogeneous in length per cell and less straight compared with EP$^{-/-}$ and a fortiori to WT microvilli (Figure 2, A and B). This was confirmed by the significantly increased coefficient of variation of the length of microvilli per cell in the VEP$^{-/-}$ compared with WT cells (2.54 ± 1.37%, n_{WT} = 7 cells, and 10.85 ± 4.90%, $n_{VEP-/-}$ = 7 cells; Mann-Whitney $p < 0.01$). In conclusion, the absence of the three known actin-bundling proteins reduces microvillar length but does not prevent microvillar protrusion. Providing that no additional actin-bundling protein compensates for the triple KO, it would appear that actin-bundling proteins are not required for membrane protrusion.

The loss of the three bundlers appears not to be compensated

To look for a fourth, unknown actin-bundling protein or for a protein compensating for the absence of the three bundlers that would account for the protrusion of microvilli in the VEP$^{-/-}$ enterocytes, we performed mass spectrometric analysis of the total protein content of WT and VEP$^{-/-}$ isolated brush borders. The list of actin-related proteins found in the analysis of WT brush borders is presented in Supplemental Table S1. All the additional proteins found in the analysis of VEP$^{-/-}$ brush borders are listed in Table S2, and the proteins missing in the VEP$^{-/-}$ compared with the WT brush borders are in Table S3. The potential cross-linkers harmonin and Eps8 could be detected in WT and VEP$^{-/-}$ brush borders. However, only the short harmonin isoform, harmonin a, which lacks the actin-bundling region (Verpy *et al.*, 2000), but not the cross-linking isoform b (Boeda *et al.*, 2002), could be detected in WT and VEP$^{-/-}$ brush borders by Western blot analysis using a pan-harmonin antibody (Supplemental Figure S1B). The capping protein Eps8 has also been recently proposed to have cross-linking activity in vitro that is enhanced by binding to IRSp53 (Disanza *et al.*, 2006; Hertzog *et al.*, 2010). IRSp53 was absent from both WT and VEP$^{-/-}$ brush borders, as we could neither find it in the proteomic data nor detect it by Western blotting (Figure S1A). Moreover, Eps8 expression levels were unchanged between WT and VEP$^{-/-}$ brush borders and, importantly, Eps8 was strictly localized at the very tip, as expected, and did not extend along the shaft of the microvilli in the VEP$^{-/-}$ samples (Figure S1A). Eps8 is thus not ectopically recruited and does not compensate for the loss of the actin-bundling proteins in VEP$^{-/-}$ intestinal microvilli. Finally, two interesting nucleators of linear actin filaments were detected in this proteomic study: cordon-bleu and diaphanous homologue 1. Cordon-bleu localized to the terminal web region and not to the tips of microvilli, as demonstrated by immunofluorescence (Figure S1C), and is thus unlikely to have a role in microvilli protrusion. The presence of diaphanous homologue 1 was confirmed by Western blotting (Figure S1C), but the lack of antibodies suitable for immunofluorescence prevented us from addressing its localization. No extra actin-bundling or cross-linking proteins could be detected in the VEP$^{-/-}$ brush borders compared with WT (Table S2). Thus the formation of microvilli in VEP$^{-/-}$ mice does not appear to be due to the compensatory recruitment of a fourth bundler but is more likely explained by the presence of the remaining actin-binding proteins normally present in microvilli.

The organization of F-actin into a bundle is lost in VEP$^{-/-}$ microvilli

We next addressed the precise organization of actin filaments, which were detected in microvilli after phalloidin staining (Figure 1D). The longitudinal striation due to the actin bundle was easily detectable by TEM in the double KO microvilli, whereas it was no longer distinguishable in the VEP$^{-/-}$ microvilli (Figure 2B). TEM of transverse sections of WT microvilli demonstrated a sharp, electron-dense, dotted pattern that corresponded to transverse sections of individual actin filaments (Figure 3A, insets). This pattern was absent in VEP$^{-/-}$ samples, which displayed only a few, indistinct darker areas that likely correspond to actin filaments (Figure 3A). This prevented the quantification of the number of filaments in VEP$^{-/-}$ samples. Noticeably, although the reticular organization of microvilli was unaffected as measured by the angle between three adjacent microvilli (65.9 ± 9.7°, n_{WT} = 115; 62.4 ± 9.4°, $n_{VEP-/-}$ = 151), the transverse area of microvilli was strongly decreased in VEP$^{-/-}$ versus WT animals (5231.1 ± 836.7 nm^2, $n_{VEP-/-}$ = 91, and 8909.5 ± 1097.9 nm^2, n_{WT} = 137; *t* test $p < 0.0001$; Figure 3B). As the number of filaments in the bundle influences the diameter of a protrusion (Tilney and Tilney, 1988), this could indicate a reduced number of filaments in the VEP$^{-/-}$ microvilli. In support of this hypothesis, Western blotting revealed that the actin content of the purified brush borders was reduced in VEP$^{-/-}$ mice compared with WT controls, whereas the actin content of enterocytes remained unmodified between WT and VEP$^{-/-}$ total lysates (Figure 3C).

To achieve better resolution of the actin filaments in microvilli, we performed TEM on isolated brush borders from WT and VEP$^{-/-}$ mice. This technique eliminates most of the background generated by the cytoplasmic elements, while the brush border actin cytoskeleton and its associated plasma membrane are preserved. As demonstrated by phalloidin staining, VEP$^{-/-}$ brush borders appeared thinner than WT brush borders and retained F-actin (Figure 3, D and E, insets). TEM revealed that longitudinal actin filaments were still present in VEP$^{-/-}$ microvilli. However, they lost the normal bundled structure present in the WT situation (compare Figure 3E with 3D): the number of filaments seemed to be reduced, and their spacing was highly irregular. In some areas, actin filaments appeared compacted and indistinguishable from each other, or even interrupted, which could be due to wavy filaments going out of the section. In other areas, the spacing between two filaments was enlarged compared with the WT bundle. This disorganization explains the lack of sharp actin dots in the transverse sections (Figure 3A). On the contrary, actin filaments in WT microvilli showed the expected highly

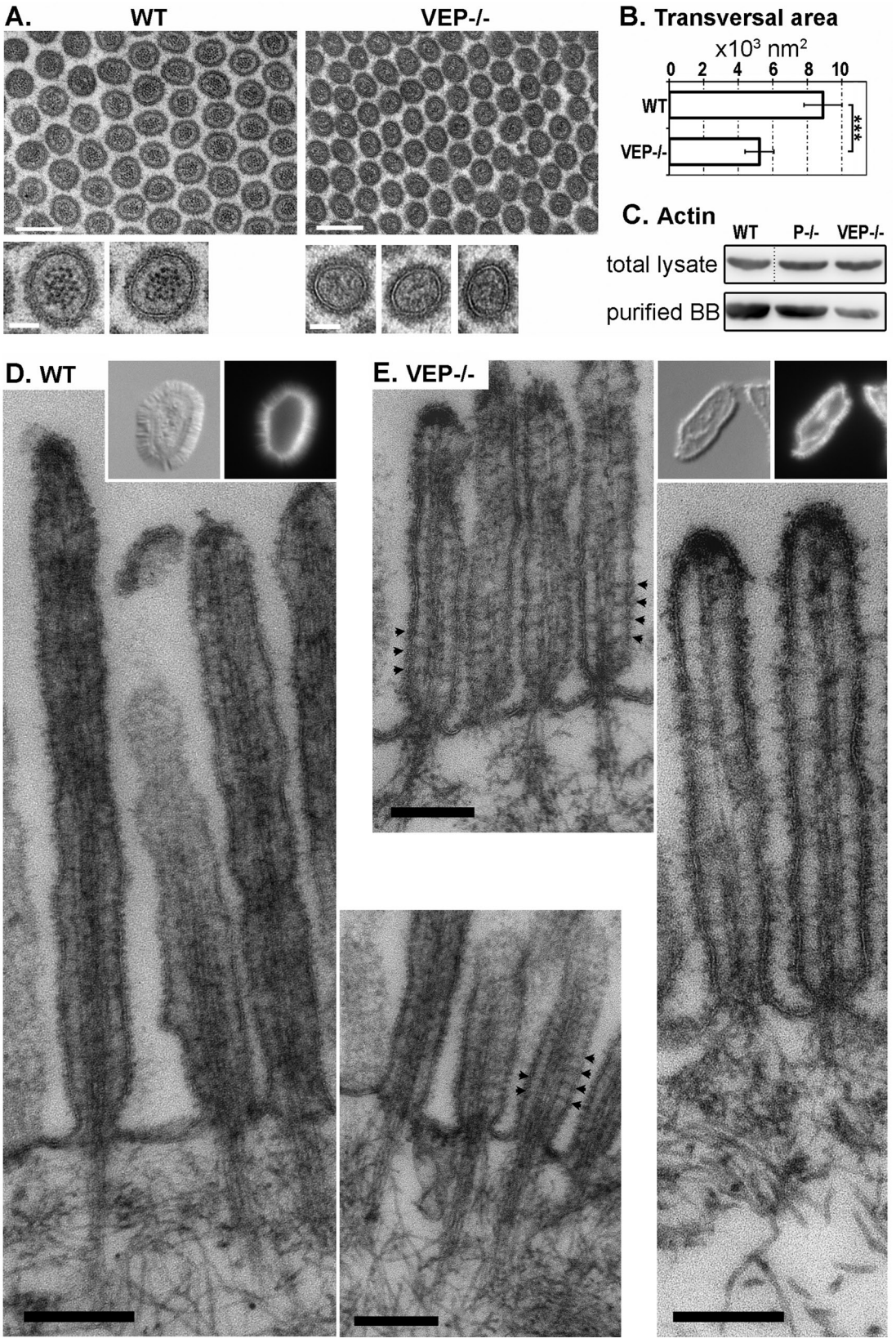

FIGURE 3: The organization of the actin bundle is affected in the VEP$^{-/-}$ microvilli. (A) Transmission electron micrographs of transversal sections of the microvilli of WT and VEP$^{-/-}$ mice. Scale bars: 200 nm; insets: 50 nm. (B) Histograms depicting the average area of transversal sections of microvilli depending on the genotype: 5231.1 ± 836.7 nm^2, $n_{VEP-/-}$ = 91 and 8909.5 ± 1097.9 nm^2, n_{WT} = 137. *** *t* test $p < 0.001$. (C) Western blotting against actin on total lysates or lysates from isolated brush borders (loaded for equal total protein). (D and E) Transmission electron micrographs of isolated brush borders from (D) WT and (E) VEP$^{-/-}$ mice. Typical isolated brush borders are shown in insets (left: Nomarski; right, phalloidin staining). Arrowheads highlight actin-membrane bridges. Scale bars: 200 nm.

regular bundle pattern resembling striae (Figure 3D). The short or missing rootlets in VEP$^{-/-}$ mice look similar to those reported for P$^{-/-}$ mice (Grimm-Gunter *et al.*, 2009). Actin-membrane bridges, known to be myosin-1a–based in WT animals, could still be detected in some VEP$^{-/-}$ samples (Figure 3, D and E, arrowheads). These bridges cannot be detected in all sectioned microvilli, even in WT mice; therefore their number and arrangement cannot be reliably evaluated. Taken together, these data indicate that although actin filaments are still present in VEP$^{-/-}$ microvilli, they are sparse and no longer packed in parallel bundles.

As VEP$^{-/-}$ mice have reduced microvillar transverse area and length, their intestine absorptive surface could be significantly compromised and have an impact on growth. On the basis of the measured length, area, and density of microvilli in WT, EP$^{-/-}$, and VEP$^{-/-}$ intestine, we calculated the respective brush border membrane surfaces per square micrometer of apical domain, approximating microvilli to cylinders ($S_{WT} = 24.8 \pm 6.9\ \mu m^2$, $S_{EP-/-} = 12.0 \pm 2.5\ \mu m^2$, $S_{VEP-/-} = 14.4 \pm 2.8\ \mu m^2$; maximal SDs were calculated according to the Gaussian error-propagation law). The brush border membrane surface was strongly reduced in VEP$^{-/-}$ enterocytes compared with WT, but not EP$^{-/-}$, enterocytes. As the EP$^{-/-}$ and VEP$^{-/-}$ absorptive surfaces are similar, the effect of smaller microvilli on the VEP$^{-/-}$ growth retardation phenotype can be ruled out. The growth delay of VEP$^{-/-}$ mice is thus not due to a reduction in the absorptive surface of the epithelium but could be linked to a defect in actin bundle organization.

Digestive enzymes do not properly localize in the apical domain

One important step toward understanding the phenotype of the VEP$^{-/-}$ mice is to define how the disorganization of the actin network accounts for growth retardation. Trafficking toward the basolateral domain did not appear to be affected, as illustrated by the basolateral localization of the Na^+/K^+-ATPase in VEP$^{-/-}$ enterocytes (Figure S3B). We therefore analyzed the localization of digestive enzymes that are normally exposed at the apical surface of the enterocytes using a variety of apical trafficking routes. As the VEP$^{-/-}$ mouse demonstrates the major terminal web defects previously reported in the plastin-1 KO (Grimm-Gunter *et al.*, 2009), and as we need to unravel the specificity of the VEP$^{-/-}$ samples, we used both WT and P$^{-/-}$ samples as controls in this study (Figure 4). The lipid raft–associated aminopeptidase N (APN) still localized properly in the VEP$^{-/-}$ brush border (Figure S3A). Nevertheless, several enzymes presented an impressive subapical accumulation in the VEP$^{-/-}$ enterocytes, with partial localization in the microvilli (Figure 4A, stars). This was the case for raft-independent lactase phlorizin hydrolase (LPH), raft-associated sucrase-isomaltase (SI), and peptide transporter protein PepT1. Moreover, Western blot analyses performed on lysates from purified brush borders showed that the amount of these enzymes that still localized to the microvilli was reduced in the VEP$^{-/-}$ compared with the WT or P$^{-/-}$ samples (Figure 4B). To a much lesser extent, LPH could be seen accumulating subapically in some areas of the plastin-1 KO (Figure 4A) and its combinations (Figure S2). In the VP$^{-/-}$ enterocytes, SI also appeared delocalized and PepT1 showed some slight subapical accumulation but much less strikingly than in the VEP$^{-/-}$ samples (Figure S2). The amount of dipeptidyl-peptidase IV (DPPIV), an enzyme following a transcytotic pathway, was strongly reduced in the VEP$^{-/-}$ microvilli, as demonstrated both by Western blotting (Figure 4B) and immunostaining (Figure 4A, circle), but DPPIV did not show the intense subapical accumulations reported above. Finally, the glycosylphosphatidylinositol-anchored intestinal alkaline phosphatase (IAP) presented both a very strong decrease in the VEP$^{-/-}$ brush border, observed by Western blotting and immunostaining, and a significant subapical accumulation (Figure 4, A, star and circle, and B). The subapical accumulations reported by immunofluorescence were in agreement with the high vesicular content of the VEP$^{-/-}$ cytoplasm detected by TEM (Figure 2). Compared with the WT cell and brush border lysates, a reproducible shift in the size of the bands detected by Western blotting occurred for LPH, SI, DPPIV, and APN in the P$^{-/-}$ and VEP$^{-/-}$ samples (Figures 4A and S3A). This shift could be suppressed by treating the samples with glycosidases and therefore reflects a difference in the glycosylation pattern (Figure S5). This unexpected phenomenon is not responsible for the phenotype of the VEP$^{-/-}$ mice, because it already occurs in the P$^{-/-}$ samples and thus must be due solely to the depletion of plastin-1.

To directly assess an absorption defect in the VEP$^{-/-}$ mice, we measured the kinetics of glucose absorption of fasted WT, P$^{-/-}$, and VEP$^{-/-}$ mice following oral glucose load. The glucose absorptive capacity of VEP$^{-/-}$ intestine was strongly and significantly reduced compared with both WT and P$^{-/-}$ animals, as depicted by the measurements of glucose blood level plotted against time after gavage (Figure 4C). Interestingly, the blood glucose level in VEP$^{-/-}$ mice was significantly reduced by 75% at 30 min. Such an early time point directly represents an alteration of the glucose absorption capacity of the enterocytes, as the adaptive physiological response to high glycemia has not yet occurred.

The study of the triple KO enterocytes therefore reveals a major disruption in apical delivery and/or retention of enzymes at the apical membrane associated with malabsorption and subsequent growth delay that develops predominantly after weaning in the VEP$^{-/-}$ mice. The slight apical localization defects observed in the VP$^{-/-}$ samples are not sufficient to cause such a growth delay in these mice (Figure 1B).

Apical membrane retention is deficient and myosin-1a is mislocalized

To decipher the apical transport or anchorage mechanisms that are defective in the VEP$^{-/-}$ mice, we analyzed the subcellular localization of several players in apical targeting and delivery. The organization of the Golgi was not affected in the VEP$^{-/-}$ enterocytes, as the Golgi marker giantin and the GTP-binding protein Rab6, which is implicated in intra-Golgi transport, retained the localization observed in WT enterocytes (Figure S4A). The Golgi apparatus appeared morphologically unaltered, suggesting that a later step in the apical transport could be defective. Cargoes are known to go through Rab11- and Rab8-positive compartments en route to the apical pole. Although the subnuclear localization of Rab11 was not affected in the VEP$^{-/-}$ animals (Figure S4A), Rab8 subapical concentration looked slightly decreased when observed by immunofluorescence (Figure S4B). However, this reduced Rab8 apical localization could not be confirmed by Western blotting (Figure S4B). Whereas the apical delivery route did not appear affected, the early endosomal marker EEA1 exhibited an enlarged subapical localization in the VEP$^{-/-}$ enterocytes (Figure 5A) and strongly colocalized with the accumulation of apical markers, as shown for SI (Figure 5B). These results suggest that endocytosis, rather than apical delivery, is responsible for the mislocalization of apical enzymes and transporters in the VEP$^{-/-}$ mice. Is endocytosis therefore enhanced in the absence of a proper actin bundle or are these apical components more prone to endocytosis? To discriminate between these two possibilities, we compared in vivo the kinetics of global endocytosis using the vital membrane stain FM dye as an endocytic probe perfused in the intestinal lumens of WT and

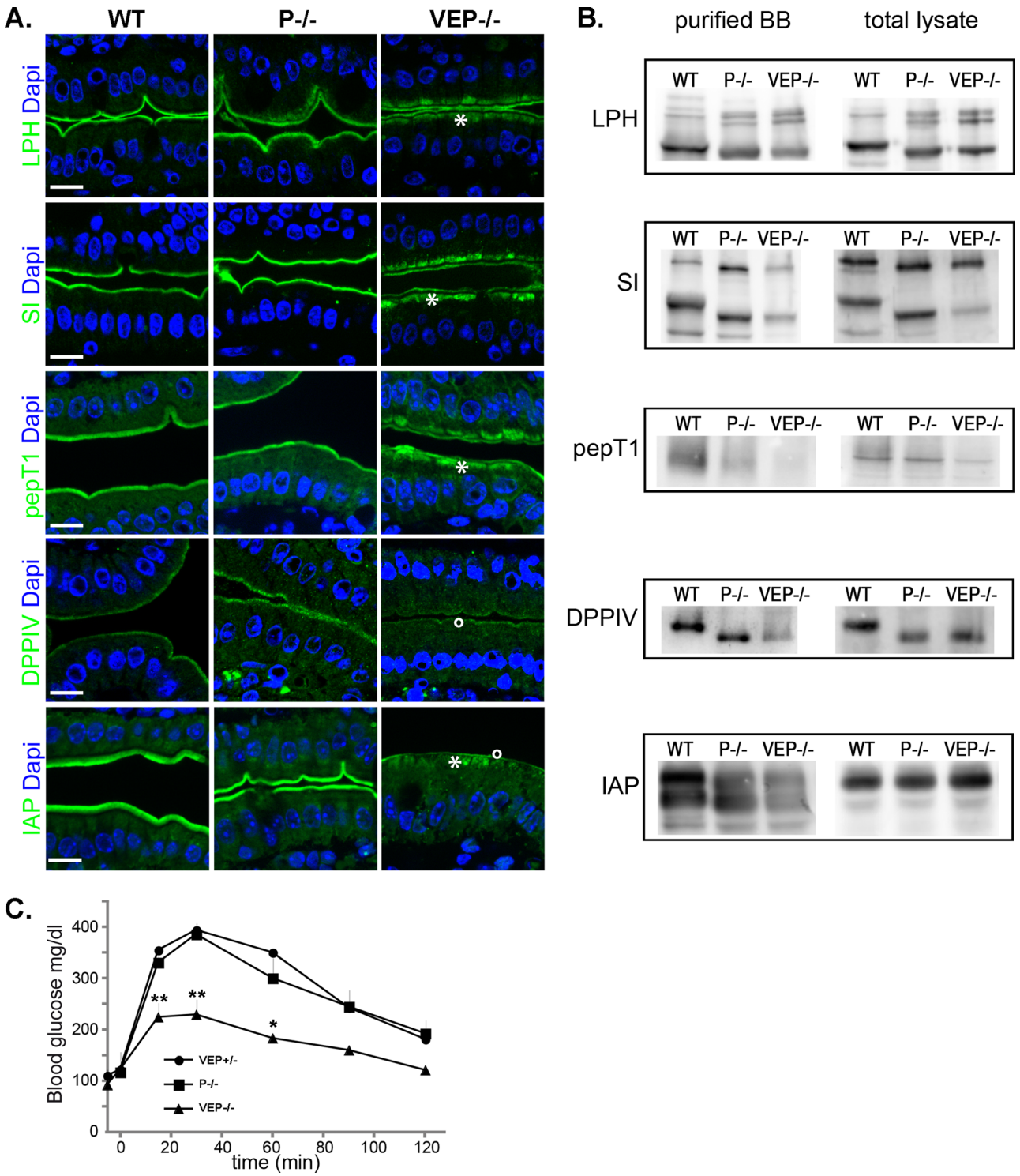

FIGURE 4: VEP$^{-/-}$ mice show apical localization defects of major digestive and absorptive brush border components. (A) Histological sections of jejunum from WT, P$^{-/-}$ and VEP$^{-/-}$ animals immunostained for LPH, SI, PepT1, DPPIV, and IAP (green). DAPI (blue) labels nuclei. Scale bars: 10 μm. (B) Western blots against LPH, SI, PepT1, DPPIV, and IAP were performed on total or isolated brush borders lysates (loaded for equal total protein). (C) Blood glucose concentrations plotted over time during oral glucose tolerance test in mice fasted overnight ($n_{VEP+/-}$ = 3; $n_{P-/-}$ = 5; $n_{VEP-/-}$ = 3; Mann-Whitney: **, $p < 0.01$, *, $p < 0.05$).

VEP$^{-/-}$ mice (Hansen *et al.*, 2009). A modification in the internalization of the dye in the KO enterocytes could not be detected at any of the time points analyzed from 5 to 90 min (Figure 5C). The global endocytosis rate is therefore not increased in the VEP$^{-/-}$ enterocytes, and the accumulation of apical digestive components in EEA1-positive compartments is most likely due to their deficient stabilization at the apical membrane.

The mechanisms allowing membrane retention of apical enzymes and transporters are widely unknown. To date, only the actin motor myosin-1a, a brush border myosin, has been implicated in the

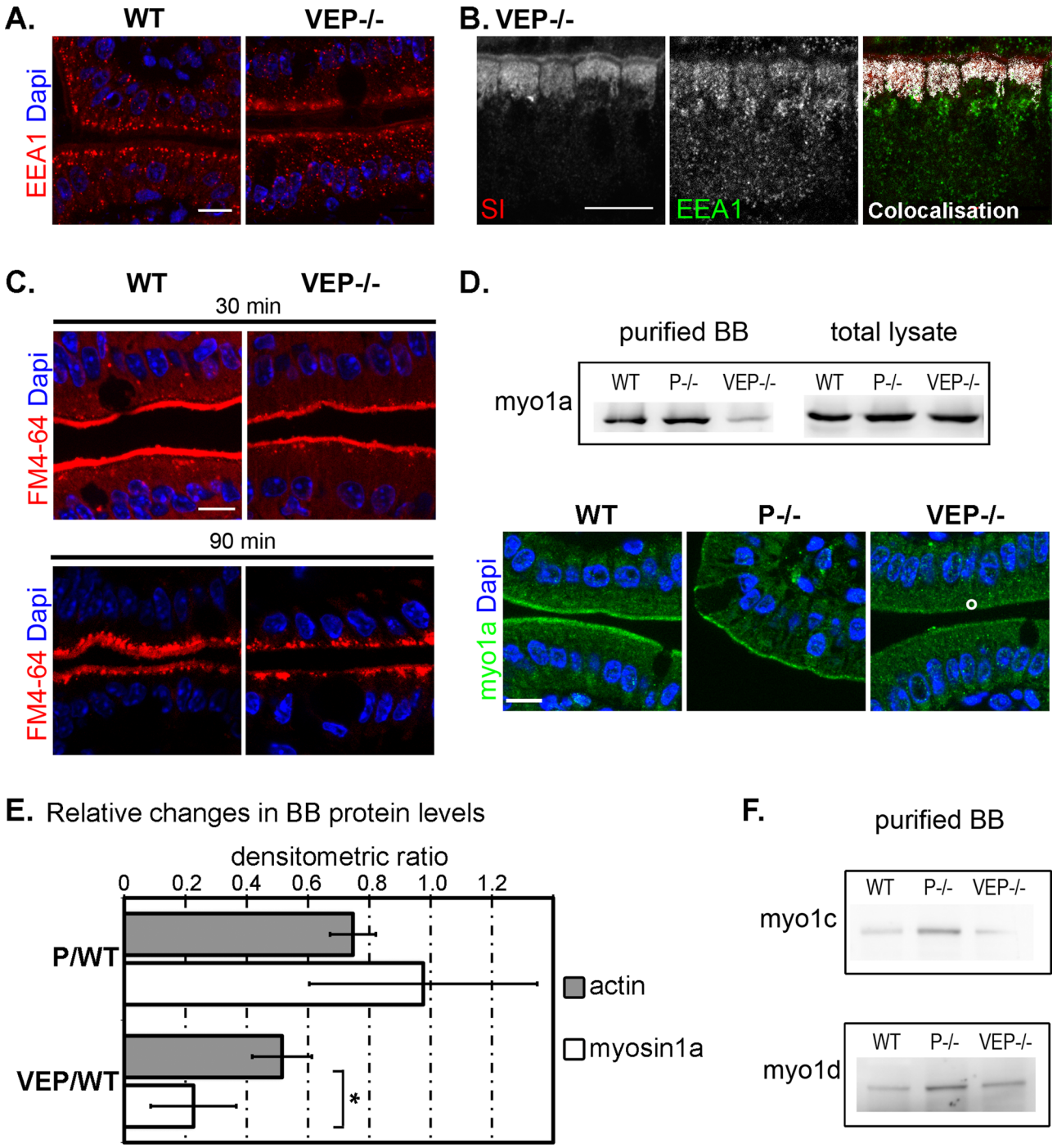

FIGURE 5: The apical domain retention machinery is affected in VEP$^{-/-}$ mice. (A) Immunostaining against the early endosomal marker EEA1 in WT and VEP$^{-/-}$ enterocytes. (B) Colocalization (white) of EEA1 (green) with the subapical accumulations of the enzyme SI (red) by immunostaining. (C) Unchanged global endocytosis rate analyzed by the internalization of the vital membrane dye FM4-64 (red), shown at 30- and 90-min time points. (D) Western blots and immunostaining against myosin-1a on WT, P$^{-/-}$, and VEP$^{-/-}$ samples. Western blot analysis was performed on total and isolated brush border lysates. DAPI labels nuclei (blue). Scale bars: 10 µm. (E) Histograms depicting the relative changes of actin and myosin-1a protein content between P$^{-/-}$ or VEP$^{-/-}$ and WT brush borders (P/WT and VEP/WT, respectively). Values are densitometric ratios of Western blotting performed on brush border lysates (P/WT: 0.98 ± 0.37, n_{myo1a} = 3, and 0.75 ± 0.07, n_{actin} = 5; VEP/WT: 0.23 ± 0.14, n_{myo1a} = 3, and 0.52 ± 0.10, n_{actin} = 5). *Wilcoxon two-sample test $p < 0.05$. (F) Western blotting performed on isolated brush border lysates against myosins-1c and -1d on WT, P$^{-/-}$, and VEP$^{-/-}$ samples showing that the decrease in myosin-1a is not accompanied by their compensatory recruitment to the brush borders.

anchorage of some apical enzymes (Tyska and Mooseker, 2004). Remarkably, whereas it is properly concentrated in the microvilli of WT and P$^{-/-}$ enterocytes, myosin-1a was substantially lost in VEP$^{-/-}$ microvilli, as detected by Western blotting on isolated brush border lysates and by immunofluorescence (Figure 5D). As the actin content was also diminished in VEP$^{-/-}$ brush borders (Figure 3C), we

wondered whether the reduction in myosin-1a was directly due to the loss of the actin-bundling proteins or solely a reflection of the lower actin content. We quantified by densitometric analysis of Western blots the relative changes in actin and myosin-1a content between WT and $P^{-/-}$ or $VEP^{-/-}$ brush borders (Figure 5E). The densitometric ratio of $P^{-/-}$ over WT brush border samples was not significantly different between actin and myosin-1a (0.98 ± 0.37, $n_{myo1a} = 3$, and 0.75 ± 0.07, $n_{actin} = 5$, $p \leq 0.8$). In contrast, the densitometric ratio of $VEP^{-/-}$ over WT brush border samples was significantly reduced for myosin-1a compared with actin (0.23 ± 0.14, $n_{myo1a} = 3$, and 0.52 ± 0.10, $n_{actin} = 5$; Mann-Whitney $p < 0.05$). This demonstrates that $VEP^{-/-}$ brush borders lost approximately two times more myosin-1a than actin and that the decrease in myosin-1a was not merely due to a decrease in brush border actin. Although myosin-1a brush border level was strongly decreased, it was not completely absent. We could still detect some myosin-1a bridges by TEM (Figure 3E), and the myosin-1a–based extrusion of vesicular membranes (McConnell and Tyska, 2007) was still detected upon ATP-induced myosin activation on isolated $VEP^{-/-}$ brush borders (Figure S6). The KO of myosin-1a in mouse enterocytes does not cause defects at the whole-animal level (Tyska *et al.*, 2005). This lack of phenotype has been accounted for by the compensatory recruitment of at least two other myosins, myosin-1c and -1d, in the brush border (Tyska *et al.*, 2005; Benesh *et al.*, 2010). We therefore used Western blotting to analyze the brush border content of these class I myosins in our samples. The level of these two myosins did not increase between $VEP^{-/-}$ and WT brush borders (Figure 5F). Neither of them became ectopically recruited to the microvilli in the absence of the three actin-bundling proteins, although myosin-1a was almost absent from $VEP^{-/-}$ microvilli. Thus the absence of the three actin-bundling proteins is associated with defects in the brush border localization of at least one player in apical enzyme retention, myosin-1a.

DISCUSSION

How to build microvilli without actin-bundling proteins?

As discussed in the *Introduction*, a number of experimental data strongly suggest a role for actin-bundling proteins in the formation of membrane protrusions. It is therefore surprising that mice devoid of actin bundlers still form microvilli. However, biophysical and modeling studies have questioned this presupposed requirement (Janmey *et al.*, 1992; Miyata *et al.*, 1999; Mogilner and Rubinstein, 2005). Actin polymerization alone would be sufficient to produce a force that can overcome the resistance of the membrane to bending (Peskin *et al.*, 1993; Mogilner and Rubinstein, 2005). Our results are in favor of such a dispensable role for actin-bundling proteins in microvilli protrusions in vivo. As actin filaments are flexible, the force they generate after reaching a critical protrusion length is limited by buckling that occurs in response to the membrane resilience force. This critical length is dependent on the number of filaments and on their rigidity, the latter being increased by their physical bundling (Mogilner and Rubinstein, 2005; Atilgan *et al.*, 2006; Claessens *et al.*, 2006; Bathe *et al.*, 2008). In agreement with these biophysical models, we demonstrate that actin-bundling proteins do not act redundantly in the protrusion of microvilli but do regulate their length. A role for plastin-1 in microvillar lengthening has already been reported in vivo (Grimm-Gunter *et al.*, 2009). In contrast to their reported roles in LLCPK-1 cells (Loomis *et al.*, 2003), we show that espin plays a positive role in regulating microvillar length only in the absence of plastin-1, whereas villin clearly has no effect. The three bundlers are therefore not equivalent in their contributions to microvillar morphogenesis. Nevertheless, they do cooperatively contribute to the paracrystalline, bundled organization of filaments that is lost in the $VEP^{-/-}$ mice compared with the single or double KO.

Although actin-bundling proteins are dispensable, many additional mechanisms can provide sufficient organization to the network for membrane protrusion to occur. It has been proposed that the membrane itself participates in the organization of actin filaments in parallel arrays within protrusions (Liu *et al.*, 2008). In stereocilia and filopodia, the role of actin-binding proteins in the tip complex is well documented (Tokuo and Ikebe, 2004; Pellegrin and Mellor, 2005; Rzadzinska *et al.*, 2009). Eps8 is localized at the tip of microvilli and participates in their morphogenesis (Croce *et al.*, 2004; Tocchetti *et al.*, 2010). Eps8 cross-linking activity (Disanza *et al.*, 2006; Hertzog *et al.*, 2010) combined with its restricted localization make it a credible molecular bond between the polymerizing ends of actin filaments. This tip connection and the remaining myosin bridges linking actin filaments to the membrane may be sufficient to maintain the longitudinal filaments observed in $VEP^{-/-}$ microvilli. Moreover, the nucleator mDia1 has been identified in our proteomic analysis. If present in the tip complex, this nucleator is likely to initiate and elongate unipolar arrays of actin filaments (Campellone and Welch, 2010), as formins do in filopodia (Mellor, 2010). In future studies, it will be of interest to investigate the function of mDia1 in microvilli.

Defective apical retention and increased internalization of membrane proteins?

The malabsorption and growth retardation reported for the $VEP^{-/-}$ mice cannot be explained by microvillar shortening, because similar shortening and reduction of membrane surface are also present in non-growth-retarded $EP^{-/-}$ mice. It is more likely due to defective enterocyte absorption caused by the large defects in the apical localization of transporters and enzymes required for this process. We demonstrate that, although the endocytic rate is unmodified, these membrane proteins accumulate in EEA1-positive compartments. SI and LPH-associated vesicles traverse endosomal compartments en route to the apical pole, but they do not normally associate with EEA1 (Cramm-Behrens *et al.*, 2008). Moreover, digestive enzymes are highly stable at the apex, presenting a very low basal rate of endocytosis and recycling (Matter *et al.*, 1990; Hansen *et al.*, 2009). Our results clearly argue in favor of a highly increased susceptibility to internalization via normal endocytic pathways in the $VEP^{-/-}$ animals. Interaction with the cytoskeleton is essential for membrane protein stabilization, but little is known about the molecular mechanisms involved (Nelson and Veshnock, 1987; Tyska and Mooseker, 2004). In enterocytes, myosin-1a has been implicated in the retention of SI within the brush border (Tyska and Mooseker, 2004; Tyska *et al.*, 2005). Its strong mislocalization in this study, in the absence of a structured actin network, provides good evidence of the general mechanism at the origin of the retention defects, but myosin-1a is most probably not the only cytoskeletal linker affected—the others being still undiscovered.

In myosin-1a KO microvilli, enzymes appear to localize fairly normally, and no overt phenotype was detected (Tyska and Mooseker, 2004; Tyska *et al.*, 2005), most probably due to compensatory recruitment of myosin-1c and -1d (Tyska *et al.*, 2005; Benesh *et al.*, 2010). This recruitment solely in the absence of myosin-1a is due to differential actin-binding affinities and competition for actin-binding sites (Tyska *et al.*, 2005; Benesh *et al.*, 2010). Equivalent ectopic redistributions are not detected in the $VEP^{-/-}$ enterocytes, even if myosin-1a is substantially lost from the microvilli. This suggests that the abnormality that affects the recruitment of myosin-1a could be

structural, residing in the disorganization of the actin network, and would hence also perturb the recruitment of any other possible compensatory class I myosin, causing the apical defects observed.

Actin bundle architecture is critical for the efficient recruitment of proteins

Compared with single and double KO microvilli, those of VEP$^{-/-}$ demonstrate an additional structural defect: the lack of organization of actin filaments into a bundle. The literature increasingly reports the importance of specific actin architecture for the selective binding of proteins (Temm-Grove *et al.*, 1998; Tang and Ostap, 2001; DesMarais *et al.*, 2002; Nagy *et al.*, 2008; Nagy and Rock, 2010; Brawley and Rock, 2009). In the VEP$^{-/-}$ enterocytes, because myosin-1 is not efficiently recruited to the microvilli, myosins are of particular interest. Different classes of unconventional myosins have been shown to select specific actin filament subpopulations in cells (Brawley and Rock, 2009). The filopodium myosin-X selects actin bundles for processive movement (Nagy *et al.*, 2008; Nagy and Rock, 2010; Ricca and Rock, 2010). Moreover, the architecture and dynamics of the bundle regulate the differential concentration of actin-binding molecules in the bundle (Naoz *et al.*, 2008). Loss of the stabilizing effect of actin-bundling proteins (Zigmond *et al.*, 1992; Tilney *et al.*, 2003; Prost *et al.*, 2007) is therefore likely to modify the localization of myosins and other associated molecules (Naoz *et al.*, 2008). Finally, the radial "barber pole" distribution of myosin-1a along the microvillar axis relies on the precise paracrystalline hexagonal arrangement of actin filaments together with the sterical hindrance generated by the bundlers (Brown and McKnight, 2010). Alterations to the concentration and localization of myosin-1a in the brush borders of VEP$^{-/-}$ mice most likely reflect the different architectural organization of the actin network. It is thus conceivable that myosin-1a, and other actin-binding proteins present in the brush border, do not efficiently bind or move along the unstructured VEP$^{-/-}$ actin network.

In conclusion, the function of actin-bundling proteins is not to power the morphogenesis of microvilli per se but to grant the actin network a precise architecture that allows the selective recruitment of proteins implicated in apical retention. This work highlights in vivo the importance of local cytoskeletal organization in the proper regulation of subcellular membrane specializations.

MATERIALS AND METHODS

KO mice

The double and triple KO mice used in this study were generated by successive crossing between the villin (Ferrary *et al.*, 1999), espin (Zheng *et al.*, 2000), and plastin-1 (Grimm-Gunter *et al.*, 2009) KO, as described previously. The espin KO (jerker) mice, which carry a natural autosomal recessive mutation in the gene encoding the bundlers of the espin family, were purchased from the Jackson Laboratory (Bar Harbor, ME). They were all genotyped by PCR. Animal experiments were carried out under the authority of the Curie Institute veterinarian, under permission granted to the Robine laboratory (number 75-433, Préfecture de Police—Direction des Services Vétérinaires de Paris).

Growth curves

To analyze the growth of VEP$^{-/-}$ animals, mice born from crosses of VEP$^{-/-}$ males with VEP$^{-/-}$ females were compared with half-siblings born from the same males crossed with WT females. The double KO VP$^{-/-}$ litters were from intercrosses of double KO parents. The weights of 86 mice from 12 different litters with the three different genotypes were measured every 2 d during the first 60 d after birth. We analyzed the growth time series by adjusting a mixed-effect model in order to assess the significance of the genotype effect. The fixed effects accounted for in the model are the genotype, the sex, and the time, while the litter is considered a random effect. For more details, see Supplemental Material.

Sampling and preparation of the tissues

The intestine of adult mice was isolated and divided into three parts of identical length corresponding to the duodenum, jejunum, and ileum. The intestinal tube was washed with phosphate-buffered saline (PBS). To prepare tissue for paraffin sectioning, we fixed short pieces of jejunum in 4% paraformaldehyde (PFA), in Carnoy solution (60% ethanol, 30% chloroform, 10% acetic acid), or in 70% methanol for 2 h at room temperature or overnight at 4°C. The samples were then ethanol- or methanol-dehydrated and embedded in paraffin. For cryosections, tissues were fixed for 2 h in PFA and incubated overnight in a 30% glucose solution. They were then embedded in optimal cutting temperature compound (OCT) and frozen at −80°C. For histological analysis, sections of 5 µm were prepared from paraffin-embedded tissues and stained with hematoxylin eosin–safranin according to standard histological procedures.

Oral glucose tolerance test

Mice were fasted overnight and then received a glucose load of 4 mg/kg. The blood glucose level was assessed at different time points using an ACCU-CHEK Compact Plus meter system (Roche, Basel, Switzerland). At least three animals per genotype were included in the study.

Immunohistochemistry

Sections of 5 µm were prepared from paraffin- or OCT-embedded tissues depending on the antibody used. For paraffin sections, paraffin was removed by two 5-min washes in xylene. Sections were then hydrated with ethanol solutions of decreasing concentrations. Unmasking of the epitopes was performed by boiling for 20 min in Antigen Unmasking Solution (Vector Laboratories, Burlingame, CA). Sections were incubated for 45 min at room temperature in blocking buffer (3% fetal calf serum [FCS] in PBS) and then overnight at 4°C with primary antibody (see Supplemental Material) diluted in 3% FCS. After several washes, secondary fluorescent antibody was added for 90 min. Representative images from immunostaining were acquired using an Apotome system with a 63× water Plan-Apochromat lens (Zeiss, Jena, Germany). All images were further processed and pseudocolored using ImageJ (National Institutes of Health). All images comparing different genotypes were acquired and postprocessed with identical parameters. Colocalization analyses were performed using the Colocalization Highlighter plug-in for ImageJ.

TEM

Small pieces of tissue (~1–2 mm) were fixed for 2 h at room temperature in 2.5% glutaraldehyde and 2% PFA in cacodylate buffer (80 mM cacodylate buffer, pH 7.2, 0.05% $CaCl_2$). After being washed with cacodylate buffer, tissues were postfixed for 30 min at 4°C with 1% OsO_4 and 1.5% potassium ferrocyanide in 80. mM cacodylate buffer (pH 7.2), and then treated at room temperature for 1 h with 2% uranyl acetate in 40% ethanol. The samples were dehydrated in a series of graded ethanol solutions and then embedded in Epon before ultrathin sectioning. The observations were made with a Philips CM120 electron microscope (FEI, Eindhoven, The Netherlands). Images were acquired with a KeenView camera,

and measurements were made with the iTEM software (Olympus Soft Imaging Solutions GMBH, Münster, Germany).

Brush border isolation

Intestines from two adult mice were collected, cut into three pieces, and soaked in ice cold saline (150 mM NaCl, 2 mM imidazole, pH 7.2). Segments were washed with saline and opened longitudinally. They were then cut into pieces (~2 cm) and stirred in a beaker containing 20 ml of ice cold sucrose dissociation solution buffer A (200 mM sucrose, 12 mM EDTA, 19 mM KH_2PO_4, 78 mM Na_2HPO_4) for 30 min in a cold room. The buffer A containing the enterocytes was centrifuged at 300 × *g* for 8 min. During this spin, another 20 ml of buffer A was poured into the beaker and stirred. This second 20-ml cell collection was added to the cell pellets obtained from the first collection. The isolated enterocytes were washed three times in buffer A by centrifugation at 300 × *g* for 8 min. The cell pellet was then resuspended with 20 ml of homogenization buffer (10 mM imidazole, pH 7.2, 4 mM EDTA, 1 mM ethylene glycol tetraacetic acid [EGTA], 1 mM dithiothreitol [DTT], protease inhibitor cocktail [Sigma-Aldrich, St. Louis, MO], pH 7.2), poured into a blender, and homogenized with two 15-s bursts at high speed. The blender was rinsed once with 20 ml of buffer B (75 mM KCl, 5 mM $MgCl_2$, 1 mM EGTA, 10 mM imidazole, pH 7.4, 1 mM DTT, and protease inhibitor cocktail). The homogenate was then centrifuged (1000 × *g* for 8 min) to pellet the brush borders. The pellet containing isolated brush borders was washed four times by centrifugation in buffer B (1000 × *g* for 8 min).

For TEM, isolated brush borders were incubated in buffer B containing 15 mM $MgCl_2$. To let them adhere, they were incubated for 1 h at 4°C on glass coverslips coated with polylysine. Coverslips were washed once before fixation in 0.1 M Na-phosphate buffer (pH 7.0) containing 2% glutaraldehyde and 2 mg/ml tannic acid for 1 h at 4°C. After being washed in PBS, brush borders were postfixed in 1% OsO_4, in 0.1 M phosphate buffer at pH 6.0 for 45 min and then with 0.5% uranyl acetate for 2 h. The brush borders were dehydrated in a series of graded ethanol solutions and then embedded in Epon before ultrathin sectioning.

For one-dimensional analysis, brush border pellets were frozen in liquid nitrogen and kept at −80°C before being processed as described in the following section. For Western blotting, the pellets were processed the same way as for tissue samples.

Tissue lysis and Western blotting

Frozen jejunal tissues were homogenized with a Dounce homogenizer in a solution containing 50 mM Tris- HCl (pH 7.5), 150 mM NaCl, 20 mM MgCl2, 5 mM EDTA, 1% Triton X-100, 1% NP-40, 0.5% SDS, and protease inhibitor cocktail (Sigma-Aldrich, St. Louis, MO). Proteins were extracted after centrifugation at 15,000 × *g* for 10 min at 4°C. Fifty micrograms of total protein was used for electrophoresis on 7.5% SDS-polyacrylamide gels under reducing conditions, and transferred to a nitrocellulose membrane using standard procedures. Immunogens were visualized using the enhanced chemiluminescence method (Thermo Scientific, Lafayette, CO). The primary antibodies used for immunoblots in these experiments were the same as those described for immunohistochemistry, and were used at 1:1000. In addition, polyclonal rabbit β-actin (Cell Signaling Technology, Danvers, MA), monoclonal mDia1 (BD Biosciences, Franklin Lakes, NJ), polyclonal rabbit myosin-1c (from P. Gillespie), polyclonal rabbit anti–myosin-1d (from M. Bähler), and monoclonal IRSp53 (from G. Scita) antibodies were used, also at 1:1000. Harmonin isoforms were detected using a rabbit serum at 1:200 (from C. Petit). Protein lysates were deglycosylated using the Protein Deglycosylation Mix (New England BioLabs, Ipswich, MA).

Densitometry measurements were carried out using the software ImageJ. The densitometric value of each band was corrected by subtracting the background value of the corresponding lane before applying the ratio calculations.

Global endocytosis assay

Intestinal segments from anesthetized mice were isolated using sewing cotton. A solution of the vital membrane stain FM4-64 FX (Invitrogen, Carlsbad, CA) diluted in PBS-$MgCl_2$-$CaCl_2$ at 100 µg/ml was injected into the isolated segments and incubated for different times at 37°C. The mice were then killed, and isolated segments were fixed and processed for cryosectioning. Endocytic activity was assessed by the internalization of labeled membranes observed by fluorescence microscopy.

ACKNOWLEDGMENTS

We are grateful to A. Quaroni (Cornell University), R. Jacob (Philipps-Universität Marburg, Marburg, Germany), E.M. Danielsen (Panum Institute, University of Copenhagen, Denmark), A.L. Hubbard (Johns Hopkins University, Baltimore, MD), G. Kellett (University of York, Heslington, UK), F. Jaisser (INSERM U872, Centre de recherche des Cordeliers, Paris, France), M. Mooseker (Yale University, New Haven, CT), P.G. Gillepsie (Oregon Health & Science University, Portland, OR), M. Bähler (Westfälische Wilhems-Universität Münster, Münster, Germany), J. Klingensmith (Duke University, Durham, NC), C. Petit (Institut Pasteur, Paris, France), and T. Galli (Institut Jacques Monod, Paris, France) for kindly supplying antibodies. We thank G. Raposo for the collaboration on TEM and M. Arpin, E. Coudrier, E. Ferrary, D. Vignjevic, and S. Duffy for advice and careful reading of the manuscript. We thank J. Mandel and the bioinformatics platform for the analysis of the growth curves; all members of the animal house facility and in particular Stéphanie Boissel; C. Backeland, W. Faigle, and V. Masson from the proteomics platform; and the PICT@BDD imaging facility, especially O. Renaud and O. Leroy. The Curie Institute Foundation funded this work. C.R. was supported by the CNRS and Association pour la Recherche sur le Cancer; F.U. was supported by the Ministère de la Recherche et de la Technologie and by Fondation pour la Recherche Médicale. The Laboratory of Proteomic Mass Spectrometry is supported by Cancéropôle Ile-de-France and Institut National du Cancer (INCA).

REFERENCES

Atilgan E, Wirtz D, Sun SX (2006). Mechanics and dynamics of actin-driven thin membrane protrusions. Biophys J 90, 65–76.

Bartles JR (2000). Parallel actin bundles and their multiple actin-bundling proteins. Curr Opin Cell Biol 12, 72–78.

Bathe M, Heussinger C, Claessens MM, Bausch AR, Frey E (2008). Cytoskeletal bundle mechanics. Biophys J 94, 2955–2964.

Benesh AE, Nambiar R, McConnell RE, Mao S, Tabb DL, Tyska MJ (2010). Differential localization and dynamics of class I myosins in the enterocyte microvillus. Mol Biol Cell 21, 970–978.

Boeda B *et al.* (2002). Myosin VIIa, harmonin and cadherin 23, three Usher I gene products that cooperate to shape the sensory hair cell bundle. EMBO J 21, 6689–6699.

Brawley CM, Rock RS (2009). Unconventional myosin traffic in cells reveals a selective actin cytoskeleton. Proc Natl Acad Sci USA 106, 9685–9690.

Brown JW, McKnight CJ (2010). Molecular model of the microvillar cytoskeleton and organization of the brush border. PLoS One 5, e9406.

Campellone KG, Welch MD (2010). A nucleator arms race: cellular control of actin assembly. Nat Rev Mol Cell Biol 11, 237–251.

Claessens MM, Bathe M, Frey E, Bausch AR (2006). Actin-binding proteins sensitively mediate F-actin bundle stiffness. Nat Mater 5, 748–753.

Coluccio LM, Bretscher A (1989). Reassociation of microvillar core proteins: making a microvillar core in vitro. J Cell Biol 108, 495–502.

Costa de Beauregard MA, Pringault E, Robine S, Louvard D (1995). Suppression of villin expression by antisense RNA impairs brush border assembly in polarized epithelial intestinal cells. EMBO J 14, 409–421.
Cramm-Behrens CI, Dienst M, Jacob R (2008). Apical cargo traverses endosomal compartments on the passage to the cell surface. Traffic 9, 2206–2220.
Croce A, Cassata G, Disanza A, Gagliani MC, Tacchetti C, Malabarba MG, Carlier MF, Scita G, Baumeister R, Di Fiore PP (2004). A novel actin barbed-end-capping activity in EPS-8 regulates apical morphogenesis in intestinal cells of *Caenorhabditis elegans*. Nat Cell Biol 6, 1173–1179.
DesMarais V, Ichetovkin I, Condeelis J, Hitchcock-DeGregori SE (2002). Spatial regulation of actin dynamics: a tropomyosin-free, actin-rich compartment at the leading edge. J Cell Sci 115, 4649–4660.
Disanza A *et al*. (2006). Regulation of cell shape by Cdc42 is mediated by the synergic actin-bundling activity of the Eps8-IRSp53 complex. Nat Cell Biol 8, 1337–1347.
Ferrary E *et al*. (1999). In vivo, villin is required for Ca^{2+}-dependent F-actin disruption in intestinal brush borders. J Cell Biol 146, 819–830.
Franck Z, Footer M, Bretscher A (1990). Microinjection of villin into cultured cells induces rapid and long-lasting changes in cell morphology but does not inhibit cytokinesis, cell motility, or membrane ruffling. J Cell Biol 111, 2475–2485.
Friederich E, Huet C, Arpin M, Louvard D (1989). Villin induces microvilli growth and actin redistribution in transfected fibroblasts. Cell 59, 461–475.
Grimm-Gunter EM, Revenu C, Ramos S, Hurbain I, Smyth N, Ferrary E, Louvard D, Robine S, Rivero F (2009). Plastin 1 binds to keratin and is required for terminal web assembly in the intestinal epithelium. Mol Biol Cell 20, 2549–2562.
Gruneberg H, Burnett JB, Snell GD (1941). The origin of jerker, a new gene mutation of the house mouse, and linkage studies made with it. Proc Natl Acad Sci USA 27, 562–565.
Hansen GH, Rasmussen K, Niels-Christiansen LL, Danielsen EM (2009). Endocytic trafficking from the small intestinal brush border probed with FM dye. Am J Physiol Gastrointest Liver Physiol 297, G708–G715.
Hertzog M *et al*. (2010). Molecular basis for the dual function of Eps8 on actin dynamics: bundling and capping. PLoS Biol 8, e1000387.
Hirokawa N, Cheney RE, Willard M (1983). Location of a protein of the fodrin-spectrin-TW260/240 family in the mouse intestinal brush border. Cell 32, 953–965.
Hirokawa N, Tilney LG, Fujiwara K, Heuser JE (1982). Organization of actin, myosin, and intermediate filaments in the brush border of intestinal epithelial cells. J Cell Biol 94, 425–443.
Janmey PA, Lamb J, Allen PG, Matsudaira PT (1992). Phosphoinositide-binding peptides derived from the sequences of gelsolin and villin. J Biol Chem 267, 11818–11823.
Liu AP, Richmond DL, Maibaum L, Pronk S, Geissler PL, Fletcher DA (2008). Membrane-induced bundling of actin filaments. Nat Phys 4, 789–793.
Loomis PA, Zheng L, Sekerkova G, Changyaleket B, Mugnaini E, Bartles JR (2003). Espin cross-links cause the elongation of microvillus-type parallel actin bundles in vivo. J Cell Biol 163, 1045–1055.
Matter K, Stieger B, Klumperman J, Ginsel L, Hauri HP (1990). Endocytosis, recycling, and lysosomal delivery of brush border hydrolases in cultured human intestinal epithelial cells (Caco-2). J Biol Chem 265, 3503–3512.
McConnell RE, Tyska MJ (2007). Myosin-1a powers the sliding of apical membrane along microvillar actin bundles. J Cell Biol 177, 671–681.
Mellor H (2010). The role of formins in filopodia formation. Biochim Biophys Acta 1803, 191–200.
Miyata H, Nishiyama S, Akashi K, Kinosita K., Jr. (1999). Protrusive growth from giant liposomes driven by actin polymerization. Proc Natl Acad Sci USA 96, 2048–2053.
Mogilner A, Rubinstein B (2005). The physics of filopodial protrusion. Biophys J 89, 782–795.
Nagy S, Ricca BL, Norstrom MF, Courson DS, Brawley CM, Smithback PA, Rock RS (2008). A myosin motor that selects bundled actin for motility. Proc Natl Acad Sci USA 105, 9616–9620.
Nagy S, Rock RS (2010). Structured post-IQ domain governs selectivity of myosin X for fascin-actin bundles. J Biol Chem 285, 26608–26617.
Naoz M, Manor U, Sakaguchi H, Kachar B, Gov NS (2008). Protein localization by actin treadmilling and molecular motors regulates stereocilia shape and treadmilling rate. Biophys J 95, 5706–5718.
Nelson WJ, Veshnock PJ (1987). Ankyrin binding to (Na^+ + K^+)ATPase and implications for the organization of membrane domains in polarized cells. Nature 328, 533–536.
Pellegrin S, Mellor H (2005). The Rho family GTPase Rif induces filopodia through mDia2. Curr Biol 15, 129–133.
Peskin CS, Odell GM, Oster GF (1993). Cellular motions and thermal fluctuations: the Brownian ratchet. Biophys J 65, 316–324.
Pinson KI, Dunbar L, Samuelson L, Gumucio DL (1998). Targeted disruption of the mouse villin gene does not impair the morphogenesis of microvilli. Dev Dyn 211, 109–121.
Prost J, Barbetta C, Joanny JF (2007). Dynamical control of the shape and size of stereocilia and microvilli. Biophys J 93, 1124–1133.
Revenu C, Athman R, Robine S, Louvard D (2004). The co-workers of actin filaments: from cell structures to signals. Nat Rev Mol Cell Biol 5, 635–646.
Ricca BL, Rock RS (2010). The stepping pattern of myosin X is adapted for processive motility on bundled actin. Biophys J 99, 1818–1826.
Rodriguez-Boulan E, Kreitzer G, Musch A (2005). Organization of vesicular trafficking in epithelia. Nat Rev Mol Cell Biol 6, 233–247.
Rzadzinska AK, Nevalainen EM, Prosser HM, Lappalainen P, Steel KP (2009). MyosinVIIa interacts with Twinfilin-2 at the tips of mechanosensory stereocilia in the inner ear. PLoS One 4, e7097.
Saotome I, Curto M, McClatchey AI (2004). Ezrin is essential for epithelial organization and villus morphogenesis in the developing intestine. Dev Cell 6, 855–864.
Sato T *et al*. (2007). The Rab8 GTPase regulates apical protein localization in intestinal cells. Nature 448, 366–369.
Tang N, Ostap EM (2001). Motor domain-dependent localization of myo1b (myr-1). Curr Biol 11, 1131–1135.
Temm-Grove CJ, Jockusch BM, Weinberger RP, Schevzov G, Helfman DM (1998). Distinct localizations of tropomyosin isoforms in LLC-PK1 epithelial cells suggests specialized function at cell–cell adhesions. Cell Motil Cytoskeleton 40, 393–407.
Tilney LG, Connelly PS, Ruggiero L, Vranich KA, Guild GM (2003). Actin filament turnover regulated by cross-linking accounts for the size, shape, location, and number of actin bundles in *Drosophila* bristles. Mol Biol Cell 14, 3953–3966.
Tilney LG, Connelly PS, Vranich KA, Shaw MK, Guild GM (1998). Why are two different cross-linkers necessary for actin bundle formation in vivo and what does each cross-link contribute? J Cell Biol 143, 121–133.
Tilney LG, Tilney MS (1988). The actin filament content of hair cells of the bird cochlea is nearly constant even though the length, width, and number of stereocilia vary depending on the hair cell location. J Cell Biol 107, 2563–2574.
Tilney LG, Tilney MS, Guild GM (1995). F actin bundles in *Drosophila* bristles. I. Two filament cross-links are involved in bundling. J Cell Biol 130, 629–638.
Tocchetti A *et al*. (2010). Loss of the actin remodeler Eps8 causes intestinal defects and improved metabolic status in mice. PLoS One 5, e9468.
Tokuo H, Ikebe M (2004). Myosin X transports Mena/VASP to the tip of filopodia. Biochem Biophys Res Commun 319, 214–220.
Tyska MJ, Mackey AT, Huang JD, Copeland NG, Jenkins NA, Mooseker MS (2005). Myosin-1a is critical for normal brush border structure and composition. Mol Biol Cell 16, 2443–2457.
Tyska MJ, Mooseker MS (2004). A role for myosin-1A in the localization of a brush border disaccharidase. J Cell Biol 165, 395–405.
Verpy E *et al*. (2000). A defect in harmonin, a PDZ domain-containing protein expressed in the inner ear sensory hair cells, underlies Usher syndrome type 1C. Nat Genet 26, 51–55.
Vignjevic D, Kojima S, Aratyn Y, Danciu O, Svitkina T, Borisy GG (2006). Role of fascin in filopodial protrusion. J Cell Biol 174, 863–875.
Weisz OA, Rodriguez-Boulan E (2009). Apical trafficking in epithelial cells: signals, clusters and motors. J Cell Sci 122, 4253–4266.
Yamashiro S, Yamakita Y, Ono S, Matsumura F (1998). Fascin, an actin-bundling protein, induces membrane protrusions and increases cell motility of epithelial cells. Mol Biol Cell 9, 993–1006.
Zheng L, Sekerkova G, Vranich K, Tilney LG, Mugnaini E, Bartles JR (2000). The deaf jerker mouse has a mutation in the gene encoding the espin actin-bundling proteins of hair cell stereocilia and lacks espins. Cell 102, 377–385.
Zigmond SH, Furukawa R, Fechheimer M (1992). Inhibition of actin filament depolymerization by the *Dictyostelium* 30,000-D actin-bundling protein. J Cell Biol 119, 559–567.

During my PhD, I also had the opportunity to collaborate with the team of Tom Kirchhausen from Harvard. In this article, Boulant et al. investigate the role of actin dynamics during clathrin mediated endocytosis in epithelial cells. They started from the already known observation that actin assembly is required during clathrin coated pits assembly on the apex of epithelial cells whereas it is dispensable at the basolateral pole and in non-polarized cells. Since membrane tension is higher at the apex of epithelial cells, they reasoned that actin dynamics is required to overcome the membrane resistance in highly tensed cells to allow the vesicle budding. Accordingly, using various biophysical approaches and live imaging they demonstrate the importance of actin to achieve clathrin mediated endocytosis in a tensed environment. They additionally hypothesized that microvilli which crowd the apices of epithelial cells are responsible for this selective actin requirement, possibly by increasing the tensile properties of the apical membrane. To clarify these points, Steeve Boulant, first author of this study, contacted us seeking for advices and tools. We provided several reagents, molecular tools and cell lines that were used in this study. We moreover actively participate in the design of the experiments focused on microvilli.

C. Publication II

Actin dynamics counteract membrane tension during clathrin-mediated endocytosis.

Boulant S, Kural C, Zeeh JC, Ubelmann F, Kirchhausen T.

Nat Cell Biol. 2011 Aug 14;13(9):1124-31.

nature cell biology

Actin dynamics counteract membrane tension during clathrin-mediated endocytosis

Steeve Boulant[1,2,4], Comert Kural[1,2,4], Jean-Christophe Zeeh[1,2], Florent Ubelmann[3] and Tomas Kirchhausen[1,2,5]

Clathrin-mediated endocytosis is independent of actin dynamics in many circumstances but requires actin polymerization in others. We show that membrane tension determines the actin dependence of clathrin-coat assembly. As found previously, clathrin assembly supports formation of mature coated pits in the absence of actin polymerization on both dorsal and ventral surfaces of non-polarized mammalian cells, and also on basolateral surfaces of polarized cells. Actin engagement is necessary, however, to complete membrane deformation into a coated pit on apical surfaces of polarized cells and, more generally, on the surface of any cell in which the plasma membrane is under tension from osmotic swelling or mechanical stretching. We use these observations to alter actin dependence experimentally and show that resistance of the membrane to propagation of the clathrin lattice determines the distinction between 'actin dependent and 'actin independent'. We also find that light-chain-bound Hip1R mediates actin engagement. These data thus provide a unifying explanation for the role of actin dynamics in coated-pit budding.

The coordinated action of a large number of structural and regulatory proteins and lipids is required for the assembly–disassembly of a clathrin-coated vesicle. Budding coated pits and other clathrin-coated structures can be followed in living cells by labelling component proteins with fluorescent markers[1–7]. Recent live-cell imaging studies reveal unexpected modes of endocytic coat assembly, with distinct kinetics, recruitment of associated proteins, requirements for the participation of actin and its accessory proteins, and mechanisms of membrane deformation[7–13].

Electron microscopy of B-lymphoblastoid cells showed association of actin microfilaments with clathrin-coated structures[14], indicating that actin may participate in coated-vesicle assembly by pulling the membrane inward. In cultured mammalian cells, actin polymerization is usually dispensable for coated-pit formation[7,15], but in some circumstances actin and a subset of regulators of short-branch actin assembly, including Arp2/3 (actin-related protein-2/3), cortactin and N-Wasp (also known as Wasl, Wiskott-Aldrich syndrome-like; refs 16–19), are recruited to clathrin-containing structures at or near the time of membrane scission. One such actin-dependent structure, termed a coated plaque, assembles at adherent surfaces of cultured mammalian cells[11,20]. Actin dynamics are essential for membrane invagination and scission associated with coated-plaque uptake. Actin dynamics also rescue the clathrin-mediated uptake of elongated (180 nm) vesicular stomatitis virus particles[6] (VSV), which block closure of the curved pit, causing endocytosis to stall. Coordinated actin polymerization and inward movement of the partially clathrin-coated virus narrows the neck between the pit and the plasma membrane, leading to dynamin-induced scission. Thus, actin assembly is a pathway required under stringent conditions, rather than an essential process under more permissive ones[10]. In contrast, clathrin-mediated internalization is constitutively actin dependent in yeast cells[9] where actin dynamics are needed to counteract the inhibition of endocytosis induced by elevated membrane tension[21].

Inhibition of actin dynamics blocks endocytosis from the apical but not the basolateral surface of polarized cells[22–29]. We sought an explanation for this difference by combining live-cell, spinning-disc confocal imaging with electron microscopy. We show in polarized MDCK cells, that pharmacologically inhibiting actin dynamics or disrupting the link between actin and clathrin (by blocking the interaction between clathrin and Hip1R, Huntingtin interacting protein 1 related; refs 11,30) selectively traps apical clathrin-coated pits at a late stage of assembly. More generally, if we raise membrane tension and inhibit actin dynamics, coated pits stall at a late stage of assembly in BSC1 or MDCK cells. Local actin dynamics seem to prevent stalling by imparting additional constriction force.

We compared the dynamics of endocytic clathrin adaptor protein 2 (AP-2)-coated structures at the apical and basolateral surfaces of polarized MDCK cells[1] (Fig. 1a). Most fluorescent AP-2 spots on the

[1]Department of Cell Biology, Harvard Medical School, Boston, Massachusetts 02115, USA. [2]Immune Disease Institute and Program in Cellular and Molecular Medicine at Children's Hospital, Boston, Massachusetts 02115, USA. [3]Laboratoire de Morphogénèse et Signalisation Cellulaires, Institut Curie Paris, Paris, Cedex 05, France. [4]These authors contributed equally to this work.
[5]Correspondence should be addressed to T.K. (e-mail: kirchhausen@crystal.harvard.edu)

Received 21 January 2011; accepted 27 June 2011; published online 14 August 2011; DOI: 10.1038/ncb2307

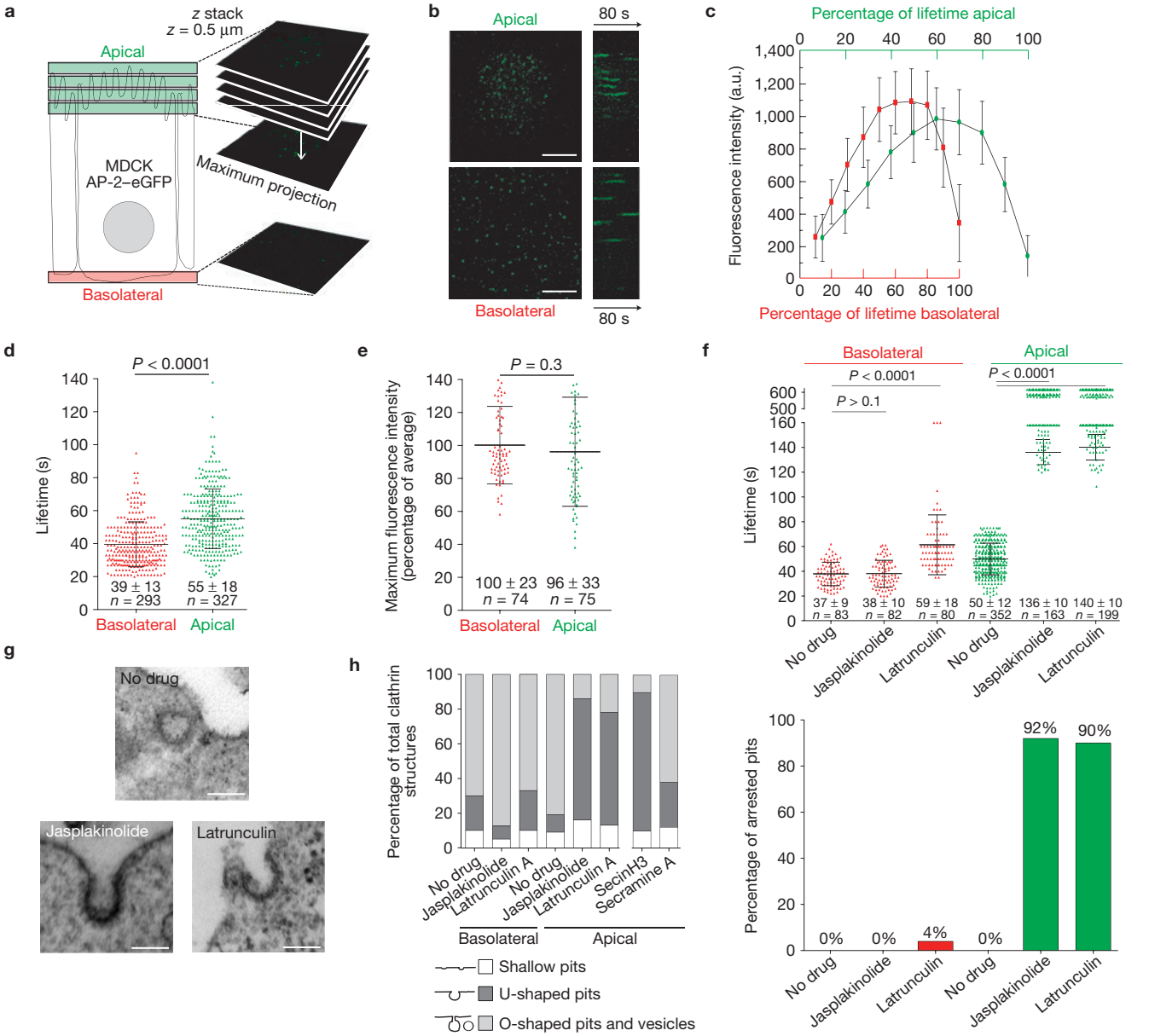

Figure 1 Formation of endocytic coated pits and vesicles at the apical and basolateral surfaces of polarized MDCK cells. (**a**) Imaging procedures used to visualize the dynamics of pit formation at the apical and basolateral surfaces of polarized MDCK cells. Movies from the dome-like apical surface are from 3D time series acquired at 2 s intervals from 3–5 serial optical sections spaced by 0.5 µm and using 100 ms exposures; 2D time series were created from maximum-intensity *z*-projection sets. Movies from the basolateral surface are 2D time series acquired at 2 s intervals from a single optical section. (**b**) Snapshot from a maximum-intensity projection (left) and representative kymograph (right) of coated-pit formation at the apical and basolateral surfaces from the same polarized MDCK cell; AP-2 labelled with σ2–eGFP; scale bars, 5 µm. (**c**) Average fluorescence intensity of AP-2 structures forming at the apical and basolateral surfaces of polarized MDCK cells ($n = 3$), normalized to the lifetime of each individual pit analysed (percentage of lifetime). Each point represents average ± s.d. (**d**) Scatter plot of individual lifetimes of coated structures from seven polarized MDCK cells. Each data set represents average ±s.d. *n* is the number of objects analysed. Statistical significances for lifetime differences are shown. (**e**) Scatter plot of individual maximum fluorescence intensities for coated structures. (**f**) Scatter plots of lifetimes for individual AP-2 spots at the apical and basolateral surfaces of polarized MDCK cells stably expressing σ2–eGFP in the absence or presence of jasplakinolide or latrunculin A. The upper and lower data sets are from distinct time series of 10 and 2.5 min in duration, respectively. Bottom, fraction of AP-2 objects with longer duration than the time series (percentage of arrested pits). (**g**) Morphological analysis of clathrin-coated structures on the apical surface of polarized MDCK cells treated with jasplakinolide, latrunculin A, SecinH3 or secramine A. Representative electron microscopy images of the most abundant clathrin-coated-pit profiles. Scale bars, 100 nm. The coated structures were classified as shallow, U-shaped or nearly-mature Ω- and fully-mature O-shaped vesicles. (**h**) Relative frequency of profiles in about 45 cells per condition.

basolateral surface belonged to a single class of diffraction-limited objects, with the properties characteristic of canonical coated pits and vesicles, ~100–200 nm in diameter[1,5,7,11] (Fig. 1b,c and Supplementary Movie S1). Their mean lifetime was 39 ± 13 s (Fig. 1d). The mean lifetime of clathrin-coated pits on the apical surface of the same polarized MDCK cells was significantly longer (55 ± 18 s; $P < 0.001$;

Fig. 1d and Supplementary Movie S1), although both had a similar maximum fluorescence intensity (Fig. 1c,e) and hence reached a similar final size[1,11]. Disturbance of actin assembly in polarized MDCK cells with latrunculin or jaskplakinolide resulted in a marked increase in the lifetime of apical pits. About 90% of the pits arrested and remained for at least 10 min (the upper limit of the time series), and the remaining ~10% had lifetimes significantly longer than at the apical surface in non-treated cells (Fig. 1f and Supplementary Movie S2) and transferrin endocytosis ceased[22,23,25] (Supplementary Figs S1a,b). In contrast, basolateral pits from the same cells were unaffected by jaskplakinolide and showed a small increase in lifetime (from 37 s to 59 s) and in the fraction of arrested pits (from 0% to 4%) in response to latrunculin (Fig. 1f and Supplementary Movie S2). The dependence on actin dynamics required cell polarization. Incubation with jaskplakinolide did not affect the formation and lifetime of dorsal pits in non-polarized MDCK cells (Supplementary Fig. S2).

We ruled out the possibility that cessation of coat growth at the apical surface resulted from depletion of free cytosolic coat components by transiently exposing the cells to 1-butanol, which induces coat disassembly[7]. Incubation of jasplakinolide-treated polarized MDCK cells for 3 min with 1-butanol led to rapid disappearance (~10 s) of all AP-2 spots (Supplementary Fig. S3a, 1-butanol). Removal of the 1-butanol with jasplakinolide still present led to synchronous appearance of newly formed apical coated pits that again stalled at late assembly (Supplementary Fig. S3a,b). The fluorescence intensity of the long-lived apical pits in jaskplakinolide-treated cells was on average 10% less than the maximum intensity in untreated cells (Supplementary Fig. S3b). As fluorescence intensity is proportional to coat size[11], this indicates that the long-lived pits may arrest at a late stage of coat assembly, but before full completion. Electron microscopy of MDCK cells treated with jasplakinolide or latrunculin showed a substantial increase (from 10 to ~70%) in the fraction of coated pits at the apical surface linked to the plasma membrane by wide necks (U-shaped), representing incomplete coats arrested at a relatively late stage of assembly (Fig. 1g,h). Narrower necks were less common, and we saw no long tubules decorated at their end by clathrin coats. Untreated control cells showed the expected distribution of coated profiles (Fig. 1g,h). Jaskplakinolide or latrunculin did not affect the distribution of basolateral coated profiles (Fig. 1h). Dynamin associates with the neck of a fully formed coated pit and promotes release of a coated vesicle[1,4,31]. Dynamin does not associate with the wide neck of incomplete pits, and indeed very few (~5%) of the long-lived apical pits generated by jasplakinolide treatment recruited a detectable amount of dynamin-2 (Supplementary Fig. S4a,b). The apical pits of untreated cells recruited dynamin normally (~30% of pits co-localize with the relatively strong dynamin signal; Supplementary Fig. S4b). We conclude that clathrin-coated pits assembling on the apical surface of polarized MDCK cells require actin dynamics for closure but not for initiation, whereas coat assembly on the basolateral surface is actin independent.

We next examined the differential effects at the two surfaces of inhibiting the small GTPases Cdc42, Rac1 and Arf6 (regulators of Arp2/3-mediated actin polymerization[26,32]) and of blocking clathrin binding of Hip1R. Cdc42 inhibition did not arrest pit formation, had only a small effect on the formation and lifetime of apical or basolateral pits (Fig. 2a) and had no evident influence on the distribution of apical coat morphologies (Fig. 1h). Rac1 inhibition seemed to arrest apical-pit assembly, as a large fraction of the pits (60%) were present throughout the complete movie; it also retarded basolateral pit assembly by about twofold, with a modest effect on completion and budding (15% arrest). Arf6 has been linked to clathrin-based endocytosis in HeLa cells[33] and at the apical surface of polarized MDCK cells[24]. Arf6 inhibition similarly arrested most of the apical pits (76%), but had no detectable effect on basolateral coat dynamics. In all cases, the fluorescence intensity of the arrested coated pits was equivalent to the maximum intensity of pits imaged in untreated cells, indicating that the coats arrested at a late stage of assembly. Consistent with this conclusion, we found by electron microscopy an accumulation of U-shaped coats at the apical surfaces of polarized MDCK cells following SecinH3 treatment (Fig. 1h). These inhibitors had no effect on pit assembly in non-polarized MDCK cells.

Hip1R interacts with F-actin, cortactin and clathrin light chains[34–36] and connects the actin cytoskeleton with clathrin coats[34]. It is essential for assembly of coated plaques[11] and for endocytosis of VSV (ref. 6), but not for completion of coated pits in non-polarized cells[11]. We detected a role for Hip1R in apical-pit assembly by blocking the association of Hip1R with clathrin—either by overexpression of a dominant-negative form of clathrin light chain B (CLCb-EED/QQN), which binds the clathrin heavy chain but does not recruit Hip1R (refs 10, 11,30), or by depletion with short interfering RNA (siRNA) of both forms of the clathrin light chain. CLCb-EED/QQN overexpression in non-polarized cells does not inhibit clathrin-mediated endocytosis[11,30]; it prevents formation of clathrin-coated plaques, but not of coated pits[11]. Overexpression in polarized MDCK cells inhibited completion of apical pits (60% arrest, as defined by pits with lifetimes longer than the upper limit of the time series we recorded) but affected basolateral pits in the same cells only modestly, increasing their lifetimes from 47 s to 86 s and generally permitting complete assembly (15% arrest; Fig. 2b). Overexpression of wild-type LCb had no detectable effect on pit dynamics[11] (Fig. 2b), confirming that failure of the mutated light chain to recruit Hip1R had produced the observed late-stage arrest. siRNA-mediated knockdown of light chains led to late-stage arrest of pits at the apical but not at the basolateral surface (Fig. 2b). Results from Hip1R depletion were not interpretable because of the massive upregulation of the number of actin filaments throughout the cells[17,35,37] (Supplementary Fig. S3c), the increase in the level of cytosolic AP-2 and the general arrest of coated-pit formation at the apical and basolateral surfaces of polarized MDCK cells (Supplementary Fig. S3d), explaining the previously observed partial inhibition of transferrin uptake[35]. Thus, under actin-independent conditions, inhibiting Hip1R recruitment has no influence on clathrin-mediated endocytosis[30] or on coat assembly[11]. When actin dynamics are required to finish coat assembly, however, blocking Hip1R recruitment has the same effect (late-stage arrest) as blocking actin dynamics. As for Hip1R, the light chains are dispensable for initiation and early growth of coats under all conditions examined.

Apical surfaces of polarized epithelial cells have large numbers of microvilli. Treatment of polarized MDCK cells with a short hairpin RNA (shRNA) probe specific for ezrin, on which microvilli depend, resulted in substantial loss of the protein and disappearance of microvilli (Supplementary Fig. S5a). Following ezrin depletion, actin was no longer required for apical-pit completion (Supplementary Fig. S5b). Moreover, overexpression of villin-1–Cherry in non-polarized BSC1 cells generated a large number of microvilli-like

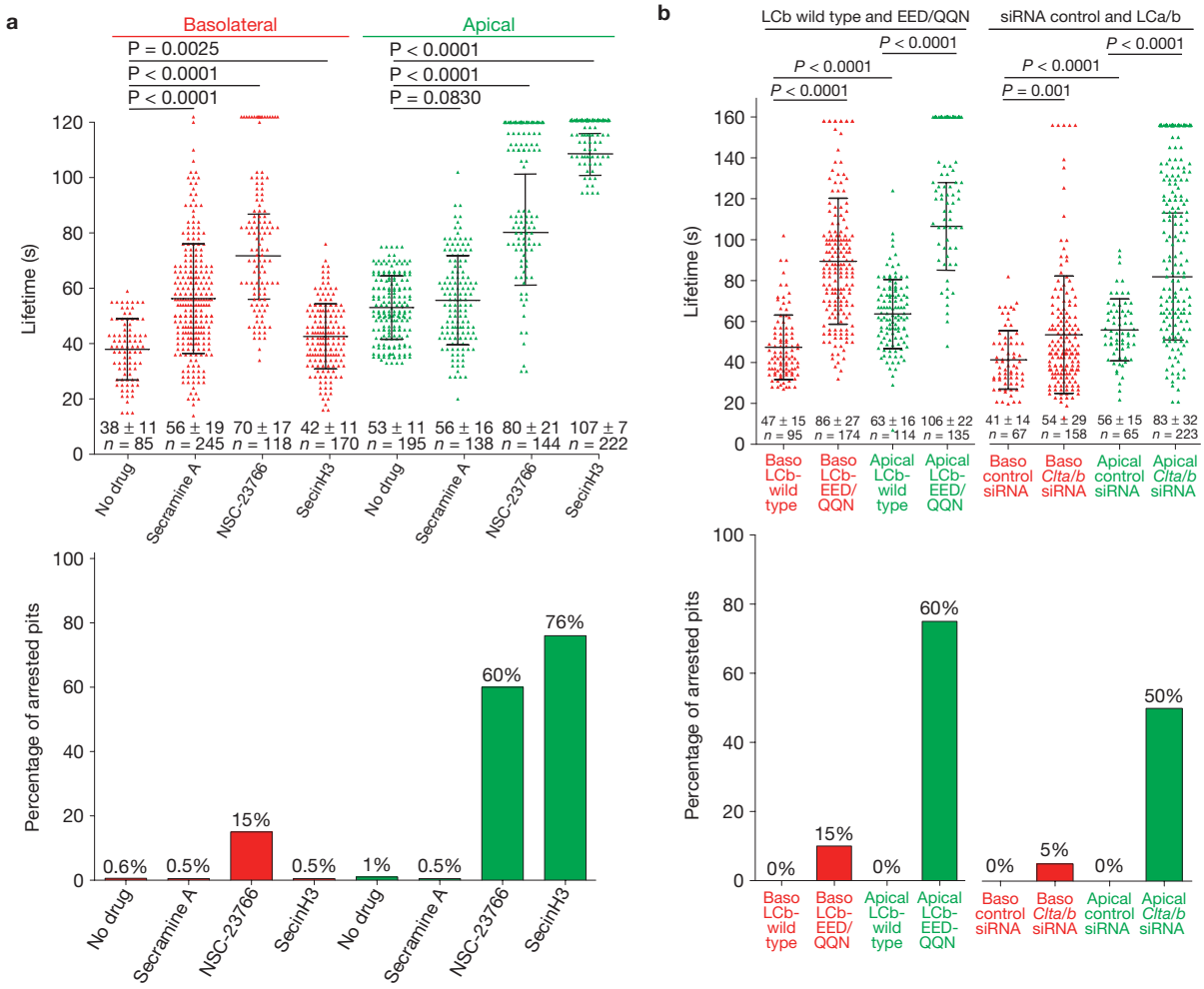

Figure 2 Disruption of apical coat formation by pharmacological interference with the small GTPases Rac1 and Arf6 and interference with the function of clathrin light chains. (**a**) Top, scatter plots of lifetimes for individual AP-2 spots. Polarized MDCK cells stably expressing σ2–eGFP were treated for 10 min before imaging with secramine A, NSC-23766 or SecinH3, small molecule inhibitors of Cdc42, Rac1 and Arf6, respectively. Each data set represents average ±s.d. for objects whose duration was fully included in the time series. *n* is the number of objects analysed. Statistical significances for the differences in lifetimes are shown. Bottom, fraction of AP-2 objects with longer duration than the time series. (**b**) Top, scatter plots of lifetimes for individual AP-2 spots imaged at the apical and basolateral (Baso) surfaces of polarized MDCK cells stably expressing σ2–eGFP and transiently expressing wild-type or mutant clathrin light chain B fused to Cherry (left) or depleted of both clathrin light chains by *Clta* and *Cltb* siRNA (right). Each data set represents average ±s.d. *n* is the number of objects analysed. Bottom, fraction of AP-2 objects with longer duration than the 160 s time series.

structures (Supplementary Fig. S5c) and caused actin-dependent coated-pit maturation (Supplementary Fig. S5d). Thus, the actin dependence of coat completion correlates with a property imparted to the plasma membrane in response to the formation of microvilli or microvillus-related structures.

Membrane tension in polarized cells is greater in apical than in basolateral regions[38]. We investigated whether clathrin-coat assembly might be sufficient to deform the underlying membrane completely under conditions of low membrane tension, whereas an additional activity associated with actin dynamics might be needed under conditions of high membrane tension. Increasing membrane tension by exposing cells to hypotonic medium (Fig. 3) revealed strong correlation between the severity of the hypotonic treatment and the appearance of arrested pits in non-polarized cells treated with jaskplakinolide (Fig. 3 and Supplementary Movie S3) and at the basolateral surface of polarized MDCK cells treated first with jasplakinolide (not shown). The actin requirement induced by hypotonic treatment was reversible (data not shown). Electron microscopy of jaskplakinolide-treated BSC1 cells incubated with hypotonic medium confirmed that most apical coated pits had U-shaped structures. The pits from these cells also failed to accumulate dynamin (not shown). We also increased membrane tension by laterally stretching cells growing on an elastic support. Pits at the basolateral surface of control, unstretched MDCK cells had an average lifetime of 43 s that was insensitive to jasplakinolide (Fig. 4b), comparable to pits in MDCK cells grown on glass coverslips (Fig. 1d). Linear stretching by 25% led to a small but statistically significant increase in pit lifetime (from 43 s to 52 s) and pit arrest (from 4% to 8%). Jaskplakinolide treatment of the stretched cells resulted in a marked increase in pit lifetimes and percentage of arrested pits (from 8% to 60%; Fig. 4b). Thus, local actin dynamics must coordinate with clathrin assembly to achieve complete vesiculation following increased membrane tension.

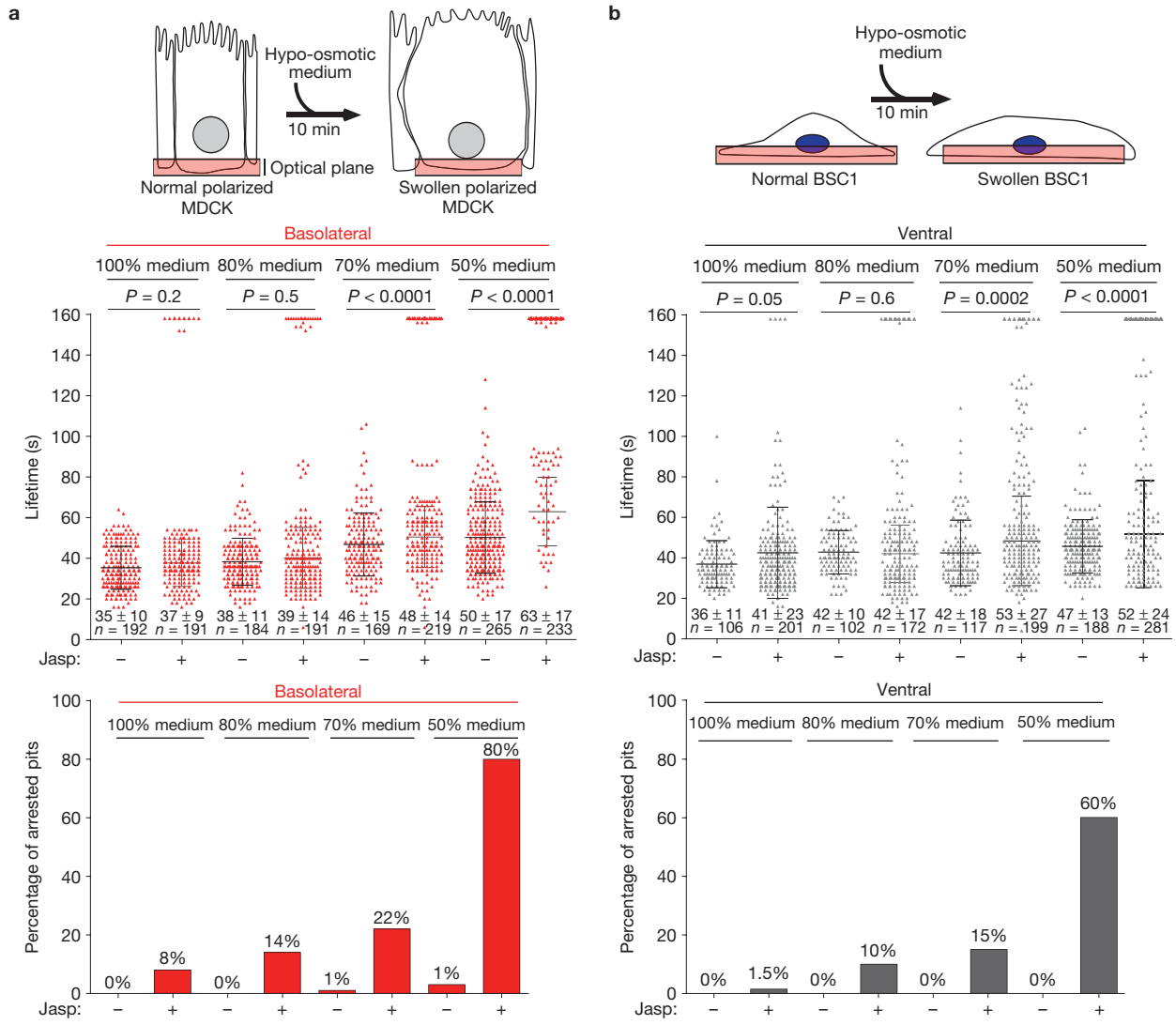

Figure 3 Actin dependence for endocytic coat formation in cells swelled by hypo-osmotic treatment. Polarized MDCK or non-polarized BSC1 cells incubated for 10 min in serially diluted medium (from 100% to 50%) of decreasing osmolarity, ranging from 311 to 174 mOsM, were analysed for the effects of altering actin dynamics on the lifetimes of their AP-2-coated structures. Each data set represents average ± s.d.; *n* is the number of objects analysed. (**a**) Top, schematic representation of polarized MDCK cells stably expressing σ2–eGFP exposed to hypo-osmotic medium. Middle, scatter plots of lifetimes for individual basolateral AP-2 spots of cells exposed for 10 min to hypo-osmotic media in the absence and presence of jasplakinolide (Jasp). Bottom, fraction of AP-2 objects with longer duration than the time series. (**b**) Top, schematic representation of BSC1 cells stably expressing σ2–eGFP exposed to hypo-osmotic medium. Middle, scatter plots of lifetimes for individual ventral AP-2 spots of cells exposed for 10 min to hypo-osmotic media in the absence and presence of jasplakinolide. Bottom, fraction of AP-2 objects with longer duration than the time series.

Thus, we show that interfering with actin dynamics induces arrest of canonical coated-pit assembly under some circumstances, but not under others. Indeed, actin activity is essential for efficient completion of coated pits at the apical surfaces of polarized cells in culture, but not at the basolateral surfaces of the same cells. Coat assembly in various non-polarized cells does not ordinarily depend on actin[7,11,15]. Furthermore, the actin dependence of coated-pit assembly can be modulated experimentally by modifying membrane tension: coat formation in a non-polarized cell can be rendered actin dependent by exposure to hypotonic medium, by stretching the substrate or by inducing the formation of microvillus-like structures; coat formation at the apical surface of a polarized cell can be rendered actin independent by shrinking its apical microvilli. In addition, interfering with actin dynamics under conditions that require actin activity causes coats to stall late in assembly. Most AP-2 complexes are recruited during earlier stages[11,20,39]. Therefore, we estimate (from the fluorescence intensity of tagged AP-2 and from the appearance of the U-shaped pits that accumulate) that the stalled coats are roughly two-thirds to three-quarters complete. At this stage of completion, the 'neck' is probably not yet narrow enough to allow dynamin recruitment, as the dynamin burst normally associated with maturation of a coated pit into a coated vesicle was not detected. Finally, we show that perturbing actin dynamics does not directly affect coat initiation[7]. Thus, canonical coated pits differ in this respect from coated plaques, which require actin dynamics for both initiation and invagination[11].

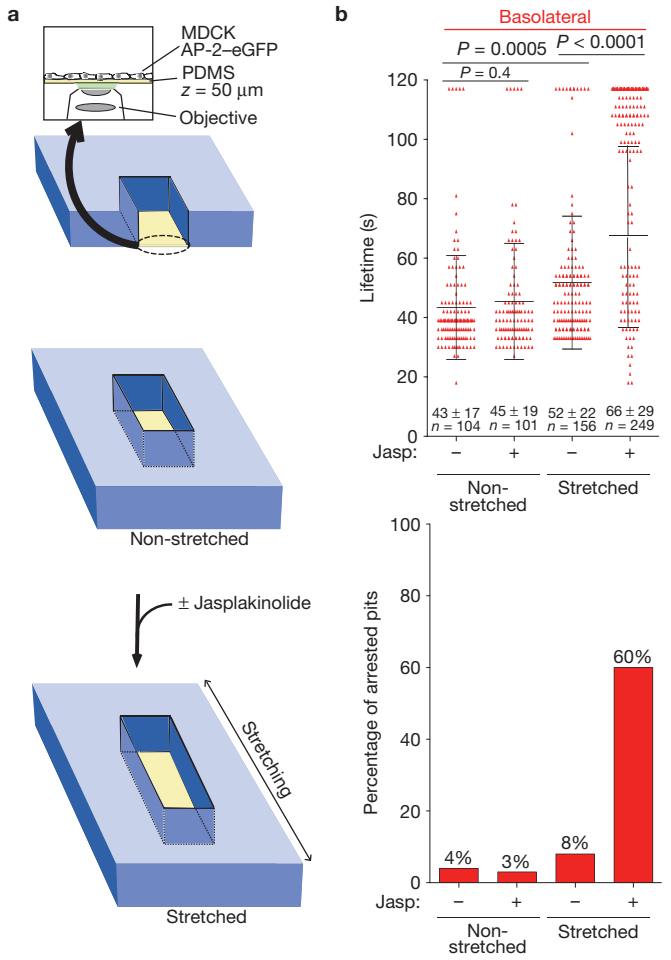

Figure 4 Actin dependence of endocytic coat formation in mechanically stretched cells. (**a**) Schematic representation of the device used to image mechanically stretched, non-polarized MDCK cells. An optically clear, stretchable silicon holder made of PDMS, about 50 μm thick, which could make contact with the oil above a ×63 objective lens was placed at the bottom of the stretching device. Cells were grown for 24 h on the PDMS surface pre-coated with fibronectin and then imaged by spinning-disc confocal microscopy; the spherical-aberration-correction device was essential for detecting the diffraction-limited coated structures containing AP-2–eGFP. (**b**) Dynamics of coated pits before and after ~25% linear stretching. Top, scatter plots for lifetimes of individual AP-2 spots from the ventral surface of cells subjected to controlled stretching in the presence or absence of jasplakinolide. Each data set represents average ± s.d. *n* is the number of objects analysed. Bottom, fraction of AP-2 objects with longer duration than the time series.

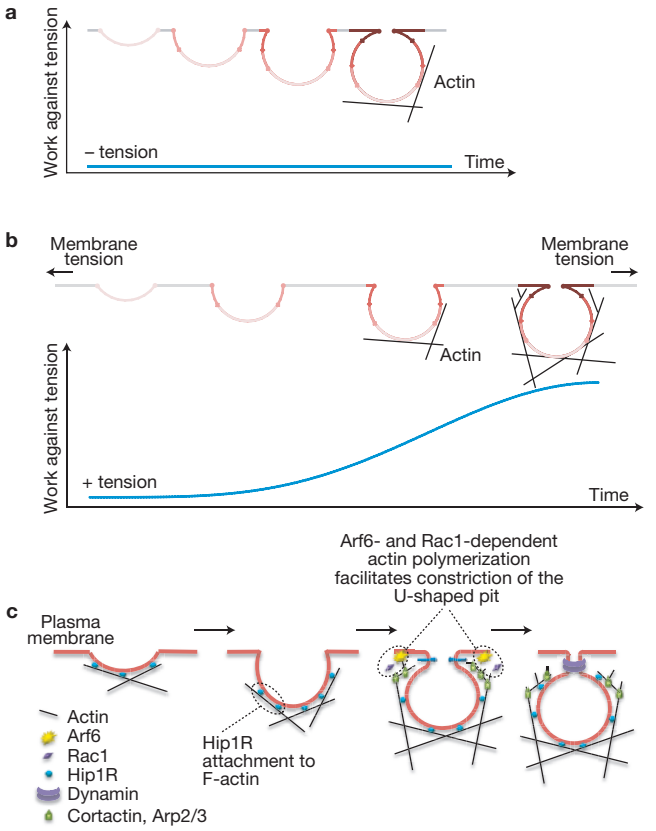

Figure 5 Model depicting the role of actin polymerization during the formation of endocytic clathrin-coated pits. (**a**) Under non-stringent conditions and low membrane tension, assembly of the clathrin coat is sufficient to deform the membrane into a tightly constricted coated pit. (**b**) Under more stringent conditions of high membrane tension, clathrin assembly is not sufficient and membrane invagination stalls; actin polymerization then provides the additional work needed to complete membrane bending. Hip1R links the assembling clathrin coat to actin polymers, and if sufficient time is allowed, then assembly of short-branched actin rescues the stalled coat. The two main forces resisting membrane deformation are bending and tension. The bending work per unit area depends inversely on the curvature and hence is uniform for a spherical or nearly spherical vesicle. The work done against a constant membrane tension depends on the net increase in membrane area—that is, the area of the invaginated membrane minus the area of the opening it covers. The plot represents the cumulative work required to counteract membrane tension, and does not include the work required to create the membrane vesicle. The cumulative work was calculated according to $W = \pi r^2 T(1-\cos\alpha)^2$, where T is the membrane tension and α is the angle (in radians) between the pole of the budding pit and the position at which the curved pit intersects the plane of the plasma membrane (see Methods). When the neck begins to constrict ($\alpha = \pi/2$), the area of the opening decreases and the net increase in area rises sharply. When the pit is complete, $\alpha = \pi$. (**c**) Hip1R links actin filaments with the clathrin coat by interactions with F-actin and clathrin light chains. Branched actin filaments grow towards the plasma membrane through new filament assembly at the barb end of the stabilized actin filaments; this growth relies on Arp2/3 stimulation, mediated by cortactin and by small GTPases such as Arf6 and Rac1.

We investigated what determines actin engagement if coat assembly stalls. In principle, there may be a 'sensor' of assembly arrest. Alternatively, actin may be engaged constitutively, but with at most a small contribution to observable coat dynamics except in circumstances of elevated membrane tension. The distinction between 'actin dependent' and 'actin independent' would then be determined by the threshold of membrane tension (or other resistance to propagation of the coat lattice) at which the free energy of clathrin–clathrin contacts can no longer overcome membrane resistance to generating a constricted neck. Our experiments, in which we switch from actin dependence to actin independence and vice versa, are consistent with this threshold picture. Indeed, increased tension is a common feature in which actin dynamics are required for coated-pit maturation beyond the 'U' stage. One explanation for why coated-pit assembly may stall at this point is embodied in Fig. 5. Under conditions of constant membrane tension, the work needed to invaginate the first hemisphere of a coated vesicle is substantially less than that needed to complete the second hemisphere (see Methods). Extreme levels of tension will

probably block invagination altogether; an intermediate level may stall the process when the work needed to counteract the tension is greater than incremental coat assembly can contribute.

Clathrin-mediated uptake in yeast cells depends constitutively on actin dynamics. Initial steps in coat formation precede local actin assembly, which is essential for invagination and inward movement[9]. Increased turgor diminishes internalization[21], in agreement with our observations on membrane tension in mammalian cells. Exposure to hyperosmotic medium, which reduces turgor to below-normal levels, rescues internalization of a fluid phase marker, even when actin dynamics are blocked[21], but it is not clear whether the rescue involves a clathrin-coated structure.

We have shown that actin polymerization takes over from clathrin polymerization in driving membrane invagination, when the latter process stalls. Actin is engaged at the coat by clathrin-light-chain-bound Hip1R. We have not determined whether actin simply pushes the plasma membrane away from the coat, or whether branching at Arp2/3 helps constrict the neck. Actin polymerization similarly takes over when clathrin polymerization and assembly stalls because of steric interference from cargo (for example, VSV; refs 6,10), and actin alone drives the remaining membrane invagination and constriction. Coated plaques are also examples of this phenomenon, in which adhesion of cell-surface proteins to the substrate generates the steric interference. □

METHODS

Methods and any associated references are available in the online version of the paper at http://www.nature.com/naturecellbiology

Note: Supplementary Information is available on the Nature Cell Biology website

ACKNOWLEDGEMENTS

This work was supported by NIH grant National Institutes of Health GM 075252 (T.K.) and a Harvard Digestive Disease Consortium Feasibility Award (S.B.). We express gratitude to E. Marino (supported by NIH grant U54 AI057159, New England Regional Center of Excellence in Biodefense and Emerging Infectious Diseases) for maintaining the imaging resource used in this study and to S.C. Harrison for help with describing the force contributed by membrane tension and for editorial assistance. We gratefully acknowledge M. Ericsson and I. Kim for preparation of samples for electron microscopic analysis and members of the Kirchhausen laboratory for thought-provoking discussions. We thank M. Arpin (Centre National de la Recherche Scientifique (CNRS)/Morphogenèse et Signalisation cellulaires, Paris, France) and C. Revenu (Centre National de la Recherche Scientifique/Institut Curie, Paris, France) for the antibody specific for villin-1. We also acknowledge S. Robine for important suggestions involving the villin-1/villin-2 depletion experiments.

AUTHOR CONTRIBUTIONS

S.B., C.K. and T.K. designed experiments; S.B. and C.K. carried out experiments; S.B. and C.K. analysed data; C.K. developed the analytical tools to analyse the 3D data. F.U. provided expression vectors specific for the experiments with villin-1/villin-2, contributed to the experimental design of the experiments involved in villin-1/villin-2 depletion and created the LLCPK1 cell line. S.B. and T.K. wrote the manuscript. All authors discussed the results and contributed to the final manuscript.

COMPETING FINANCIAL INTERESTS

The authors declare no competing financial interests.

Published online at http://www.nature.com/naturecellbiology
Reprints and permissions information is available online at http://www.nature.com/reprints

1. Ehrlich, M. *et al.* Endocytosis by random initiation and stabilization of clathrin-coated pits. *Cell* **118,** 591–605 (2004).
2. Conibear, E. Converging views of endocytosis in yeast and mammals. *Curr. Opin. Cell Biol.* **22,** 513–518 (2010).
3. Kaksonen, M., Toret, C. P. & Drubin, D. G. A modular design for the clathrin- and actin-mediated endocytosis machinery. *Cell* **123,** 305–320 (2005).
4. Merrifield, C. J., Feldman, M. E., Wan, L. & Almers, W. Imaging actin and dynamin recruitment during invagination of single clathrin-coated pits. *Nat. Cell Biol.* **4,** 691–698 (2002).
5. Boucrot, E., Saffarian, S., Zhang, R. & Kirchhausen, T. Roles of AP-2 in clathrin-mediated endocytosis. *PloS ONE* **5,** e10597 (2010).
6. Cureton, D. K., Massol, R. H., Saffarian, S., Kirchhausen, T. L. & Whelan, S. P. J. Vesicular stomatitis virus enters cells through vesicles incompletely coated with clathrin that depend upon actin for internalization. *PLoS Pathog.* **5,** e1000394 (2009).
7. Boucrot, E., Saffarian, S., Massol, R., Kirchhausen, T. & Ehrlich, M. Role of lipids and actin in the formation of clathrin-coated pits. *Exp. Cell Res.* **312,** 4036–4048 (2006).
8. Perrais, D. & Merrifield, C. J. Dynamics of endocytic vesicle creation. *Dev. Cell* **9,** 581–592 (2005).
9. Kaksonen, M., Toret, C. P. & Drubin, D. G. Harnessing actin dynamics for clathrin-mediated endocytosis. *Nat. Rev. Mol. Cell Biol.* **7,** 404–414 (2006).
10. Cureton, D. K., Massol, R. H., Whelan, S. P. J. & Kirchhausen, T. The length of vesicular stomatitis virus particles dictates a need for actin assembly during clathrin-dependent endocytosis. *PLoS Pathog.* **6,** e1001127.
11. Saffarian, S., Cocucci, E. & Kirchhausen, T. Distinct dynamics of endocytic clathrin-coated pits and coated plaques. *PLoS Biol.* **7,** e1000191 (2009).
12. Kirchhausen, T. Imaging endocytic clathrin structures in living cells. *Trends Cell Biol.* **19,** 596–605 (2009).
13. Mettlen, M. *et al.* Endocytic accessory proteins are functionally distinguished by their differential effects on the maturation of clathrin-coated pits. *Mol. Biol. Cell* **20,** 3251–3260 (2009).
14. Salisbury, J. L., Condeelis, J. S. & Satir, P. Role of coated vesicles, microfilaments, and calmodulin in receptor-mediated endocytosis by cultured B lymphoblastoid cells. *J. Cell Biol.* **87,** 132–141 (1980).
15. Fujimoto, L. M., Roth, R., Heuser, J. E. & Schmid, S. L. Actin assembly plays a variable, but not obligatory role in receptor-mediated endocytosis in mammalian cells. *Traffic* **1,** 161–171 (2000).
16. Merrifield, C. J., Perrais, D. & Zenisek, D. Coupling between clathrin-coated-pit invagination, cortactin recruitment, and membrane scission observed in live cells. *Cell* **121,** 593–606 (2005).
17. Le Clainche, C. *et al.* A Hip1R-cortactin complex negatively regulates actin assembly associated with endocytosis. *EMBO J.* **26,** 1199–1210 (2007).
18. Merrifield, C. J., Qualmann, B., Kessels, M. M. & Almers, W. Neural Wiskott Aldrich Syndrome Protein (N-WASP) and the Arp2/3 complex are recruited to sites of clathrin-mediated endocytosis in cultured fibroblasts. *Eur. J. Cell Biol.* **83,** 13–18 (2004).
19. Benesch, S. *et al.* N-WASP deficiency impairs EGF internalization and actin assembly at clathrin-coated pits. *J. Cell Sci.* **118,** 3103–3115 (2005).
20. Saffarian, S. & Kirchhausen, T. Differential evanescence nanometry: live-cell fluorescence measurements with 10-nm axial resolution on the plasma membrane. *Biophys. J.* **94,** 2333–2342 (2008).
21. Aghamohammadzadeh, S. & Ayscough, K. R. Differential requirements for actin during yeast and mammalian endocytosis. *Nature Cell Biol.* **11,** 1039–1042 (2009).
22. Gottlieb, T. A., Ivanov, I. E., Adesnik, M. & Sabatini, D. D. Actin microfilaments play a critical role in endocytosis at the apical but not the basolateral surface of polarized epithelial cells. *J. Cell Biol.* **120,** 695–710 (1993).
23. Jackman, M. R., Shurety, W., Ellis, J. A. & Luzio, J. P. Inhibition of apical but not basolateral endocytosis of ricin and folate in Caco-2 cells by cytochalasin D. *J. Cell Sci.* **107,** 2547–2556 (1994).
24. Altschuler, Y. *et al.* ADP-ribosylation factor 6 and endocytosis at the apical surface of Madin-Darby canine kidney cells. *J. Cell Biol.* **147,** 7–12 (1999).
25. Shurety, W., Bright, N. A. & Luzio, J. P. The effects of cytochalasin D and phorbol myristate acetate on the apical endocytosis of ricin in polarised Caco-2 cells. *J. Cell Sci.* **109,** 2927–2935 (1996).
26. Hyman, T., Shmuel, M. & Altschuler, Y. Actin is required for endocytosis at the apical surface of Madin-Darby canine kidney cells where ARF6 and clathrin regulate the actin cytoskeleton. *Mol. Biol. Cell* **17,** 427–437 (2006).
27. Da Costa, S. R. *et al.* Impairing actin filament or syndapin functions promotes accumulation of clathrin-coated vesicles at the apical plasma membrane of acinar epithelial cells. *Mol. Biol. Cell* **14,** 4397–4413 (2003).
28. Shmuel, M. *et al.* ARNO through its coiled-coil domain regulates endocytosis at the apical surface of polarized epithelial cells. *J. Biol. Chem.* **281,** 13300–13308 (2006).
29. Buss, F., Arden, S. D., Lindsay, M., Luzio, J. P. & Kendrick-Jones, J. Myosin VI isoform localized to clathrin-coated vesicles with a role in clathrin-mediated endocytosis. *EMBO J.* **20,** 3676–3684 (2001).
30. Poupon, V. *et al.* Clathrin light chains function in mannose phosphate receptor trafficking via regulation of actin assembly. *Proc. Natl Acad. Sci. USA* **105,** 168–173 (2008).
31. Macia, E. *et al.* Dynasore, a cell-permeable inhibitor of dynamin. *Dev. Cell* **10,** 839–850 (2006).

32. Rohatgi, R. *et al*. The interaction between N-WASP and the Arp2/3 complex links Cdc42-dependent signals to actin assembly. *Cell* **97,** 221–231 (1999).
33. Paleotti, O. *et al*. The small G-protein ARF6GTP recruits the AP-2 adaptor complex to membranes. *J. Biol. Chem.* **280,** 21661–21666 (2005).
34. Chen, C.-Y. & Brodsky, F. M. Huntingtin-interacting protein 1 (Hip1) and Hip1-related protein (Hip1R) bind the conserved sequence of clathrin light chains and thereby influence clathrin assembly *in vitro* and actin distribution *in vivo*. *J. Biol. Chem.* **280,** 6109–6117 (2005).
35. Engqvist-Goldstein, A. E. *et al*. The actin-binding protein Hip1R associates with clathrin during early stages of endocytosis and promotes clathrin assembly *in vitro*. *J. Cell Biol.* **154,** 1209–1223 (2001).
36. Wilbur, J. D. *et al*. Actin binding by Hip1 (huntingtin-interacting protein 1) and Hip1R (Hip1-related protein) is regulated by clathrin light chain. *J. Biol. Chem.* **283,** 32870–32879 (2008).
37. Engqvist-Goldstein, A. E. *et al*. RNAi-mediated Hip1R silencing results in stable association between the endocytic machinery and the actin assembly machinery. *Mol. Biol. Cell* **15,** 1666–1679 (2004).
38. Dai, J. & Sheetz, M. P. Membrane tether formation from blebbing cells. *Biophys. J.* **77,** 3363–3370 (1999).
39. Fotin, A. *et al*. Structure determination of clathrin coats to subnanometer resolution by single particle cryo-electron microscopy. *J. Struct. Biol.* **156,** 453–460 (2006).

DOI: 10.1038/ncb2307

METHODS

Reagents. Rabbit polyclonal antibodies against dynamin-2 (Hudy-1, Millipore; 1:1,000), villin (provided by M. Arpin; 1:2,000) and ezrin (Cell Signaling Technology; 1:1,000), mouse monoclonal antibodies against ZO-1 (Invitrogen; 1:2,000) and clathrin light chains (CON-1 generated from hybridoma cells; 1:500), and Alexa Fluor 488, 546 or 647 secondary antibodies and Alexa 647 human-transferrin (Molecular Probes/Invitrogen; 1:1,000) were used.

Jasplakinolide (Alexis Biochemical), latrunculin A, NSC-23766 (Rac1 inhibitor[40]), SecinH3 (inhibitor for cytohesins[41], small guanine nucleotide exchange factors (GEFs) for Arf factors including Arf6; Calbiochem) and secramine (inhibitor of Cdc42; ref. 42) were used at 1 μM, 1 μM, 50 μM and 1 μM, respectively.

Cell culture and transfections. MDCK and BSC1 cells stably expressing σ2–eGFP (the small subunit of AP-2 fused to enhanced green fluorescent protein, eGFP) were grown in DMEM medium containing 10% FCS, penicillin and streptomycin. The MDCK cells expressing σ2–eGFP were generated by transfection with Fugen HD selected with G418. Plasmids encoding Cherry fused to wild-type and mutant bovine clathrin light chain B (Cherry–LCb and Cherry–LCb-EED/QQN) were made by exchange of eGFP with Cherry from eGFP–LCb and eGFP–LCb-EED/QQN (P. McPherson). Transient expression of villin–Cherry, Cherry–LCb and Cherry–LCb-EED/QQN was carried out using TransIT-LT1 (Mirus Bio LL) and cells were analysed 12–16 h after transfection unless otherwise indicated.

Gene silencing. Simultaneous depletion of clathrin light chains A and B was achieved in MDCK cells stably expressing σ2–eGFP by siRNA-mediated gene silencing as described previously[11].

Depletion of villin-1 and ezrin was achieved by shRNA. siRNA sequences specific for villin-1 (5′-CCGGGCCAAGATGAAATTACAGCATCTCGAGATGCTGTAATTTCATCTTGGCTTTTTG-3′) and ezrin genes 5′-CCGGCCTGGAAATGTATGGAATCAACTCGAGTTGATTCCATACATTTCCAGGTTTTTG-3′) were incorporated into the lentivirus vector pLKO.1 (Addgene). MDCK cells (1×10^6) stably expressing σ2–eGFP were transduced with 50–100 μl of thawed supernatants, and cells containing integrated viral sequences were selected by serial passage in medium containing 4 μg ml^{-1} puromycin.

Osmotic swelling. MDCK or BSC1 cells kept at 37 °C and in the presence of humidified 5% CO_2 were exposed for 10 min to diluted medium (311, 251, 220 and 174 mOsM) prepared by mixing 100, 80, 70 or 50% of phenol red-free DMEM containing 10% FCS serum with 0, 20, 30 or 50% water containing 10% FCS serum. Live-cell imaging time series were acquired immediately before and after the hypo-osmotic treatment. In some experiments, jasplakinolide was added after 10 min of exposure to the hypotonic medium; in other experiments, jasplakinolide was included before and during the treatment with the hypotonic medium. Both protocols elicited the same actin dependence on the dynamics of clathrin coat formation. The actin dependence imparted by osmotic swelling of cells incubated for 10 min with 50% medium was fully lost on incubation for 10 min with normal medium.

Controlled stretching. To form the support chamber, first a thin sheet of polydimethylsiloxane (PDMS; 50 μm in thickness; Specialty Silicone Products) was placed on the bottom of a 35-mm-diameter glass Petri dish. An optically flat-ended fused silica rod (Techspec, Edmund Optics) was placed on top of the PDMS sheet and used to cast the lateral walls of the PDMS chamber. The chamber was made by pouring PDMS (Sylgard 184 silicone elastomer kit; Ellsworth Adhesives) degassed for about 20 min until no more bubbles formed, and then cured for 2 h at 65 °C. After extensive washes with water, the PDMS sheet was coated overnight at 4 °C with 50 μg ml^{-1} fibronectin (dissolved in water) and then washed once more with PBS. About 1×10^4 cells were plated for 16 h at 37 °C. The PDMS chamber with cells was attached to a 37 °C pre-equilibrated stretching device equipped with a micrometre screw and then mounted on the temperature-controlled stage of the microscope. Imaging was done before and immediately after ∼25% mechanical stretching along one horizontal axis.

Immunofluorescence microscopy. Cells were fixed for 15 min at room temperature with 4% w/v paraformaldehyde in PBS, followed by sequential incubation with primary and secondary antibodies in PBS containing 0.05% w/v Triton X-100 and 2% FCS.

Electron microscopy. Electron microscopy was carried out as described previously[10].

Live-cell spinning-disc confocal imaging. About 1×10^5 BSC1 cells were plated 16 h before imaging on 25-mm-diameter glass No. 1.5 coverslips; a similar number of MDCK cells were plated 1 day or 3 days (to allow for cell polarization) before imaging. Imaging medium was phenol red-free DMEM with 10% FCS and 20 mM HEPES. For imaging, the coverslips were placed on a temperature-controlled 5% CO_2-humidified chamber (20/20 Technologies) mounted on the stage of a Mariana imaging system (Intelligent Imaging Innovations) based on an Axiovert 200 M inverted microscope (Carl Zeiss), a CSU-X1 spinning-disc confocal unit (Yokogawa Electric Corporation), a spherical-aberration-correction device (SAC; Infinity Photo-Optical) and a ×63 objective lens (Plan-Apochromat, NA 1.4, Carl Zeiss)[10]. The SAC resolved the severe spherical aberration especially noticeable on the apical surface located 8–10 μm away from the coverslip using SAC values of 1,100 and 850 for basolateral/bottom and apical surfaces of cells on glass coverslips, and 0 for bottom (attached) surfaces of cells on PDMS. Two-dimensional (2D) and 3D time series were obtained using Slidebook 5 (3I).

Data acquisition, image processing and statistical analysis. 2D movies from the attached surfaces (basolateral for polarized and ventral for non-polarized cells) were obtained with 100 ms exposures from a single optical plane. 3D movies from the free surface (apical for polarized and dorsal for non-polarized) correspond to z stacks of 3–5 consecutive optical planes spaced 0.5 μm acquired at a frequency of 0.5 Hz per stack and 100 ms exposure; a 2D movie was then obtained by generating for each time point a maximum-intensity z projection. The 3D movies had a duration of 120–160 s, sufficient to fully track the few non-arrested AP-2 spots; the remaining ones had lifetimes longer than 10 min when stalled by the absence of actin dynamics. Time series from the bottom surface were acquired from a single optical plane because the intensity and lifetime data obtained from these 2D movies were equivalent to data obtained from 3D movies, thus minimizing potential photobleaching and phototoxicity effects.

AP-2 spots were identified and tracked using a MATLAB routine (Kural, C., Boulant, S. & Kirchhausen, T., manuscript in preparation) using three sequential steps composed of 2D Gaussian and Laplacian filtering followed by a local maxima-finding algorithm. The intensity profile as a function of time was used to characterize the dynamics of each of the AP-2 spots selected according to the following criteria: fluorescent objects were diffraction limited; dynamic, non-arrested objects appeared and disappeared within the time window of the time series with lifetimes of at least 20 s (thus, shorter-lived objects corresponding to abortive pits were not included for analysis); arrested objects were those present throughout the duration of the time series; the fluorescent objects did not collide with each other.

Statistical tests. The statistical significance for the differences between the lifetime or maximum fluorescence intensity of the data determined under specific experimental conditions was established using a two-tailed Student t-test.

Estimate of the work required to deform a membrane vesicle under conditions of membrane tension. We estimate the work done against tension as the product of the tension and the net increase in membrane area required to advance the bud to the point in question. During budding of the initial hemisphere, the increase in membrane area in the pit is accompanied by a decrease in area in the plane of the cell surface. However, when the membrane starts to constrict, both areas increase together (Fig. 5). Measured membrane tensions for cells in culture are in the range 10–50 mN m^{-1}. To generate a typical coated pit, which encloses a vesicle of diameter ∼700 Å in a shell of about 60–80 clathrin trimers (∼200 heavy chains), from a membrane under 30 mN m^{-1} tension, the work needed to form the first hemisphere is about 10^{-19} J or 60 kJ mol^{-1} (15 kcal mol^{-1}), whereas the work needed to complete the second hemisphere is three times that value. If 100 heavy chains contribute to the lattice surrounding the initial hemisphere, the corresponding membrane deformation requires only about 0.6 kJ mol^{-1} of net free energy per heavy chain beyond the free energy needed to generate a membrane-free clathrin lattice—that is, a contribution considerably less than $k_B T$, where k_B is Boltzmann's constant and T is temperature. Note that the estimated work required to bend a membrane into a hemisphere is roughly ten times this amount, but still only the equivalent of 1–2 well-placed hydrogen bonds per heavy chain and therefore easily within the free energy likely to come from assembly of the clathrin lattice. If the tension rises 10-fold (from cytoskeletal stretching, osmotic changes and so on), to levels comparable to the tension of cytoskeletally constrained red blood cell membranes[38,43], the work needed to overcome tension becomes comparable to the bending work. Our observations indicate that in the absence of actin dynamics this contribution is enough to stall invagination. Addition of one actin monomer to a growing filament generates a force of about 10 pN (refs 44,45) and a displacement at the tip by about 3 nm, for example about 3×10^{-20} J or 18 kJ mol^{-1}. Thus, the addition of about 20 actin monomers

to each of 5–10 filaments can do more than enough work, in concert with the contribution from clathrin polymerization, to deform the second hemisphere and to displace the invaginating membrane by about 60 nm—nearly a full vesicle diameter.

40. Gao, Y., Dickerson, J. B., Guo, F., Zheng, J. & Zheng, Y. Rational design and characterization of a Rac GTPase-specific small molecule inhibitor. *Proc. Natl Acad. Sci. USA* **101,** 7618–7623 (2004).
41. Hafner, M. *et al.* Inhibition of cytohesins by SecinH3 leads to hepatic insulin resistance. *Nature* **444,** 941–944 (2006).
42. Pelish, H. E. *et al.* Secramine inhibits Cdc42-dependent functions in cells and Cdc42 activation *in vitro*. *Nat. Chem. Biol.* **2,** 39–46 (2006).
43. Hochmuth, F. M., Shao, J. Y., Dai, J. & Sheetz, M. P. Deformation and flow of membrane into tethers extracted from neuronal growth cones. *Biophys. J.* **70,** 358–369 (1996).
44. Noireaux, V. *et al.* Growing an actin gel on spherical surfaces. *Biophys. J.* **78,** 1643–1654 (2000).
45. Upadhyaya, A., Chabot, J. R., Andreeva, A., Samadani, A. & van Oudenaarden, A. Probing polymerization forces by using actin-propelled lipid vesicles. *Proc. Natl Acad. Sci. USA* **100,** 4521–4526 (2003).

D. Publication III

Microvilli.

Ubelmann F, Louvard D, Robine S

Chapter 13 from the book “Cellular domains” edited by Ivan R. Nabi

J. Wiley & sons Ed.; 2011